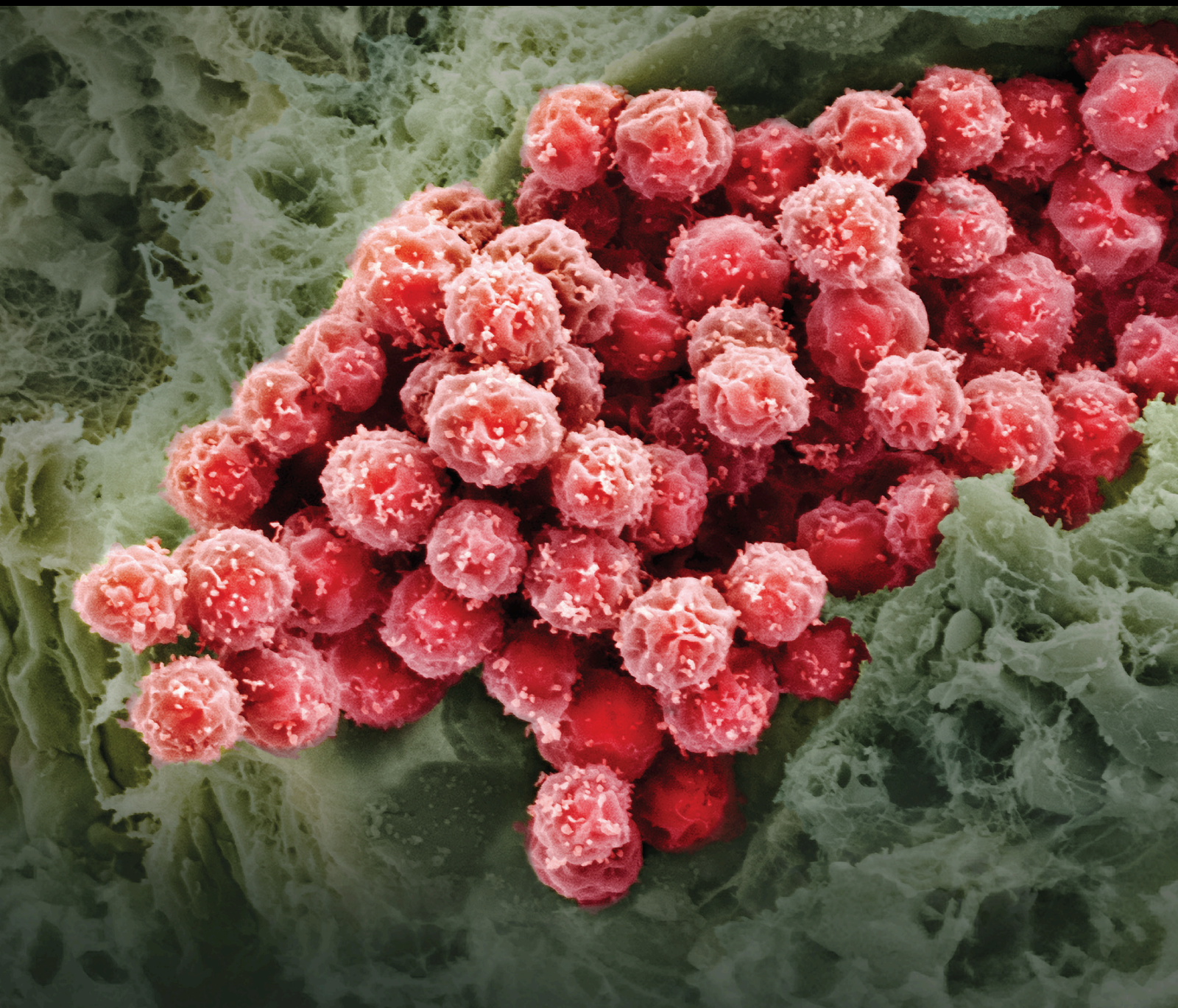


# Application of Stem Cells in the Oral and Maxillofacial Region

Lead Guest Editor: Toru Ogasawara

Guest Editors: Edward C. Ko and Jiashing Yu





---

# **Application of Stem Cells in the Oral and Maxillofacial Region**

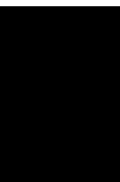
Stem Cells International

---

## **Application of Stem Cells in the Oral and Maxillofacial Region**

Lead Guest Editor: Toru Ogasawara

Guest Editors: Edward C. Ko and Jiashing Yu



---

Copyright © 2020 Hindawi Limited. All rights reserved.

This is a special issue published in "Stem Cells International." All articles are open access articles distributed under the Creative Commons Attribution License, which permits unrestricted use, distribution, and reproduction in any medium, provided the original work is properly cited.

# Chief Editor

Renke Li, Canada

## Editorial Board

James Adjaye, Germany  
Cinzia Allegrucci, United Kingdom  
Eckhard U Alt, USA  
Francesco Angelini, Italy  
James A. Ankrum, USA  
Sarnowska Anna, Poland  
Stefan Arnhold, Germany  
Marta Baiocchi, Italy  
Andrea Ballini, Italy  
Dominique Bonnet, United Kingdom  
Philippe Bourin, France  
Daniel Bouvard, France  
Anna T. Brini, Italy  
Annelies Bronckaers, Belgium  
Silvia Brunelli, Italy  
Stefania Bruno, Italy  
Bruce A. Bunnell, USA  
Kevin D. Bunting, USA  
Benedetta Bussolati, Italy  
Leonora Buzanska, Poland  
Antonio C. Campos de Carvalho, Brazil  
Stefania Cantore, Italy  
Yilin Cao, China  
Marco Cassano, Switzerland  
Alain Chapel, France  
Sumanta Chatterjee, USA  
Isotta Chimenti, Italy  
Mahmood S. Choudhery, Pakistan  
Pier Paolo Claudio, USA  
Gerald A. Colvin, USA  
Mihaela Crisan, United Kingdom  
Radbod Darabi, USA  
Joery De Kock, Belgium  
Frederic Deschaseaux, France  
Marcus-André Deutsch, Germany  
Valdo Jose Dias Da Silva, Brazil  
Massimo Dominici, Italy  
Leonard M. Eisenberg, USA  
Georgina Ellison, United Kingdom  
Alessandro Faroni, United Kingdom  
Francisco J. Fernández-Avilés, Spain  
Jess Frith, Australia  
Ji-Dong Fu, USA  
Manuela E. Gomes, Portugal


Cristina Grange, Italy  
Hugo Guerrero-Cazares, USA  
Jacob H. Hanna, Israel  
David A. Hart, Canada  
Alexandra Harvey, Australia  
Yohei Hayashi, Japan  
Tong-Chuan He, USA  
Xiao J. Huang, China  
Thomas Ichim, USA  
Joseph Itskovitz-Eldor, Israel  
Elena A. Jones, United Kingdom  
Christian Jorgensen, France  
Oswaldo Keith Okamoto, Brazil  
Alexander Kleger, Germany  
Diana Klein, Germany  
Valerie Kouskoff, United Kingdom  
Andrzej Lange, Poland  
Laura Lasagni, Italy  
Robert B. Levy, USA  
Tao-Sheng Li, Japan  
Shinn-Zong Lin, Taiwan  
Yupo Ma, USA  
Risheng Ma, USA  
Marcin Majka, Poland  
Giuseppe Mandraffino, Italy  
Athanasios Mantalaris, United Kingdom  
Cinzia Marchese, Italy  
Katia Mareschi, Italy  
Hector Mayani, Mexico  
Jason S. Meyer, USA  
Eva Mezey, USA  
Susanna Miettinen, Finland  
Toshio Miki, USA  
Claudia Montero-Menei, France  
Christian Morscheck, Germany  
Patricia Murray, United Kingdom  
Federico Mussano, Italy  
Mustapha Najimi, Belgium  
Norimasa Nakamura, Japan  
Bryony A. Nayagam, Australia  
Karim Nayernia, United Kingdom  
Krisztian Nemeth, USA  
Francesco Onida, Italy  
Sue O'Shea, USA

Gianpaolo Papaccio, Italy  
Kishore B. S. Pasumarthi, Canada  
Yuriy Petrenko, Czech Republic  
Alessandra Pisciotta, Italy  
Stefan Przyborski, United Kingdom  
Bruno P#ault, USA  
Peter J. Quesenberry, USA  
Pranela Rameshwar, USA  
Francisco J. Rodríguez-Lozano, Spain  
Bernard A. J. Roelen, The Netherlands  
Alessandro Rosa, Italy  
Peter Rubin, USA  
Hannele T. Ruohola-Baker, USA  
Benedetto Sacchetti, Italy  
Ghasem Hosseini Salekdeh, Iran  
Antonio Salgado, Portugal  
Fermin Sanchez-Guijo, Spain  
Heinrich Sauer, Germany  
Coralie Sengenès, France  
Dario Siniscalco, Italy  
Shimon Slavin, Israel  
Sieghart Sopper, Austria  
Valeria Sorrenti, Italy  
Giorgio Stassi, Italy  
Ann Steele, USA  
Alexander Storch, Germany  
Bodo Eckehard Strauer, Germany  
Hirotaka Suga, Japan  
Gareth Sullivan, Norway  
Masatoshi Suzuki, USA  
Kenichi Tamama, USA  
Corrado Tarella, Italy  
Daniele Torella, Italy  
Hung-Fat Tse, Hong Kong  
Marc L. Turner, United Kingdom  
Aijun Wang, USA  
Darius Widera, United Kingdom  
Bettina Wilm, United Kingdom  
Dominik Wolf, Austria  
Wasco Wruck, Germany  
Qingzhong Xiao, United Kingdom  
Takao Yasuhara, Japan  
Zhaohui Ye, USA  
Holm Zaehres, Germany  
Elias T. Zambidis, USA  
Ludovic Zimmerlin, USA  
Ewa K. Zuba-Surma, Poland




Eder Zucconi, Brazil  
Maurizio Zuccotti, Italy  
Nicole Isolde zur Nieden, USA

## Contents




### **Application of Stem Cells in the Oral and Maxillofacial Region**

Toru Ogasawara , Edward Chengchuan Ko, and Jiashing Yu  
Editorial (2 pages), Article ID 2421453, Volume 2020 (2020)





### **Bone Defect Repair Using a Bone Substitute Supported by Mesenchymal Stem Cells Derived from the Umbilical Cord**

Michal Kosinski , Anna Figiel-Dabrowska, Wioletta Lech, Lukasz Wieprzowski, Ryszard Strzalkowski, Damian Strzemecki, Lukasz Cheda, Jacek Lenart, Krystyna Domanska-Janik , and Anna Sarnowska   
Research Article (15 pages), Article ID 1321283, Volume 2020 (2020)


### **Deciduous Dental Pulp Stem Cells for Maxillary Alveolar Reconstruction in Cleft Lip and Palate Patients**

Daniela Y. S. Tanikawa , Carla C. G. Pinheiro , Maria Cristina A. Almeida, Claudia R. G. C. M. Oliveira, Renata de Almeida Coudry, Diógenes Laercio Rocha, and Daniela Franco Bueno   
Research Article (9 pages), Article ID 6234167, Volume 2020 (2020)


### **Aging Induced p53/p21 in Genioglossus Muscle Stem Cells and Enhanced Upper Airway Injury**

Lu-Ying Zhu, Li-Ming Yu , Wei-Hua Zhang, Jia-Jia Deng, Shang-Feng Liu, Wei Huang, Meng-Han Zhang, Yan-Qin Lu , Xin-Xin Han , and Yue-Hua Liu   
Research Article (13 pages), Article ID 8412598, Volume 2020 (2020)






### **Human Fat-Derived Mesenchymal Stem Cells Xenogenically Implanted in a Rat Model Show Enhanced New Bone Formation in Maxillary Alveolar Tooth Defects**

Andrew Wofford, Austin Bow, Steven Newby, Seth Brooks, Rachel Rodriguez, Tom Masi, Stacy Stephenson, Jack Gotcher, David E. Anderson, Josh Campbell, and Madhu Dhar   
Research Article (14 pages), Article ID 8142938, Volume 2020 (2020)





### **Bone Tissue Regeneration in the Oral and Maxillofacial Region: A Review on the Application of Stem Cells and New Strategies to Improve Vascularization**

Vivian Wu, Marco N. Helder, Nathalie Bravenboer, Christiaan M. ten Bruggenkate, Jianfeng Jin, Jenneke Klein-Nulend , and Engelbert A. J. M. Schulten  
Review Article (15 pages), Article ID 6279721, Volume 2019 (2019)








### **Evaluation of Chitosan Hydrogel for Sustained Delivery of VEGF for Odontogenic Differentiation of Dental Pulp Stem Cells**

Si Wu , Yachuan Zhou , Yi Yu, Xin Zhou, Wei Du, Mian Wan, Yi Fan, Xuedong Zhou , Xin Xu , and Liwei Zheng   
Research Article (14 pages), Article ID 1515040, Volume 2019 (2019)

### **Is There a Noninvasive Source of MSCs Isolated with GMP Methods with Better Osteogenic Potential?**



Carla C. G. Pinheiro , Alessandro Leyendecker Junior , Daniela Y. S. Tanikawa , José Ricardo Muniz Ferreira, Reza Jarrahy, and Daniela F. Bueno   
Research Article (14 pages), Article ID 7951696, Volume 2019 (2019)

### **Dental Follicle Cells: Roles in Development and Beyond**

Tao Zhou , Jinhai Pan, Peiyao Wu, Ruijie Huang, Wei Du , Yachuan Zhou , Mian Wan, Yi Fan, Xin Xu , Xuedong Zhou , Liwei Zheng , and Xin Zhou 

Review Article (17 pages), Article ID 9159605, Volume 2019 (2019)

### **Local Application of Semaphorin 3A Combined with Adipose-Derived Stem Cell Sheet and Anorganic Bovine Bone Granules Enhances Bone Regeneration in Type 2 Diabetes Mellitus Rats**

Xiaoru Xu , Kaixiu Fang, Lifeng Wang, Xiangwei Liu, Yuchao Zhou, and Yingliang Song 

Research Article (14 pages), Article ID 2506463, Volume 2019 (2019)

### **New Insights on Properties and Spatial Distributions of Skeletal Stem Cells**

Jun-qi Liu, Qi-wen Li , and Zhen Tan 

Review Article (11 pages), Article ID 9026729, Volume 2019 (2019)



## Editorial

# Application of Stem Cells in the Oral and Maxillofacial Region

**Toru Ogasawara** <sup>1</sup>, **Edward Chengchuan Ko**,<sup>2</sup> and **Jiashing Yu**<sup>3</sup>

<sup>1</sup>*The University of Tokyo, Tokyo, Japan*

<sup>2</sup>*Kaohsiung Medical University, Kaohsiung, Taiwan*

<sup>3</sup>*National Taiwan University, Taiwan*

Correspondence should be addressed to Toru Ogasawara; [togasawara-tky@umin.ac.jp](mailto:togasawara-tky@umin.ac.jp)

Received 13 March 2020; Accepted 14 March 2020; Published 13 April 2020

Copyright © 2020 Toru Ogasawara et al. This is an open access article distributed under the Creative Commons Attribution License, which permits unrestricted use, distribution, and reproduction in any medium, provided the original work is properly cited.

## 1. Introduction

Conditions such as trauma-induced bone or cartilage defects and tumor or congenital defects are common in the oral and maxillofacial region. To repair irreversible skeletal damage or defects, bone grafts are the current gold standard. However, problems such as a shortage of bone graft material and donor-site morbidity affect the availability of bone grafts. It is also still difficult to restore salivary glands that have been severely damaged by radiation therapy and to counteract the neurodegeneration induced by trauma or surgery. In addition, due to the limited self-healing ability of the teeth, dental caries is treated by fillings (e.g., composite resin) or crowns, and missing teeth are replaced through dental bridges, removable dentures, or dental implants.

It is thus necessary to establish new treatment strategies for these conditions. One of the most effective strategies is to introduce stem cell-based tissue engineering technology in the oral and maxillofacial region. Accordingly, numerous studies have been conducted and many promising results have been reported. Stem cell-based tissue engineering therapy in this region of the body remains challenging to perfect, however.

The cutting-edge review by J.-Q. Liu et al. emphasized four bone sites (growth plate, perivascular areas, periosteum, and cranial suture) as possible sources of skeletal stem cells (SSCs) and evaluated these cells from a SSC perspective. To make the best use of SSCs, they considered it necessary to clarify the mechanism underlying their fate commitment.

X. Xu et al. evaluated the effect of local application of Semaphorin 3A (Sema3A) combined with adipose-derived

stem cell sheets and anorganic bovine bone granules in type 2 diabetes mellitus (T2DM) rats. Their results suggested that this combination can be useful to improve bone healing for T2DM patients.

T. Zhou et al. comprehensively reviewed roles of dental follicle cells (DFCs) in tooth development as well as such characteristics of DFCs as their multilineage differentiation, immunosuppression capability, excellent amplification ability, and tissue engineering potential. They concluded that DFCs can act as groups of excellent cells in future cell-based treatment for tissue repair and regeneration.

C. C. G. Pinheiro et al. studied the osteogenic potential of three types of stem cells (umbilical cord, orbicularis oris muscle, and deciduous dental pulp), aiming at alveolar cleft bone tissue engineering. Their results suggested that dental pulp and orbicularis oris muscles are the best sources of mesenchymal stem cells (MSCs) for bone tissue engineering for cleft lip and palate (CLP) patients. The review by V. Wu et al. presented and discussed the advancement of stem cell application, vascularization, and bone regeneration in the oral and maxillofacial region, with an emphasis on the human jaw. In addition, they proposed new strategies to improve the current techniques, which may lead to feasible clinical applications.

A biomaterial-based approach is one of the technical advances shown to improve both cell engraftment and survival after transplantation. In their original research article, S. Wu et al. evaluated a chitosan/ $\beta$ -glycerophosphate (CS/ $\beta$ -GP) hydrogel as a vascular endothelial growth factor-(VEGF-) sustained release system and explored its effects on dental pulp stem cells (DPSCs). They hypothesized that

thermosensitive chitosan hydrogel could effectively deliver VEGF protein in a sustained release pattern to stimulate differentiation and mineralization of DPSCs.

The original research article by A. Wofford et al. demonstrated that xenogeneic human adipose tissue-derived MSCs, which were delivered to and contained at the bone injury site via a bioinert scaffold, promoted enhanced regeneration of maxillary alveolar tooth defects in rats.

Muscle regeneration is also one of the important topics in the oral and maxillofacial region. With the goal of providing a therapeutic basis for the repair of obstructive sleep apnea (OSA) upper airway injury, L.-Y. Zhu et al. studied the function of genioglossus (GG) muscles and muscle stem cells (MuSCs). Their results highlighted the important role of p53/p21 on the GG muscle during the aging process.

In summary, this special issue encompasses both comprehensive reviews and original research articles highlighting advances in stem cell and biomaterial research relative to the regeneration of the oral and maxillofacial region. We sincerely hope that the articles published in this special issue can help researchers to better understand the recent trends in the application of stem cells in the oral and maxillofacial region.

### **Conflicts of Interest**

The editors declare that they have no conflicts of interest regarding the publication of this Special Issue.




### **Acknowledgments**

We would like to thank all the authors and reviewers who contributed to this special issue. We would also like to express our gratitude to the editorial board members and the editorial office members of this journal for their support throughout the review process.

*Toru Ogasawara  
Edward Chengchuan Ko  
Jiashing Yu*

## Research Article

# Bone Defect Repair Using a Bone Substitute Supported by Mesenchymal Stem Cells Derived from the Umbilical Cord

Michał Kosinski <sup>1</sup>, Anna Figiel-Dabrowska,<sup>1</sup> Wioletta Lech,<sup>2</sup> Lukasz Wieprzowski,<sup>3</sup> Ryszard Strzalkowski,<sup>4</sup> Damian Strzemecki,<sup>5</sup> Lukasz Cheda,<sup>6</sup> Jacek Lenart,<sup>7</sup> Krystyna Domanska-Janik <sup>2</sup>, and Anna Sarnowska <sup>1</sup>

<sup>1</sup>Translational Platform for Regenerative Medicine, Mossakowski Medical Research Centre, Polish Academy of Sciences, Poland

<sup>2</sup>Department of Stem Cell Bioengineering, Mossakowski Medical Research Centre, Polish Academy of Sciences, Poland

<sup>3</sup>Paediatric Surgery Clinic, Institute of Mother and Child, Poland

<sup>4</sup>Electron Microscopy Platform, Mossakowski Medical Research Centre, Polish Academy of Sciences, Poland

<sup>5</sup>Department of Experimental Pharmacology, Mossakowski Medical Research Centre, Polish Academy of Sciences, Poland

<sup>6</sup>Faculty of Chemistry, Biological and Chemical Research Centre, University of Warsaw, Poland

<sup>7</sup>Department of Neurochemistry, Mossakowski Medical Research Centre, Polish Academy of Sciences, Poland

Correspondence should be addressed to Anna Sarnowska; [a\\_sarnowska@tlen.pl](mailto:a_sarnowska@tlen.pl)

Received 4 October 2019; Revised 10 January 2020; Accepted 13 February 2020; Published 18 March 2020

Guest Editor: Toru Ogasawara

Copyright © 2020 Michał Kosinski et al. This is an open access article distributed under the Creative Commons Attribution License, which permits unrestricted use, distribution, and reproduction in any medium, provided the original work is properly cited.

**Objective.** Bone defects or atrophy may arise as a consequence of injury, inflammation of various etiologies, and neoplastic or traumatic processes or as a result of surgical procedures. Sometimes the regeneration process of bone loss is impaired, significantly slowed down, or does not occur, e.g., in congenital defects. For the bone defect reconstruction, a piece of the removed bone from ala of ilium or bone transplantation from a decedent is used. Replacement of the autologous or allogenic source of the bone-by-bone substitute could reduce the number of surgeries and time in the pharmacological coma during the reconstruction of the bone defect. Application of mesenchymal stem cells in the reconstruction surgery may have positive influence on tissue regeneration by secretion of angiogenic factors, recruitment of other MSCs, or differentiation into osteoblasts. **Materials and Methods.** Mesenchymal stem cells derived from the umbilical cord (Wharton's jelly (WJ-MS)) were cultured in GMP-grade DMEM low glucose supplemented with heparin, 10% platelet lysate, glucose, and antibiotics. *In vitro* WJ-MSs were seeded on the bone substitute Bio-Oss Collagen® and cultured in the StemPro® Osteogenesis Differentiation Kit. During the culture on the 1st, 7th, 14th, and 21st day (day in vitro (DIV)), we analyzed viability (confocal microscopy) and adhesion capability (electron microscopy) of WJ-MS on Bio-Oss scaffolds, gene expression (qPCR), and secretion of proteins (Luminex). *In vivo* Bio-Oss® scaffolds with WJ-MS were transplanted to trepanation holes in the cranium to obtain their overgrowth. The computed tomography was performed 7, 14, and 21 days after surgery to assess the regeneration. **Results.** The Bio-Oss® scaffold provides a favourable environment for WJ-MS survival. WJ-MSs in osteodifferentiation medium are able to attach and proliferate on Bio-Oss® scaffolds. Results obtained from qPCR and Luminex® indicate that WJ-MSs possess the ability to differentiate into osteoblast-like cells and may induce osteoclastogenesis, angiogenesis, and mobilization of host MSCs. In animal studies, WJ-MSs seeded on Bio-Oss® increased the scaffold integration with host bone and changed their morphology to osteoblast-like cells. **Conclusions.** The presented construct consisted of Bio-Oss®, the scaffold with high flexibility and plasticity, approved for clinical use with seeded immunologically privileged WJ-MS which may be considered reconstructive therapy in bone defects.

## 1. Introduction

Bone defects resulting from a birth defect, injury, or ongoing disease processes often require reconstruction. So far as a standard procedure, own bone transplants were used. This means an additional procedure and sometimes health complications for the patient. According to scientific studies, such bone transplants undergo more often atrophy than tested biomaterial scaffolds. By introducing the bone scaffold into the human body, it is assumed that it will perform a specific function for a long time. Good anastomosis of the implant with the bone and its proper elasticity could create conditions that accompany the normal healing process of bone defect.

One of the biomaterials commonly used in stomatology is Bio-Oss<sup>®</sup> manufactured by Geistlich Pharma AG. This material is approved for clinical use in orthodontic surgeries. Bio-Oss<sup>®</sup> is composed of bovine bones deprived from lipids, blood components, and proteins; due to that after transplantation, graft rejection does not occur. Bio-Oss<sup>®</sup> has very similar structure to human cancellous bone, is flexible, and is elastic with high porosity which allows for cell adhesion and survival.

In recent years, biomedical field shows high interest in mesenchymal stem cells as a potential booster of endogenous regeneration of tissues. MSC expresses surface markers such as CD73, CD90, and CD105 and has potency to renewing and differentiating into preferred cell types such as bone and fat cells as well as chondrocytes. Every year, a number of clinical trials with MSC isolated from the bone marrow or adipose tissue increase. The role of those cells is not fully explained, but in the skeletal system, dermatology and ophthalmology are based on differentiation into targeted cell lines as well as on immunomodulatory and proangiogenic functions [1].

Mesenchymal stem cells were firstly isolated from the bone marrow; since then, those cells were characterized extensively and used frequently. Except the bone marrow, MSCs are isolated from the adipose tissue and umbilical cord. The number of isolated MSCs varies from 0.001 to 0.01% of total cells obtained from the bone marrow aspirate, approx. 2% in case of adipose tissue to approx. 25% in Wharton jelly of the umbilical cord [2]. Collection of the bone marrow as well as adipose tissue is associated with invasive procedures in contrast to the umbilical cord which is a waste during babies' delivery. Moreover, there are additional benefits from usage of fetal sources of MSC stem cells for regeneration purposes due to their expansive growth and higher spectrum of differentiation [3]. WJ-MSc is characterized by great plasticity and can be differentiated into bone and fat cells and chondrocytes and into sweat gland cells [4], Schwann cells [5, 6], and pancreas cells [7] or even neural-like cells [8]. Cells isolated from adult tissues due to longer exposure to environmental conditions may be characterized by reduced proliferation and regeneration potency and faster ageing what is connected to shorter telomeres. Compared to those cells, MSC from the umbilical cord has primary potency and unchanged properties due to its fetus origin [9].

The very important advantage of the WJ-MSCs is their low immunogenicity, which allows the use of those cells not only in autologous but also in allogeneic transplants with

minimal risk of rejection. WJ-MSc is characterized by low protein expression of primary histocompatibility class I (MHC-I) and lack of MHC-II; thus, they are protected against lysis by NK cells [10]. Low immunogenicity is probably also associated with the lack of CD40, CD80, and CD86 as immunologic response costimulants on the surface of cells and simultaneous expression of its inhibitors—indoleamine 2,3-dioxygenase (IDO) and prostaglandin E2. In addition, WJ-MSc expresses human leukocyte antigens HLA-G5 (human leukocyte antigen G5) and HLA-G6, which are involved in the process of fetal tolerance in the mother's uterus by inhibiting lymphocyte proliferation. WJ-MSc does not form teratomas after transplantation into mice with weakened immune systems, and so far, no such cases have been reported in patients whom WJ-MSCs were transplanted [11, 12].

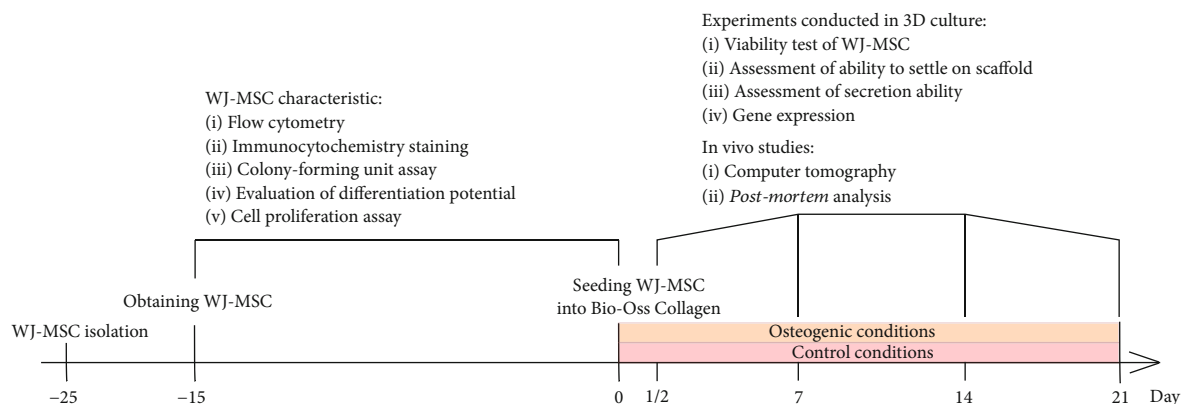
## 2. Materials and Methods

Our experiments were conducted according to Scheme 1.

**2.1. Isolation and Culture of WJ-MSc.** The umbilical cords (UC) were taken from the University Medical Center for Women and the Newborn of the Medical University of Warsaw with consents of mothers and Local Ethical Comity. The UCs were transported in PBS with 100 j/ml penicillin and streptomycin and 0.25 µg/ml amphotericin B. Isolation procedures were performed in less than 24 h after birth. The UCs were sliced into 1-2 mm pieces. 2 mm biopsy pieces were taken from perivascular zone of Wharton's jelly and placed on 6-well cell culture plates. Tissues were cultured in 90% DMEM (Macopharma), 10% platelet lysate (Macopharma), 2 j/ml heparin, 1% (v/v) antibiotics (Gibco), 1% (v/v), and 100 mg/ml glucose in 5% O<sub>2</sub>. Medium was changed every 2-3 days. Cells migrated out from tissue pieces were harvested with Accutase (BD).

**2.2. Flow Cytometry Analysis.** To determine MSC markers, cells were harvested from cell culture flask with Accutase. Cells were stained by mouse anti-human antibodies conjugated with fluorochromes: fluorescein isothiocyanate (FITC), phycoerythrin (PE), peridinin-chlorophyll-cyanine protein complex (PerCP-Cy<sup>™</sup>), or allophycocyanin (APC): CD90-FITC, CD44-PE, CD105-PerCP-Cy<sup>™</sup>, CD73-APC (BD Stemflow<sup>™</sup> hMSC Analysis Kit). Cells were analyzed by a FACSCalibur II (Becton Dickinson).

**2.3. Immunocytochemical Analysis.** Cells were seeded onto coverslips with polylysine in 24-well cell culture plate. Cells were fixed with 4% paraformaldehyde for 10 min, permeabilized with Triton X-100 (Sigma-Aldrich) for 15 min (not apply when stained for CD73 and CD90), and blocked with 10% goat serum (10% donkey serum when stained for osteopontin) with 1% bovine serum albumin (Sigma-Aldrich) for 1 h. Cells were incubated with mouse anti-human primary antibodies CD73, CD90, osteocalcin, goat anti-human osteopontin, and rabbit anti-mouse primary antibodies Ki67 overnight in 4°C (Table 1). Antibodies were washed few times with PBS and secondary antibodies goat anti-mouse/rabbit or for osteopontin donkey anti-goat antibodies were



SCHEME 1: Schematic illustration of the conducted experiments.

TABLE 1: Primary antibodies used for immunocytochemistry.

Primary antibody	Source	Isotype	Dilution	Company
CD73	Mouse monoclonal	IgG3	1 : 200	Dako
CD90	Mouse monoclonal	IgG1	1 : 200	Dako
Ki67	Mouse monoclonal	IgG1	1 : 400	Novocastra
Osteocalcein	Mouse monoclonal	IgG3	1 : 200	Thermo Fisher Scientific
Osteopontin	Goat polyclonal	IgG	1 : 100	Thermo Fisher Scientific

added for 1 h in RT. Cell nuclei were counterstained with Hoechst 33342. Immunocytochemical staining for osteocalcein was performed on freshly isolated cells and 21 days after osteodifferentiation and examined under a fluorescent microscope Zeiss AxioVert.A1. Immunocytochemical staining for osteopontin was performed on cells cultured 21 days on Bio-Oss® Collagen scaffold in osteodifferentiation medium and examined under a confocal microscope Zeiss LSM780.

**2.4. Colony-Forming Unit Assay.** The umbilical cord was cut into half. One part was frozen in 80% PBS, 10% 2 M sucrose, and 10% DMSO. The second one was used for fresh isolation. WJ-MSCs on the 4<sup>th</sup> passage were seeded 10 cells/well on 6-well cell culture plate in duplicates. After 10-12 days, cells were fixed with 4% paraformaldehyde for 15 min and stained with 0.5% solution of toluidine blue for 20 min in RT. Cells were examined under confocal microscope Zeiss LSM780. The number of CFU-F was counted in ZEN 2.3 lite software. After 1-month storage of frozen tissue, the UC was thawed and all steps were conducted as for fresh UC. Experiment was performed in 3 repetitions.

**2.5. Osteogenic, Chondrogenic, and Adipogenic Differentiation of WJ-MSC.** Cells were seeded in a 24-well cell culture plates at a density of  $5 \times 10^3$  cells/cm<sup>2</sup> for osteogenesis and  $1 \times 10^4$  cells/cm<sup>2</sup> for adipogenesis. After reaching 50-60% confluency of WJ-MSC for osteogenesis and 70% confluency for adipogenesis, standard growth medium was replaced by StemPro® Osteogenesis/Adipogenesis Differentiation Kit. For chondrogenesis, 1 µl droplets of  $1.6 \times 10^7$  cells/ml solution were seeded in the centre of the wells, and after 10 min in high-humidity conditions, the StemPro® Chondrogenesis Differ-

entiation Kit was gently added. After 21 days of culture in osteodifferentiation medium, 14 days in adipodifferentiation medium, and 14 days of chondrodifferentiation medium, cells were fixed in 4% paraformaldehyde and stained with Alizarin Red S, Oil Red O, and 1% Alcian Blue solution, respectively. When cells were cultured in differentiation mediums, cell culture plates were transferred into 21% O<sub>2</sub> as recommended by the manufacturer.

**2.6. Cell Proliferation Assay.** WJ-MSCs were seeded 3000 cells/cm<sup>2</sup> in 96-well cell culture plates. Cells were cultured in standard culture medium and in StemPro® Osteogenesis Differentiation Kit for 8 days, 6 wells for each condition, one plate for each day. After  $19.5 \text{ h} \pm 0.5 \text{ h}$ , mediums were changed onto DMEM w/o phenol red with platelet lysate, heparin, glucose, and antibiotics. 10 µl of MTT salt was added into the wells and incubated for 4.5 h. 25 µl of solution was left in the wells and 50 µl of DMSO was added. Absorbance was measured in FLUOstar Omeg (BMG Labtech). Procedure was repeated every day for 8 days. Population doubling time was obtained for each condition according to the following formula:  $(t - t_0) \times \log 2 / (\log N - \log N_0)$  where  $t$  is the day of experiment,  $t_0$  is the initial day of experiment,  $N$  is a number of cells in a particular day, and  $N_0$  is an initial number of cells in  $t_0$ .

**2.7. Seeding Cells into the Scaffold.** Bio-Oss® Collagen was purchased from Geistlich Pharma SA. 100 mg cube was cut into 16 smaller pieces by scalpel. 30 µl of 8,000,000 cells/ml cell solution was injected into the scaffolds. Scaffolds with cells were transferred into 24-well cell culture plates, with a maximum of 3 cubes into 1 well. Bio-Oss® Collagen with WJ-MSC was cultured in standard culture medium and in

StemPro® Osteogenesis Differentiation Kit for 21 days. After 24 h, scaffolds were transferred into new wells.

**2.8. Cell Viability Test on Bio-Oss® Collagen.** Cells were seeded into the scaffolds as mentioned before. Cell viability test was performed on culture in standard culture medium and StemPro® Osteogenesis Differentiation Kit in days 1, 7, 14, and 21. In each time point, scaffolds with cells were stained by ethidium homodimer-1 and calcein AM in DMEM for 20 min in RT. After washing with PBS, scaffolds were examined under confocal microscope Zeiss LSM780 in Z-plane from which 2D pictures were generated.

**2.9. Assessment of the Settlement of WJ-MSC on Bio-Oss® Collagen.** Cells were seeded into the scaffolds according to Seeding Cells into the Scaffold. Assessment was performed in days 1, 7, 14, and 21. For each time point and condition, the scaffold without cells was prepared as a negative control. In each time point, scaffolds were transferred into fixation solution for electron microscopy. Scaffolds were examined under a scanning electron microscope JSM-6390LV (JEOL).

**2.10. WJ-MSC Protein Secretion in 3D Culture.** Cells were seeded into the scaffolds according to Seeding Cells into the Scaffold. There are 3 scaffolds for each time point in each condition. In days 2, 7, 14, and 21, medium was collected from all wells and coupled into one falcon tube for each condition, frozen and stored at -80°C. 24 h before collection, mediums were changed into fresh ones. Standard culture medium and StemPro® Osteogenesis Differentiation Kit were collected as a negative control. Experiment was conducted in 3 repetitions. All mediums were thawed and centrifuged in 500 x g for 5 min. 3 ml of each supernatant was transferred into Spin-X 6 UF concentrators (SIGMA) with cut-off 5 kDa and centrifuged 1800 x g for 15 min. BMP-2, FGF-23, IL-6, osteoprotegerin, RANKL, Dkk-1, IL-1 $\alpha$ , osteopontin, TNF- $\alpha$ , VEGF-D, and TGF- $\beta$ 1 were analyzed in Luminex® assay. All steps were conducted following the manufacturer's instructions. Luminex® plates were read in Luminex BioPlex® 200 System.

**2.11. RNA Isolation and qPCR Analysis.** Cells were seeded into the scaffolds as mentioned before, 3 scaffolds for each time point in each condition. In days 2, 7, 14, and 21, scaffolds were collected and suspended in 400  $\mu$ l of phenosol, frozen and stored at -80°C. Experiment was conducted in 3 repetitions. Total RNA was isolated from scaffolds with Total RNA Mini Plus (A&A Biotechnology), cleaned, and concentrated with Clean-Up RNA Concentrator (A&A Biotechnology) following the manufacturer's instructions. 19 ng of RNA from each probe was reverse-transcribed using RNA-to-cDNA kit (Thermo Fisher) following the manufacturer's instructions. cDNA was preamplified with SsoAdvanced Pre-Amp Supermix following the manufacturer's instructions. 25  $\mu$ l of cDNA was added into 225  $\mu$ l of water for each probe. 5  $\mu$ l of cDNA solution, primers, and a mix from 3color RT HS-PCR Mix Sybr® were used for each qPCR reaction. PCR was performed with specific primers for human *GAPDH*, *B2M*, *RPL13A*, *HPRT1*, *TBP*, *PPIA*, *BGLAP*, *ALPL*, *RUNX2*, *COL1A1*, *VDR*, and *SNAI1*. qPCR conditions are 300 s in

95°C, 40 cycles of 15 s in 95°C, and 60 s in 60°C. The reference gene was determined by geNorm and NormFinder. The reference gene was used: TBP. GeneEx 6.1 software (MultiD Analyses AB, Göteborg, Sweden) was used to analyze the data by the Pfaffl method [13] (the quantification cycle (Cq) values and the baseline settings automatically calculated by the qPCR instrument software) from LightCycler® 96 Software (Roche Diagnostics GmbH, Mannheim, Germany) (Table 2).

**2.12. In Vivo Transplantation.** Four Wistar rats were used in the following experiments. Under anesthesia, 4 trepanation holes (~0.2 cm width) were made in the scalp of each rat. One was left empty, one was filled with Bio-Oss® Collagen, one was filled with Bio-Oss® Collagen with injected cells, one was filled with Bio-Oss® Collagen with injected cells, and additional injection of cell solution was applied on the place of transplantation. Rats were kept for 21 days after surgery.

**2.13. Computed Tomography.** After 7, 14, and 21 days, rats' scalps were examined in computed tomography under the anesthesia. Computed tomography was made with Albira PET/SPECT/CT Preclinical Imaging System (Bruker). In time of each imaging, rats get anesthetized with isoflurane (Baxter Polska Sp. z o.o.) in oxygen applied through a nose cone and respiration was monitored. CT scan parameters were set as follows: tube voltage was 45 kVp, tube current was 400  $\mu$ A, and number of projections was 1000. Minimal resolution of CT was 90  $\mu$ m. 3D reconstruction of scalps was made, and comparison of bone regeneration between time points was done in PMOD software, version 3.307, module View Tool [PBAS] (PMOD Technologies LLC). All procedures made on animals were approved by the First Local Ethical Committee of the Warsaw University Biology Department (Permission No. 560/2018).

**2.14. Postmortem Analysis.** After rats were sacrificed, cranial vaults were isolated and submerged into 2 j/ml of collagenase for 2 h in 37°C with shaking. Soft tissues were removed from the scalps and pictures were made with binocular with camera.

**2.15. Statistics.** Statistical analysis of the raw data was conducted using GraphPad Prism 5 software. The Kolmogorov-Smirnov test was used as a normality test. The Student *t*-test for a pair of group or one-way ANOVA followed by Tukey's multiple comparison test for comparison inside the group was used: \**p* < 0.05, \*\**p* < 0.01, \*\*\**p* < 0.001, and \*\*\*\**p* < 0.0001. Results represent three independent experiments, each in at least four replicates. Results presented at the graphs were shown as mean with standard.

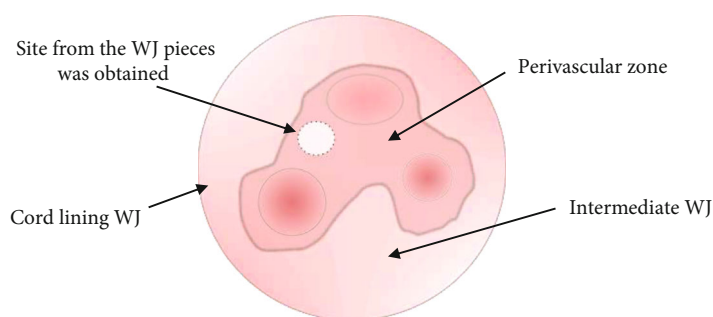
### 3. Results

**3.1. Isolation Efficiency and WJ-MSC Characteristic.** WJ-MSCs were isolated from fresh and frozen UC tissue from Wharton's jelly obtained from perivascular zone (Scheme 2).

Cells migrated out from tissue pieces showed typical fibroblast-like morphology (Figure 1(a)). Difference in efficiency of isolation between fresh and frozen UC was observed but did not affect ability to isolate WJ-MSC

TABLE 2

Gene symbol	Gene name	NCBI reference gene	Primer sequence	Product length	Product efficiency E (%)
<i>GAPDH</i>	Glyceraldehyde-3-phosphate dehydrogenase	NM_001289745.2	F: GGTGTGAACCATGAGAAGTATGA R: GAGTCCTTCCACGATACCAAAG	123	1.91
<i>B2M</i>	Beta-2-microglobulin	XM_005254549.3	F: CCAGCGTACTCCAAAGATTCA R: TGGATGAAACCCAGACACATAG	94	1.85
<i>RPL13A</i>	Ribosomal protein L13a	NM_001270491.1	F: CGAGAAGAACGTGGAGAAGAAA R: GGCAACGCATGAGGAATTAAC	105	1.92
<i>HPRT1</i>	Hypoxanthine phosphoribosyltransferase 1	NM_000194.2	F: CGAGATGTGATGAAGGAGATGG R: TTGATGTAATCCAGCAGGTCAG	98	2.22
<i>TBP</i>	TATA-box binding protein	NM_003194.4	F: TCTTGGCGTGTGAAGATAACC R: GCTGGAACCTCGTCTCACTATTC	100	1.87
<i>PPIA</i>	Peptidylprolyl isomerase A	XM_024446809.1	F: GGTCCCAAAGACAGCAGAAA R: GTCACCACCCTGACACATAAA	115	1.87
<i>BGLAP</i>	Bone gamma-carboxyglutamate protein	NM_199173.5	F: AAATAGCCCTGGCAGATTCC R: CAGCCTCCAGCACTGTTTAT	105	1.96
<i>ALPL</i>	Alkaline phosphatase	XM_006710546.3	F: GGAGTATGAGAGTGACGAGAAAAG R: GAAGTGGGAGTGCTTGTATCT	103	—
<i>RUNX2</i>	Runt-related transcription factor 2	NM_001278478.1	F: TGTCATGGCGGGTAACGAT R: AAGACGGTTATGGTCAAGGTGAA	147	1.95
<i>COL1A1</i>	Collagen type I alpha 1 chain	XM_005257058.4	F: GAGGGCCAAGACGAAGACATC R: CAGATCACGTCATCGCACAAAC	140	1.92
<i>VDR</i>	Vitamin D receptor	NM_001017536.1	F: TCTCCTGCCTACTCAGATAA R: GCTACTGCCCGTGAGAATATAA	105	—
<i>SNAI1</i>	Snail family transcriptional repressor 1	NM_005985.3	F: CCACGAGGTGTGACTAACTATG R: ACCAAACAGGAGGCTGAAATA	126	—



SCHEME 2: Cross section of the umbilical cord with a marked site from the Wharton's jelly (WJ) pieces was obtained.

(Figure 1(b)). WJ-MSCs were able to form CFU-F from a single cell. In average, 40% of cells were capable of clonogenicity from fresh and frozen isolation (Figure 1(c)).

Flow cytometry analysis showed around 97% of isolated cells with expression of CD73, CD90, and CD105 with lack of CD45, CD34, CD19, and CD11b markers (Figures 2(a)–2(c)).

Immunocytochemical staining showed CD73 and CD90 expressions in WJ-MSC. In few cells, osteocalcin was observed in undifferentiated cells but not the osteopontin. After osteodifferentiation, WJ-MSC expressed in  $89.6 \pm 7\%$  osteocalcin. In undifferentiated cells, great number of Ki67 expression was observed (Figure 3).

WJ-MSCs differentiated into adipocytes, chondrocytes, and osteocytes which was confirmed by positive staining for Oil Red O, Alcian Blue, and Alizarin Red, respectively (Figure 4).

There was no noticeable difference in doubling time of WJ-MSC from day 1 to day 8 for cells in standard culture medium and in osteodifferentiation medium which was approximately 30 h (Figure 5).

**3.2. Cell Viability Test and Assessment of the Settlement of WJ-MSC on Bio-Oss® Collagen.** On the first day in both conditions, viability of the cells on Bio-Oss® Collagen was

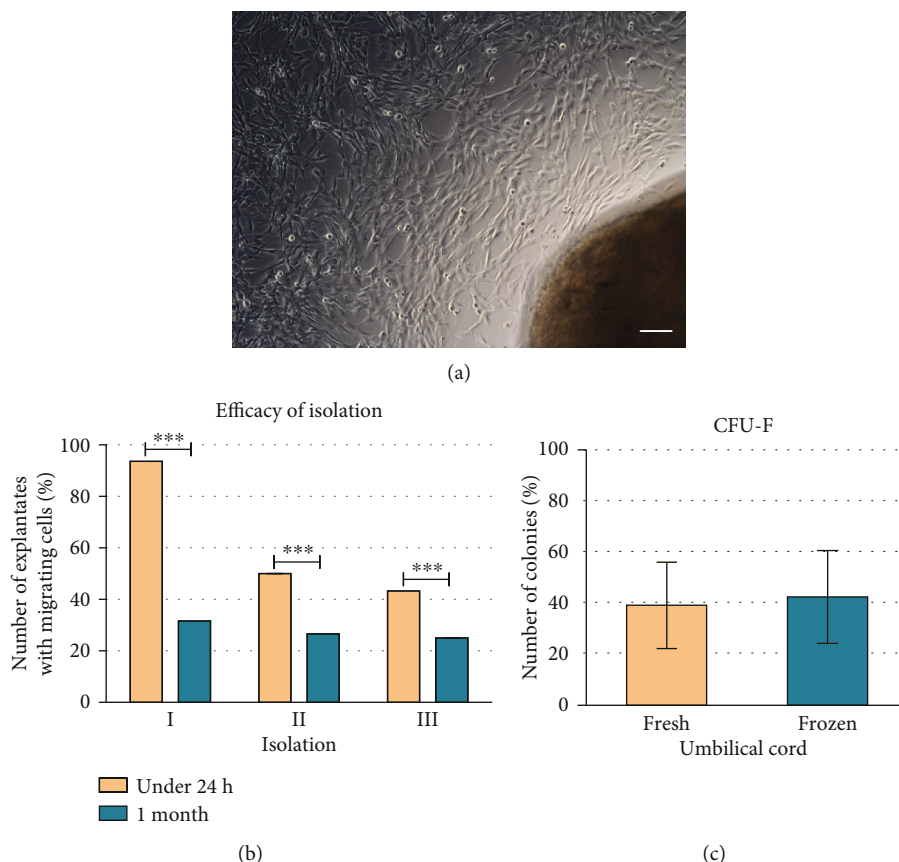


FIGURE 1: Picture from light microscopy of WJ-MSC migrated from Wharton's jelly explantate after 10 days in culture (a). Size of scale bar: 100  $\mu$ m. Number of explantates with migrating cells after isolation from the fresh and frozen umbilical cord in three repetitions (b). Number of colonies formed from single cells when 10 cells were seeded on a 6-well dish from cells derived from Wharton's jelly from the fresh and frozen umbilical cord (c).

comparable, but in osteodifferentiation, medium cells had fibroblast-like morphology. On the 7<sup>th</sup> day, viability of cells was similar in both conditions. In osteodifferentiation, medium cells become shorter and wider and approximately whole surface of the scaffold was covered by a layer of cells compared to few cells attached to scaffold in control conditions. Boundaries between cells in osteodifferentiation conditions are blurred making hard to distinguish separate cells. Until the end of experiments, similar observations were noticed with even a greater reduction of the number of cells in control condition and more osteoblast-like morphologies in osteodifferentiation condition (Figure 6).

Immunocytochemical staining of WJ-MSC cultured on Bio-Oss® Collagen showed osteopontin expression in those cells (Figure 7). WJ-MSC expressed osteopontin in  $47.3 \pm 13\%$ .

**3.3. Protein Secretion in 3D Culture.** WJ-MSC secretes cytokines which are crucial during bone regeneration process (Scheme 3). From days 2 to 21 in osteodifferentiation medium, increase in protein concentration of BMP2 secreted by seeded cells can be observed. In control medium, this tendency does not occur. Similar changes in protein concentration were observed for FGF-23 which level increased until day 7<sup>th</sup> when reached plateau only in osteodifferentiation medium.

For VEGF in control medium, protein amount decreases from the 2<sup>nd</sup> day to the 14<sup>th</sup> day. Reverse results can be observed in differentiation medium where from the 2<sup>nd</sup> day to the 7<sup>th</sup> day, concentration increases and holds that level until the end of the experiment.

In control conditions, osteopontin concentration increased in the 2<sup>nd</sup> day followed by decrease of protein level through next time points, whereas in osteodifferentiation medium, constant increase in protein amount was noticed from the beginning until the end of the experiment.

Osteoprotegerin concentration slightly increased in control condition through a time, but in differentiation medium, great increase can be observed from the 7<sup>th</sup> day and its stable secretion until the 21<sup>st</sup> day.

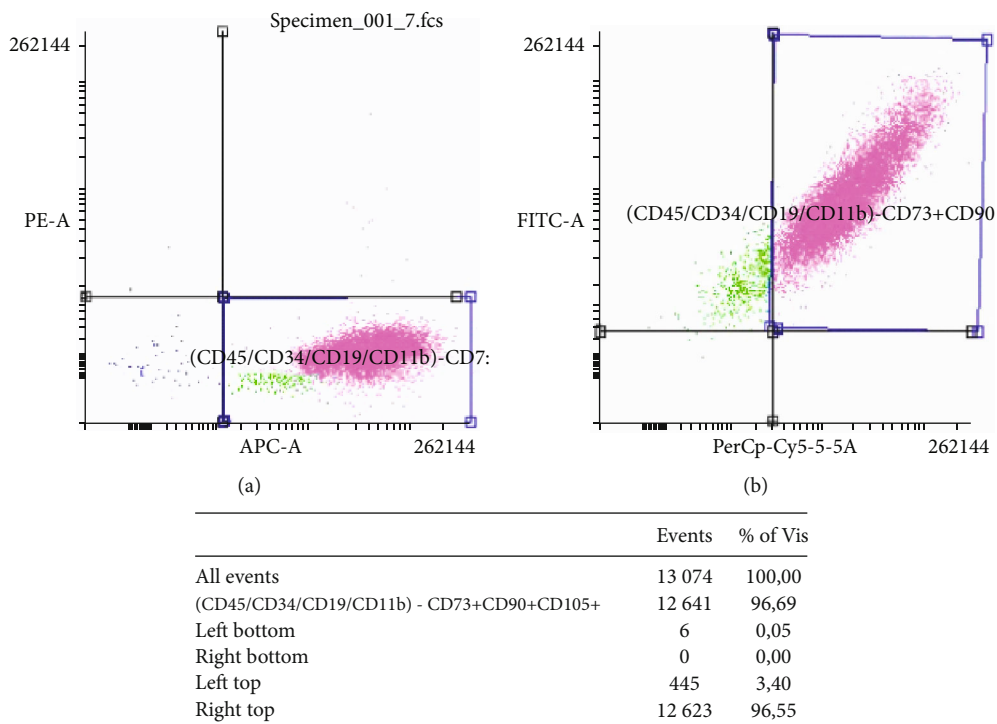
In control conditions, a slight decrease of RANKL level can be observed from days 2 to 21, whereas in osteodifferentiation medium, a 2.5-fold increase is observed in day 7 and this level is stable until the end of experiment.

In both conditions, tendency to increased secretion of TGF- $\beta$ 1 from days 2 to 21 can be observed.

In both conditions, in day 2, great amounts of IL-6 were secreted and in the next day level, this protein drastically dropped.

Through 21 days of experiments in control conditions, secretion of Dkk-1 is almost not observed compared to a





(c)

FIGURE 2: Flow cytometry analysis. Representative gating for CD45/CD34/CD19/CD11b-negative and CD73-positive markers (a) and for CD90- and CD105-positive markers (b). Table with results obtained from flow cytometry (c).

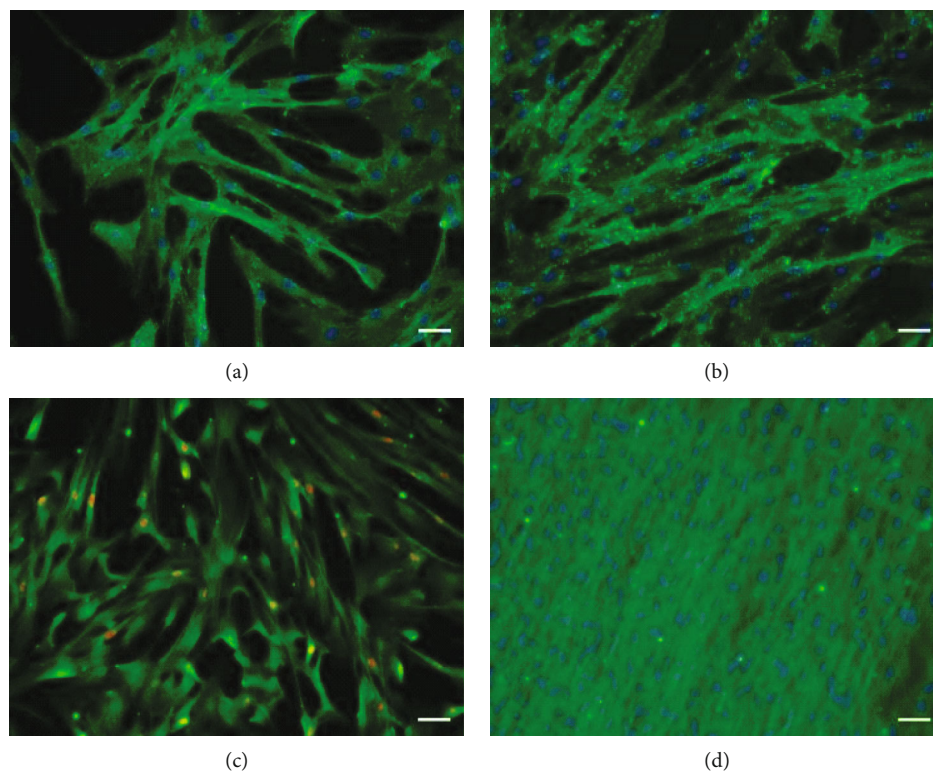


FIGURE 3: Immunocytochemistry staining of WJ-MSC. CD73 (green; a), CD90 (green; b), osteocalcin (green; c, d), and Ki67 staining (red; c). (a, b, d) Nuclei were counterstained with Hoechst 33342. Size of scale bar: 50  $\mu$ m.

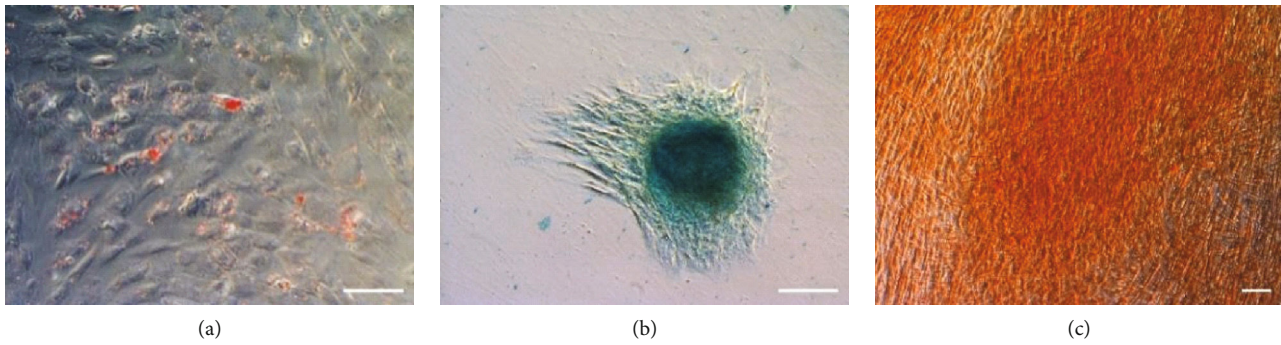


FIGURE 4: Evaluation of differentiation potential of WJ-MSC. WJ-MSC differentiated into adipocytes (a), chondrocytes (b), and osteocytes (c). Cell cultures were stained with Oil Red O, Alcian Blue, and Alizarin Red S, respectively. Size of scale bar: 100  $\mu\text{m}$ .

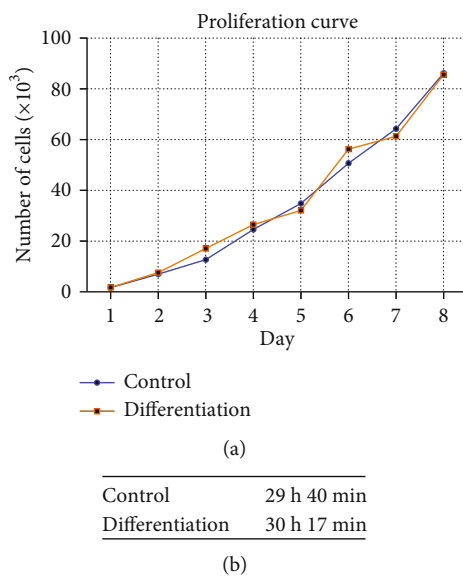


FIGURE 5: Cell proliferation analysis. Graph represents the proliferation curve for cells cultured in control medium and cultured in osteodifferentiation medium during 8 days of culture (a). Mean of the doubling time is written in the table for control and for differentiation conditions (b). Doubling time was calculated based on the following equation:  $(t - t_0) \times \log 2 / (\log N - \log N_0)$ .

great amount and its tendency to increasement of protein level in osteodifferentiation medium until the last day.

Concentration of IL-1 and TNF- $\alpha$  in control conditions decreased from day 2. In osteodifferentiation conditions, reverse tendency can be observed and until day 7 increasement of protein level can be observed and then secretion of those protein stabilizes on certain level until the end of experiment (Figure 8).

**3.4. Gene Expression (qPCR).** After analysis of 6 reference genes, the two most stable genes were chosen by geNorm software—TATA binding protein (*TBP*) and peptidylprolyl isomerase A (*PPIA*) and one gene chosen by NormFinder software—*TBP* (Figure 9). For the next analysis, *TBP* gene was used as a reference gene.

After procedures of RNA isolation from WJ-MSC cultured on Bio-Oss® Collagen in standard culture medium,

there was shortage of material needed for qPCR. Due to that, comparison of gene expression in material from WJ-MSC cultured in 2D in standard culture medium was used. A 7-fold increase of *BGLAP* and a 5-fold increase of *ALPL* expression were observed from day 2 to day 21. A 6-fold decrease of *COL1A1* expression was observed in day 2 and 8-fold from days 7 to 21. On the day 2 of experiment, a 3-fold increase in expression was observed for *SNAIL1*; on days 7 and 14, expression dropped to a 1-fold increase compared to control; on day 21, expression increased again to 2-fold. *VDR* expression elevated 10-folds from day 2 to day 21. Expression of *RUNX2* slightly decreased, approximately 1-fold during 21 days of experiment (Figure 10).

Computed tomography scans on days 7, 14, and 21 show a lack of regeneration in place of empty hole after trepanation (Figure 11). In case of trepanations, scans on holes filled with scaffolds show radiological regeneration. Up to 21 days, there is no difference between variants of injected cells.

After scalp incubation in collagenase solution and removal of soft tissues with gauze, scaffold without cells fell out from the hole. Scaffolds in which cells were injected show connection with bone tissue of the scalp (Figure 12).

## 4. Discussion

Wharton jelly (umbilical cord stroma) due to its fully noninvasive collection and high availability might be the most convenient source of MSC (WJ-MSC) for future clinical therapy. The advantage of cells isolated from the after-birthing is their early developmental stage, which makes them less differentiated, with higher proliferative potential than somatic MSC and with higher clonogenic abilities and a slower aging rate. Moreover, WJ-MSC shows negligible immunogenicity. This is due to the very low expression of MHC class I antigens (HLA-ABC) and the lack of MHC class II antigens (HLA-DR) and costimulatory antigens such as CD80 and CD86 involved in the activation of both T lymphocyte responses and B lymphocytes. Considering both the availability and the ability to administer cells in an allogeneic system, it seems that WJ-MSC might be the better source for clinical use than bone marrow-derived MSC. In order to obtain the largest possible amount of WJ-MSC with high proliferative and clonogenic potential and good survival, we have developed

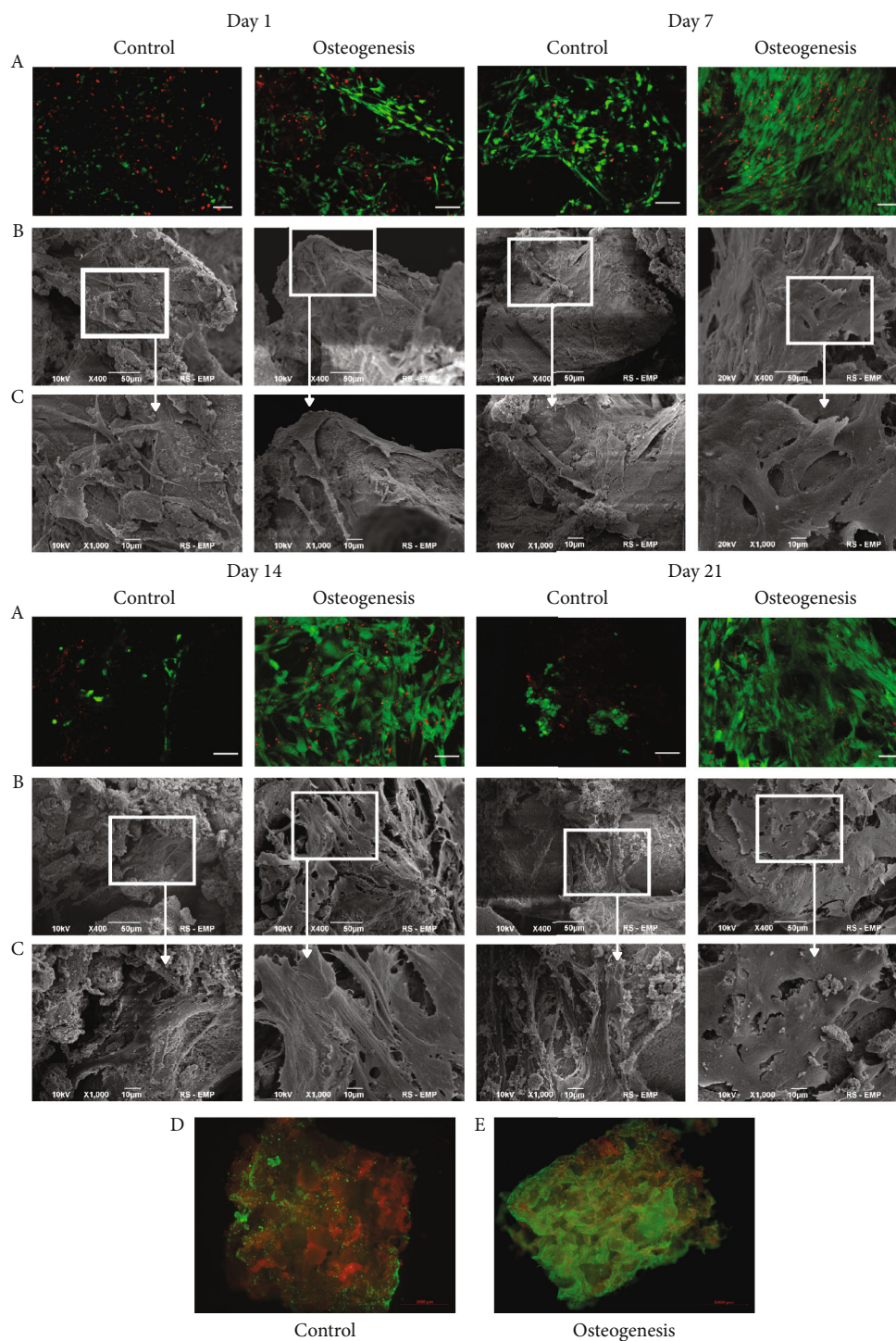


FIGURE 6: WJ-MSC on the Bio-Oss® Collagen scaffold cultured in control medium and osteodifferentiation medium. Pictures from a confocal microscope (a)—cells were stained with calcein AM (alive cells—green staining) and ethidium homodimer (dead cells—red staining). Pictures from an electron microscope (b, c). Scale bar in (a) row: 100  $\mu\text{m}$ . Image of the entire scaffold cultured with WJ-MSC in control (d) and osteodifferentiation (e) medium (green—calcein AM; red—ethidium homodimer). Scale bar: 1000  $\mu\text{m}$

a protocol for isolation from specific regions of umbilical cord. Similarly to Subramanian group [14], we isolate cells with mechanical technique from the perivascular region. The best results were obtained using biopunch with 2 mm diameter.

Technique used in our laboratory for WJ-MSC isolation gives high yield of cells with their good quality. CFU-F of isolated cell population reach up to 40% which is a positive result compared to 10-30% MSC population reported by other scientists [2, 9, 15]. Wharton's jelly isolated with our

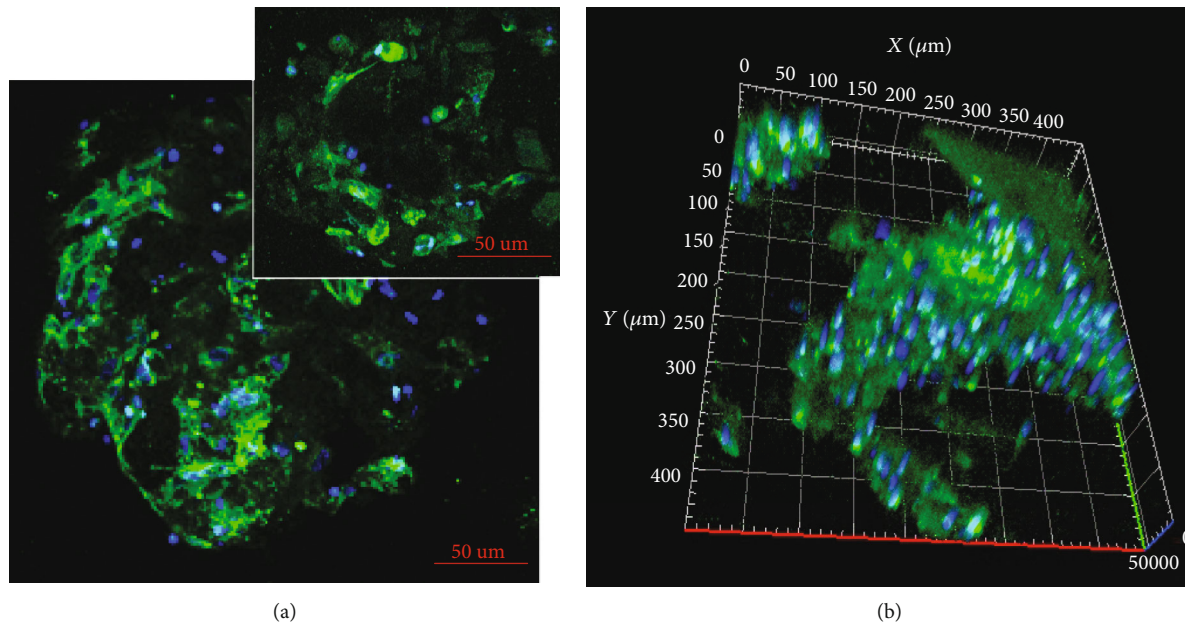
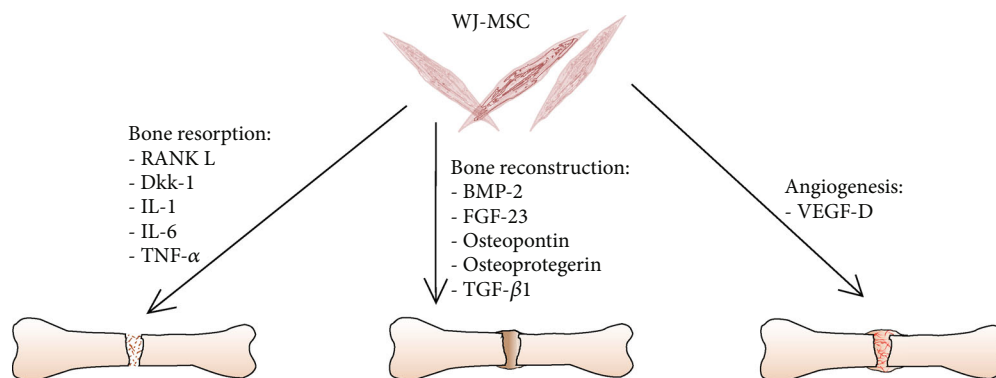


FIGURE 7: The immunocytochemical analysis of osteopontin (green) expression in WJ-MSC cultured on the Bio-Oss® Collagen scaffold after osteodifferentiation. (a) Confocal imaging shows osteopontin expression in single cells; specific staining was localized to the cytoplasm. (b) 3D cross-sectional image illustrates the distribution of WJ-MSC expressing osteopontin inside the skeleton. The nuclei were stained with Hoechst (blue). Scale bar: 50  $\mu\text{m}$ .



SCHEME 3: Schematic illustration of cytokines involved in the process of bone regeneration secreted by WJ-MSC.

method can be frozen without reduction of the MSC population after isolation what contradicts Chatzistamatiou who states that efficient isolation of MSC from umbilical cord is possible only from fresh tissue [16].

To date, MSC isolated from the bone marrow have been the most commonly used in orthopedic surgery. In our previous papers [8], we compared BM-MSC and WJ-MSC underlying some properties of WJ-MSC unique only for this fraction. WJ-MSC preferentially differ into mesodermal cell lineages as Chen and Avercenc-L  ger show in their works ([17, 18]), but its differentiation potency is not limited only to one germ layer. WJ-MSC can also differentiate toward cell lineages from ectoderm and endoderm germ layer which was proven by Maher Atari and our team ([19–21]). Thus, plasticity of those cells shows their high therapeutic potential.

For bone reconstruction, transplanted cells must possess the ability to differentiate toward osteoblasts (OB). From the

literature, there is known that these cells are recruited during remodeling from host stem/stromal mesenchymal cells. In some clinical situations, the number of host precursors is insufficient that is why human MSCs are now being introduced into the clinic.

MSCs play multidirectional function. In addition to osteoblast differentiation, MSC supports osteoclast development. Osteoclast development requires cell-to-cell contact between osteoclast progenitors which come from hematopoietic cells. Osteopontin seems to be the factor that plays a key role in this process. Osteopontin is expressed during the early stage of the differentiation of osteoblast and osteoclast progenitors and its cell adhesion properties are important for osteoclastogenesis. It is responsible for attachment of cells to matrix substances or other cells facilitating the interactions. Yamate et al. [22] described antiosteopontin antibody or RGD-containing peptide inhibits that process, whereas

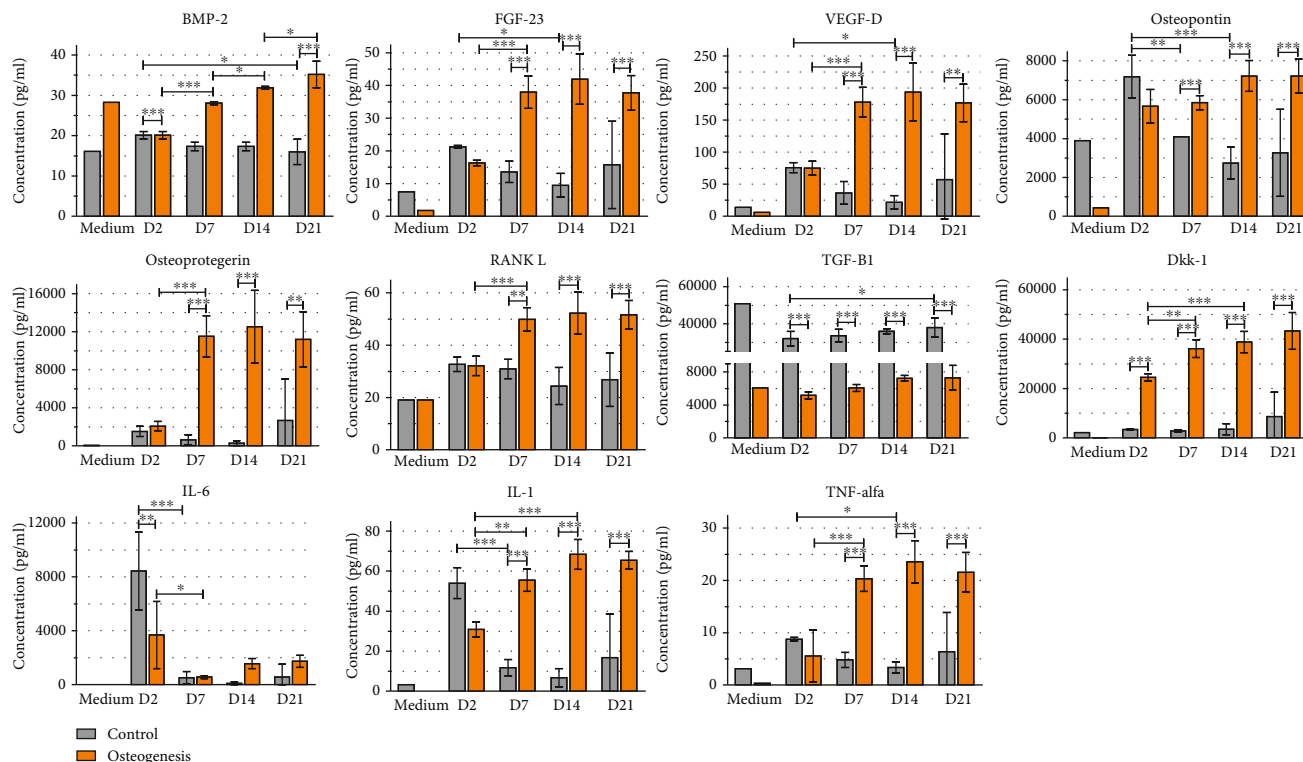


FIGURE 8: Luminex analysis of protein secretion produced by WJ-MSC cultured in control medium and osteodifferentiation medium in days 2, 7, 14, and 21 cultured on 3D scaffolds. “Medium” bars represent the basic level of proteins in the medium.

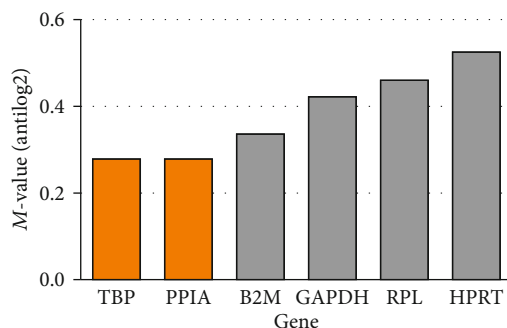


FIGURE 9: Analysis of reference genes for WJ-MSC by geNorm software.

freshly isolated WJ-MSCs secrete osteopontin but the secretion significantly declines during cell culture; in differentiating conditions, its level is constantly increasing.

Moreover, osteopontin is thought to potentiate the secretive potential of MSC that in turn promote proliferation and differentiation of the hematopoietic precursors.

WJ-MSC isolated and cultured in described conditions can similar to BM-MSC contribute to bone regeneration directly by differentiation into osteoblast-like cells, and indirectly by stimulation of maturation of osteoblasts and osteoclasts as well as the activation of angiogenesis by secretion of VEGF-D.

Bone reconstruction takes place in several stages with different crucial factors (Scheme 3). The first stage concerns a resorption of the bone. During this stage, secretion of

Dkk-1, IL-6, IL-1, and TNF- $\alpha$  increases what is a booster for osteoclastogenesis [23, 24]. In the next stage of regeneration, formation of the new bone takes place. BMP-2 accumulated in ECM [25] counteract with osteoblasts receptors which induce bone formation. During our experiments, secretion of BMP-2 increased. Similar tendency was observed for FGF-23, a protein which maintains homeostasis of ions and mineralization of the bone [26]. During 3D culture, cells were adherent to the scaffold, alive, and capable of migration. Those features were correlated with the increase of osteopontin secretion which also contributes to bone remodelling, stress response, and repair ([27]). Resorption and formation of the new bone have to be balanced. It is maintaining by osteoprotegerin (OPG) and RANKL. OPG is a competitive inhibitor of RANKL which is responsible for osteoclast maturation and bone resorption, appropriate ratio between OPG and RANKL which is necessary for maintaining proper bone volume [28, 29]. Both protein levels increased during experiments. For correct bone regeneration, a simultaneous angiogenesis is required. The supply of nutrients to cells that settle a damaged tissue fragment is critical to the bone regeneration process [30]. VEGF-D, which stimulates the proliferation and migration of endothelial cells, belongs to important proangiogenic factors. Despite the observations described by the Amable group, which found that WJ-MSCs do not secrete VEGF [31], during our experiments, we observed a significant increase in VEGF-D level in the differentiating medium from days 2 to 7 and maintaining this level until day 21. In line with my observations, the proangiogenic properties of WJ-MSC have also been described by

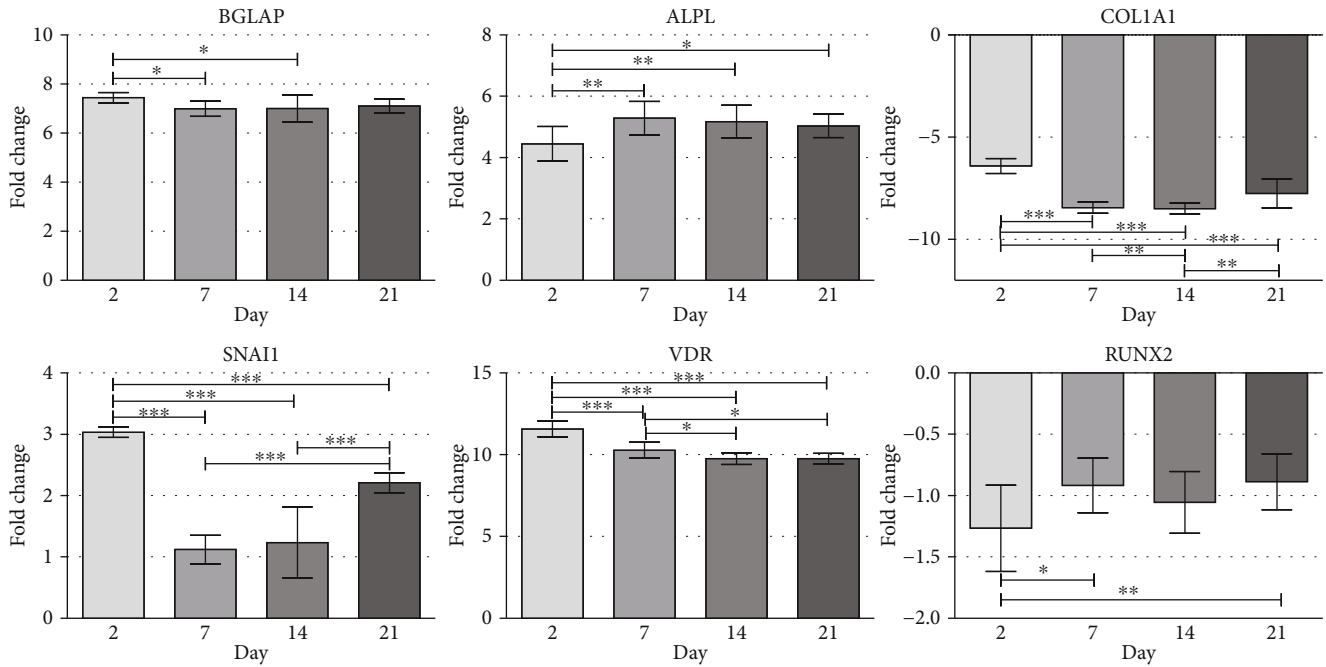


FIGURE 10: Canonical gene expression of BGLAP, ALPL, RUNX2, VDR, SNAI1, and COL1A1 during osteoblast differentiation of WJ-MSC cultured on scaffolds in osteodifferentiation medium obtained by the  $2^{-\Delta\Delta Ct}$  method. The y-axis of each plot represents gene expression fold change, relative to day 0 (nondifferentiated cells). The x-axis represents the time point post-OB induction (day 2, day 7, day 14, and day 21). Error bars represent the standard error of the mean, and measurements are based on 3 replicates.

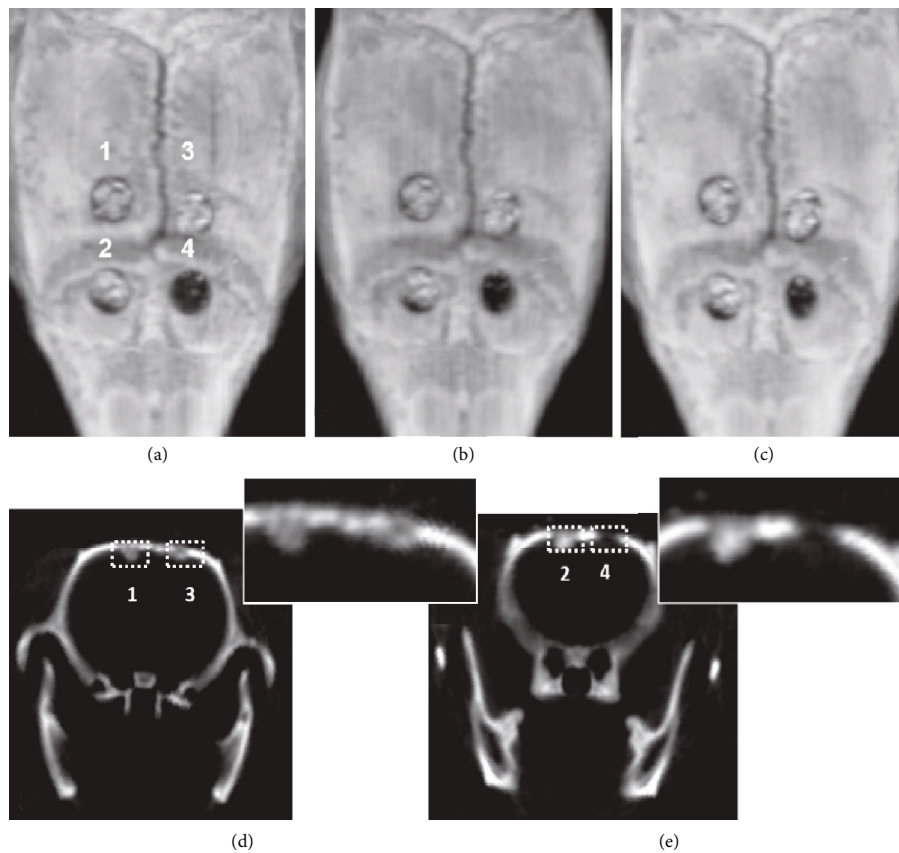


FIGURE 11: Computed tomography images of the rat scalp. (a–c) Transversal sections: 7 (a), 14 (b), and 21 (c) days after scaffold transplantation. 1—Bio-Oss® with injected WJ-MSC into and onto the scaffold; 2—Bio-Oss® with injected WJ-MSC; 3—Bio-Oss; 4—empty hole after trepanation ( $n = 4$ ). (d, e) Cross-coronal sections.

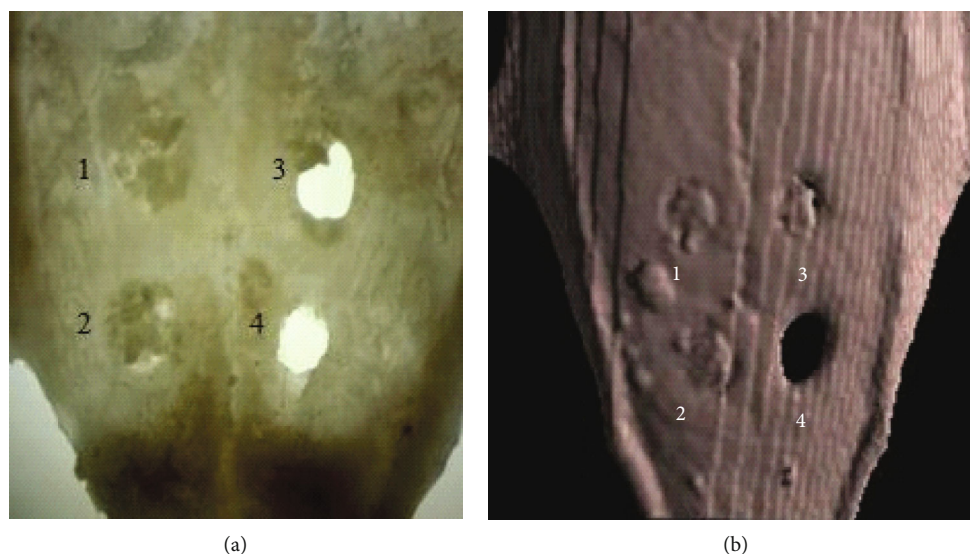


FIGURE 12: Cranial vaults of the rat skull after removal of soft tissues. 1—Bio-Oss® with injected WJ-MSC into and onto the scaffold; 2—Bio-Oss® with injected WJ-MSC; 3—Bio-Oss® alone; 4—empty hole after trepanation. (a) Light binocular. (b) Computed tomography.

Obtulowicz et al. and Widowati et al. [21, 32]. It can therefore be assumed that WJ-MSCs by stimulating VEGF-D production promote formation of new blood vessels and thus support and accelerate the regeneration of tissue (Scheme 3).

In the case of extensive defects in bone tissue, the use of cell therapy alone does not bring the expected results due to the lack of scaffolding needed to cell growth and tissue regeneration could occur. It is necessary to apply a combination therapy using bone graft material along with cells that will accelerate the regeneration of the structure and support the linking of the introduced material with the patient's bone through the above secretory, inductive, and differentiation properties of mesenchymal stem cells [33]. Numerous works have shown that the appropriately selected material from which the 3D skeleton is created may, due to its biophysical properties, e.g., elasticity, shape, or porosity, influence the differentiation of mesenchymal cells [34–36]. Unfortunately, sometimes the biochemical composition of such materials despite meeting the topographic conditions may prevent proper cell survival, adhesion, and differentiation. Some of the materials tested cannot be used for clinic; the others are not biodegradable. That is why research on selection of the optimal skeletons for the regeneration is still ongoing.

In our *in vitro* studies, we have shown that WJ-MSCs are able to colonize the Bio-Oss® Collagen scaffold, and the resulting construct is characterized by high cell survival and allows the formation of complex osteoblastic structures with a characteristic disappearance of the boundaries between individual cells. Moreover, MSC seeded into the scaffold and cultured in osteo medium secreted crucial for osteoblast and osteoclast differentiation.

Observation in the natural environment *in vivo* is necessary to confirm the ability to integrate and differentiate MSCs toward osteoblast-like cells. In our experience, *in vivo* examinations carried out using the rat model, we demonstrated presence of Bio-Oss® Collagen scaffold seeded with alive

WJ-MSC 21 days after transplantation. In order to verify the complete integration of the bone substitute with the bone tissue of the rat, a similar observation would have to be made several months after the transplantation [37]. However, despite such a short time, after postmortem examination, it can be concluded that the scaffolds with injected cells have become more integrated with the skull bones than the empty skeleton alone, which may result from the formation of cartilage, impossible to visualize in computed tomography. Similar results were described for maxillary sinus elevation with different bone substitutes and BMSCs [38], although the low survival rate of grafted BMSCs was reported, which resulted from acute inflammation and mechanical damage [39] and indisposed to use the therapy in a clinic.

## 5. Conclusions

The reconstruction of the bone defects is a procedure that requires materials other than the mandible, long bones, or skull. By applying computed tomography, the shape of the defect can be clearly visualized. However, still the border between the graft and the patient's bone should be defaced. For this purpose, the used material must be elastic, easy to remodel, and flexible during surgery. The addition of 10% collagen in Bio-Oss® Collagen scaffold makes it formable and easy to handle. Moreover, it favours the cells to attach to the scaffold and leads to better survival and differentiation. According to our observations, the skeleton can be placed and fitted to the defect-like plasticine and then injected with cells. This will not disturb cell colonization or reduce cell survival. Thanks to the appropriate porosity, the cells will create inside local niches. On the other hand, we proved that WJ-MSC might be the optimal cell source for reconstructive therapy in clinic. They possess the same capacity for osteogenesis and secretion of factors necessary for bone formation as other MSCs, and at the same time, they are less immunogenic, which allows even allogeneic transplantation. In addition, they are

more readily available and, with the appropriate isolation and culture method, their potential for survival and proliferation is very high. Presented in the manuscript graft consisted of clinically used scaffold, and the nature of WJ-MSC has a chance to be immediately used in a clinic in the reconstruction of bone defects.

## Data Availability

The data from presented study are available from the corresponding author upon request.

## Conflicts of Interest

The authors declare that there is no competing financial interest or conflict of interest regarding the publication of this paper.

## Acknowledgments

The studies were performed in the Electron Microscopy Platform, Mossakowski Medical Research Centre Polish Academy of Sciences, Warsaw, Poland, transmission electron microscope model JEM-1011 (JEOL) equipped with a model EDS INCA (Oxford) analyzer. This work was partially supported by the National Centre for Research and Development (Grant no. Strategmed 1/234261/2/NCBR/2014).

## References

- [1] A. Oryan, A. Kamali, A. Moshiri, and M. Baghaban Eslaminejad, "Role of mesenchymal stem cells in bone regenerative medicine: what is the evidence?," *Cells Tissues Organs*, vol. 204, no. 2, pp. 59–83, 2017.
- [2] Q. Wang, Q. Yang, Z. Wang et al., "Comparative analysis of human mesenchymal stem cells from fetal-bone marrow, adipose tissue, and Wharton's jelly as sources of cell immunomodulatory therapy," *Human Vaccines & Immunotherapeutics*, vol. 12, no. 1, pp. 85–96, 2016.
- [3] D. J. Eve, P. R. Sanberg, L. Buzanska, A. Sarnowska, and K. Domanska-Janik, "Human somatic stem cell neural differentiation potential," in *Human Neural Stem Cells: From Generation to Differentiation and Application*, L. Buzanska, Ed., pp. 21–87, Results and Problems in Cell Differentiation. Springer International Publishing, Cham, 2018.
- [4] Y. Xu, S. Huang, K. Ma, X. Fu, W. Han, and Z. Sheng, "Promising new potential for mesenchymal stem cells derived from human umbilical cord Wharton's jelly: sweat gland cell-like differentiative capacity," *Journal of Tissue Engineering and Regenerative Medicine*, vol. 6, no. 8, pp. 645–654, 2012.
- [5] Y. Kuroda, M. Kitada, S. Wakao, and M. Dezawa, "Mesenchymal stem cells and umbilical cord as sources for Schwann cell differentiation: their potential in peripheral nerve repair," *The Open Tissue Engineering and Regenerative Medicine Journal*, vol. 4, no. 1, pp. 54–63, 2011.
- [6] J. Peng, Y. Wang, L. Zhang et al., "Human umbilical cord Wharton's jelly-derived mesenchymal stem cells differentiate into a Schwann-cell phenotype and promote neurite outgrowth *in vitro*," *Brain Research Bulletin*, vol. 84, no. 3, pp. 235–243, 2011.
- [7] L.-F. Wu, N.-N. Wang, Y.-S. Liu, and X. Wei, "Differentiation of Wharton's jelly primitive stromal cells into insulin-producing cells in comparison with bone marrow mesenchymal stem cells," *Tissue Engineering Part A*, vol. 15, no. 10, pp. 2865–2873, 2009.
- [8] K. Drela, W. Lech, A. Figiel-Dabrowska et al., "Enhanced neuro-therapeutic potential of Wharton's jelly-derived mesenchymal stem cells in comparison with bone marrow mesenchymal stem cells culture," *Cytotherapy*, vol. 18, no. 4, pp. 497–509, 2016.
- [9] W. Lech, A. Figiel-Dabrowska, A. Sarnowska et al., "Phenotypic, functional, and safety control at preimplantation phase of MSC-based therapy," *Stem Cells International*, vol. 2016, 2016.
- [10] I. Kalaszczynska and K. Ferdyn, "Wharton's jelly derived mesenchymal stem cells: future of regenerative medicine? Recent findings and clinical significance," *BioMed Research International*, vol. 2015, Article ID 430847, 11 pages, 2015.
- [11] D.-C. Ding, Y.-H. Chang, W.-C. Shyu, and S.-Z. Lin, "Human umbilical cord mesenchymal stem cells: a new era for stem cell therapy," *Cell Transplantation*, vol. 24, no. 3, pp. 339–347, 2015.
- [12] J. Prasanna and S. Jahnavi, "Wharton's jelly mesenchymal stem cells as off-the-shelf cellular therapeutics: a closer look into their regenerative and immunomodulatory properties," *The Open Tissue Engineering and Regenerative Medicine Journal*, vol. 4, no. 1, pp. 28–38, 2011.
- [13] M. W. Pfaffl, "A new mathematical model for relative quantification in real-time RT-PCR," *Nucleic Acids Research*, vol. 29, no. 9, 2001.
- [14] A. Subramanian, C.-Y. Fong, A. Biswas, and A. Bongso, "Comparative characterization of cells from the various compartments of the human umbilical cord shows that the Wharton's jelly compartment provides the best source of clinically utilizable mesenchymal stem cells," *PLoS One*, vol. 10, no. 6, 2015.
- [15] U. Nekanti, L. Mohanty, P. Venugopal, S. Balasubramanian, S. Totey, and M. Ta, "Optimization and scale-up of Wharton's jelly-derived mesenchymal stem cells for clinical applications," *Stem Cell Research*, vol. 5, no. 3, pp. 244–254, 2010.
- [16] T. K. Chatzistamatiou, A. C. Papassavas, E. Michalopoulos et al., "Optimizing isolation culture and freezing methods to preserve Wharton's jelly's mesenchymal stem cell (MSC) properties: an MSC banking protocol validation for the Hellenic Cord Blood Bank," *Transfusion*, vol. 54, no. 12, pp. 3108–3120, 2014.
- [17] L. Avercenc-Léger, P. Guerci, J.-M. Virion et al., "Umbilical cord-derived mesenchymal stromal cells: predictive obstetric factors for cell proliferation and chondrogenic differentiation," *Stem Cell Research & Therapy*, vol. 8, no. 1, pp. 1–13, 2017.
- [18] M.-Y. Chen, P.-C. Lie, Z.-L. Li, and X. Wei, "Endothelial differentiation of Wharton's jelly-derived mesenchymal stem cells in comparison with bone marrow-derived mesenchymal stem cells," *Experimental Hematology*, vol. 37, no. 5, pp. 629–640, 2009.
- [19] A. Al Madhoun, H. Ali, S. AlKandari et al., "Defined three-dimensional culture conditions mediate efficient induction of definitive endoderm lineage from human umbilical cord Wharton's jelly mesenchymal stem cells," *Stem Cell Research & Therapy*, vol. 7, no. 1, 2016.
- [20] K. Drela, A. Sarnowska, P. Siedlecka et al., "Low oxygen atmosphere facilitates proliferation and maintains undifferentiated state of umbilical cord mesenchymal stem cells in an hypoxia



- inducible factor-dependent manner,” *Cytotherapy*, vol. 16, no. 7, pp. 881–892, 2014.
- [21] P. Obtulowicz, W. Lech, L. Strojek, A. Sarnowska, and K. Domanska-Janik, “Induction of endothelial phenotype from Wharton’s jelly-derived MSCs and comparison of their vasoprotective and neuroprotective potential with primary WJ-MSCs in CA1 hippocampal region *ex vivo*,” *Cell Transplantation*, vol. 25, no. 4, pp. 715–727, 2016.
- [22] T. Yamate, H. Mocharla, Y. Taguchi, J. U. Igjetseme, S. C. Manolagas, and E. Abe, “Osteopontin expression by osteoclast and osteoblast progenitors in the murine bone marrow: demonstration of its requirement for osteoclastogenesis and its increase after ovariectomy,” *Endocrinology*, vol. 138, no. 7, pp. 3047–3055, 1997.
- [23] K. Tat, M. P. Steeve, S. Théoleyre, D. Heymann, and Y. Fortun, “IL-6, RANKL, TNF-alpha/IL-1: interrelations in bone resorption pathophysiology,” *Cytokine & Growth Factor Reviews*, vol. 15, no. 1, pp. 49–60, 2004.
- [24] J. J. Pinzone, B. M. Hall, N. K. Thudi et al., “The role of Dickkopf-1 in bone development, homeostasis, and disease,” *Blood*, vol. 113, no. 3, pp. 517–525, 2009.
- [25] S. Scarfi, “Use of bone morphogenetic proteins in mesenchymal stem cell stimulation of cartilage and bone repair,” *World Journal of Stem Cells*, vol. 8, no. 1, pp. 1–12, 2016.
- [26] Y.-C. Guo and Q. Yuan, “Fibroblast growth factor 23 and bone mineralisation,” *International Journal of Oral Science*, vol. 7, no. 1, pp. 8–13, 2015.
- [27] Q. Chen, P. Shou, L. Zhang et al., “An osteopontin-integrin interaction plays a critical role in directing adipogenesis and osteogenesis by mesenchymal stem cells,” *Stem Cells*, vol. 32, no. 2, pp. 327–337, 2014.
- [28] K. Oshita, K. Yamaoka, N. Udagawa et al., “Human mesenchymal stem cells inhibit osteoclastogenesis through osteoprotegerin production,” *Arthritis and Rheumatism*, vol. 63, no. 6, pp. 1658–1667, 2011.
- [29] W. E. Sharaf-Eldin, N. Abu-Shahba, M. Mahmoud, and N. el-Badri, “The modulatory effects of mesenchymal stem cells on osteoclastogenesis,” *Stem Cells International*, vol. 2016, Article ID 1908365, 13 pages, 2016.
- [30] Q. Ge, H. Zhang, J. Hou et al., “VEGF secreted by mesenchymal stem cells mediates the differentiation of endothelial progenitor cells into endothelial cells via paracrine mechanisms,” *Molecular Medicine Reports*, vol. 17, no. 1, pp. 1667–1675, 2018.
- [31] P. Amable, M. V. Teixeira, R. B. Carias, J. Granjeiro, and R. Borojevic, “Protein synthesis and secretion in human mesenchymal cells derived from bone marrow, adipose tissue and Wharton’s jelly,” *Stem Cell Research & Therapy*, vol. 5, no. 2, p. 53, 2014.
- [32] W. Widowati, H. Widyastuti, H. Murti et al., “Interleukins and VEGF secretome of human Wharton’s jelly mesenchymal stem cells-conditioned medium (hWJMSCs-CM) in different passages and oxygen tensions,” *Bioscience Research*, vol. 14, no. 4, pp. 776–787, 2017.
- [33] A. Polini, D. Pisignano, M. Parodi, R. Quarto, and S. Scaglione, “Osteoinduction of human mesenchymal stem cells by bioactive composite scaffolds without supplemental osteogenic growth factors,” *PLoS One*, vol. 6, no. 10, 2011.
- [34] S. J. Lee, J. S. Choi, K. S. Park, G. Khang, Y. M. Lee, and H. B. Lee, “Response of MG63 osteoblast-like cells onto polycarbonate membrane surfaces with different micropore sizes,” *Biomaterials*, vol. 25, no. 19, pp. 4699–4707, 2004.
- [35] S. K. Maiti, A. R. Ninu, P. Sangeetha et al., “Mesenchymal stem cells-seeded bio-ceramic construct for bone regeneration in large critical-size bone defect in rabbit,” *Journal of Stem Cells & Regenerative Medicine*, vol. 12, no. 2, pp. 87–99, 2016.
- [36] A. Matsiko, J. P. Gleeson, and F. J. O’Brien, “Scaffold mean pore size influences mesenchymal stem cell chondrogenic differentiation and matrix deposition,” *Tissue Engineering Part A*, vol. 21, no. 3–4, pp. 486–497, 2015.
- [37] P. J. Harwood, J. B. Newman, and A. L. R. Michael, “(ii) An update on fracture healing and non-union,” *Orthopaedics and Traumatology*, vol. 24, no. 1, pp. 9–23, 2010.
- [38] L. Yu, Y. Wu, J. Liu et al., “3D culture of bone marrow-derived mesenchymal stem cells (BMSCs) could improve bone regeneration in 3D-printed porous Ti6Al4V scaffolds,” *Stem Cells International*, vol. 2018, 2018.
- [39] M. Uemura, M. M. Refaat, M. Shinoyama, H. Hayashi, N. Hashimoto, and J. Takahashi, “Matrigel supports survival and neuronal differentiation of grafted embryonic stem cell-derived neural precursor cells,” *Journal of Neuroscience Research*, vol. 88, no. 3, pp. 542–551, 2010.

## Research Article

# Deciduous Dental Pulp Stem Cells for Maxillary Alveolar Reconstruction in Cleft Lip and Palate Patients

**Daniela Y. S. Tanikawa** <sup>1,2</sup>, **Carla C. G. Pinheiro** <sup>1</sup>, **Maria Cristina A. Almeida**,<sup>2</sup>  
**Claudia R. G. C. M. Oliveira**,<sup>1</sup> **Renata de Almeida Coudry**,<sup>1</sup> **Diógenes Laercio Rocha**,<sup>1</sup>  
and **Daniela Franco Bueno** <sup>1,2</sup>

<sup>1</sup>Instituto Sírio-Libanês de Ensino e Pesquisa, Hospital Sírio-Libanês, São Paulo, SP, Brazil

<sup>2</sup>Departamento de Fissura Lábio Palatina, Hospital Municipal Infantil Menino Jesus, São Paulo, SP, Brazil

Correspondence should be addressed to Daniela Franco Bueno; [daniela.fbueno@hsl.org.br](mailto:daniela.fbueno@hsl.org.br)

Received 24 October 2019; Accepted 3 February 2020; Published 12 March 2020

Guest Editor: Edward C. Ko

Copyright © 2020 Daniela Y. S. Tanikawa et al. This is an open access article distributed under the Creative Commons Attribution License, which permits unrestricted use, distribution, and reproduction in any medium, provided the original work is properly cited.

**Background.** To reduce morbidity to cleft patients, new approaches have been developed and here, we report for the first time the use of deciduous dental pulp stem cells (DDPSC) associated with a hydroxyapatite-collagen sponge (Bio-Oss Collagen® 250 mg, Geistlich) for closing alveolar defects during secondary dental eruption, further comparing these results to historical controls. **Methods.** Six patients, aged 8 to 12, were selected. Autologous DDPSC were isolated from each patient, then associated with the biomaterial and this bone tissue engineered set was used to fill the alveolar defect. Computed tomography was performed to assess both preoperative and 6- and 12-month postoperative outcomes. Overall morbidity was recorded. Historical controls consisted of sixteen patients previously selected and randomly assigned to group one (rhBMP-2) or group two (iliac crest bone graft). **Results.** DDPSC could be isolated and characterized as mesenchymal stem cells. Progressive alveolar bone union has occurred in all patients. Similarly to group two 75.4%, SD ± 4.0,  $p > 0.999$ , but statistically different from group one (59.6%, SD ± 9.9,  $p = 0.001$ ), completion of the defect with 75.6% (SD ± 4.8) of bone filling was detected 6 months postoperatively. Dental eruption routinely occurred in 66.7% of patients. No complications were detected, in comparison to significant swelling in 37.5% of group one patients and significant donor site pain in 87.5% of group two. **Conclusion.** For this selected group of patients, DDPSC therapy resulted in satisfactory bone healing with excellent feasibility and safety, which adds significantly to the prospect of stem cell use in clinical settings. **Clinical Question/Level of Evidence.** Therapeutic, II. This trial is registered with <https://clinicaltrials.gov/ct2/show/NCT01932164?term=NCT01932164&rank=1>.

## 1. Introduction

To overcome donor site morbidity during secondary maxillary alveolar reconstruction in cleft lip and palate (CLP) patients, many innovative efforts regarding various bone substitutes have been reported [1, 2].

However, the lack of bioactivity, biomechanical weakness, and susceptibility to infection are still detrimental to the use of most of them; [3] and even for bone morphogenetic proteins, recently suggested as an effective alternative [4–7], significant restraints concerning high costs and severe adverse events have emerged [8–11].

Diversely, tissue engineering strategies arise as a new therapeutic option and one of the research hotspots in recent years [2, 12–16]. Therefore, considering that during the mixed dentition every child has deciduous exfoliating teeth, we decided to carry out a phase 1 clinical study using deciduous dental pulp stem cells (DDPSC) for maxillary alveolar cleft reconstruction (Figure 1) [17, 18].

The results of this prospective cohort of patients were then compared to historical controls, which received either the traditional iliac crest bone graft or bone morphogenetic protein 2 (rhBMP-2) [6]. Outcomes of interest were the alveolar cleft bone filling, the new bone's ability to withstand dental eruption, and the occurrence of complications.

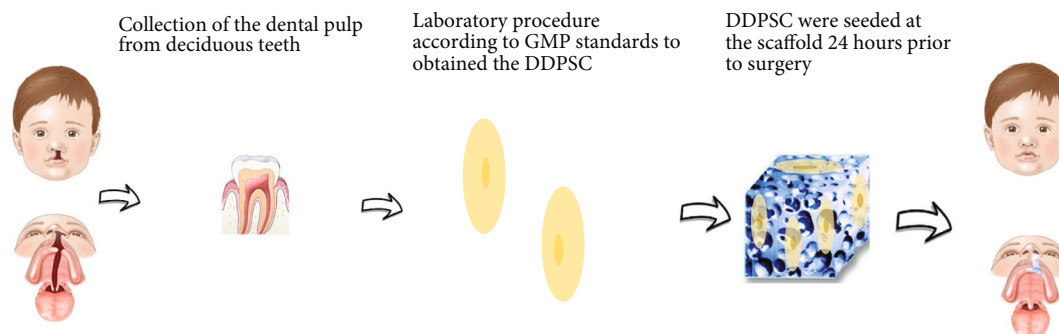


FIGURE 1: Representative strategy for autologous bone tissue engineering using DDPSC.

## 2. Methods

**2.1. Study Design.** This study is a retrospective review of a prospective cohort and a historical group of patients who previously had been submitted to a randomized, controlled, observer-blinded, and surgical trial with two parallel comparison groups.

**2.2. Trial Population and Eligibility Criteria.** For this phase I trial, six patients with unilateral alveolar cleft defects, aged 8 to 12 years old, were selected at Hospital Municipal Infantil Menino Jesus (HMIMJ). All patients underwent preoperative orthodontic expansion of maxillary segments. Exclusion criteria used were previous alveolar surgery, previous eruption of the canine, presence of comorbidities, or incomplete records. Informed consent was obtained for each subject at study entry (written and verbal guidelines).

**2.3. Interventions.** Patients underwent maxillary alveolar reconstruction using a hydroxyapatite-collagen sponge (Bio-Oss Collagen® 250 mg, Geistlich) associated with DDPSC ( $N = 6$ ). Historical controls met the same eligibility criteria and consisted of subjects who previously underwent maxillary alveolar reconstruction with either rhBMP-2 (group one,  $N = 8$ ) or the traditional iliac crest bone graft (group two,  $N = 8$ ).

**2.4. Collection and Expansion of DDPSC.** Extraction of the deciduous teeth was performed at the dental office at HMIMJ. By endodontic removal, the deciduous tooth pulps were obtained and immediately added to a sterile collector with 2 mL DMEM-F12 solution (Dulbecco's Modified Eagle Medium/Nutrient Mixture F12, Gibco Invitrogen, Grand Island, NY). Then, they were transported to the laboratory of good practices of manipulation (GMP) at Centro de Tecnologia Celular-Hospital Sírio-Libanês (HSL) up to 24 hours after the collection. With the use of a solution containing 1 mg/mL trypsin (TrypLE, Gibco Invitrogen, Grand Island, NY) in PBS (pH 7.4, Gibco Invitrogen, Grand Island, NY) for 30 minutes at 37°C, stem cells were obtained. Then, pulp tissues were fragmented and cultured in Dulbecco Modified Water/Nutrient Modules F12 (Gibco, Grand Island, NY) supplemented with 15% bovine fetal serum (HyClone, GE Health Care Life Sciences), preferably distributed in different wells and maintained with DMEM-F12 medium (Gibco, Grand Island, NY), 2% NEAA (MEM nonessential amino

acid solution, Gibco, Grand Island, NY), and 2% penicillin and streptomycin (Gibco, Grand Island, NY) and incubated at 37°C in an atmosphere of 10% CO<sub>2</sub>. Culture medium was changed every three days, and only the DPSC that had been cultured for three to five passages were used in this study.

**2.5. Identification and Characterization of DDPSC.** The cellular characterization was performed by flow cytometry on FACSCalibur (BD Biosciences, Becton Dickinson, Franklin Lakes, NJ) and analyzed in their own CellQuest program (BD Biosciences). Cells obtained from cell cultures at a concentration of  $1 \times 10^6$  cells in 100  $\mu$ L were labeled with monoclonal antibodies—CD29-PE, CD31-FITC, CD34-FITC, CD44-PE, CD45-PE, CD73-FITC, CD90-FITC, CD105-PE, IgG-FITC, and IgG-PE (BD Biosciences)—for 30 minutes at room temperature, in the dark.

Next, DDPSC were tested for their ability to differentiate into adipocytes, chondrocytes, and osteoblasts in accordance to the methods previously described [17, 18]. To analyze the presence of aerobic, anaerobic bacteria, and fungi in the culture, the automated microbial detection system BacT/Alert 3D (BacT/Alert-bioMérieux-Durham, NC) was used. Any positive samples were discharged, and then, new dental pulp collection was recommended.

**2.6. Tissue-Engineered Bone Graft.** One million DDPSC were seeded at 250 mg Bio-Oss Collagen® (Geistlich Biomaterials AG, Wolhusen, Germany) 24 hours prior to surgical procedure, and for each patient, two to four sets were prepared.

**2.7. Electron Microscopy.** Cells were fixed at the biomaterial 250 mg Bio-Oss Collagen® (Geistlich Biomaterials AG, Wolhusen, Germany) during 24 hours at 4°C using the modified Karnovsky solution, which contains 2.5% glutaraldehyde and 2% paraformaldehyde in 0.1 M (pH 7.4) sodium cacodylate buffer. The specimens were postfixed in 2% osmium tetroxide solution and rinsed in distilled water for one hour at room temperature. Then, the cells were dehydrated using ethanol and cleansed in an ultrasonic apparatus (Gerador DA 200, Thornton Inpec Eletronica SA, São Paulo, SP, Brazil) for one hour. The samples were mounted on metal stubs and covered with gold in a sputter coater apparatus (Balzers Union SCD-040, Liechtenstein). The specimens were

TABLE 1: Immunophenotype profile (% positive reaction).

Patient ID	CD29	CD31	CD34	CD44	CD45	CD73	CD90	CD105
1	80	0.8	0.26	97.6	0.09	89.5	98.06	88
2	80	0.7	0.06	97.5	0.5	94.48	95.7	94.21
3	94	0.65	0.31	98.43	0.5	90.38	96.48	96.45
4	90.58	0.05	0.08	80	0.02	97.46	99.68	98.17
5	95.23	2	0.03	97.94	0.14	80	90	98.2
6	95.12	0.81	1.17	83.43	1.06	81.09	92.83	98.52

examined in a scanning electron microscope at 20.0 kV (Jeol 6460LV, Tokyo, Japan).

**2.8. Surgical Procedure.** The surgical procedure and the alveolar defect exposure were performed in the same standardized manner and by the same surgical team of historical controls, as previously described [6]. In accordance with its size, two to three bone tissue-engineered sets, each one composed of 250 mg Bio-Oss Collagen® (Geistlich Biomaterials AG, Wolhusen, Germany) with one million DDPSC, were placed into the alveolar defect.

For the historical controls, the 2.8 mL kit of Infuse® Bone Graft (Medtronic, Memphis, TN) with a dose range of 3.2 to 4.2 mg was used as bone morphogenetic protein source in group one and in group two, a volume range of 20 to 40 mL of iliac crest cancellous bone was removed and applied into the defect.

**2.9. Clinical Assessment.** Preoperative variables included age, sex, and CLP classification. Length of hospital stay was recorded. Postoperatively, patients were asked to return for follow-up appointments on the 1<sup>st</sup>, 2<sup>nd</sup>, and 3<sup>rd</sup> weeks and on the 6<sup>th</sup> and 12<sup>th</sup> months. On each follow-up visit, surgical complications such as bleeding, infection, oronasal fistula, bone graft exposure, or signs of ectopic bone formation were assessed and recorded.

**2.10. Radiographic Assessment.** For bone healing assessment, a computed tomography (CT) was performed, using Somatom Force AF2 Siemes Healthcare GmbH, Munich, Germany, preoperatively as well as on the 6<sup>th</sup> and 12<sup>th</sup> months postoperatively, as previously described [6]. A volumetric analysis of the alveolar defect on both cleft and noncleft sides was performed through the Osirix Dicom Viewer (Apple Inc. Website). By superimposing the coordinates on anatomical landmarks, preoperative and 6- and 12-month postoperative images were adjusted, unified, and compared. Anatomical landmarks were the pyriform aperture superiorly and the cemento-enamel junction inferiorly. The difference between preoperative and postoperative defect volume was defined as the bone filling volume, and the percentage ratio between the bone filling volume and the preoperative defect volume was defined as the bone filling percentage. Dental eruption was assessed 12 months postoperatively.

**2.11. Statistical Analysis.** Statistical and inferential analyses were performed through the Statistical Package for the Social Sciences software (SPSS for Windows 13). The assumptions of normal distribution in each group and the homogeneity

of variances between groups were evaluated, respectively, with Shapiro-Wilk and Levene's tests. In all inferential analysis a type I ( $\alpha$ ) error probability of 0.05 was considered. A statistical analysis of the data was carried out using the ANOVA for linear mixed effects models followed by the Bonferroni method.

### 3. Results

**3.1. Characterization of DDPSC.** Mesenchymal stem cells were isolated from dental pulps, showing fibroblast-like morphology. Flow cytometry analysis showed positive reactions for mesenchymal markers (CD29, CD44, CD73, CD90, and CD105) and negative reactions for endothelial (CD31) and hematopoietic markers (CD34 and CD45) (Table 1).

DDPSC were also characterized by inducing cellular differentiation into bone, cartilage, and fat. This was observed in all strains, demonstrating their multipotent capability (Figure 2).

**3.2. Electron Microscopy.** Good attachment of DDPSC to the scaffold 250 mg Bio-Oss Collagen® (Geistlich Biomaterials AG, Wolhusen, Germany) could be routinely detected by electron microscopy (Figure 3).

**3.3. Study Population and Surgical Variables.** Six patients were enrolled in the study (three males and three females). Three patients had complete unilateral clefts, and the others had unilateral cleft lip and alveolus. Mean age at surgery was ten years and two months old (range 8 to 12). All these variables were comparable to historical controls.

**3.4. Morbidity.** For patients receiving DDPSC, there were no surgical complications. In group one, 37.5% developed significant swelling in the early postoperative period, and in group two, 87.5% complained about significant donor site pain at week two. Mean length of stay was longer for group two at day three, compared to patients receiving dental pulp stem cells and group one at day one postoperatively.

**3.5. Bone Healing.** Preoperative and follow-up examinations revealed progressive alveolar bone union in all 6 patients that has received bone tissue engineering alveolar bone graft (DDPSC associated with 250 mg Bio-Oss Collagen®). Partial or total graft loss, wound breakdown, or ectopic bone formation were not observed in all patients that has received DDPSC associated with 250 mg Bio-Oss Collagen® (Geistlich Biomaterials AG, Wolhusen, Germany), Figure 4.

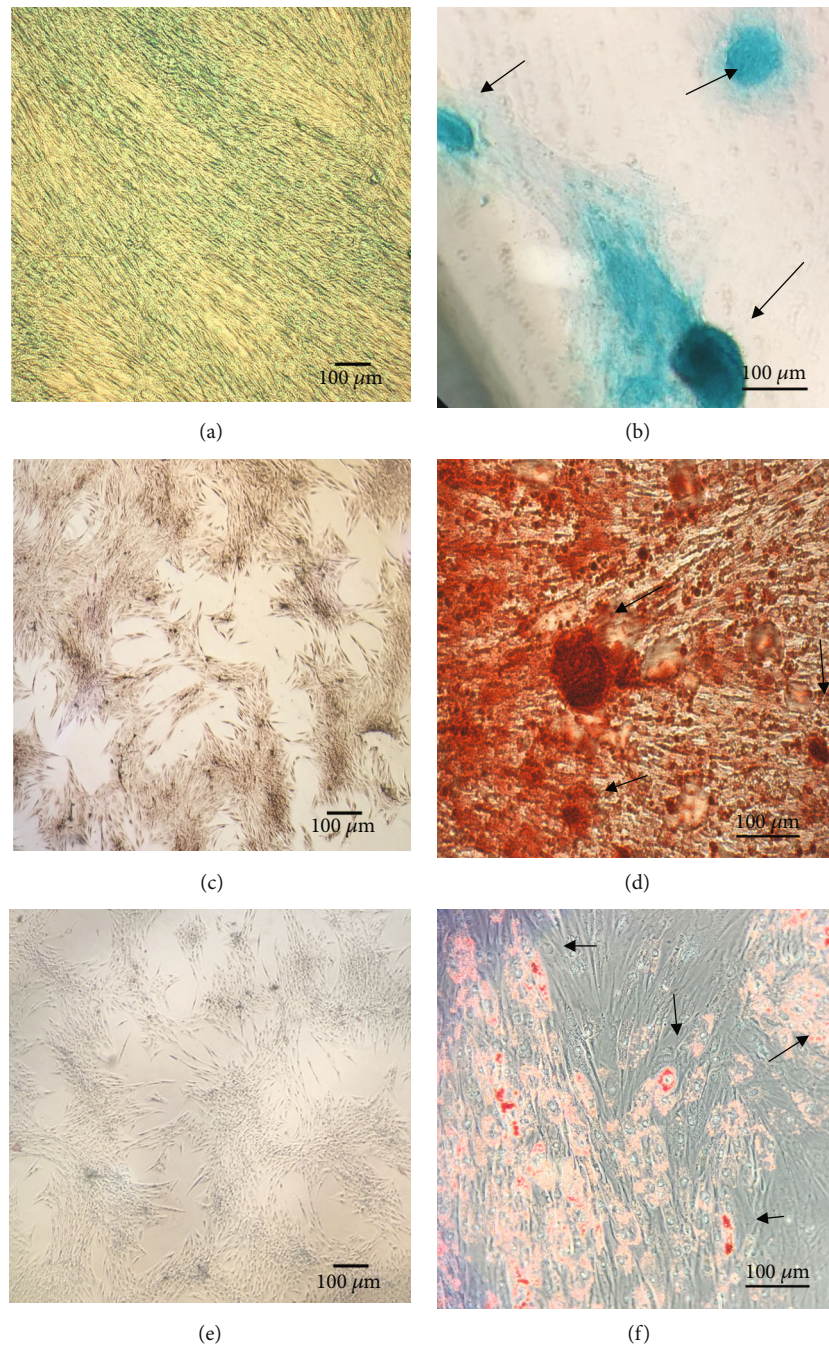


FIGURE 2: Multilineage differentiation “in vitro”. (a) The control group of DDPSC chondrogenic differentiation. (b) Chondrogenic differentiation after three weeks of DDPSC induction stained with Alcian Blue; black arrows show the extracellular matrix formation—mucopolysaccharides. (c) The control group of DDPSC osteogenic differentiation. (d) Osteogenic differentiation after three weeks of DPSC induction stained with Alizarin Red S; the black arrows show the calcium nodules. (e) Control group of DDPSC. (f) Adipocytes stained with Oil Red obtained after the adipogenic induction of DPSC during 18 days; black arrows show the fat vesicles. All the scale bars represent 100  $\mu\text{m}$ .

Through volumetric analysis, mean preoperative defect was 1028.6  $\text{mm}^3$  (SD 212.6), resembling groups one and two ( $p = 0.841$ ). At the 6-month follow-up examination, mean postoperative defect was 253.2  $\text{mm}^3$  (SD 85.8) in group one and in group two 260.4  $\text{mm}^3$  (SD 98.5); it was smaller than that in group one (393.6  $\text{mm}^3$ , SD 144.7,  $p = 0.048$ ). However, at the 12-month follow-up examination, mean postoperative

defect became similar in all groups ( $p = 0.569$ ) (Figure 5(a) and Table 2).

Regarding bone filling percentage, there was a significant difference at the 6-month follow-up between patients receiving DDPSC (75.6%, SD 4.8) and group one (59.6%, SD 9.9,  $p = 0.001$ ), but at the 12-month follow-up examination, this difference disappeared ( $p = 0.233$ ) (Figure 5(b) and Table 3).

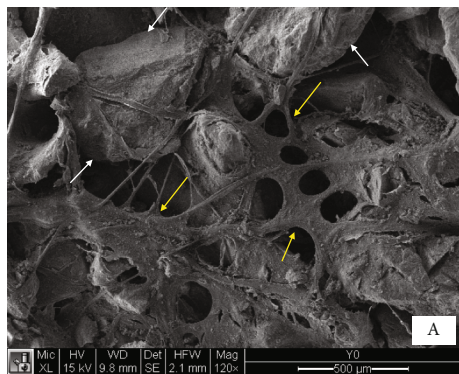


FIGURE 3: Electron microscopy. Scaffold 250 mg Bio-Oss Collagen® (Geistlich Biomaterials AG, Wolhusen, Germany) seeded with DDPSC; yellow arrows show DDPSC, and white arrows show the scaffold (Bio-Oss®).

The patients biopsy twelve months after the use of bone tissue engineering to do their alveolar cleft rehabilitation using DDPSC associated with Bio-Oss Collagen® showed in the histology the presence of good young bone with only some reminiscent of the biomaterial (Bio-Oss®, Geistlich), Figure 6.

Dental eruption routinely occurred with 66.7% of patients. Canine impingement was detected in two patients, for which the canine tooth was drawn using orthodontic strategies. In groups one and two, no adverse event regarding dental eruption was detected.

#### 4. Discussion

For the past two decades, the advent of bone tissue engineering represents a very promising alternative that circumvents several limitations of autografting. Currently, there are vigorous investigations on new strategies such as gene therapy, stem cells, and osteoinductive growth factors, but so far, only small series of patients in few controlled human clinical trials describe its use in the craniofacial surgical field [2, 5–7, 15, 16, 19–21].

For instance, the discovery of rhBMP-2 has prompted a spurt of activity to apply this growth factor into a variety of bone defects. Primarily observed in embryonic and skeletal development, small amounts of these proteins are found in mature skeletons for bone repair and maintenance [22].

However, for the recombinant human forms currently available, superphysiological doses with approximately 200,000 times the naturally occurring dose are detected. Thus far, rhBMP-2 has been approved by the US Food and Drug Administration (FDA) for autograft replacement for interbody spinal fusion, treatment of orthopedic trauma, sinus floor augmentations, and localized alveolar ridge augmentations for tooth extract defects in skeletally mature patients [23]. Several studies have shown successful rhBMP-2-induced bone formation in the craniofacial skeleton [5–7]. However, in spite of some exciting data from these human reports, major complications, adverse events, and reoperations have increasingly been attributed to the “off-label” use of rhBMP-2 in spine surgery, including heterotopic ossifica-

tion, osteolysis, increased neurological deficits, and cancer, [9, 10, 24, 25] and for maxillofacial surgery, Neovius et al. and Goss et al. reported severe swelling, while high rates of postoperative nasal stenosis were described in cleft children [8, 11]. Because of this, a second FDA warning was issued against the use of this product in the pediatric population out of concern for insufficient data to demonstrate long-term efficacy or safety in children.

Diversely, tissue engineering strategies using scaffolds and mesenchymal stem cells are potential treatments for filling bone defects in the growing craniofacial skeleton, including alveolar clefts. For alveolar bone tissue engineering, the first clinical use was published in 2006 [12], and to date, few cases have been reported [2, 13–15]. After using osteoblasts cultured on demineralized bone matrix Osteovit® (Braun, Melsungen, Germany), Pradel and Lauer reported that 40.9% of the cleft defect was ossified [15]. In 2012, mesenchymal stem cells on biphasic scaffolds Reprobone® (Ceramisys, Sheffield, England) resulted in 51.3% of bone filling three months postoperation; [14] in Bajestan’s study, cell therapy was successful in two out of five subjects [16]. In all these reports, less than half of the bone’s defect was filled; in addition, the bone marrow had been the stem cell donor, which implies that their acquisition required prior harvesting procedure with drawbacks in both time and patient comfort.

In this study, we report for the first time the use of DDPSC for maxillary alveolar reconstruction in CLP patients. With similar properties and differentiation abilities to those derived from bone marrow [26], proangiogenic properties [27], and adipogenic, myogenic, neurogenic, and odontogenic potential [17, 26], DDPSC are easily accessible with very little morbidity from deciduous teeth during the mixed dentition. Besides, from only one deciduous tooth, it is possible to obtain  $1 \times 10^4$  DDPSC, and after five passages, that the number turns into  $1 \times 10^{20}$  cells. Considering that an average of two to three biomaterials embedded with  $1 \times 10^6$  cells was used in this study, we highlight that the number of cells needed could be easily obtained in approximately one month after dental extraction, which is a short period. Furthermore, in this study, we could observe by electronic microscopy that these DDPSC have a good interaction and adhesion to the biomaterial (Bio-Oss collagen®; Geistlich Biomaterials AG, Wolhusen, Germany).

Regarding scaffolding matrices, we previously observed that the collagen sponge carrier of rhBMP-2 lacked structural stability, causing the collapse of soft tissue walls in the grafted area [6]. Thus, to aid in maintaining bone induction space to occur during new bone formation, a hydroxyapatite-collagen sponge was selected for this study. Hydroxyapatite has inherent osteoconductive and osteoinductive properties; therefore, a hydroxyapatite-collagen sponge mixture takes advantage of the architectural strength of hydroxyapatite and the rapid dissolution profile of collagen. The Bio-Oss collagen® (Geistlich Biomaterials AG, Wolhusen, Germany) is characterized by a sponge structure and interconnected pore system that may facilitate cell adherence and vascular in-growth [28, 29]. However, due to its high degree of radiolucency, it cannot be

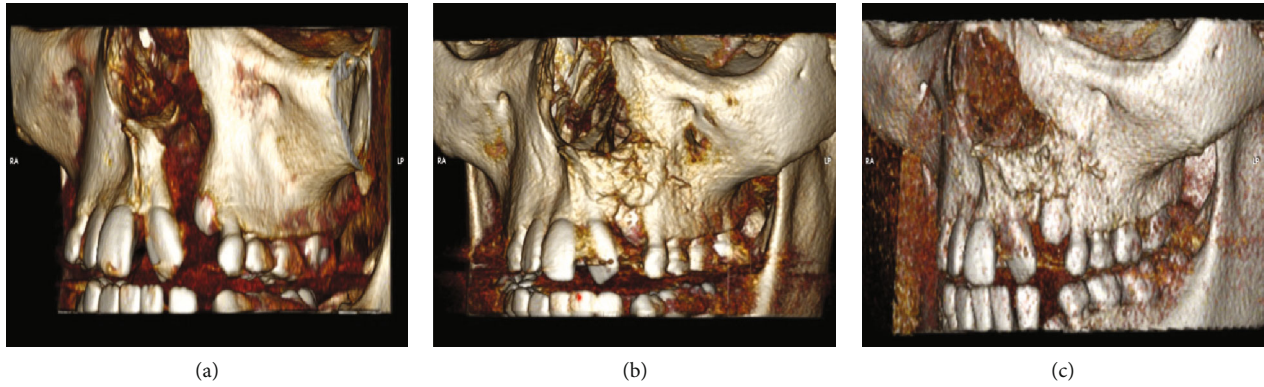


FIGURE 4: Patient that has received alveolar bone tissue engineering graft (DDPSC associated with 250 mg Bio-Oss Collagen®). Computed tomography images of the same patient showing the alveolar cleft fill by bone 6 and 12 months after the use of bone tissue engineering strategies (DDPSC associated with Bio-Oss Collagen®) and the canine tooth eruption after 12 months. (a) Preoperative—presence of alveolar cleft; (b) 6 months postoperatively—the alveolar cleft filled by new bone, and (c) 12 months postoperatively—canine tooth eruption in the new bone formed using the DDPSC associated with Bio-Oss Collagen®.

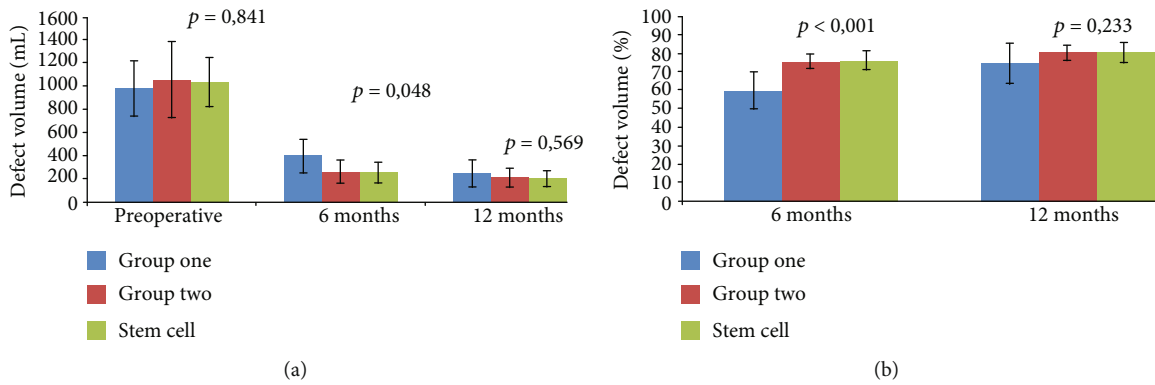


FIGURE 5: Analysis of volumetric and bone filling. (a) Volumetric representative graph. (b) Bone filling representative graph.

TABLE 2: Defect volume analysis.

	Preoperative		6-month follow-up		12-month follow-up	
	Mean (mm <sup>3</sup> )	SD	Mean (mm <sup>3</sup> )	SD	Mean (mm <sup>3</sup> )	SD
Group one (N = 8)	974.8	236.8	393.6	144.7	247.1	112.8
Group two (N = 8)	1052.4	326.0	260.4	98.8	207.8	77.9
Stem cell (N = 6)	1028.6	212.6	253.2	85.8	200.2	67.0
<i>p</i>	0.841		<b>0.048*</b>		0.569	

SD: standard deviation. \*Statistically significant difference.

TABLE 3: Bone filling percentage analysis.

	6-month follow-up		12-month follow-up	
	%	SD	%	SD
Group one (N = 8)	59.6	9.9	74.4	10.8
Group two (N = 8)	75.4	4.0	80.2	4.1
Stem cell (N = 6)	75.6	4.8	80.4	5.3
<i>p</i>	<b>&lt;0.001*</b>		0.233	

\*Statistically significant difference.

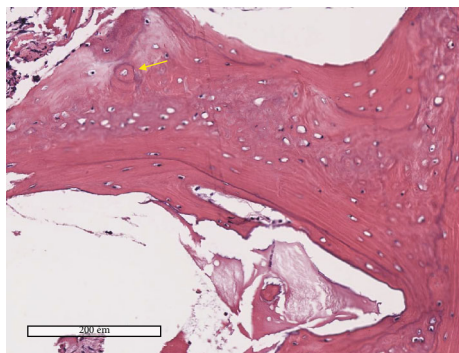


**FIGURE 6:** Histology of the bone formed with DDPSC associated with Bio-Oss Collagen® after 12 months. Histology of the bone formed after 12 months of the use of bone tissue engineering strategy (DDPSC associated with Bio-Oss Collagen® (Geitlich) to close the alveolar bone cleft of cleft lip and palate patients. The scale bars represent 200  $\mu\text{m}$ . The yellow arrow shows the presence of young bone (Haversian canal), and the black arrows show the presence of remaining biomaterial (Bio-Oss Collagen®, Geitlich) that was not reabsorbed in twelve months.

detected by X-ray or CT examination until it has been replaced by autogenous bone. Our experimental study in minipigs, which employed CT, histologic, histomorphometric, and immunohistochemical analyses, provides evidence that the hydroxyapatite-collagen scaffolds seeded with DDPSC are more proficient than unseeded scaffolds for osteogenesis and new bone formation. These data unequivocally demonstrate that the addition of stem cells to a bone-mimetic biomaterial can improve the regenerative capacity of the tissue-engineered bone (unpublished data).

Objective parameters such as bone volume, labiolingual morphology, and bone architecture were assessed using the Osirix Dicom Viewer software (Apple Inc.). In all patients, it was detected that progressive alveolar bone union successfully occurred. However, while grafted cancellous bone is quickly incorporated and vascularized, being anatomically indistinguishable by CT at the 6-month follow-up examination, in the stem cell group, a slow resorption rate of the hydroxyapatite component was verified and at the 6 and 12-month follow-up examinations and small amounts of this product could still be detected. Still, the volume increase between 6 and 12 months postoperative suggests that this volume was replaced by autologous bone. Furthermore, when specifically evaluating interalveolar bone height and the distance between the apex and cemento-enamel junction of both mesial and distal teeth, we detected a bone bridge formation with bone mineralization greater than 75% in all patients receiving stem cell therapy.

Nevertheless, for the stem cell group, canine impingement was observed in 33% of patients. In the literature, it has been shown that patients with alveolar clefts have a 20-fold increased risk for canine impaction based on canine position compared with the reported 1-2% prevalence of impacted canines in the general population [30, 31]. Therefore, these results are in accordance to recent reported rates of 35% and 18.9% for canine impaction in patients with clefts [32, 33].

Despite the lack of biomechanical analysis, we believe that a predisposing factor for canine impingement might be the slow resorption rate of the hydroxyapatite component, and not an unusual hardness of the regenerated bone, as suggested by Giuliani et al. [34] Three years after transplants in human mandibles, they showed that collagen sponge seeded with DPSC regenerated a compact rather than a spongy bone. In this study, 12 months postoperatively, bone biopsies could be collected from the treated sites in two patients: one from the stem cell group and the other from the iliac crest bone graft group. For both, the histological analysis demonstrated complete mineralization of the new bone and its integration with the intact bone boundaries, without any other difference between them, except for the small amounts of hydroxyapatite still present in the stem cell patient.

No ectopic bone growth related to the immature skeleton was detected in this study, whereas some investigative reports of ectopic bone formation have been associated with rhBMP-2. Hence, in this preliminary report, bone formation induced by DDPSC appears to have similar behavior to iliac crest bone engraftment, but canine impaction needs to be further investigated.

Many investigators are concerned about the potential complications of stem cell therapy. Therefore, we kept monitoring clinical parameters and, thus far (for up to five years), no complications or hazards associated with this new therapy modality have been detected.

As the first clinical report of alveolar bone tissue engineering using DDPSC in children, our study has the limitation of a small sample size in a series of patients. Despite the comparison to a historical cohort, randomized controlled trials are still necessary to substantiate the evidence for this strategy in various clinical circumstances.

## 5. Conclusion

In conclusion, we demonstrated that stem cell therapy results in satisfactory bone regeneration with dental eruption and reduced morbidity compared to traditional iliac crest bone grafting and rhBMP-2. These observations point out that stem cells can be potentially applied in reconstructing other insults in the craniofacial surgical field. Particularly, when it comes to rehabilitating the alveolar bone in CLP patients, the use of the DDPSC has the advantage of eliminating the need for a second surgical intervention (to obtain the iliac crest bone graft), thus having the potential to reduce operative time, intraoperative blood loss, postoperative pain, costs, and length of hospital stay—factors that could render regenerative medicine a reliable alternative for the current cleft care.

## Abbreviations

rhBMP-2:	Recombinant human bone morphogenetic protein-2
CLP:	Cleft lip and palate
DDPSC:	Deciduous dental pulp stem cells
CT:	Computed tomography



HMIMJ:	Hospital Municipal Infantil Menino Jesus
SPSS:	Statistical Package for the Social Sciences software
CD:	Cluster of differentiation
DMEM-F12:	Dulbecco's Modified Eagle Medium/Nutrient Mixture F12
SD:	Standard deviation
PROADI-SUS:	Programa de Apoio ao Desenvolvimento Institucional do SUS.

## Data Availability

The corresponding author had full access to all the data in the study and had final responsibility for the decision to submit for publication. Please contact author for data requests.

## Ethical Approval

This project is approved by Plataforma Brasil number: 12406113.7.0000.5461 (<http://plataformabrasil.saude.gov.br/login.jsf;jsessionid=5DB7672DD900C8AC431388F40C2F1B3A.server-plataformabrasil-srvjpdf130>) and ethics committee in number: 5461 Hospital Sírío Libanês and registers in the public record site: <https://clinicaltrials.gov/ct2/show/NCT01932164?term=NCT01932164&rank=1>.

## Consent

Consent was received from the patients and/or legally responsible person.

## Conflicts of Interest

The authors declare that they have no competing interests.

## Authors' Contributions

Tanikawa DYS contributed to the conceptualization, data curation, formal analysis, methodology, investigation, visualization, and writing—original draft preparation (all project); Pinheiro CCG contribution includes resources, image editing, and validation (laboratory processes). Resources and validation were also contributed by Almeida MCA (odontology analyses), Oliveira CRGCM: (histopathological analyses), Coudry RA (histopathological analyses), and Rocha DL (performed the surgeries). Bueno DF did the conceptualization, data curation, formal analysis, methodology, investigation, visualization, writing, project administration, and supervision (all project). All authors read and approved the final manuscript.

## Acknowledgments

The sources of funding were the Brazilian Ministry of Health and Hospital Sírío-Libanês through a PROADI-SUS project; these institutions' involvement are as follows: the Brazilian Ministry of Health financed the development of new health techniques for cleft lip and palate patient treatment and Hospital Sírío-Libanês provided the physical structure (laboratories), equipment, and researchers. The Hospital

Municipal Infantil Menino Jesus provides the multidisciplinary care for cleft lip and palate patients where the surgeries were performed. We thank the "Sociedade Beneficente de Senhoras do Hospital Sírío-Libanês" and "Instituto de Responsabilidade Social Sírío-Libanês" through Hospital Municipal Infantil Menino Jesus for providing multidisciplinary care for cleft lip and palate patients in São Paulo, Brazil, with endless encouragement to the development of new strategies that could improve patient quality of life and reduce their morbidity. We thank the philanthropy of Hospital Sírío-Libanês through the PROADI office staff for their support to this project development. We thank Isac de Castro for the assistance with the statistical data analysis and education and research team of Hospital Sírío-Libanês for the administration support.

## References

- [1] B. L. Eppley and A. M. Sadove, "Management of alveolar cleft bone grafting—state of the art," *The Cleft Palate-Craniofacial Journal*, vol. 37, no. 3, pp. 229–233, 2000.
- [2] M. Gimbel, R. K. Ashley, M. Sisodia et al., "Repair of alveolar cleft defects: reduced morbidity with bone marrow stem cells in a resorbable matrix," *Journal of Craniofacial Surgery*, vol. 18, no. 4, pp. 895–901, 2007.
- [3] Y. R. Cho and A. K. Gosain, "Biomaterials in craniofacial reconstruction," *Clinics in Plastic Surgery*, vol. 31, no. 3, pp. 377–385, 2004.
- [4] M. H. Carstens, M. Chin, T. Ng, and W. K. Tom, "Reconstruction of #7 facial cleft with distraction-assisted in situ osteogenesis (DISO): role of recombinant human bone morphogenetic protein-2 with Helistat-activated collagen implant," *Journal of Craniofacial Surgery*, vol. 16, no. 6, pp. 1023–1032, 2005.
- [5] B. P. Dickinson, R. K. Ashley, K. L. Wasson et al., "Reduced morbidity and improved healing with bone morphogenetic protein-2 in older patients with alveolar cleft defects," *Plastic and Reconstructive Surgery*, vol. 121, no. 1, pp. 209–217, 2008.
- [6] N. Alonso, D. Y. S. Tanikawa, R. S. Freitas, L. Canan Jr., T. O. Ozawa, and D. L. Rocha, "Evaluation of maxillary alveolar reconstruction using a resorbable collagen sponge with recombinant human bone morphogenetic protein-2 in cleft lip and palate patients," *Tissue Engineering Part C: Methods*, vol. 16, no. 5, pp. 1183–1189, 2010.
- [7] L. W. Canan Jr., R. da Silva Freitas, N. Alonso, D. Y. S. Tanikawa, D. L. Rocha, and J. C. U. Coelho, "Human bone morphogenetic protein-2 use for maxillary reconstruction in cleft lip and palate patients," *Journal of Craniofacial Surgery*, vol. 23, no. 6, pp. 1627–1633, 2012.
- [8] E. Neovius, M. Lemberger, A. C. Docherty Skogh, J. Hilborn, and T. Engstrand, "Alveolar bone healing accompanied by severe swelling in cleft children treated with bone morphogenetic protein-2 delivered by hydrogel," *Journal of Plastic, Reconstructive & Aesthetic Surgery*, vol. 66, no. 1, pp. 37–42, 2013.
- [9] N. E. Epstein, "Complications due to the use of BMP/INFUSE in spine surgery: the evidence continues to mount," *Surgical Neurology International*, vol. 4, Supplement 5, pp. S343–S352, 2013.
- [10] E. L. Lord, J. R. Cohen, Z. Buser et al., "Trends, costs, and complications of anterior cervical discectomy and fusion with and without bone morphogenetic protein in the United States

- Medicare population,” *Global Spine Journal*, vol. 7, no. 7, pp. 603–608, 2017.
- [11] J. A. Goss, M. S. Hunter, E. S. Armbrrecht, and A. Y. Lin, “Higher dosages of BMP-2 in alveolar cleft repair result in higher rates of postoperative nasal stenosis,” *Plastic and Reconstructive Surgery*, vol. 136, p. 4, 2015.
- [12] H. Hibi, Y. Yamada, M. Ueda, and Y. Endo, “Alveolar cleft osteoplasty using tissue-engineered osteogenic material,” *International Journal of Oral and Maxillofacial Surgery*, vol. 35, no. 6, pp. 551–555, 2006.
- [13] H. Behnia, A. Khojasteh, M. Soleimani et al., “Secondary repair of alveolar clefts using human mesenchymal stem cells,” *Oral Surgery, Oral Medicine, Oral Pathology, Oral Radiology, and Endodontology*, vol. 108, no. 2, pp. e1–e6, 2009.
- [14] H. Behnia, A. Khojasteh, M. Soleimani, A. Tehrani, and A. Atashi, “Repair of alveolar cleft defect with mesenchymal stem cells and platelet derived growth factors: a preliminary report,” *Journal of Cranio-Maxillofacial Surgery*, vol. 40, no. 1, pp. 2–7, 2012.
- [15] W. Pradel and G. Lauer, “Tissue-engineered bone grafts for osteoplasty in patients with cleft alveolus,” *Annals of Anatomy*, vol. 194, no. 6, pp. 545–548, 2012.
- [16] M. N. Bajestan, A. Rajan, S. P. Edwards et al., “Stem cell therapy for reconstruction of alveolar cleft and trauma defects in adults: a randomized controlled, clinical trial,” *Clinical Implant Dentistry and Related Research*, vol. 19, no. 5, pp. 793–801, 2017.
- [17] A. de Mendonça Costa, D. F. Bueno, M. T. Martins et al., “Reconstruction of large cranial defects in nonimmunosuppressed experimental design with human dental pulp stem cells,” *The Journal of Craniofacial Surgery*, vol. 19, no. 1, pp. 204–210, 2008.
- [18] D. F. Bueno, I. Kerkis, A. M. Costa et al., “New source of muscle-derived stem cells with potential for alveolar bone reconstruction in cleft lip and/or palate patients,” *Tissue Engineering Part A*, vol. 15, no. 2, pp. 427–435, 2009.
- [19] W. Pradel, E. Tausche, J. Gollogly, and G. Lauer, “Spontaneous tooth eruption after alveolar cleft osteoplasty using tissue-engineered bone: a case report,” *Oral Surgery, Oral Medicine, Oral Pathology, Oral Radiology, and Endodontology*, vol. 105, no. 4, pp. 440–444, 2008.
- [20] R. d’Aquino, A. De Rosa, V. Lanza et al., “Human mandible bone defect repair by the grafting of dental pulp stem/progenitor cells and collagen sponge biocomplexes,” *European Cells and Materials*, vol. 18, pp. 75–83, 2009.
- [21] M. Nagata, H. Hoshina, M. Li et al., “A clinical study of alveolar bone tissue engineering with cultured autogenous periosteal cells: coordinated activation of bone formation and resorption,” *Bone*, vol. 50, no. 5, pp. 1123–1129, 2012.
- [22] M. Chin, T. Ng, W. K. Tom, and M. Carstens, “Repair of alveolar clefts with recombinant human bone morphogenetic protein (rhBMP-2) in patients with clefts,” *Journal of Craniofacial Surgery*, vol. 16, no. 5, pp. 778–789, 2005.
- [23] W. F. McKay, S. M. Peckham, and J. M. Badura, “A comprehensive clinical review of recombinant human bone morphogenetic protein-2 (INFUSE® Bone Graft),” *International Orthopaedics*, vol. 31, no. 6, pp. 729–734, 2007.
- [24] M. C. Wang, L. Chan, D. J. Maiman, W. Kreuter, and R. A. Deyo, “Complications and mortality associated with cervical spine surgery for degenerative disease in the United States,” *Spine*, vol. 32, no. 3, pp. 342–347, 2007.
- [25] D. Benglis, M. Y. Wang, and A. D. Levi, “A comprehensive review of the safety profile of bone morphogenetic protein in spine surgery,” *Operative Neurosurgery*, vol. 62, Supplement 5, pp. ONS423–ONS431, 2008.
- [26] S. Gronthos, M. Mankani, J. Brahimi, P. G. Robey, and S. Shi, “Postnatal human dental pulp stem cells (DPSCs) in vitro and in vivo,” *Proceedings of the National Academy of Sciences of the United States of America*, vol. 97, no. 25, pp. 13625–13630, 2000.
- [27] A. Bronckaers, P. Hilken, Y. Fanton et al., “Angiogenic properties of human dental pulp stem cells,” *PLoS One*, vol. 8, no. 8, article e71104, 2013.
- [28] M. Payer, B. Lohberger, E. Stadelmeyer, C. Bartmann, R. Windhager, and N. Jakse, “Behaviour of multipotent maxillary bone-derived cells on  $\beta$ -tricalcium phosphate and highly porous bovine bone mineral,” *Clinical Oral Implants Research*, vol. 21, no. 7, pp. 699–708, 2010.
- [29] S. Bose, M. Roy, and A. Bandyopadhyay, “Recent advances in bone tissue engineering scaffolds,” *Trends in Biotechnology*, vol. 30, no. 10, pp. 546–554, 2012.
- [30] K. A. D. D. S. Russell and C. E. McLeod, “Canine eruption in patients with complete cleft lip and palate,” *The Cleft Palate-Craniofacial Journal*, vol. 45, no. 1, pp. 73–80, 2008.
- [31] T. B. Bass, “Observations on the misplaced upper canine tooth,” *Dental Practitioner and Dental Record*, vol. 18, no. 1, pp. 25–33, 1967.
- [32] H. Enemark, J. Jensen, and C. Bosch, “Mandibular bone graft material for reconstruction of alveolar cleft defects: long-term results,” *Cleft Palate-Craniofacial Journal*, vol. 38, no. 2, pp. 155–163, 2001.
- [33] K. Matsui, S. Echigo, S. Kimizuka, M. Takahashi, and M. Chiba, “Clinical study on eruption of permanent canines after secondary alveolar bone grafting,” *Cleft Palate-Craniofacial Journal*, vol. 42, no. 3, pp. 309–313, 2005.
- [34] A. Giuliani, A. Manescu, M. Langer et al., “Three years after transplants in human mandibles, histological and in-line holo-tomography revealed that stem cells regenerated a compact rather than a spongy bone: biological and clinical implications,” *Stem Cells Translational Medicine*, vol. 2, no. 4, pp. 316–324, 2013.

## Research Article

# Aging Induced p53/p21 in Genioglossus Muscle Stem Cells and Enhanced Upper Airway Injury

Lu-Ying Zhu,<sup>1</sup> Li-Ming Yu ,<sup>2,3</sup> Wei-Hua Zhang,<sup>2,3</sup> Jia-Jia Deng,<sup>2,3</sup> Shang-Feng Liu,<sup>2</sup> Wei Huang,<sup>2</sup> Meng-Han Zhang,<sup>2,3</sup> Yan-Qin Lu ,<sup>1</sup> Xin-Xin Han ,<sup>2</sup> and Yue-Hua Liu ,<sup>2,3</sup>

<sup>1</sup>Xiangya School of Stomatology, Xiangya Stomatological Hospital, Central South University, Changsha 410078, China

<sup>2</sup>Oral Biomedical and Engineering Laboratory, Shanghai Stomatological Hospital, Fudan University, Shanghai 200001, China

<sup>3</sup>Department of Orthodontics, Shanghai Stomatological Hospital, Fudan University, Shanghai 200001, China

Correspondence should be addressed to Yan-Qin Lu; [lu\\_yanqin@163.com](mailto:lu_yanqin@163.com), Xin-Xin Han; [xxhan@fudan.edu.cn](mailto:xxhan@fudan.edu.cn), and Yue-Hua Liu; [liuyuehua@fudan.edu.cn](mailto:liuyuehua@fudan.edu.cn)

Received 7 November 2019; Revised 18 January 2020; Accepted 8 February 2020; Published 4 March 2020

Guest Editor: Toru Ogasawara

Copyright © 2020 Lu-Ying Zhu et al. This is an open access article distributed under the Creative Commons Attribution License, which permits unrestricted use, distribution, and reproduction in any medium, provided the original work is properly cited.

Aging of population brings related social problems, such as muscle attenuation and regeneration barriers with increased aging. Muscle repair and regeneration depend on muscle stem cells (MuSCs). Obstructive sleep apnea (OSA) rises in the aging population. OSA leads to hypoxia and upper airway muscle injury. However, little is known about the effect of increasing age and hypoxia to the upper airway muscle. The genioglossus (GG) is the major dilator muscle to keep the upper airway open. Here, we reported that muscle fiber and MuSC function declined with aging in GG. Increasing age also decreased the migration and proliferation of GG MuSCs. p53 and p21 were high expressions both in muscle tissue and in GG MuSCs. We further found that hypoxia inhibited GG MuSC proliferation and decreased myogenic differentiation. Then, hypoxia enhanced the inhibition effect of aging to proliferation and differentiation. Finally, we investigated that hypoxia and aging interact to form a vicious circle with upregulation of p53 and p21. This vicious hypoxia plus aging damage accelerated upper airway muscle injury. Aging and hypoxia are the major damage elements in OSA patients, and we propose that the damage mechanism of hypoxia and aging in GG MuSCs will help to improve upper airway muscle regeneration.

## 1. Introduction

The root source of obstructive sleep apnea (OSA) is repeated hypoxia during sleep [1, 2], and OSA has a higher prevalence at advanced age [3, 4]. Genioglossus (GG), a major upper airway dilator, is key to OSA pathophysiology. Compared with other skeletal muscles, genioglossus has high specific gravity of oxidized muscle fiber and is sensitive to oxygen [5]. The upper airway muscle collapses more easily with aging [6], and there is an age-related change in the fiber-type distribution of the upper airway muscle [7]. However, the effect of increasing age to GG function and the related mechanism remains to be elucidated.

Muscle stem cells (MuSCs) are responsible for muscle growth and injury repair throughout the life [8]. After stimuli, MuSCs can differentiate into myocytes and then fuse

with each other to repair damaged muscle [9, 10]. Muscle is a homeostatic tissue and can tolerate daily wear-and-tear by repair and regeneration [11]. With increasing age, the important reason of progressive weaken and regenerative dysfunction is the functional decline muscle MuSCs [12]. In aging cells, there are also inactivated antioxidative pathways, increased reactive oxygen species, and apoptosis [13]. GG repair and regeneration are very important to OSA patients. However, the influence of aging to GG MuSCs is still unknown.

p53 is a famous tumor suppressor and mutated in a large proportion of cancers [14]. Meanwhile, p53 is a transcription factor involved in many cell processes, such as cell-cycle control, DNA repair, apoptosis, and cellular stress responses [15]. p53 also is a downstream member of aging and hypoxia signaling pathway [16, 17]. p53 increases its expansion and

encourages in aging skeletal muscle. An apoptotic environment is encouraged by p53 in muscle tissue [18]. Then, p53 is sensitive to hypoxia and may suppress muscle cell proliferation by interacting with p21 and hypoxia-inducible factor-1 $\alpha$  (HIF-1 $\alpha$ ) [19]. p21 plays an important role in muscle differentiation after injury [20]. Limited reports show that hypoxia promotes autophagy and modulates mitochondrial function of the GG MuSCs [1, 2]. However, the mechanism of aging GG MuSCs under hypoxia and whether p53 and p21 are involved in this process are still unclear.

Repeated airway collapse and obstruction caused hypoxia in OSA patients. This hypoxia aggravates upper airway muscle damage. Muscle damage further increases obstruction and forms a vicious cycle. Some studies have reported that the prevalence of OSA increases with aging [3, 4]. Our previous work has showed that hypoxia inhibits the myogenic differentiation of GG MuSCs and causes muscle disturbances [21–23]. However, the mechanism of aging and hypoxia damage to GG MuSCs has few reported. In this study, we hypothesized that aging and hypoxia might injure the GG MuSCs by upregulating p53 and p21.

## 2. Materials and Methods

**2.1. Animals and Ethical Issues.** C57BL/6 mice (male, 1 to 12 months old) were obtained from Shanghai Bikai Biotechnology. Mice were kept under natural aging conditions in the animal house facility, with a 12:12 h light and dark cycle. All animals were anesthetized and euthanized. The mouse GG were removed, then frozen in liquid nitrogen and stored at  $-80^{\circ}\text{C}$  rapidly for subsequent quantitative polymerase chain reaction (qPCR) measurements. This research complied with the Animal Ethics Committee of Shanghai Stomatology Hospital, Fudan University.

**2.2. Cell Cultures and Proliferation Assays.** Under sterile conditions, the GG were excised. Firstly, the tissues were cut into  $1\text{ mm}^3$  size. Next, the muscle slurry was digested with 0.1% type I collagenase (Gibco, USA) and 0.05% trypsin-EDTA (Gibco, Canada) at  $37^{\circ}\text{C}$  each for 30 min. Then, the digestion was stopped by the addition of Dulbecco's Modified Eagle Medium (DMEM, Gibco, UK) supplemented with 10% fetal bovine serum (FBS, Gibco, New Zealand). Finally, cells were plated on the culture dishes, and twice repeated differential attachment treatment was used to remove fibroblasts. In the next experiments, to avoid fibroblasts taking over the other cell populations and becoming the predominant cell type in the culture, we only used MuSCs from passage 1. Once the cells reached 90% confluence, they were differentiated by incubation 2% horse serum (Hyclon, USA) in DMEM.  $\text{CoCl}_2$  was dissolved to  $200\text{ }\mu\text{M}$  for actual use in DMEM.

The proliferation of GG MuSCs was assessed using cell counting kit-8 (CCK-8, Dojindo, Japan) assays. Briefly, cells were seeded in 96-well plates at a density of  $5 \times 10^3$  cells per well. After 6 days culture, cells were treated with 10% CCK8 in DMEM for 2 h. Optical density (OD) of each well was measured at 430 nm on a microplate reader at  $37^{\circ}\text{C}$ .

**2.3. Wound Healing Assay and Transwell Cell Migration Assay.** For wound healing assay, GG MuSCs from four age groups were seeded in 6 well plates. After nearly 100% confluence, a single wound was created with a sterile  $200\text{ }\mu\text{l}$  plastic pipette tip in the center of the well, then washed with PBS twice to remove the cellular debris and cultured by 1% FBS in DMEM for 24 h. The wound was captured at 0 and 24 h. The size of the wound healing was measured using Image J 1.5 software.

For migration assay, GG MuSCs ( $1 \times 10^5$ ) were seeded in the transwell inserts (Costar, China, pore size: 8 mm). The assays and counting of migrating cells were performed as described previously [24]. After incubation at  $37^{\circ}\text{C}$  for 24 h, GG MuSCs remaining on the upper chamber membrane were removed with cotton swabs. The migrated cells were fixed in ice-cold 4% PFA for 10 min and stained with a 1% crystal violet solution for 10 min. Images were captured five field at  $100\times$  magnification.

**2.4. Electromyography of the GG Muscle ( $\text{EMG}_{\text{GG}}$ ).**  $\text{EMG}_{\text{GG}}$  was acquired and analyzed as previously described [25]. In brief, mice were anesthetized with 1% pentobarbital, then we turned over the digastric muscle and exposed the genioglossus muscle. Next, two Teflon-insulated wire loop electrodes were used to record  $\text{EMG}_{\text{GG}}$ . The  $\text{EMG}_{\text{GG}}$  signal was amplified, band-pass filtered from 1 to 1000 Hz (ADInstrument Australia), and digitized at a sampling rate of 1000 Hz (LabChart 8). The  $\text{EMG}_{\text{GG}}$  was rectified, and a 1 s time constant was applied to compute the moving average (LabChart 8).

**2.5. Hematoxylin and Eosin and Masson Trichrome Staining.** The GG were collected from four age groups male C57BL/6 mice and were fixed in ice-cold 4% PFA. Then, GG were embedded in paraffin and cut into  $4\text{ }\mu\text{m}$  thick sections by a paraffin slicer. Sections were mounted on glass slides, then were stained with hematoxylin and eosin (H&E, Solarbio, Beijing, China) staining for observing the muscle fiber morphology, and Masson trichrome staining (Servicebio, Wuhan, China) was performed to analyze collagen content in muscle fibers.

**2.6. Immunohistochemistry (IHC) and Immunofluorescence (IF) Assay of Tissues.** For IHC assay, the  $4\text{ }\mu\text{m}$  sections embedded in paraffin were deparaffinized and rehydrated. Then, slides were incubated with 10% goat serum seal (Novus Biologicals, USA) solution at room temperature for 30 min. Next, slides were incubated with primary antibodies against p53 (1:500, Santa Cruz Biotechnology) and p21 (1:500, Santa Cruz Biotechnology) overnight at  $4^{\circ}\text{C}$ . Then, the slides were incubated with the second antibody (1:1000, Abcam, UK) at room temperature for 1 h. Enzyme conjugate was applied for 10 min at room temperature followed by development with AEC (Solarbio, Beijing, China). Each section was captured three times using a light microscope. For the negative control, PBS was used in place of primary antibody.

For IF assay, the  $4\text{ }\mu\text{m}$  sections were rehydrated. After rehydrated, 0.25% Triton X-100 in PBS was used as a

TABLE 1: Primer sequences for qPCR.

Gene	Forward	Reverse
$\beta$ -Actin	GTGACGTTGACATCCGTAAGA	GCCGGACTCATCGTACTCC
p53	CCCCTGTCATCTTTTGTCCCT	AGCTGGCAGAATAGCTTATTGAG
p21	CGAGAACGGTGGAACTTTGAC	CCAGGGCTCAGGTAGACCTT
p16	GCTCAACTACGGTGCAGATTC	GCACGATGTCTTGATGTCCC
MyHC	GCGAATCGAGGCTCAGAACAA	GTAGTTCCGCCTTCGGTCTTG
MyoD	CGGGACATAGACTTGACAGGC	TCGAAACACGGGTCATCATAGA
BAX	AGACAGGGGCCTTTTGTCTAC	GTAGTTCCGCCTTCGGTCTTG
BCL-2	GCTACCGTCGTGACTTTCGC	CCCCACCGAACTCAAAGAAGG

membrane permeability agent. Then, sections were blocked with 10% goat serum seal solution at room temperature for 30 min. Next, slides were incubated with primary antibodies against Ki67 (1:1000, Thermo scientific) and Pax7 (1:250, Abcam, UK) overnight at 4°C, and then slides were incubated with anti-rabbit secondary antibody (1:10000, Abcam, UK) in the dark at room temperature for 1 h. Finally, sections were incubated with 4',6-diamidino-2-phenylindole (1:10000, DAPI, Abcam, UK) for 10 min and photoed using fluorescence microscopy.

**2.7. Immunofluorescence Assay of Cells.** Cells were seeded in 24 well plates and stained in ice-cold 4% PFA at room temperature for 10 min on the third day. Cells were washed three times with PBS, and 0.25% Triton X-100 was used as membrane permeability agent. Next, cells were blocked with 5% bovine serum albumin (BSA) for 1 h and with primary antibodies against Ki67, Pax7, and HIF-1 $\alpha$  (1:300, Novus Biologicals, USA) at 4°C for 48 h. Phosphate-buffered saline (PBS) is the control to primary antibody. Then, cells were washed three times with phosphate-buffered saline Tween-20 (PBST) and were incubated with a second antibody for 1 h at room temperature in the dark. At last, cells were incubated with DAPI for 8 min, and pictures were captured by fluorescence microscopy.

**2.8. Quantitative Real-Time Polymerase Chain Reaction Assay.** Total RNA was extracted from cells or tissues using TRIzol (Ambion, USA) reagent and then reverse transcribed to cDNA using PrimeScript RT reagent kit (Tiangen, China). Quantitative RT-PCR was performed with 20  $\mu$ l of reaction mixture containing SYBR Green PCR Master Mix (Light cycler, USA). Primer sequences of target genes are listed in Table 1. Relative expression level of each gene was calculated using the  $2^{-\Delta\Delta Ct}$  methods. RNA expression was normalized to  $\beta$ -actin expression.

**2.9. Western Blot Analysis.** Cells were collected by 2x lysis buffer. Then, 30  $\mu$ l of total protein was separated on a 10% SDS-PAGE gel, and protein in the gel was transferred to a 0.45  $\mu$ m polyvinylidene difluoride (PVDF) membrane. Membrane was blocked by immersion in 5% milk for 1 h at room temperature. Next, membrane was incubated with primary antibodies against p53 (1:1000, Proteintech), p21 (1:1000, Abcam), MyHC (1:500, DSHB), MyoD (1:500, Millipore), and  $\beta$ -actin (1:10000, Absin, China) overnight

at 4°C. After 4  $\times$  6 min washes in TBST, secondary antibody (1:10000, Cell Signaling) was at room temperature for 2 h and the intensities of dies against p53 and p21 as a control for all other bands. Data were analyzed by Image J 1.5 software.

**2.10. Statistical Analysis.** The statistical analysis was performed by GraphPad Prism 7.0 (GraphPad Software, La Jolla, CA). All results were shown as mean  $\pm$  SD from at least 3 independent experiments. *p* value was measured for the statistical significance of a two-tailed Student's *t*-test, and data were calculated by Excel. *p* < 0.05 was considered statistically significant.

### 3. Results and Discussion

#### 3.1. Results

**3.1.1. The Structure and Function of Upper Airway Muscle Were Affected by Increasing Age.** The upper airway becomes more collapsible with aging, and the genioglossus (GG) is the major upper airway muscle to maintain pharyngeal patency [6]. Therefore, the structure and function of GG play an important role in OSA. New generation fibers are related with muscle force deficit and fatigability [26]. Compared with other skeletal muscle, genioglossus has high specific gravity of the oxidized muscle fiber and is sensitive to oxygen [5]. To investigate whether GG muscle was altered by increasing age, we first examined the cross-sectional area (CSA) of muscle fibers which derived from four age groups. Our results showed that 6-month-old or 12-month-old mice had a CSA reduction compared to 2-month-old mice and a significantly less in 1-month-old compared to 2-month-old mice (Figure 1(a)). Similar results were found in collagen content of GG, which showed that 2-month-old mouse genioglossus has highest collagen content and less collagen content in 6 and 12-month-old mice compared to 2-month-old mice (Figure 1(b)).

Then, we used electromyography to analyze if muscle damage changes with increasing age. Electromyography is a kind of potential change that occurs when skeletal muscle is excited due to the generation, conduction, and diffusion of action potential of muscle fiber. We anesthetized mice of different ages (1-month-old, 2-month-old, 6-month-old, and 12-month-old) and then examined the genioglossus electromyographic activity (EMG<sub>GG</sub>) of these mice. The results

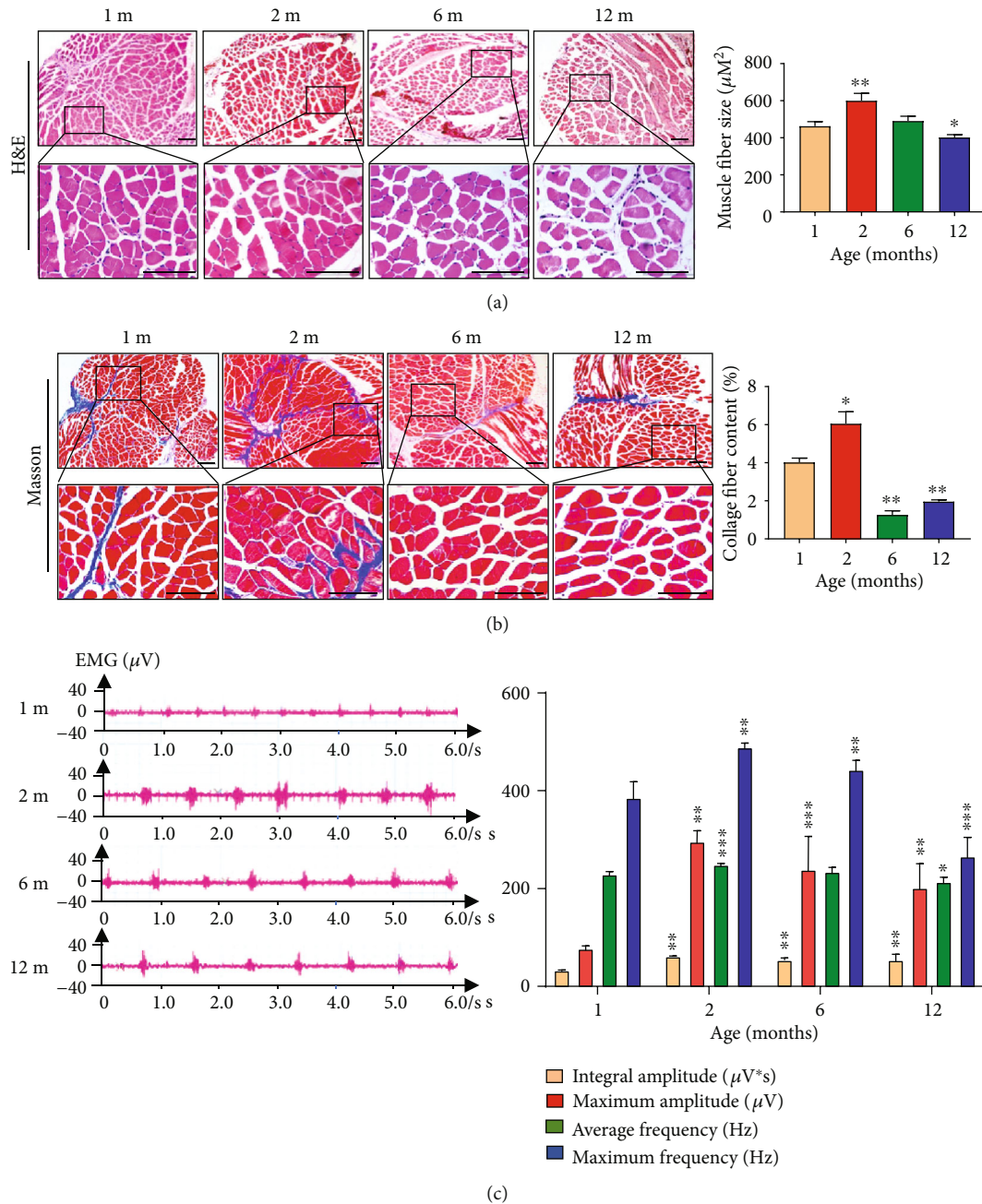


FIGURE 1: The structure and function of GG declined with aging. (a) The cross-sectional area of muscle fiber in 2-month-old significantly increased compared to other age groups. (b) The collagen content of 2-month-old was the highest among four age groups mice. (c) The genioglossus electromyographic activity in four age groups. \* $p < 0.05$ , \*\* $p < 0.01$ , and \*\*\* $p < 0.001$ . Scale bars are  $100 \mu\text{m}$ .

showed that four indexes of  $\text{EMG}_{\text{GG}}$ , including integral amplitude, maximum amplitude, average frequency, and maximum frequency, decreased with aging, except that 1-month-old was weakest (Figure 1(c)). These findings indicated that the structure and function of GG had significant reduction with increasing age in adult mice.

**3.1.2. The Renewal Ability Declined and p53/p21 Increased in Aging GG.** In order to investigate whether increasing age affected the self-renewal function of MuSCs in GG, Pax7, the expression of the paired type homeobox transcription

factor, was identified as a quantifiable marker for stem cells [27]. Therefore, we used Pax7 to detect the self-renewal function of GG MuSCs. Immunofluorescence assay showed that the Pax7-positive cells decreased gradually with aging (Figure 2(a)). We observed that the percentage of Pax7-positive cells in the GG were markedly reduced in 12-month-old (1.8%) compared to other age groups in Figure 2(e) (1 m: 3.7%; 2 m: 2.5%; and 6 m: 2.0%).

Similar results were found in proliferation ability of cells in GG. To investigate whether increasing age repaired the proliferation ability of cells in GG. Ki67, a marker protein

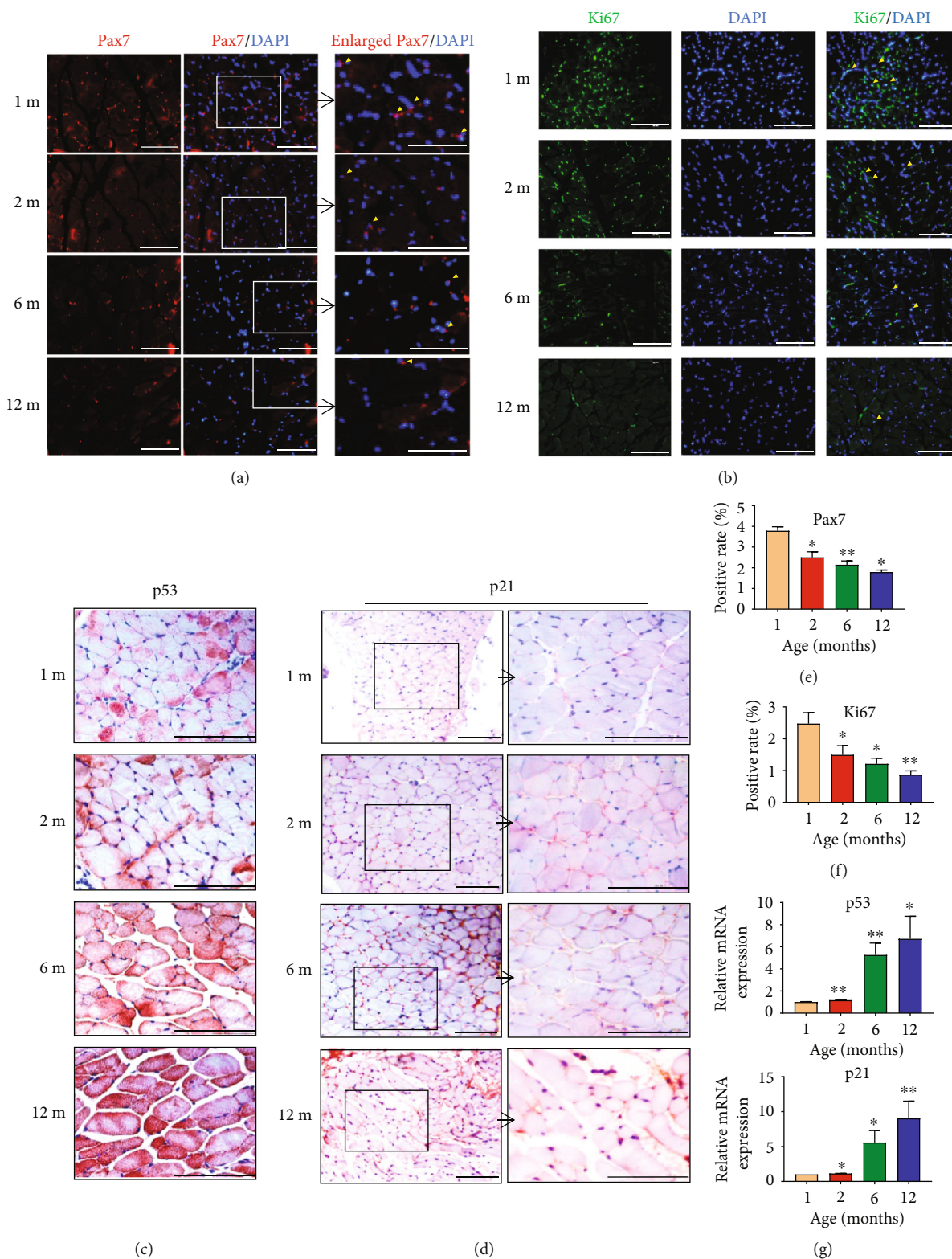


FIGURE 2: The renewal ability declined and senescence phenotype increased in aging GG. (a) Pax7, Pax7/DAPI, and enlarged Pax7/DAPI detected in GG muscles. (b) DAPI, Ki67, and Ki67/DAPI were detected in GG muscles. (c) The protein level of p53 was significantly increased in 12-month-old GG. (d) The protein level of p21 dramatically increased in 12-month-old GG compared to 1-month-old, 2-month-old, or 6-month-old. (e) Pax7-positive cells in GG significantly reduced in 12-month-old compared to 1-month-old. (f) Ki67-positive cells in GG greatly reduced in 12-month-old compared to 1-month-old. (g) The mRNA levels of p53 and p21 also upregulated in aging GG. \* $p < 0.05$  and \*\* $p < 0.01$ . Scale bars are 100  $\mu\text{m}$ .

for cell proliferation, was tested (Figure 2(b)). The results showed that Ki67-positive cells in the GG were reduced in 12-month-old (0.8%) compared with other age groups in Figure 2(f) (1 m: 2.5%; 2 m: 1.5%; and 6 m: 1.0%). Therefore, we concluded that the renewal function of GG decreased with aging.

Moreover, p53 and p21 are not only famous tumor suppressors but also members downstream of the aging and hypoxia signaling pathway [16, 17]. The senescence in GG was evaluated by the levels of p53 and p21. Immunohistochemistry analysis revealed that the protein levels of p53 and p21 were much higher in the GG of 12-month-old mice than young mice (Figures 2(c) and 2(d)). Meanwhile, p53 and p21 mRNA in 12-month-old were highest (p53  $\geq$  sixfold and p21  $\geq$  eightfold) among all age groups (Figure 2(g)). These findings discovered that p53 and p21 increased in aging GG.

**3.1.3. GG MuSCs Exhibited Worse Migration and Proliferation Abilities in Older Age.** OSA caused hypoxia and GG muscle injury. When the muscle is injured, MuSCs undergo differentiation into myocytes and fuse with each other in order to repair the injured muscle. Therefore, MuSCs are important functional cells in GG. To explore whether aging impaired GG MuSCs function, we derived GG MuSCs from four age groups of mice (Figure 3(a)). The cells were fixed after cultured 3 days. Immunofluorescence staining showed about 87% of isolated cells were Pax7-positive and 80% of cells were MyoD-positive (Figure 3(b)), which are the markers of MuSCs. The wound healing and the transwell migration chamber of GG MuSCs are shown (Figures 3(c) and 3(d)). Wound healing assay showed that the migration of GG MuSCs from 12-month-old was significantly slower than the other three groups (Figure 3(e)). The transwell migration chamber assay showed that GG MuSCs were all statistically significant among four age groups (Figure 3(e)). On the fourth day, the cell proliferation of 1-month-old mice was the fastest among the four age groups (Figure 3(f)). The GG MuSCs from 12 month-old mice exhibited decreased cell proliferation ability. These results suggested that aging impaired the migration and proliferation ability of GG MuSCs.

**3.1.4. p53/p21 Involved in Hypoxia and Aging Enhanced Hypoxia Response in GG MuSCs.** OSA is characterized by hypoxia during sleep. In order to imitate the hypoxia of OSA, cells were treated with 0  $\mu$ M and 200  $\mu$ M CoCl<sub>2</sub>, a typical chemical hypoxia model. p53 and p21 are not only famous tumor suppressors but also belong to a downstream signaling pathway of aging and hypoxia [16, 17]. Firstly, we detected the levels of p53 and p21. The results showed that p53 and p21 increased in GG MuSCs under hypoxia. The levels of p53 and p21 severely increased in 12-month-old compared to 1-month-old (Figures 4(a) and 4(b)). Meanwhile, p16 and BAX increased in hypoxia, especially in aging GG MuSCs, while BCL-2 decreased (Figure 4(c)). These results suggested that p53, p21, and p16 involved the function regulation in GG MuSCs under hypoxia. These gene

expressions were more obvious in GG MuSCs derived from aging muscle.

**3.1.5. Hypoxia Enhanced the Inhibitory Effect of Aging on GG MuSC Proliferation.** To explore whether hypoxia affected the proliferation of GG MuSCs, GG MuSCs were cultured under normoxia (0  $\mu$ M CoCl<sub>2</sub>) and hypoxia (200  $\mu$ M CoCl<sub>2</sub>). The results showed that the cell number under hypoxia was decreased to approximately 40% that of cells cultured under normoxia (Figure 5(a)). Then, we performed immunofluorescence staining for HIF-1 $\alpha$ , the master transcription factor in response to cell hypoxia [28]. Our results showed that CoCl<sub>2</sub> treatment induced high expression of HIF-1 $\alpha$ . The data confirmed its nuclear localization in the CoCl<sub>2</sub>-treated groups, while no fluorescence was detected in control cells (Figure 5(b)). Meanwhile, the results showed that the percentage of Pax7-positive cells under hypoxia (87.78%) were higher than cells under normoxia (83.53%). It demonstrated that hypoxia promoted MuSCs self-renewal function (Figure 5(b)). Ki67 is a marker protein of ribosomal RNA transcription, which is necessary for cellular proliferation [29]. The results showed that Ki67-positive cells from 12-month-old were significantly reduced compared to 1-month-old under normoxia, and the decrease was higher than that observed under hypoxia (Figure 5(c)). The results of negative control group without primary antibody were shown (Figure 5(d)). Together, our data suggested the toxicity of hypoxia and implied that hypoxia decreased the proliferation and promoted self-renewal function of GG MuSCs, especially in older age cells.

**3.1.6. Hypoxia Strengthened the Influence of Aging in the Differentiation of GG MuSCs and Increased p53 and p21 Expression.** When GG muscles are damaged, GG MuSCs differentiate into myotubes, which plays an important role in repairing the damaged tissues [30]. To explore the relationship between aging and GG MuSCs differentiation, we examined the levels of MyHC and MyoD. The results showed that under hypoxia, the number of myotubes in GG MuSCs was much less than that under normoxia. Importantly, the number of myotubes was also less in aging GG MuSCs than in young (Figure 6(a)). With increasing aging, MyHC did not have significant change, but hypoxia inhibited the MyHC expression. MyoD is immensely suppressed by hypoxia, especially in aging cells (Figures 6(b) and 6(c)). Under hypoxia, p53 and p21 proteins were accumulated. This accumulation is more obvious in aging cells (Figure 6(c)). The mRNA p53 and p21 were significantly increased under hypoxia. MyHC and MyoD mRNA were also decreased, and the reduction was more severe in aging than young cells (Figure 6(c)). In conclusion, hypoxia aggravated the influence of aging on the proliferation and differentiation of GG MuSCs and p53 and p21 involved in the process.

## 4. Discussion

The tissue homeostasis and organ function of multicellular organisms are gradually loss with aging. As aging, stem cell function has a progressive decline [31]. Therefore, the



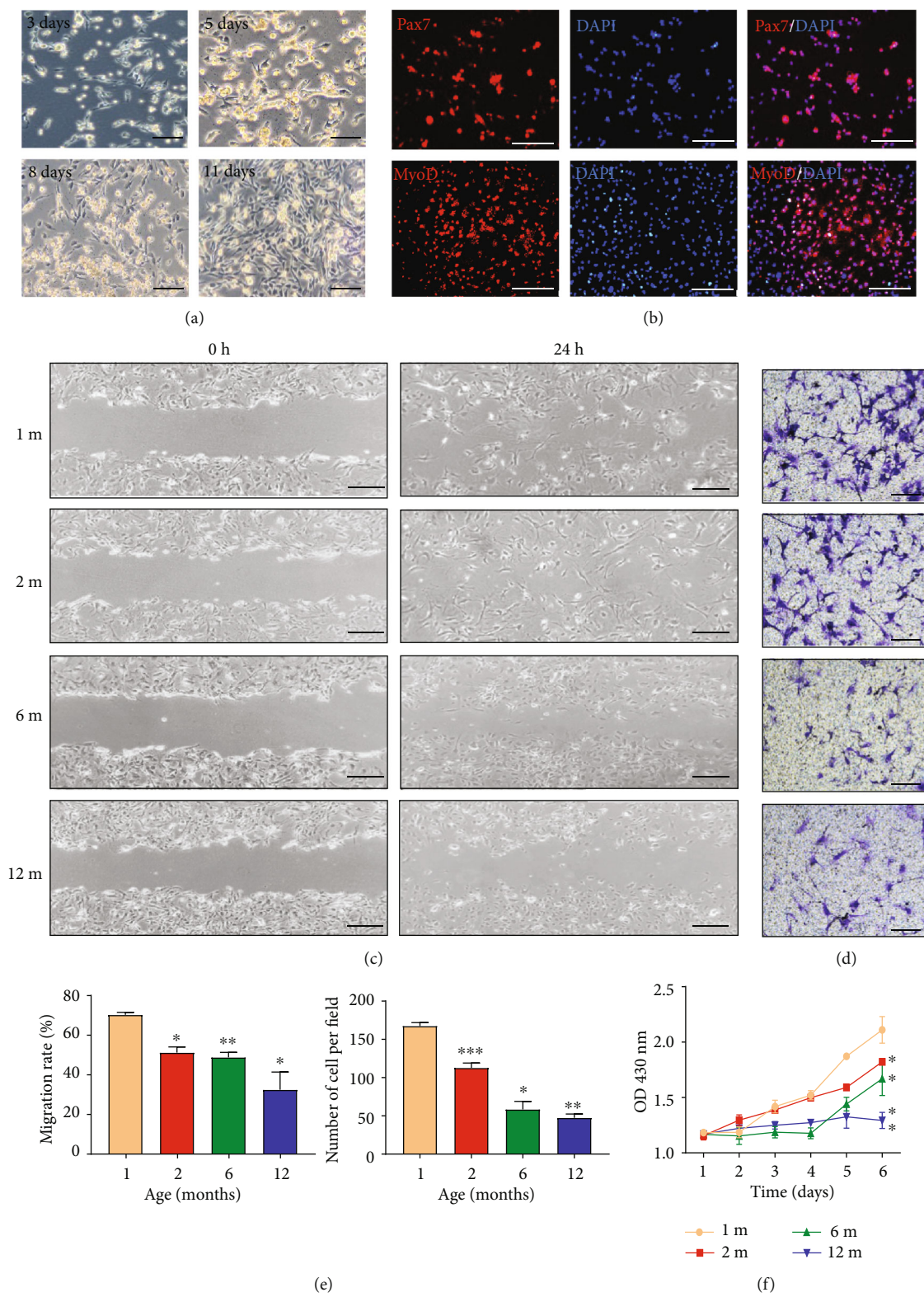


FIGURE 3: The proliferation and migration of GG MuSCs declined with aging. (a) Primary cells were obtained from GG muscle fibers, and cells showed a spindle morphology. (b) GG MuSC markers Pax7 and MyoD were positive in cells. (c) Wound healing of GG MuSCs derived from four age groups. (d) The migration of GG MuSCs derived from four age groups. (e) The wound healing and migration rate are significantly lower in 12-month-old compared to other age groups at 24 h. (f) The growth curve of GG MuSCs in four age groups. \* $p < 0.05$  and \*\* $p < 0.01$ . Scale bars are 100  $\mu\text{m}$ .

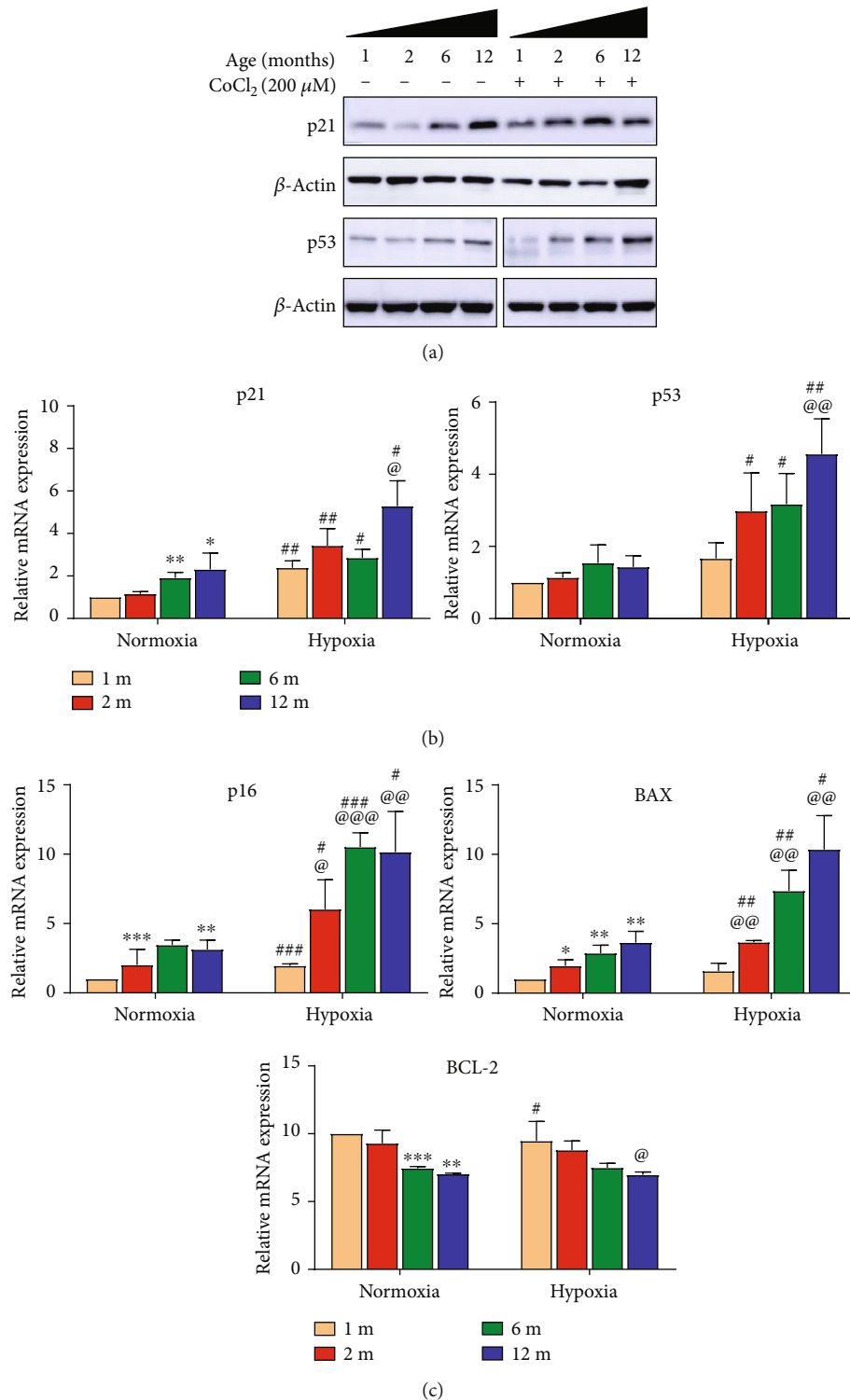


FIGURE 4: p53/p21 involved in hypoxia response in GG MuSCs. (a) The protein levels of p53 and p21 significantly increased under hypoxia, particularly in MuSCs derived from older age GG. (b) The mRNA levels of p53 and p21 also obviously grew up under hypoxia. The levels were higher in old GG MuSCs than in young. (c) The mRNA levels of p16 and BAX increased, while BCL-2 increased under hypoxia, especially in aging GG MuSCs. Statistical significance is marked as follows: \* represents the difference between normoxia and 1-month-old vs. 2-month-old vs. 6-month-old vs. 12-month-old;  $p < 0.05$ ,  $**p < 0.01$ , and  $***p < 0.001$ . @ represents the difference between hypoxia and 1-month-old vs. 2-month-old vs. 6-month-old vs. 12-month-old; @  $p < 0.05$ , @@  $p < 0.01$ , and @@@  $p < 0.001$ . # represents difference between same age and normoxia vs. hypoxia; #  $p < 0.05$ , ##  $p < 0.01$ , and ###  $p < 0.001$ .

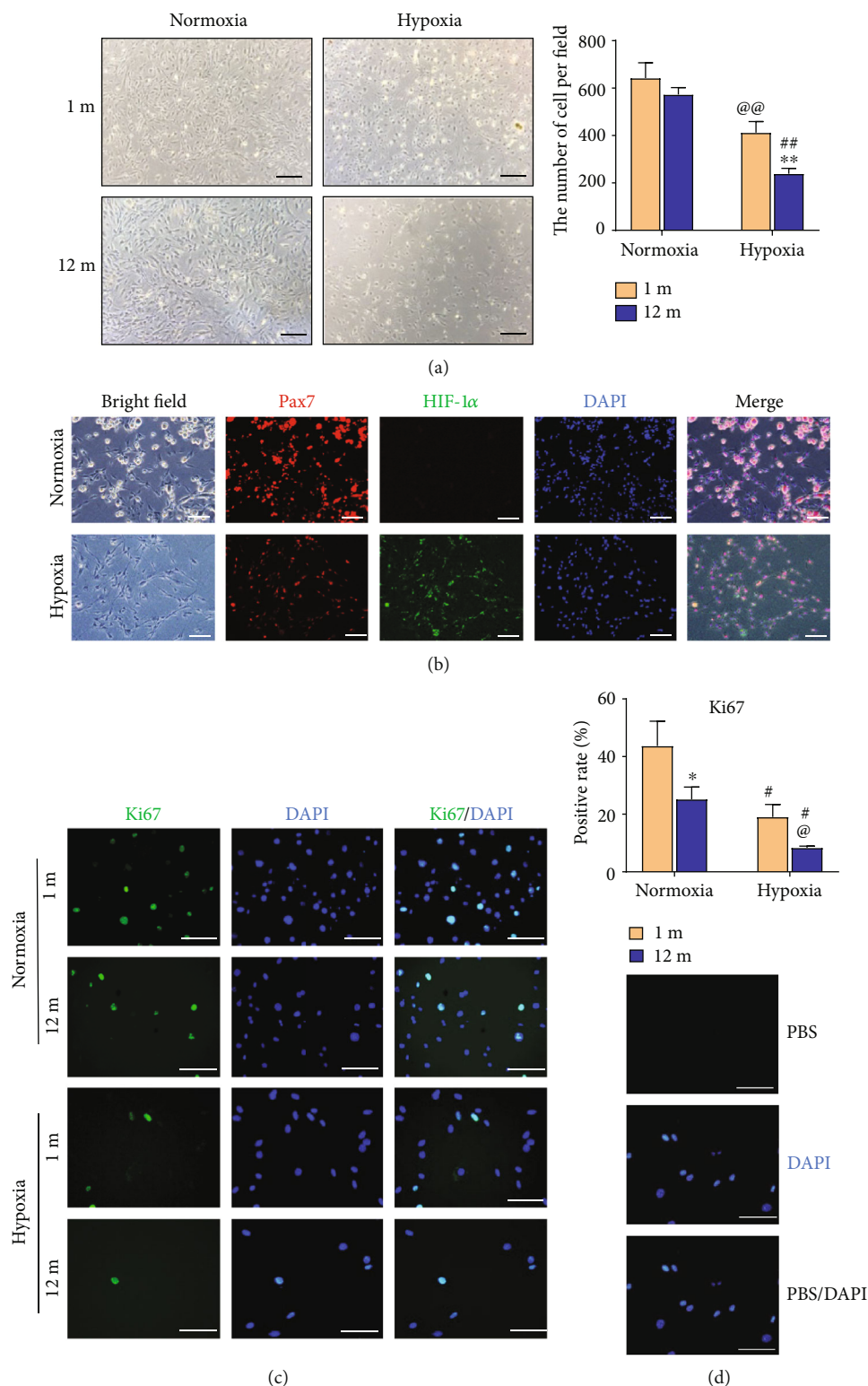
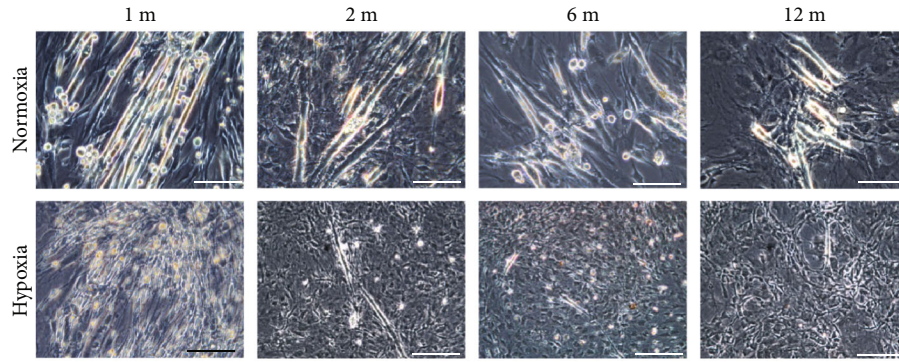
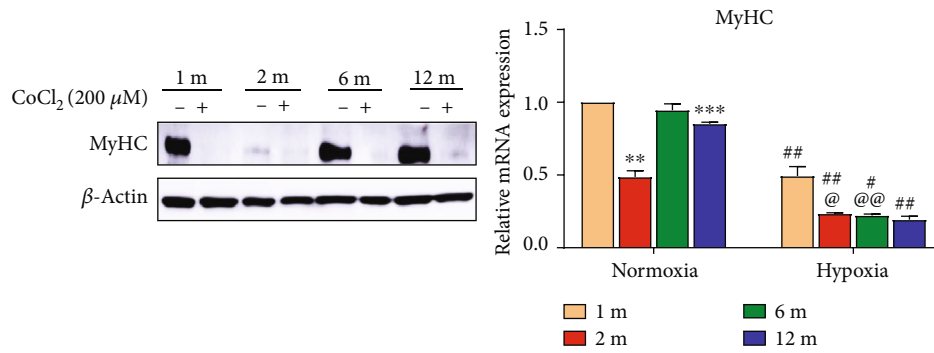


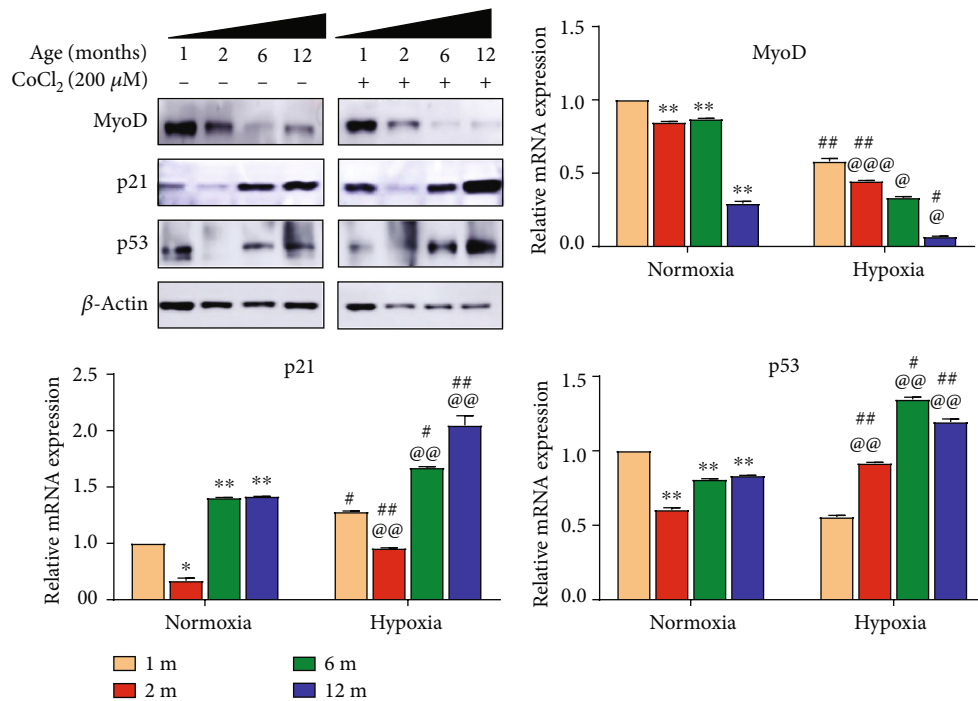
FIGURE 5: Hypoxia enhanced the inhibitory effect of aging on GG MuSC proliferation. (a) The GG MuSCs from 1-month-old and 12-month-old were treated with 0  $\mu\text{M}$  and 200  $\mu\text{M}$   $\text{CoCl}_2$  for 3 days. The cell number was decreased to approximately 40% that of untreated cells. (b) Immunofluorescence staining for Pax7 and HIF-1 $\alpha$  in MuSCs treated with or without  $\text{CoCl}_2$  for 3 days. (c) Ki67-positive cells in GG MuSCs under normoxia and hypoxia. Ki67 was observed by immunofluorescence staining. (d) The control experiment of IF. Statistical significance is marked as follows: \* represents difference between same  $\text{CoCl}_2$  and 1-month-old vs. 12-month-old; \* $p < 0.05$ , \*\* $p < 0.01$ , and \*\*\* $p < 0.001$ . @ represents the difference in 1-month-old and 0 vs. 200  $\mu\text{M}$   $\text{CoCl}_2$ ; @ $p < 0.05$  and @@ $p < 0.01$ . # represents the difference in 12-month-old and 0 vs. 200  $\mu\text{M}$   $\text{CoCl}_2$ ; # $p < 0.05$ , ## $p < 0.01$ , and ### $p < 0.001$ . Scale bars are 100  $\mu\text{m}$ .



(a)



(b)



(c)

FIGURE 6: Hypoxia strengthened the influence of aging on GG MuSC differentiation. (a) The differentiation of GG MuSCs from four age groups under normoxia and hypoxia. (b) The expression level of MyHC was tested after differentiation in normoxia and hypoxia. (c) p53, p21, and MyoD were observed after differentiation under normoxia and hypoxia. p53 and p21 significantly increased, and the expressions of MyHC and MyoD were markedly downregulated under hypoxia. Aging further inhibited the levels of MyHC and MyoD and increased the levels of p53 and p21. Statistical significance is marked as follows: \* represents the difference between normoxia and 1-month-old vs. 2-month-old vs. 6-month-old vs. 12-month-old; \* $p < 0.05$ , \*\* $p < 0.01$ , and \*\*\* $p < 0.001$ . @ represents the difference between hypoxia and 1-month-old vs. 2-month-old vs. 6-month-old vs. 12-month-old; @ $p < 0.05$ , @@ $p < 0.01$ , and @@@ $p < 0.001$ . # represents the difference between same age and normoxia vs. hypoxia; # $p < 0.05$ , ## $p < 0.01$ , and ### $p < 0.001$ . Scale bars are 100 μm in all images. Scale bars are 100 μm.

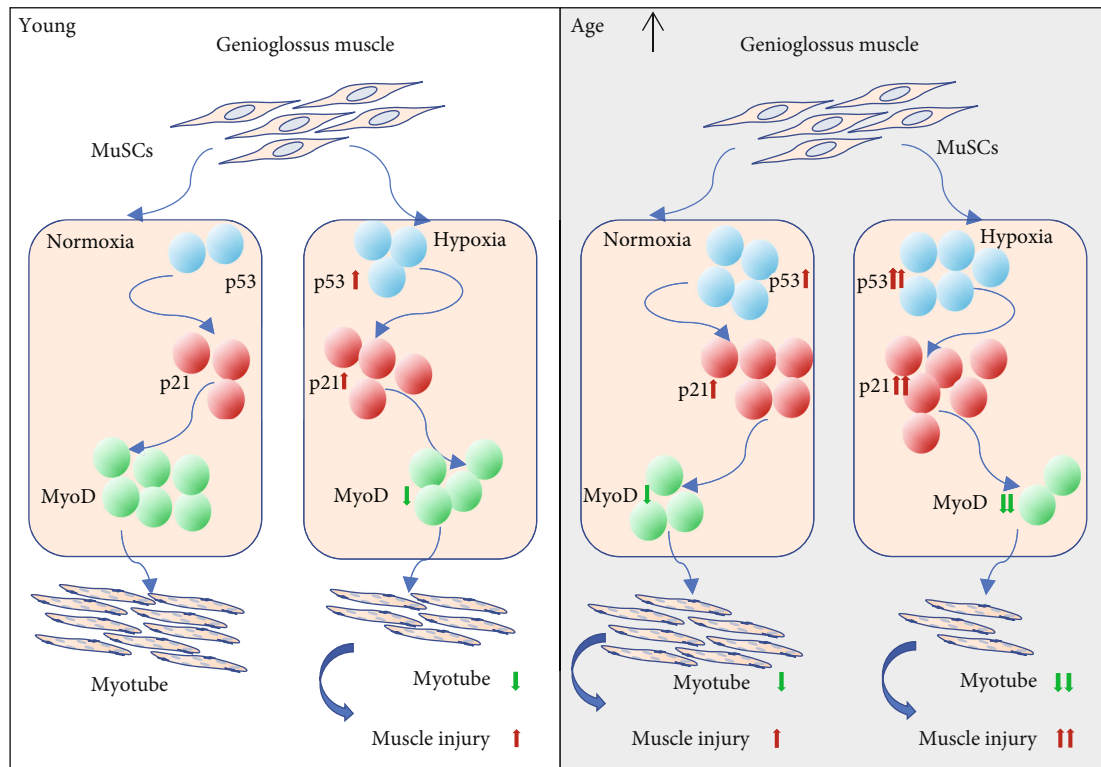


FIGURE 7: The diagrammatic sketch shows the damage mechanism of hypoxia and aging to genioglossus. Under hypoxia, increasing p53 and p21 induce the decline of MyoD. Then, low expression of MyoD leads to the reduction of myotube formation, especially in aging MuSCs. Finally, the results above enhance upper airway muscle injury.

decrease of tissue homeostasis can be attributed to an age-related decline of stem cells [12]. The genioglossus, a major upper airway dilator, has abundant blood supply and high specific gravity of the oxidized muscle fiber and is sensitive to oxygen and rapid contraction compared with other skeletal muscles [5]. In this study, we characterized the effects of aging and hypoxia on GG injury and investigated p53/p21 role in this process (Figure 7).

We firstly investigated that the tissue function, such as cross-sectional area, collagen content, genioglossus electromyographic activity, the Pax7-positive cells and the Ki67 positive cells in genioglossus, which were decreased with aging. Both mRNA and protein p53 and p21 increased in GG muscle tissue. We also displayed that the proliferation and migration of GG MuSCs decreased with aging. Therefore, we suggest that aging impaired the GG and its MuSCs function. We further verified the influence of hypoxia in MuSCs derived from aging GG. Our data suggested that the migration, proliferation, and differentiation capacity of GG MuSCs declined with aging. Hypoxia further enhanced this inhibition effect by increasing the levels of p53 and p21.

Previous reports show that the upper airway becomes more collapsible with aging [5]. The type IIa fibers have a significant decrease, and IIb fibers have an increase in aging upper airway muscles [7]. There are some age-related changes and endurance in GG muscle fiber, and aged rats showed decreased susceptibility to hypoxia-induced stress [7, 32]. Our group has reported that hypoxia inhibits the GG MuSCs proliferation and differentiation [23, 33]. How-

ever, little attention is focused on the interacting of hypoxia and aging to vicious circle on upper airway muscles. Our study firstly demonstrated the mechanism of aging and hypoxia on upper airway in molecular level.

We demonstrated that the GG MuSCs from 2-month-old mice have some abnormal changes compared to other age groups. p53 and p21 were the lowest among four age groups. It may be related to adolescent behavior. During adolescence, the development of brain changes can be dynamic [34, 35]. Neurologically, synaptic and pruning myelination are associated with brain maturation. These processes are assumed to occur in accordance with macroscopic anatomical changes. GG muscle is innervated by the sublingual nerve. When hypoglossal nerve is stimulated, the physiologic state of GG muscle changes [36]. We speculated that the changes of GG MuSCs from 2-month-old mice might be due to the development of adolescent stimuli from the hypoglossal nerve.

Our results may rich the therapeutic theory and provide some treatment base for OSA patients in aging population. Clinically, patients with OSA are regularly treated with mechanical dilation of the upper airway to alleviate the symptoms of airway collapse. These mechanical dilation methods have many shortcomings such as poor patient compliance and more complications. The older have a poorer prognosis for the treatment of mechanical dilation of the upper airway especially. Therefore, more evidence is needed to elucidate the underlying mechanisms of interactions between aging and hypoxia on GG muscle.

Our results suggested that hypoxia and aging interact to form a vicious circle with upregulation of p53 and p21, and this vicious hypoxia plus aging damage accelerated upper airway muscle injury. However, we know little about the mechanism of neurological control of EMG<sub>GG</sub>. Altered neurological control of the GG may be the primary mechanism of OSA [37]. Therefore, age-related factors altering neural control of GG may be important in the elderly. Meanwhile, more studies are expected to explore the neurological control mechanism of the aging GG.

In summary, our study displayed that the function of GG muscles and MuSCs was affected by the aging process. Meanwhile, hypoxia aggravated the influence of aging in the proliferation and differentiation of GG MuSCs by increasing p53 and p21. Our findings highlight the important role of p53/p21 on the GG muscle during the aging process, and it may provide therapeutic basis in the repair of OSA upper airway injury.

## 5. Conclusions

OSA is a serious upper airway block problem. A population of more than 100 million is tolerant to this disease. OSA brings hypoxia and upper airway muscle injury. However, the damage mechanism of hypoxia and aging to the genioglossus is still unknown. In this study, we firstly discovered the effects of aging and hypoxia on GG MuSCs and showed detailed property analysis of mouse GG MuSCs. We found that aging affected the function of GG tissue and its MuSCs. Hypoxia suppressed the proliferation of mouse GG MuSCs, especially in MuSCs derived from aging GG, by increasing the expression levels of p53/p21. Identification of p53/p21 functions to mouse GG MuSCs may be helpful to understand cell senescence. Our study may benefit to reduce the airway obstruction and benefit the OSA therapies.

## Data Availability

The data used to support the findings of this study are included within the article.

## Conflicts of Interest

The authors declare that there is no conflict of interest regarding the publication of this paper.

## Acknowledgments

We appreciate Zhi-Wen Zhou and Ling-Ling Zhang for their intellectual help on this project. The paper is supported by a National Natural Science Foundation of China grant (81901031 and 81771109), Natural Science Foundation of Shanghai grant (19ZR1445400), General Program Shanghai Municipal Health and Family Planning Commission grant (201740091), and innovation action project of Shanghai Science and Technology Commission-laboratory animal models (grant number 15140903500).

## References

- [1] W. Qin, Y. B. H. Zhang, B. L. Deng, J. Liu, H. L. Zhang, and Z. L. Jin, "miR-17-5p modulates mitochondrial function of the genioglossus muscle satellite cells through targeting Mfn2 in hypoxia," *Journal of Biological Regulators and Homeostatic Agents*, vol. 33, no. 3, pp. 753–761, 2019.
- [2] H. Wang, D. Zhang, S. Jia et al., "Effect of sustained hypoxia on autophagy of genioglossus muscle-derived stem cells," *Medical Science Monitor : international medical journal of experimental and clinical research*, vol. 24, pp. 2218–2224, 2018.
- [3] G. Magliulo, M. de Vincentiis, G. Iannella et al., "Olfactory evaluation in obstructive sleep apnoea patients," *Acta Otorhinolaryngologica Italica*, vol. 38, no. 4, pp. 338–345, 2018.
- [4] T. Young, E. Shahar, F. J. Nieto et al., "Predictors of sleep-disordered breathing in community-dwelling adults: the Sleep Heart Health Study," *Archives of Internal Medicine*, vol. 162, no. 8, pp. 893–900, 2002.
- [5] F. J. Sériès, S. A. Simoneau, S. St Pierre, and I. Marc, "Characteristics of the genioglossus and musculus uvulae in sleep apnea hypopnea syndrome and in snorers," *American Journal of Respiratory and Critical Care Medicine*, vol. 153, no. 6, pp. 1870–1874, 1996.
- [6] A. D. Ray, T. Ogasa, U. J. Magalang, J. A. Krasney, and G. A. Farkas, "Aging increases upper airway collapsibility in Fischer 344 rats," *Journal of Applied Physiology*, vol. 105, no. 5, pp. 1471–1476, 2008.
- [7] A. Oliven, N. Carmi, R. Coleman, M. Odeh, and M. Silbermann, "Age-related changes in upper airway muscles morphological and oxidative properties," *Experimental Gerontology*, vol. 36, no. 10, pp. 1673–1686, 2001.
- [8] P. Feige and M. A. Rudnicki, "Muscle stem cells," *Current Biology: CB*, vol. 28, no. 10, pp. R589–R590, 2018.
- [9] P. Bi, A. Ramirez-Martinez, H. Li et al., "Control of muscle formation by the fusogenic micropeptide myomixer," *Science*, vol. 356, no. 6335, pp. 323–327, 2017.
- [10] A. A. Cutler and B. B. Olwin, "Muscling in on the awesome proliferative power of the terrible teratoma," *Cell Stem Cell*, vol. 23, no. 1, pp. 1–2, 2018.
- [11] P. Zhu, C. Zhang, Y. Gao, F. Wu, Y. Zhou, and W. S. Wu, "The transcription factor Slug represses p16<sup>Ink4a</sup> and regulates murine muscle stem cell aging," *Nature Communications*, vol. 10, no. 1, p. 2568, 2019.
- [12] L. Li, M. Rozo, S. Yue et al., "Muscle stem cell renewal suppressed by GAS1 can be reversed by GDNF in mice," *Nature Metabolism*, vol. 1, no. 10, pp. 985–995, 2019.
- [13] S. Wang, Y. Zheng, J. Li et al., "Single-cell transcriptomic atlas of primate ovarian aging," *Cell*, vol. 180, no. 3, pp. 585–600.e19, 2020.
- [14] A. Gupta, K. Shah, M. J. Oza, and T. Behl, "Reactivation of p53 gene by MDM2 inhibitors: a novel therapy for cancer treatment," *Biomedicine & Pharmacotherapy = Biomedecine & Pharmacotherapie*, vol. 109, pp. 484–492, 2019.
- [15] A. Rufini, P. Tucci, I. Celardo, and G. Melino, "Senescence and aging: the critical roles of p53," *Oncogene*, vol. 32, no. 43, pp. 5129–5143, 2013.
- [16] L. Liu, G. W. Charville, T. H. Cheung et al., "Impaired notch signaling leads to a decrease in p53 activity and mitotic catastrophe in aged muscle stem cells," *Cell Stem Cell*, vol. 23, no. 4, pp. 544–556.e4, 2018.

- [17] T. J. Humpton and K. H. Vousden, "Regulation of cellular metabolism and hypoxia by p53," *Cold Spring Harbor perspectives in medicine*, vol. 6, no. 7, p. a026146, 2016.
- [18] M. M. Ziaaldini, E. Koltai, Z. Csende et al., "Exercise training increases anabolic and attenuates catabolic and apoptotic processes in aged skeletal muscle of male rats," *Experimental Gerontology*, vol. 67, pp. 9–14, 2015.
- [19] S. Mizuno, H. J. Bogaard, D. Kraskauskas et al., "p53 gene deficiency promotes hypoxia-induced pulmonary hypertension and vascular remodeling in mice," *American Journal of Physiology. Lung Cellular and Molecular Physiology*, vol. 300, no. 5, pp. L753–L761, 2011.
- [20] N. Chinzei, S. Hayashi, T. Ueha et al., "P21 deficiency delays regeneration of skeletal muscular tissue," *PLoS One*, vol. 10, no. 5, p. e0125765, 2015.
- [21] W. Ding and Y. Liu, "Genistein attenuates genioglossus muscle fatigue under chronic intermittent hypoxia by down-regulation of oxidative stress level and up-regulation of antioxidant enzyme activity through ERK1/2 signaling pathway," *Oral Diseases*, vol. 17, no. 7, pp. 677–684, 2011.
- [22] Y. H. Liu, Y. Huang, and X. Shao, "Effects of estrogen on genioglossal muscle contractile properties and fiber-type distribution in chronic intermittent hypoxia rats," *European Journal of Oral Sciences*, vol. 117, no. 6, pp. 685–690, 2009.
- [23] W. Li and Y. H. Liu, "Effects of phytoestrogen genistein on genioglossus function and oestrogen receptors expression in ovariectomized rats," *Archives of Oral Biology*, vol. 54, no. 11, pp. 1029–1034, 2009.
- [24] Y. Yang, M. Gao, Z. Lin et al., "DEK promoted EMT and angiogenesis through regulating PI3K/AKT/mTOR pathway in triple-negative breast cancer," *Oncotarget*, vol. 8, no. 58, pp. 98708–98722, 2017.
- [25] M. Polotsky, A. S. Elsayed-Ahmed, L. Pichard et al., "Effect of age and weight on upper airway function in a mouse model," *Journal of Applied Physiology*, vol. 111, no. 3, pp. 696–703, 2011.
- [26] S. S. K. Chan, R. W. Arpke, A. Filaretto et al., "Skeletal muscle stem cells from PSC-derived teratomas have functional regenerative capacity," *Cell Stem Cell*, vol. 23, no. 1, pp. 74–85.e6, 2018.
- [27] P. Seale, L. A. Sabourin, A. Girgis-Gabardo, A. Mansouri, P. Gruss, and M. A. Rudnicki, "Pax7 is required for the specification of myogenic satellite cells," *Cell*, vol. 102, no. 6, pp. 777–786, 2000.
- [28] S. Mason and R. S. Johnson, "The role of HIF-1 in hypoxic response in the skeletal muscle," *Advances in Experimental Medicine and Biology*, vol. 618, pp. 229–244, 2007.
- [29] R. Rahmzadeh, G. Huttman, J. Gerdes, and T. Scholzen, "Chromophore-assisted light inactivation of pKi-67 leads to inhibition of ribosomal RNA synthesis," *Cell Proliferation*, vol. 40, no. 3, pp. 422–430, 2007.
- [30] M. Buckingham and D. Montarras, "Skeletal muscle stem cells," *Current Opinion in Genetics & Development*, vol. 18, no. 4, pp. 330–336, 2008.
- [31] D. L. Jones and T. A. Rando, "Emerging models and paradigms for stem cell ageing," *Nature Cell Biology*, vol. 13, no. 5, pp. 506–512, 2011.
- [32] J. R. Skelly, R. A. O'Connell, J. F. X. Jones, and K. D. O'Halloran, "Structural and functional properties of an upper airway dilator muscle in aged obese male rats," *Respiration*, vol. 82, no. 6, pp. 539–549, 2011.
- [33] Y. Huang and Y. H. Liu, "Effects of phytoestrogens on genioglossus contractile properties in ovariectomized rats exposed to chronic intermittent hypoxia may be independent of their estrogenicity," *European Journal of Oral Sciences*, vol. 119, no. 2, pp. 128–135, 2011.
- [34] B. J. Casey, R. M. Jones, and T. A. Hare, "The adolescent brain," *Annals of the New York Academy of Sciences*, vol. 1124, pp. 111–126, 2008.
- [35] R. D. Fields, "Myelination: an overlooked mechanism of synaptic plasticity?," *The Neuroscientist*, vol. 11, no. 6, pp. 528–531, 2016.
- [36] M. F. Pengo and J. Steier, "Emerging technology: electrical stimulation in obstructive sleep apnoea," *Journal of Thoracic Disease*, vol. 7, no. 8, pp. 1286–1297, 2015.
- [37] S. C. Veasey, G. Zhan, P. Fenik, and D. Pratico, "Long-term intermittent hypoxia: reduced excitatory hypoglossal nerve output," *American Journal of Respiratory and Critical Care Medicine*, vol. 170, no. 6, pp. 665–672, 2004.

## Research Article

# Human Fat-Derived Mesenchymal Stem Cells Xenogenically Implanted in a Rat Model Show Enhanced New Bone Formation in Maxillary Alveolar Tooth Defects

Andrew Wofford,<sup>1</sup> Austin Bow,<sup>2</sup> Steven Newby,<sup>2</sup> Seth Brooks,<sup>3</sup> Rachel Rodriguez,<sup>2</sup> Tom Masi,<sup>4</sup> Stacy Stephenson,<sup>4</sup> Jack Gotcher,<sup>3</sup> David E. Anderson,<sup>2</sup> Josh Campbell,<sup>3</sup> and Madhu Dhar <sup>2</sup>

<sup>1</sup>Department of Biochemistry and Cellular and Molecular Biology, College of Arts and Sciences, University of Tennessee, Knoxville, TN 37916, USA

<sup>2</sup>Department of Large Animal Clinical Sciences, College of Veterinary Medicine, University of Tennessee, Knoxville, TN 37996, USA

<sup>3</sup>Department of Oral and Maxillofacial Surgery, University of Tennessee Medical Center, Knoxville, TN 37920, USA

<sup>4</sup>Graduate School of Medicine, Department of Surgery, University of Tennessee, Knoxville, TN 37920, USA

Correspondence should be addressed to Madhu Dhar; mdhar@utk.edu

Received 14 September 2019; Revised 21 November 2019; Accepted 13 December 2019; Published 13 January 2020

Guest Editor: Toru Ogasawara

Copyright © 2020 Andrew Wofford et al. This is an open access article distributed under the Creative Commons Attribution License, which permits unrestricted use, distribution, and reproduction in any medium, provided the original work is properly cited.

**Background.** Due to restorative concerns, bone regenerative therapies have garnered much attention in the field of human oral/maxillofacial surgery. Current treatments using autologous and allogenic bone grafts suffer from inherent challenges, hence the ideal bone replacement therapy is yet to be found. Establishing a model by which MSCs can be placed in a clinically acceptable bone defect to promote bone healing will prove valuable to oral/maxillofacial surgeons. **Methods.** Human adipose tissue-derived MSCs were seeded onto Gelfoam<sup>®</sup> and their viability, proliferation, and osteogenic differentiation was evaluated *in vitro*. Subsequently, the construct was implanted in a rat maxillary alveolar bone defect to assess *in vivo* bone healing and regeneration. **Results.** Human MSCs were adhered, proliferated, and uniformly distributed, and underwent osteogenic differentiation on Gelfoam<sup>®</sup>, comparable with the tissue culture surface. Data confirmed that Gelfoam<sup>®</sup> could be used as a scaffold for cell attachment and a delivery vehicle to implant MSCs *in vivo*. Histomorphometric analyses of bones harvested from rats treated with hMSCs showed statistically significant increase in collagen/early bone formation, with cells positive for osteogenic and angiogenic markers in the defect site. This pattern was visible as early as 4 weeks post treatment. **Conclusions.** Xenogenically implanted human MSCs have the potential to heal an alveolar tooth defect in rats. Gelfoam<sup>®</sup>, a commonly used clinical biomaterial, can serve as a scaffold to deliver and maintain MSCs to the defect site. Translating this strategy to preclinical animal models provides hope for bone tissue engineering.

## 1. Background

Several clinical studies show a need for stronger, faster, and more reliable bone formation in defects or fractures following surgery, disease, or trauma. Cell-based therapies offer the potential to overcome these challenges, especially in dental and craniofacial healing [1, 2]. This is specifically a challenge in cases of larger defects or defects that are of complex anatomical shapes and sizes and require strong,

mature bone regeneration for future implants. Additionally, in the field of oral and maxillofacial medicine, a relatively simple tooth extraction procedure, if not controlled, can lead to significant complications, including infection and osteonecrosis. Residual ridge resorption, resulting in reduced buccolingual and apicocoronal aspects at the site of extraction, is another common phenomenon that causes physical and economic concerns in human patients [3]. Furthermore, tooth extraction procedures are considered to be a major risk



factor for bisphosphonate-induced osteonecrosis of the jaw (ONJ) [4]. If not treated promptly, this disorder can lead to complex morbidities and the loss of the entire jaw bone. Hence, there is a need for therapies capable of regenerating healthy new bone after such procedures, and thus preventing further complications.

Bone tissue engineering strategies include the use of viable cells in conjunction with biomaterials or scaffolds. Several bone tissue engineering studies have shown preference for using naïve, adult mesenchymal stem cells (MSCs) instead of differentiated osteoblasts for bone formation applications. Cells alone or cells combined with biomaterials may offer advantages compared to the results associated with the use of allografts or autografts. Human MSCs (hMSCs) are naïve multipotent cells which can be isolated from any adult tissue, including the bone marrow, fat, cord blood, and dental pulp. Adult MSCs are capable of differentiation to adipocytes, myocytes, chondrocytes, and osteoblasts, with these stem cell properties having been demonstrated *in vitro* and *in vivo* [5–8]. MSCs are typically expanded in culture, evaluated for their characteristics, and induced to undergo osteogenic differentiation, *in vitro*. Subsequent to the expansion and characterization, they are transplanted *in vivo* for therapy. Their efficacy is influenced by the complex *in vivo* microenvironment as well as the cellular and molecular properties of MSCs. Human MSCs have been shown to demonstrate significant beneficial effects on bone healing and repair of the appendicular, axial, and craniomaxillofacial bones [9, 10].

Another important component of bone tissue engineering is the use of scaffolds or biomaterials capable of serving as a delivery vehicle and a containment agent to hold cells at the defect site *in vivo*. Several commercially available materials have been reported to deliver MSCs, including porous and gelatin-based scaffolds [11–13]. Even though there are a number of commercially available cell delivery materials, prohibitive factors, including high costs or technical challenges in application, restrict general use. Most importantly, an ideal bone regeneration scaffold, which is osteoinductive, osteoconductive, and osseointegrative has yet to be developed [14, 15]. As a result, autogenous bone grafts remain the gold standard.

Gelfoam®, a gelatin-based material, is commonly used as a contact hemostat in healthcare facilities. A porous, pliable, and cost-effective material, Gelfoam® is also referred to as hydrolyzed collagen and is comprised of a proteinous material, which is generally prepared by boiling skin, tendons, ligaments, and/or bones with water. Hence, Gelfoam® does not by itself demonstrate any osteogenic properties, and thus can be used to deliver and evaluate the effect of MSCs on bone healing without any confounding factors. A study showed promising results for Gelfoam® as a hMSC delivery vehicle by analyzing loading kinetics, cellular distribution, cellular density using several biochemical assays, and its biocompatibility using a rabbit joint model [16].

We hypothesized that hMSCs will readily attach and proliferate on degradable clinical grade Gelfoam® structures and that delivery of xenogenic cells via this nonbioactive vehicle in a rat maxillary tooth extraction model will promote repair

and restoration of bone tissue at defect sites. As the implanted material does not have inherent osteobiologic properties, bone tissue regeneration capacity of the examined treatment will allow for evaluation of the osteogenic potential of MSCs alone *in vivo*. Based on the potential of MSCs to differentiate toward multiple lineages, including bone, it is anticipated that the application of a reservoir of these naïve cells, maintained at the site of injury via a bioinert structure, will result in enhanced repair of damaged tissue.

## 2. Methods

**2.1. Biochemicals and Disposables.** All biochemicals, cell culture supplements, and disposable tissue culture supplies were purchased from Thermo Fisher Scientific unless otherwise noted.

**2.2. Gelfoam® as a Scaffold Material.** Commercially obtained Gelfoam®, Pfizer, is a purified gelatin material derived from porcine skin that is stored at 15–30°C until use (Pfizer USP, Michigan, USA). Materials for *in vitro* and *in vivo* experiments were cut to size from bulk sheets.

**2.3. Isolation, Ex Vivo Expansion, and In Vitro Osteogenesis of Human Mesenchymal Stem Cells.** Stromal vascular fraction of cells was obtained from human adipose tissue from patients undergoing panniculectomies in accordance to a protocol approved by the IRB at the University of Tennessee Medical Center. Informed client consent was obtained prior to the harvest. The hMSCs were isolated, *ex vivo* expanded, and induced to undergo osteogenesis as described earlier [17]. Briefly, the hMSCs were grown to 80–90% confluency and then harvested with 0.05% trypsin/EDTA for cryopreservation (80% FBS, 10% DMEM/F12, 10% DMSO), or split and seeded into new flasks for *in vitro* assays and expansion, respectively. All experiments were performed using cells from passage 2–6 in complete growth media (DMEM/F12, 1% penicillin-streptomycin/amphotericin B, 10% FBS).

MSCs obtained were confirmed for their identity by their morphology, potential to undergo trilineage differentiation, and expression of specific protein markers, using methods reported earlier [17].

*In vitro* experiments were performed on identical passage numbers of hMSCs seeded simultaneously on Gelfoam® and the tissue culture substrates. Growth and osteogenic differentiation of hMSCs on the two substrates were carried out simultaneously.

**2.4. RNA Extraction, cDNA Synthesis, and qPCR.** RNA was extracted from both control hMSC cultures, grown on a polystyrene coated tissue culture surface and Gelfoam®-embedded hMSCs at days 7 and 21 of differentiation. Total RNA was isolated using TRIzol extraction agent (Thermo Fisher) as per the manufacturer's protocol and as reported earlier [18]. Briefly, total RNA was prepared and further purified using a RNeasy mini kit (Qiagen); cDNA was prepared using a high-capacity cDNA reverse transcription kit (Applied Biosystems); and qPCR analysis of the expression of the bone-specific markers osteopontin (OPN) and osteocalcin (OCN) was carried out using SYBR green master mix

(Thermo Fisher) with GAPDH serving as the housekeeping gene using MX3005P real-time PCR cycler (Agilent).

Several preliminary experiments were run to determine ideal qPCR protocol, PCR mix, and annealing temperatures. qPCR was run using ABsolute Blue qPCR Mix (Thermo Fisher Scientific), with each reaction comprising of 5.0  $\mu$ L cDNA solution, 12.5  $\mu$ L Absolute Blue SYBR Green ROX, 5.0  $\mu$ L RNase Free Water, and 2.5  $\mu$ L of the appropriate primers. All primer sequences and PCR conditions were derived from a previously published report [5].

**2.5. Animals and Surgical Procedure.** 8-10 week old mixed gender Sprague Dawley rats ( $n = 36$ ) were commercially obtained (Harlan Laboratories).

Animal procedures were performed in accordance with a protocol approved by the University of Tennessee, Institutional Animal Care and Use Committee (IACUC). Bone defects were generated using procedures modified from those described earlier [19–21]. Briefly, rats under anesthesia were placed in a supine position, and the mandible was opened to expose the maxillary surface. 1<sup>st</sup> and the 2<sup>nd</sup> maxillary molars were removed from one side, and the resulting void spaces in the alveolar processes were then levelled using a microdrill to form a slot-shaped trough in which the scaffold could be readily implanted. Defects were washed thoroughly with sterile saline to remove residual tissue debris. Scaffold material with and without cells was firmly placed in each defect prior to closure of the site with resorbable sutures. The side opposite to the defect was left intact to serve as a reference during histological analysis. The rats were fed a soft gel (Nutra-Gel, Bio-Serv) throughout the study period to prevent damage to surgical sites by standard dry pellet form food. Animals were sacrificed at weeks 1, 4, and 12 after surgery. Rats were divided into two groups with 6 rats per group per time point. One group received Gelfoam<sup>®</sup> alone, while the other group was treated with Gelfoam<sup>®</sup> loaded with  $1 \times 10^6$  hMSCs, which were seeded onto Gelfoam<sup>®</sup> 30-60 minutes prior to implantation.

**2.6. Histomorphometry.** Samples were harvested after sacrifice and subjected to histomorphometric processing and analyses as reported earlier [18]. All bones were fixed in Decal A for at least 24 hrs, following which, they were immersed in Decal B for at least 48 hrs for decalcification. Subsequently, 5  $\mu$ m sagittal sections were obtained and stained with hematoxylin and eosin (H&E) and Masson trichrome for analysis.

H&E staining was used to subjectively evaluate adverse reaction, if any due to either the Gelfoam<sup>®</sup> or the Gelfoam<sup>®</sup>+hMSCs construct. Masson's trichrome staining was evaluated and quantitated using Fiji software [22]. Two micrograph images of each slide were taken at 2.5x. Images included both the region where the alveolar bone defect was created and the region of the corresponding contralateral intact tooth and alveolar bone. Image colors were split into channels and threshold was adjusted to generate binary masks highlighting bone tissue surface. Regions of interest (ROI) were identified by using the rectangular selection tool to set the parameters of the alveolar bone tissue where the

intact tooth is shown rooted. This selection was then transferred to an analogous site on contralateral defect side to maintain equal area and shape of the measured region. The percentage of bone tissue area coverage (BTAC) for ROIs of each image was calculated (Equation (1)). For each rat, the percentage of bone tissue area coverage in the defect region was divided by that in the intact region to obtain a bone regeneration ratio (BRR) for each defect (Equation (2)). The bone regeneration of the control (Gelfoam<sup>®</sup> only) and the Gelfoam<sup>®</sup>+hMSC-treated rats was compared at each time point of sacrifice (1, 4, and 12 weeks).

$$\frac{P \times \text{Count}_B}{P \times \text{Count}_T} = \text{BTAC} \quad (1)$$

Equation (1) is for determining bone tissue area coverage (BTAC) for a given binary image in which the tissue of interest has been set to the maximum value. The measured pixel count for maximum value pixels is divided by the total count of image pixels. This ratio represents the fractional area coverage of the tissue of interest.

$$\frac{\text{BTAC}_D}{\text{BTAC}_I} = \text{BRR} \quad (2)$$

Equation (2) is for determining the bone regeneration ratio (BRR) of a given complimentary set of intact and defect images. The bone tissue area coverage (BTAC) for the defect image of the set ( $\text{BTAC}_D$ ) is divided by that of the intact image ( $\text{BTAC}_I$ ). The ratio represents the level of bone formation within the defect site as compared with that of the native structure.

**2.7. Immunohistochemistry.** Unstained histological sections were subjected to immunohistochemical (IHC) staining to detect and analyze expression of proteins associated with bone, collagen, and vasculature structure formation. OPN and fibronectin (FN) expression correlate to early bone formation and cellular attachment, respectively, while the hematopoietic stem cell marker, CD34, represents angiogenic functions. Paraffin-embedded sections for IHC staining were prepared according to a standard protocol (Abcam IHC Protocol). Briefly, samples were deparaffinized in xylenes and rehydrated using decreasing concentrations of ethanol, ending with washing in distilled water. Antigen retrieval was performed utilizing a heated target retrieval agent (DAKO). Samples were exposed to 1% Triton in PBS and subsequent protein blocking solution prior to addition of primary antibodies. Biotinylated secondary antibody solutions targeting primary antibody host species IgG were followed by the addition of streptavidin-horseradish peroxidase (HRP). A Nova Red (Vector) kit was then utilized to stain HRP-labeled surface proteins for analysis.

Imaging of IHC-stained slides was performed with a Leica DM11 light microscope at 5x magnification. Captured images were combined utilizing a FIJI stitching plugin, designed by Dr. Preibisch, to generate full tissue section images.

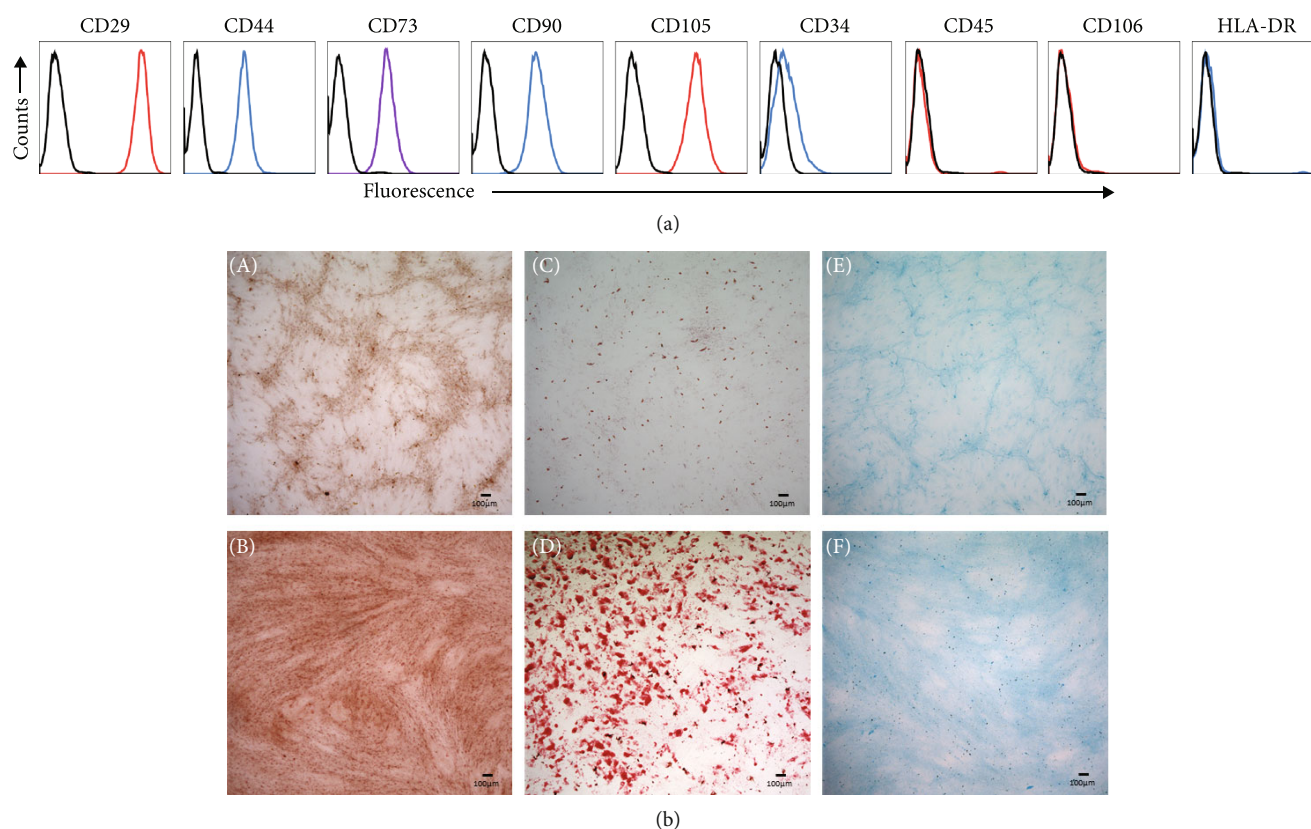


FIGURE 1: *In vitro* characterization of human MSCs. Immunophenotyping of hMSCs by flow cytometry (a) and trilineage differentiation (b). For immunophenotyping, hMSCs were stained with the indicated antibodies and then analyzed by flow cytometry. Cells strongly express the markers (CD29, CD44, CD73, CD90, CD105) associated with the MSCs, while expression of hematopoietic (CD34, CD45, HLA-DR) and endothelial (CD106) markers is markedly reduced. Black open histograms indicate isotype-matched controls for each antibody; colored open histograms represent positive reactivity. Trilineage differentiation assays of hMSCs shows representative images of alizarin red, oil-red-o, and Alcian blue staining of osteocytes (B), adipocytes (D), and chondrocytes (F), after *in vitro* differentiation. Corresponding undifferentiated hMSCs (A, C, E) are shown as controls.

**2.8. Statistical Analyses.** For the RT-qPCR gene expression analysis, expression levels of each gene were normalized with GAPDH, serving as a housekeeping gene. Gene expression of the tissue culture seeded hMSCs was evaluated to ensure the accuracy of the real-time PCR conditions. Gene expression fold levels of both the Gelfoam®+hMSCs and tissue culture seeded hMSCs groups' were analyzed at day 21 relative to day 7. Fold changes for each gene were calculated using the  $2^{-\Delta\Delta C_T}$  formula (Applied Biosystems). Data was statistically analyzed using Student's *t* test with  $p < 0.05$ .

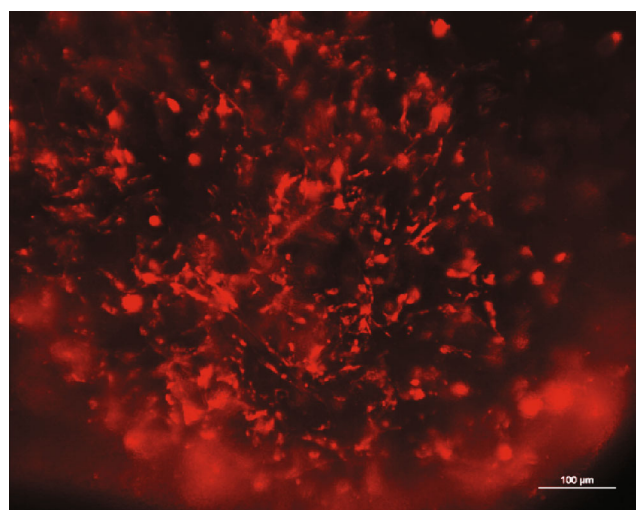
For the quantitative analysis of the rat alveolar bone healing, the level of bone formation obtained from the BRR values was analyzed using two-way ANOVA to evaluate the time (weeks of treatment) and group (scaffold alone and scaffold with MSCs) effects. Post hoc multiple comparisons were performed with Tukey's adjustment. Statistical significance was set at  $p < 0.05$ . All analyses were conducted using SAS 9.4 TS1M4 for Windows 64x (SAS Institute Inc., Cary, NC).

### 3. Results

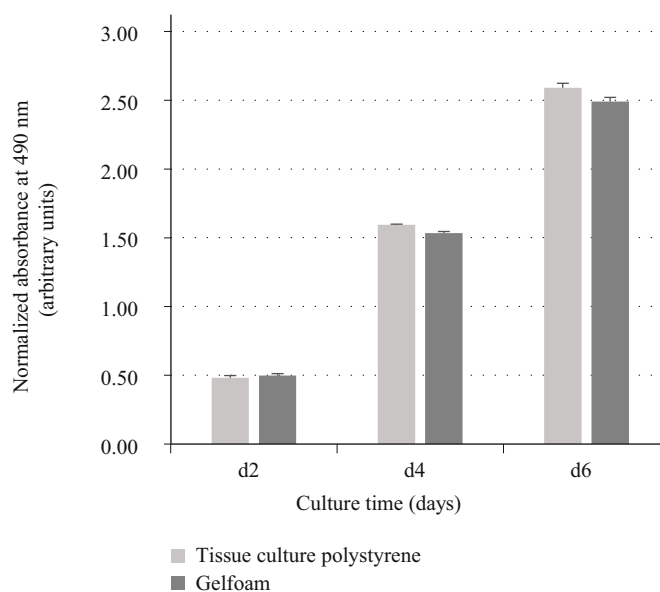
**3.1. Progenitor Cells Isolated from the Stromal Vascular Fraction Are MSCs.** Mesenchymal stromal cells were isolated from the stromal vascular fraction and subsequently

expanded *ex vivo* to generate numbers sufficient for *in vitro* and *in vivo* applications. Prior to *in vivo* applications, the expanded cells were characterized *in vitro* to prove that they are indeed MSCs. We generated primary cultures of adipose tissue-derived hMSCs, which were characterized *in vitro* using methods described earlier [17]. Subjective evaluation demonstrated that the cells adhered to the tissue culture polystyrene surface and exhibited a fibroblast-like morphology during *in vitro* culturing and serial passaging. Using flow cytometry, cells were found to be >99.8% positive for CD29, CD44, CD73, CD90, and CD105. CD34 (hematopoietic), CD106 (endothelial), CD45 (leukocyte), and HLA-DR (MHC Class II) were detected at 28.3%, 4.26%, 2.43%, and 2.49%, respectively (Figure 1(a)). During passaging, the expression of CD34 significantly reduced to <5%, suggesting that serial passaging of hMSCs under the given cell culture conditions yielded a relatively homogenous culture of cells. Thus, the overwhelming majority of the cultured cells express the expected CD markers found on MSCs with minimal contamination of other cell types.

Additionally, we demonstrated the potential of hMSCs to differentiate into osteocytes, adipocytes, and chondrocytes (trilineage differentiation) *in vitro*. When isolated MSCs were induced with lineage-specific cocktail, they did undergo



(a)



(b)

FIGURE 2: *In vitro* adherence and viability of hMSCs. The adherence and viability of hMSCs on Gelfoam® was evaluated using DiI imaging (a) and MTS assay (b). Representative image shows the red cytoplasmic fluorescence of hMSCs adhered to Gelfoam® after 6 days. A portion of the image is out of focus because of the 3D nature of the scaffold. Proliferation of hMSCs on Gelfoam® is comparable to cells seeded on tissue culture polystyrene surface for 2, 4, and 6 days. The absorbance at 490 nm is directly proportional to the number of living and proliferating cells. Tissue culture surface and Gelfoam® without any cells in the same culture conditions were used as blanks to obtain normalized values at each time point.

differentiation into the expected cell types compared to the controls, which were incubated in the absence of lineage-specific media. Alizarin red, oil-red-o, and Alcian blue staining confirmed the presence of calcium (osteocytes), lipids (adipocytes), and glycosaminoglycans (cartilage), respectively (Figure 1(b)). Therefore, the isolated progenitor cells met the specific criteria, and hence were indeed MSCs.

**3.2. Cytocompatibility of Gelfoam®.** After proving the MSC nature, cells were seeded on Gelfoam® to verify cell

adherence, distribution, and viability using DiI imaging (Figure 2(a)) and MTS proliferation assay for 6 days (Figure 2(b)), respectively. Detection of cell fluorescence and an observed linear increase in the absorbance with time indicated that cells were adhered to, were distributed uniformly on the material constructs, and that the viability and proliferation characteristics on Gelfoam® were similar to cultures grown on polystyrene surfaces. These results demonstrated that Gelfoam® is noncytotoxic, permits cell adherence, distribution, and does not hinder proliferation of MSCs. Furthermore, though Gelfoam® samples became

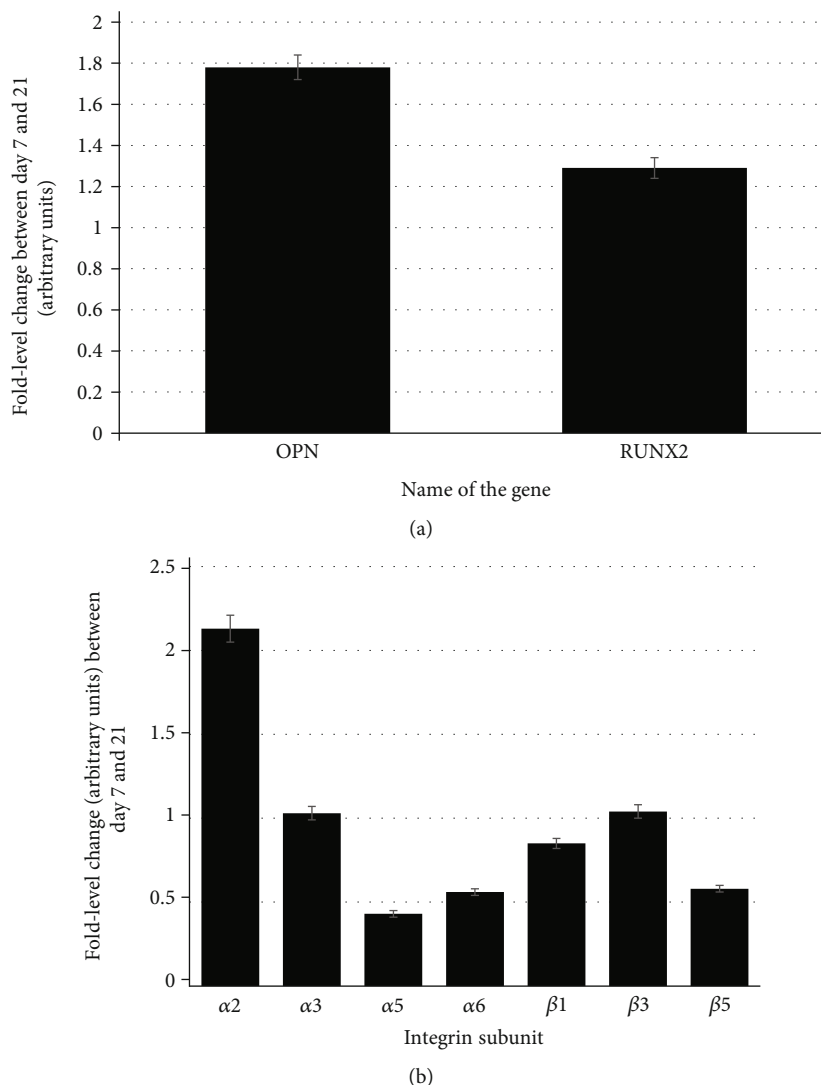


FIGURE 3: qPCR expression. Gene expression of the osteogenic-specific (a) and integrin subunit (b) genes. Relative fold differences in the expression of genes between days 7 and 21 during osteogenic differentiation of hMSCs on Gelfoam<sup>®</sup> were calculated using the delta-delta Ct method (Applied Biosystems). GAPDH was used as the housekeeping gene.

pliable and spongy after media absorption, the matrix of the material did not lose its structural integrity within the study time period. As a result, Gelfoam<sup>®</sup> served as an effective means for containing cells after initial attachment.

**3.3. hMSCs Maintain Osteogenic Capacity on Gelfoam<sup>®</sup>.** We next evaluated the osteogenic differentiation potential of hMSCs by profiling the expression of genes strongly associated with osteogenesis. We wanted to ensure that MSCs retained their osteogenic potential in presence of Gelfoam<sup>®</sup>. We used qPCR to assess the expression of two commonly used osteoblast markers, osteopontin (OPN) and the transcription factor, RUNX2 [23]. Quantitative PCR results of control cultures, i.e., hMSCs induced to undergo osteogenic differentiation on a tissue culture substrate, showed that both genes were expressed at both days 7 and 21 with significant upregulation of 4- and 2-fold difference, respectively, with time. Results confirmed that hMSCs underwent osteogenesis within this time period on the tissue culture polystyrene sur-

face and that RNA extraction, cDNA synthesis, and PCR procedures were accurate. Using the parameters validated for the control cells, the expression of both markers was detected in Gelfoam<sup>®</sup>-embedded hMSCs at both time points (Figure 3(a)). There was a significant upregulation of 1.8- and 1.2-fold difference for OPN and RUNX2 expression, respectively, when Gelfoam<sup>®</sup>-embedded hMSCs progressed from day 7 to 21. Even though the relative change is slightly less than that observed in the control cultures, the changes in OPN and RUNX2 verified that hMSCs embedded in Gelfoam<sup>®</sup> do undergo osteogenesis with time and that the presence of Gelfoam<sup>®</sup> did not affect their osteogenic potential.

**3.4. Specific Integrin Proteins May Mediate Cell Adherence and Osteodifferentiation of hMSCs on Gelfoam<sup>®</sup>.** We next evaluated the role of integrins (the major genes encoding for cell adhesion proteins), if any, in cell attachment and subsequent osteogenic differentiation processes. Using the parameters validated for the control cells (hMSCs

undergoing osteogenic differentiation on tissue culture substrate), the expression profile of integrin subunits  $\alpha 2$ ,  $\alpha 3$ ,  $\alpha 5$ ,  $\alpha 6$ ,  $\beta 1$ ,  $\beta 3$ , and  $\beta 5$  at days 7 and 21 after osteogenic induction of hMSCs embedded in Gelfoam<sup>®</sup> were analyzed (Figure 3(b)). As cells differentiated from day 7 to day 21, all the integrin subunits except  $\alpha 2$  and  $\alpha 5$  maintained relatively consistent expression profiles. The consistent expression throughout the differentiation process is evident with the fold level changes close to 1. The  $\alpha 2$  subunit showed a significant upregulation over the course of differentiation, suggesting it to be the major cell adhesion protein; while  $\alpha 5$  was downregulated indicating that it may not be involved in osteogenesis. Results suggest that the adherence, and potentially the osteogenic differentiation, of hMSCs on Gelfoam<sup>®</sup> could be mediated via specific integrin subunits.

**3.5. Rat as an Animal Model to Evaluate hMSCs in a Tooth Extraction Defect.** After confirming cytocompatibility of Gelfoam<sup>®</sup> and verifying that the material does not impede the osteogenic capacity of seeded hMSCs, we next implanted cell-seeded constructs in a rat maxillary alveolar tooth extraction defect model. All rats recovered quickly after surgery and returned to drinking, eating, and grooming within 48 hours. During the experimental period, the rats exhibited normal behavior without any weight loss or postoperative complications.

**3.6. Histomorphometric Analyses.** Special stains of H&E and Masson trichrome were used for histomorphometric analyses. As anticipated and verified by the examination of H&E-stained slides, there was no evidence of adverse reaction due to either Gelfoam<sup>®</sup> or the hMSCs when implanted *in vivo*. Masson trichrome staining was evaluated for the formation of early new bone and filling of the defects. Representative images from samples containing Gelfoam<sup>®</sup> alone and those containing Gelfoam<sup>®</sup>+hMSCs are shown (Figure 4(a)). The top panels of these images show the entire maxillary region, with the intact tooth on the left and the defect on the right side, to aid in understanding the orientation and the anatomy of the rat maxilla, whereas the lower panels show a high-resolution image of the defect subjective assessment of the Masson trichrome staining of treatment groups which showed no significant bone formation by week 1, yet soft tissue in each defect, shown in red, was apparent. Early collagen and bone formation structures attempting to refill the defect were observed at 4 weeks in the rats treated with Gelfoam<sup>®</sup> alone. Though osteoblast activity was apparent in these samples, the majority of new tissue did not appear to be solid/mineralized and instead presented as a loose and irregular connective tissue. Rats treated with Gelfoam<sup>®</sup>+hMSCs in contrast, demonstrated defects that appeared to be filled largely with structures indicating solid/mineralized bone by week 4. As some regions of the perceived bone formation lacked mineralization, this suggests that osteoblast activity was still underway. At week 12 in rats treated with Gelfoam<sup>®</sup> only, defects had been completely filled, yet the light blue to purple color of the stained tissue indicated incomplete loose bone tissue formation. Comparatively, Gelfoam<sup>®</sup>+hMSC-treated defects demonstrated com-

plete filling of the defect region with mineralized bone at week 12. Taken together, it is evident that the rats that received Gelfoam<sup>®</sup>+hMSCs showed significantly higher filling of the defect and new bone formation starting at week 4 and progressing into week 12.

The Masson trichrome-stained samples illustrated in Figure 4(a) were quantitated and analyzed and the data is shown in Figure 4(b). No significant differences were observed at any time point in the rats treated with Gelfoam<sup>®</sup> alone. In contrast, there were significant differences in early bone formation/collagen in rats treated with Gelfoam<sup>®</sup>+hMSCs between weeks 1 and 4 and between weeks 1 and 12. There was no statistical difference in bone regeneration between weeks 4 and 12. The hMSC-treated rats showed quantitatively more consistent accumulation of collagen/early bone formation structures than the rats treated with Gelfoam<sup>®</sup> alone. It appeared that the regeneration process started as early as 4 weeks. Furthermore, and most importantly, the level of bone formation between weeks 1 and 4 was roughly 2-fold significantly higher in the rats treated with Gelfoam<sup>®</sup>+hMSCs compared to the group with Gelfoam<sup>®</sup> alone. Comparatively, the level of bone formation between weeks 1 and 12 was not statistically different between the two treatment groups, suggesting an enhanced and early bone healing in presence of hMSCs.

**3.7. Immunohistochemical Assessment.** IHC evaluation of unstained histological sections for osteopontin (OPN) (Figure 5(a)), fibronectin (FN) (Figure 5(b)), and CD34 (Figure 5(c)) verified expression of these proteins within the tissue, for all rats at week 4, supporting the healing of the bone defect observed and described in the Masson trichrome-stained samples. Notable expression of OPN was observed in the soft tissue covering the palatal side as well as within the center of defects. Morphological comparison of surfaces stained for OPN within defects appeared to demonstrate a more uniform patterning within the Gelfoam<sup>®</sup>+hMSC-treated samples, in contrast to the chaotic formation in the Gelfoam<sup>®</sup>-only treated defects. FN expression was observed to be concentrated in the soft tissue covering defects, similar to OPN staining, as well as throughout the defects, indicating matrix formation within treated regions. Similar to morphological observations in OPN-stained samples, FN appeared more uniformly organized in the Gelfoam<sup>®</sup>+hMSC-treated sample as compared to the Gelfoam<sup>®</sup>-only treatment group. CD34 expression was heavily pronounced in both the treatment groups, within the defects and the surrounding tissue indicating presence of hematopoietic cells.

## 4. Discussion

Relative to bone marrow, the adipose tissue is a commonly used source of MSCs for oral/maxillofacial surgeons in bone tissue engineering [24]. The stromal vascular fraction of the adipose tissue is one of the commonly used sources of MSCs, and hence, an important tissue to regenerative medicine scientists and researchers [7, 25]. Adipose tissue-derived MSCs can be isolated relatively easily with less pain to the donor

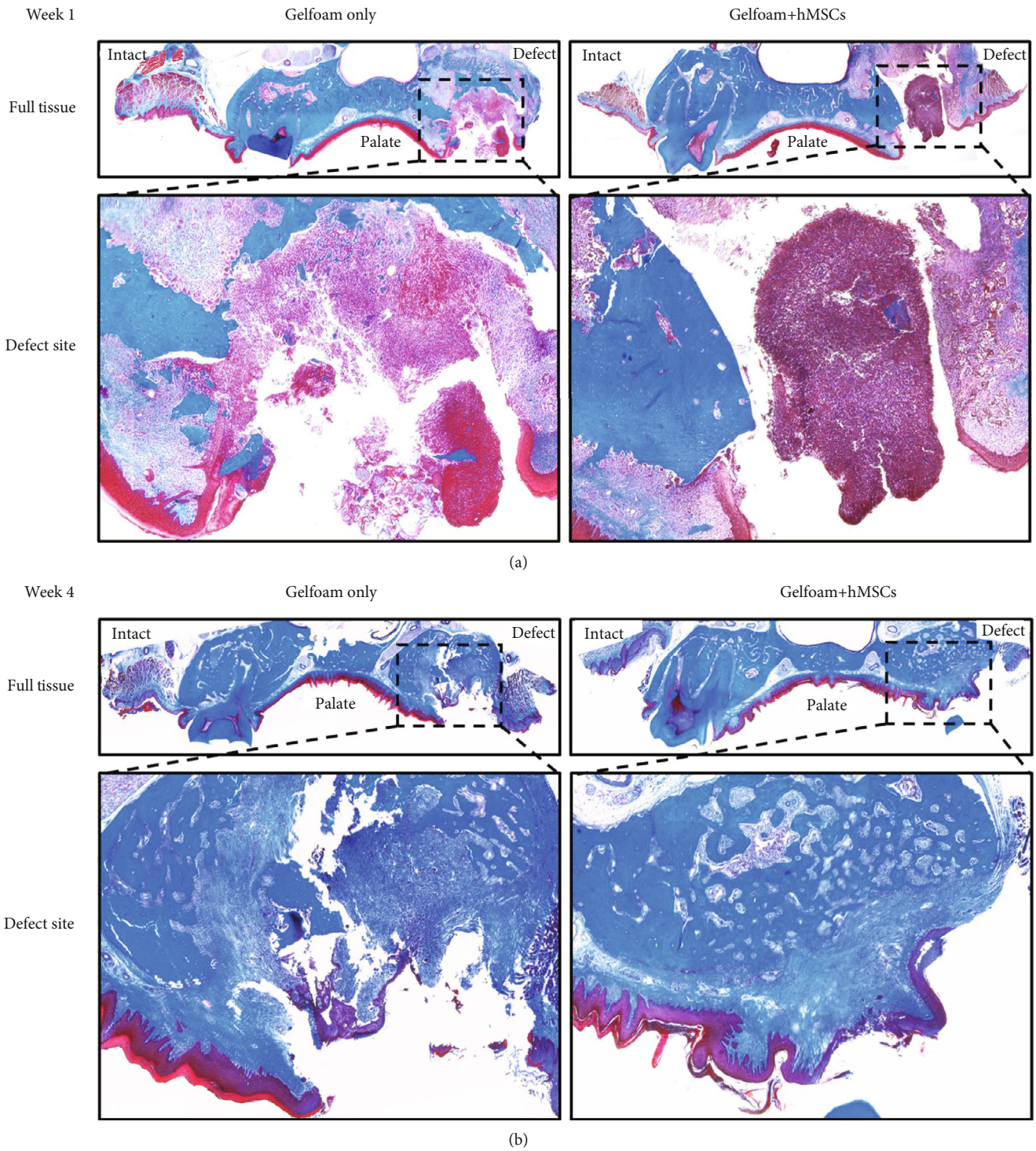
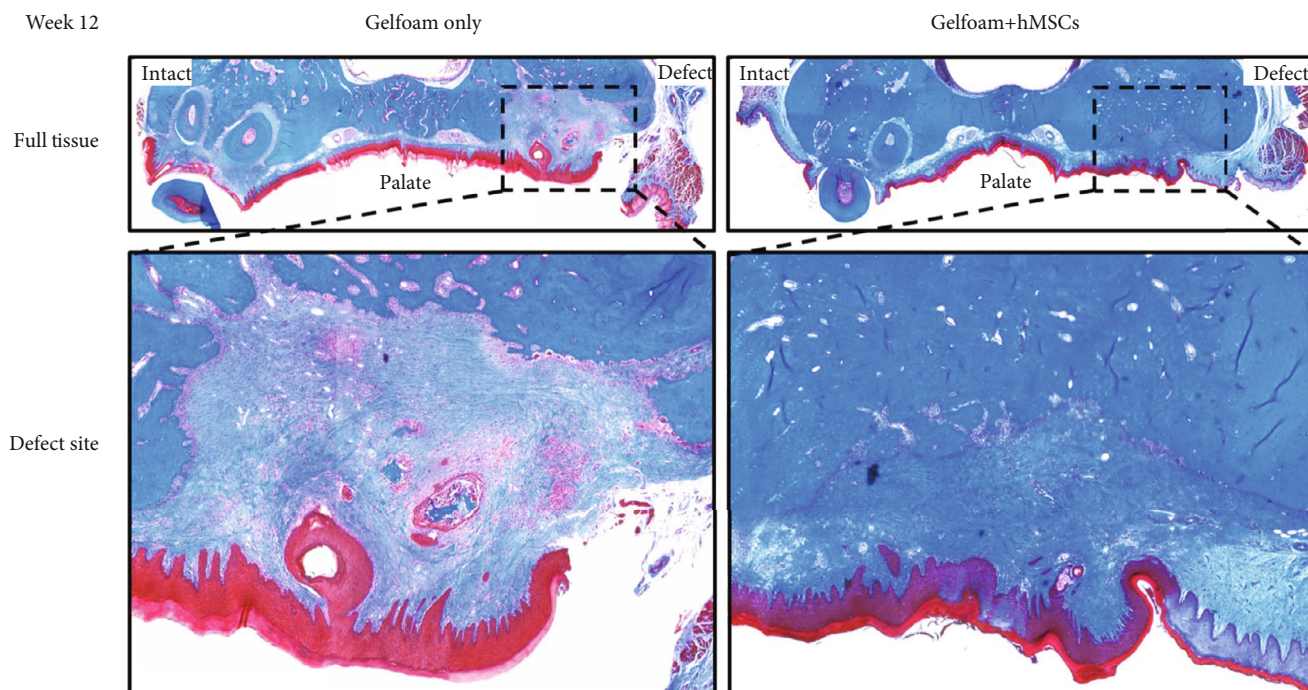
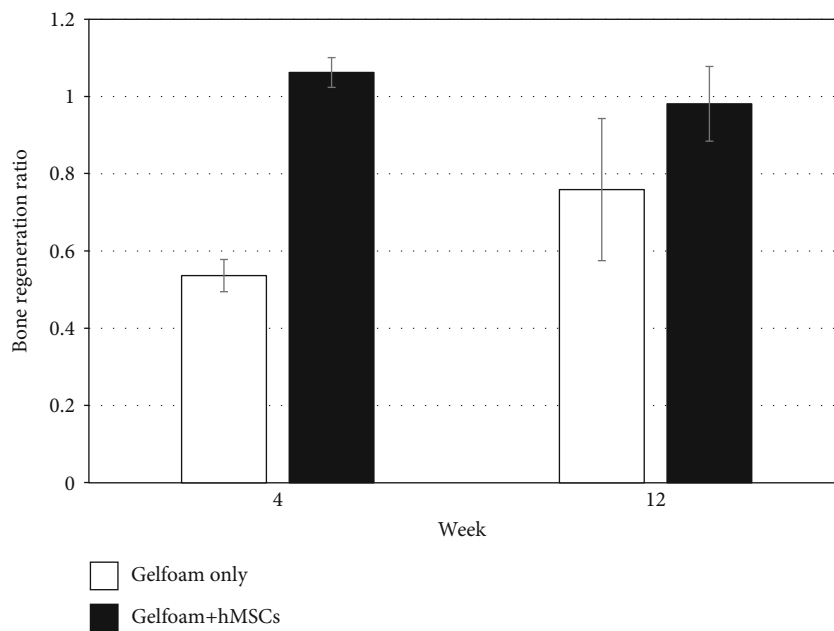


FIGURE 4: Continued.



(c)



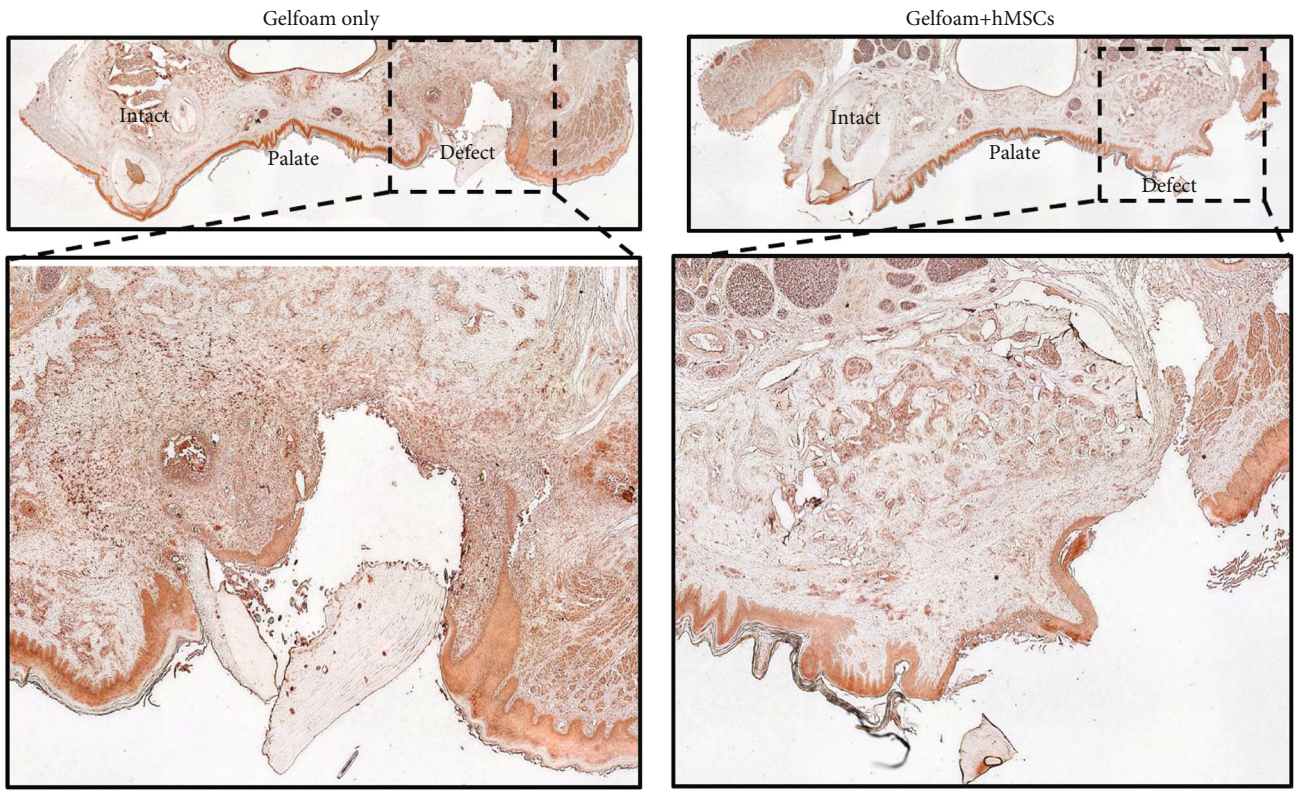
(d)

FIGURE 4: Qualitative and quantitative histomorphometry. Representative images depicting Masson trichrome stained coronal plane of the alveolar bone regions from rats treated with Gelfoam® alone and Gelfoam®+hMSCs for 1 (a), 4 (b), and 12 (c) weeks are shown. The intact and the defect sites are labelled in full tissue images, and the defect region has been expanded below respective images. Bone regeneration ratio values (d) from images demonstrate the level of bone formation within the defect site between week 1 and weeks 4 and 12, respectively, for both Gelfoam® alone and Gelfoam®+hMSCs. There is a statistically significant bone regeneration in 4 weeks in the presence of hMSCs.

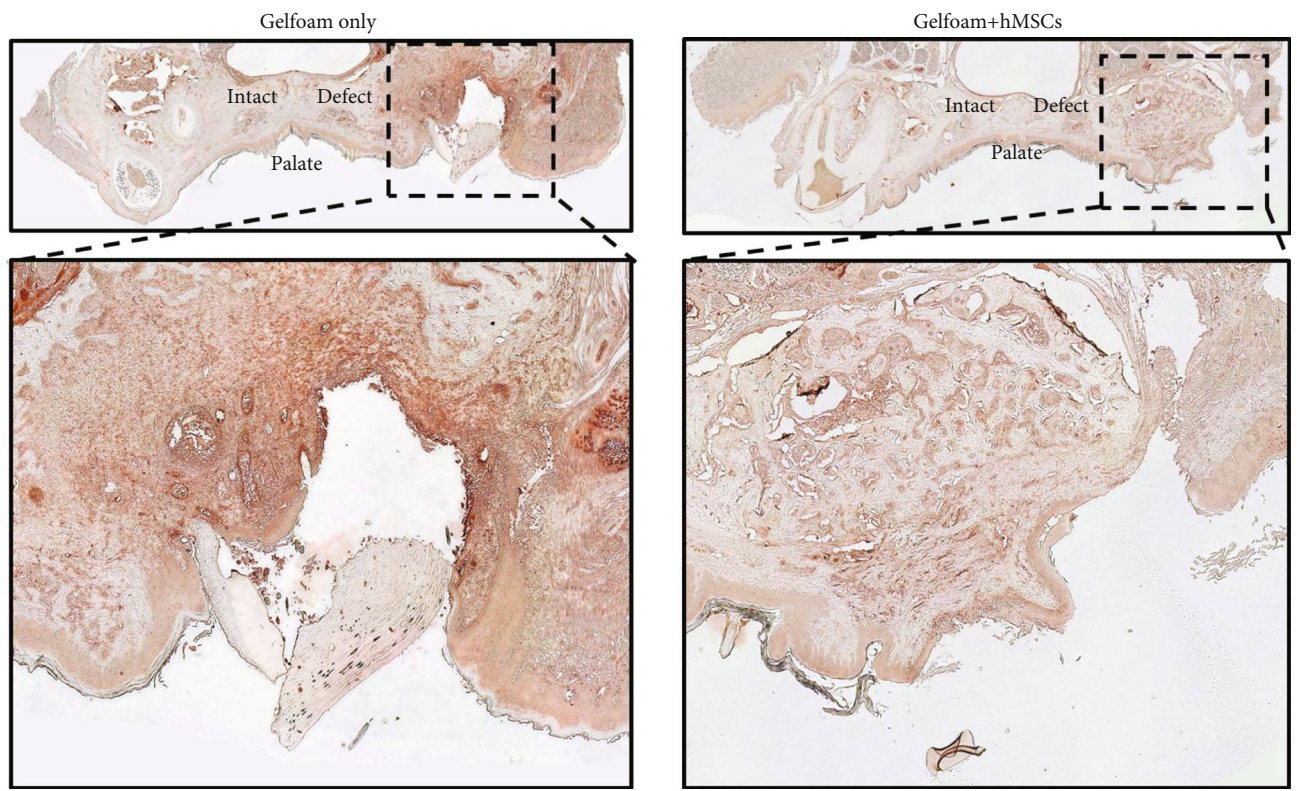
and in greater quantities. MSCs express specific markers (CD29, CD44, CD90, and CD105), demonstrate adipogenic, osteogenic, and chondrogenic potentials and enhancement of angiogenesis and immunomodulatory function, and have been used in the repair and regeneration of craniomaxillofa-

cial injuries. Multiple reports have been published demonstrating the use of MSCs in the repair of calvarial and mandibular bone defects in rodent models [26–28]. Relatively speaking, there are less reports on tooth extraction models in rats and mouse models. This can partially be





(a)



(b)

FIGURE 5: Continued.

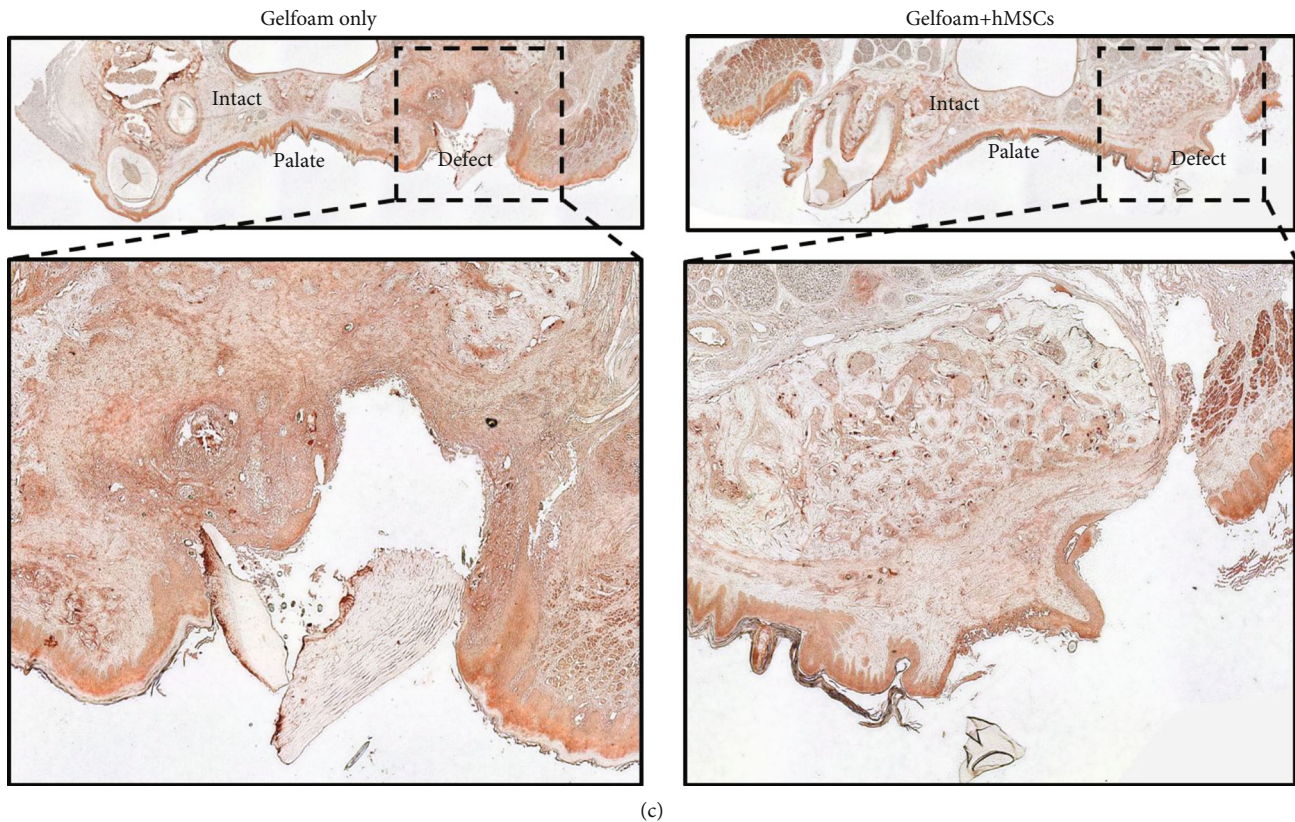


FIGURE 5: Immunohistochemistry. Representative images depicting immunohistochemical staining (Nove Red) of decalcified bone samples with OPN (a), FN (b), and CD34 (c) are shown. Histological sections from rats treated with Gelfoam® alone and Gelfoam®+hMSCs for 4 weeks are shown. The anatomical regions are labelled. Black dotted lines indicate region of interest illustrated in the 10x magnification. Note the areas of relatively organized pattern of staining in the hMSC-treated defects.

attributed towards the technical challenges associated with creating the defect and postop care in a small rodent model.

In the *in vitro* and *in vivo* assays described in this study, the bioinert scaffold, Gelfoam®, was used to deliver and contain hMSCs to the injury site. Gelfoam® is generally available and commonly used in the medical field as a hemostat. Known to be a compressible, porous, pliable, water insoluble, sponge-like material with absorptive properties, Gelfoam® also is completely absorbed by soft tissues in four to six weeks with little or no tissue reaction. We demonstrated that the material is cytocompatible with hMSCs and that cells are not hindered in the adherence, proliferation, or osteogenic potential when seeded on constructs. Though scaffolds became spongy after hydration by the media (*in vitro*) and body fluids (*in vivo*), the matrix appeared to maintain its structure throughout the study period. As Gelfoam® is not considered to be bioactive, the observed osteogenic differentiation of seeded cells is attributed to exposure to a 3D environment, which readily offers a mode of cell adhesion and permits multidirectional growth as compared to that observed along the 2D surface of the tissue culture polystyrene dish. This 3D growth pattern is more favorable to the formation of nodular cell clusters, which are hallmarks of cell osteodifferentiation [29].

Though alizarin red staining is considered to be the gold standard to evaluate *in vitro* osteogenesis, it could not be used

in this study due to nonspecific absorbance of the stain by Gelfoam®, and as a result, evaluation was carried out utilizing the expression of osteogenic-specific genes to confirm cell adhesion and osteogenic differentiation. OPN is known to be expressed in osteoblasts during bone formation and remodeling [30]. RUNX2 is a transcription factor that is expressed during osteoblast differentiation and potentially upregulates the expression of bone matrix proteins [31]. The expression profiles of OPN and RUNX2 indicated the osteogenic capacity of the hMSCs seeded on Gelfoam®.

Similarly, the expression profiles of the various integrin subunits during osteogenesis were interesting. Integrin expression is known to be a relevant biomarker of successful cell adhesion. Integrins are also important in signal transduction during differentiation and osteogenesis [32, 33]. Integrins exist and are functional in the cells as heterodimers of alpha and beta subunits, and hence, it was necessary to evaluate the expression of these subunits independently. The minor changes in expression levels from day 7 to day 21 of the integrin subunits in the hMSCs embedded in Gelfoam® indicate that all the subunits, primarily  $\alpha 2$  and not  $\alpha 5$  are needed in the adhesion and subsequent osteogenic differentiation of hMSCs. Overall, the gene expression profile of the integrin subunits and the osteogenic genes of hMSCs embedded in Gelfoam® indicated that cell adhesion and osteogenic capabilities were not affected by Gelfoam®, and hMSCs

exhibit normal molecular and cellular properties, further confirming that the material was cytocompatible.

A relatively complex and challenging rat model was used to evaluate the *in vivo* osteogenic potential of hMSCs delivered within a bioinert vehicle. This model offered a means of initial *in vivo* assessment of biocompatibility and regeneration potential of MSCs as rats tolerate the xenogenic implantation of MSCs very well. Previous studies from our laboratory demonstrate lack of immunologic or an adverse reaction when MSCs of xenogenic (goat or equine) origin are implanted in Sprague Dawley rats [34, 35]. Even though this model is convenient, cost effective, and considered to be ideal to test the performance of new implant and grafting materials in pretranslational studies, challenges due to the small animal size and the complex anatomy of the oral/maxillofacial region were apparent. Despite these challenges, histomorphometric data analyses showed that there was a statistically significant increase in the level of bone formation within 4 weeks when the defects were treated with hMSCs. This significance was observed relative to the defects treated with the Gelfoam scaffold alone, and proved our hypothesis. Subjective evaluation of the Masson trichrome staining revealed a more consistent and organized pattern of solid bone tissue regeneration in the group treated with hMSCs. This was further supported by IHC assessment of samples from both study groups at week 4 postsurgery. Stainings illustrated the presence of key osteogenic, cell matrix, and angiogenic proteins within the defect region at this time point. The Gelfoam®+hMSC-treated samples demonstrated a more organized morphological distribution of these proteins compared to the chaotic pattern in Gelfoam® alone samples. Our data strongly suggests that xenogenic adipose tissue-derived MSCs exhibit a potential to regenerate bone when delivered and contained using a scaffold. Future studies with large animal models are necessary to validate observations and elucidate mechanism(s) responsible for induced healing and repair of bone defects by MSCs.

## 5. Conclusions

We have demonstrated that xenogeneic hMSCs, delivered and contained at the bone injury site via a bioinert scaffold, promoted enhanced regeneration of maxillary bone defects. The relative availability and ease of collection for adipose-derived MSCs coupled with the observed osteogenic potential when applied and maintained within a bone defect presents a promising bioactive additive for bone tissue engineering materials. Application of such cell-based material platforms therefore offers a feasible and effective approach for the clinical restoration of oral/maxillofacial bone defects.

## Abbreviations

FN: Fibronectin  
 H&E: Hematoxylin and eosin  
 hMSCs: Human mesenchymal stem cells

HRP: Horseradish peroxidase  
 IACUC: Institutional Animal Care and Use Committee  
 ONJ: Osteonecrosis of the jaw  
 MSCs: Mesenchymal stem cells  
 OPN: Osteopontin  
 ROI: Region of interest.

## Data Availability

The data used to support the findings of this study are available from the corresponding author upon request.

## Additional Points

*Availability of Data and Material.* The datasets used and/or analyzed during the current study are available from the corresponding author on reasonable request.

## Conflicts of Interest

The authors declare that they have no competing interests in this section.

## Authors' Contributions

AW and AB carried out all the qPCR and IHC experiments and were the major contributors in compiling the data and in writing the manuscript. They both contributed equally to the manuscript. SD, SB, RR, JG, DA, and JC performed all the surgeries and were responsible for pre- and postop animal care. TM and SS were responsible for the isolation, characterization, and expansion of hMSCs. MD was responsible for the overall planning of the experiments, analyses, interpretation of results, and writing the manuscript. She was also assisted by AW, AB, TM, and SS in carrying out the experiments. All the authors read and approved the final manuscript. Andrew Wofford and Austin Bow contributed equally to this manuscript.

## Acknowledgments

We would like to acknowledge the statistical assistance of Dr. Xiaocun Sun, Ph.D., SAS Certified Advanced Programmer for SAS 9, Research Computing Support, University of Tennessee. This work was supported by a Resident Research Award from the Osteo Science Foundation. Partial funding for open access publishing of this research was provided by the University of Tennessee's Open Publishing Support Fund.

## References

- [1] E. Alsberg, E. E. Hill, and D. J. Mooney, "Craniofacial tissue engineering," *Critical Reviews in Oral Biology and Medicine*, vol. 12, no. 1, pp. 64–75, 2001.
- [2] M. Nakashima and A. H. Reddi, "The application of bone morphogenetic proteins to dental tissue engineering," *Nature Biotechnology*, vol. 21, no. 9, pp. 1025–1032, 2003.

- [3] A. Hegab, "Reconstruction of mandibular alveolar ridge defects for implant placement: critical review," *International Journal of Dentistry and Oral Health*, vol. 1, no. 6, 2015.
- [4] L. Rasmusson and J. Abtahi, "Bisphosphonate associated osteonecrosis of the jaw: an update on pathophysiology, risk factors, and treatment," *International Journal of Dentistry*, vol. 2014, Article ID 471035, 9 pages, 2014.
- [5] S. R. Chastain, A. K. Kundu, S. Dhar, J. W. Calvert, and A. J. Putnam, "Adhesion of mesenchymal stem cells to polymer scaffolds occurs via distinct ECM ligands and controls their osteogenic differentiation," *Journal of Biomedical Materials Research. Part A*, vol. 78, no. 1, pp. 73–85, 2006.
- [6] S. Schneider, M. Unger, M. van Griensven, and E. R. Balmayor, "Adipose-derived mesenchymal stem cells from liposuction and resected fat are feasible sources for regenerative medicine," *European Journal of Medical Research*, vol. 22, no. 1, article 17, 2017.
- [7] S. Kadiyala, R. G. Young, M. A. Thiede, and S. P. Bruder, "Culture expanded canine mesenchymal stem cells possess osteochondrogenic potential in vivo and in vitro," *Cell Transplantation*, vol. 6, no. 2, pp. 125–134, 1997.
- [8] M. F. Pittenger, A. M. Mackay, S. C. Beck et al., "Multilineage potential of adult human mesenchymal stem cells," *Science*, vol. 284, no. 5411, pp. 143–147, 1999.
- [9] N. Pourebahim, B. Hashemibeni, S. Shahnasari et al., "A comparison of tissue-engineered bone from adipose-derived stem cell with autogenous bone repair in maxillary alveolar cleft model in dogs," *International Journal of Oral and Maxillofacial Surgery*, vol. 42, no. 5, pp. 562–568, 2013.
- [10] V. Tollemar, Z. J. Collier, M. K. Mohammed, M. J. Lee, G. A. Ameer, and R. R. Reid, "Stem cells, growth factors and scaffolds in craniofacial regenerative medicine," *Genes & Diseases*, vol. 3, no. 1, pp. 56–71, 2016.
- [11] M. B. Eslaminejad, H. Mirzadeh, Y. Mohamadi, and A. Nickmahzar, "Bone differentiation of marrow-derived mesenchymal stem cells using beta-tricalcium phosphate-alginate-gelatin hybrid scaffolds," *Journal of Tissue Engineering and Regenerative Medicine*, vol. 1, no. 6, pp. 417–424, 2007.
- [12] R. Rohanzadeh, M. V. Swain, and M. Mason, "Gelatin sponges (Gelfoam®) as a scaffold for osteoblasts," *Journal of Materials Science. Materials in Medicine*, vol. 19, no. 3, pp. 1173–1182, 2008.
- [13] J. Y. Lee, M. H. Choi, E. Y. Shin, and Y. K. Kang, "Autologous mesenchymal stem cells loaded in Gelfoam® for structural bone allograft healing in rabbits," *Cell and Tissue Banking*, vol. 12, no. 4, pp. 299–309, 2011.
- [14] A. J. Salgado, O. P. Coutinho, and R. L. Reis, "Bone tissue engineering: state of the art and future trends," *Macromolecular Bioscience*, vol. 4, no. 8, pp. 743–765, 2004.
- [15] L. Roseti, V. Parisi, M. Petretta et al., "Scaffolds for bone tissue engineering: state of the art and new perspectives," *Materials Science & Engineering. C, Materials for Biological Applications*, vol. 78, pp. 1246–1262, 2017.
- [16] M. S. Ponticciello, R. M. Schinagl, S. Kadiyala, and F. P. Barry, "Gelatin-based resorbable sponge as a carrier matrix for human mesenchymal stem cells in cartilage regeneration therapy," *Journal of Biomedical Materials Research*, vol. 52, no. 2, pp. 246–255, 2000.
- [17] K. M. Alghazali, S. D. Newby, Z. A. Nima et al., "Functionalized gold nanorod nanocomposite system to modulate differentiation of human mesenchymal stem cells into neural-like progenitors," *Scientific Reports*, vol. 7, no. 1, article 16654, 2017.
- [18] A. Bow, S. D. Newby, R. Rifkin et al., "Evaluation of a polyurethane platform for delivery of nanohydroxyapatite and decellularized bone particles in a porous three-dimensional scaffold," *ACS Applied Bio Materials*, vol. 2, no. 5, pp. 1815–1829, 2019.
- [19] K. L. Marino, I. Zakhary, R. A. Abdelsayed et al., "Development of a rat model of bisphosphonate-related osteonecrosis of the jaw (BRONJ)," *Journal of Oral Implantology*, vol. 38, no. S1, pp. 511–518, 2012.
- [20] S. Boonyagul, W. Banlunara, P. Sangvanich, and P. Thunyakitpisal, "Effect of acemannan, an extracted polysaccharide from Aloe vera, on BMSCs proliferation, differentiation, extracellular matrix synthesis, mineralization, and bone formation in a tooth extraction model," *Odontology*, vol. 102, no. 2, pp. 310–317, 2014.
- [21] H. H. Chang, Y. L. Wang, Y. C. Chiang et al., "A novel chitosan-γPGA polyelectrolyte complex hydrogel promotes early new bone formation in the alveolar socket following tooth extraction," *PLoS One*, vol. 9, no. 3, article e92362, 2014.
- [22] J. Schindelin, I. Arganda-Carreras, E. Frise et al., "Fiji: an open-source platform for biological-image analysis," *Nature Methods*, vol. 9, no. 7, pp. 676–682, 2012.
- [23] G. R. Kirkham and S. H. Cartmell, "Genes and proteins involved in the regulation of osteogenesis," *Topics in Tissue Engineering*, N. Ashammakhi, R. Reis, and E. Chiellini, Eds., vol. 3, 2007.
- [24] M. Griffin, D. M. Kalaskar, P. E. Butler, and A. M. Seifalian, "The use of adipose stem cells in cranial facial surgery," *Stem Cell Reviews*, vol. 10, no. 5, pp. 671–685, 2014.
- [25] J. Kobolak, A. Dinnyes, A. Memic, A. Khademhosseini, and A. Mobasheri, "Mesenchymal stem cells: identification, phenotypic characterization, biological properties and potential for regenerative medicine through biomaterial micro-engineering of their niche," *Methods*, vol. 99, pp. 62–68, 2016.
- [26] P. Streckbein, S. Jackel, C. Y. Malik et al., "Reconstruction of critical-size mandibular defects in immunoincompetent rats with human adipose-derived stromal cells," *Journal of Cranio-Maxillo-Facial Surgery*, vol. 41, no. 6, pp. 496–503, 2013.
- [27] M. K. Lee, A. S. DeConde, M. Lee et al., "Biomimetic scaffolds facilitate healing of critical-sized segmental mandibular defects," *American Journal of Otolaryngology*, vol. 36, no. 1, pp. 1–6, 2015.
- [28] S. Santos Tde, R. P. Abuna, A. L. Almeida, M. M. Beloti, and A. L. Rosa, "Effect of collagen sponge and fibrin glue on bone repair," *Journal of Applied Oral Science*, vol. 23, no. 6, pp. 623–628, 2015.
- [29] H. A. Declercq, R. M. Verbeeck, L. De Ridder, E. H. Schacht, and M. J. Cornelissen, "Calcification as an indicator of osteoinductive capacity of biomaterials in osteoblastic cell cultures," *Biomaterials*, vol. 26, no. 24, pp. 4964–4974, 2005.
- [30] C. Tarquini, R. Mattera, F. Mastrangeli et al., "Comparison of tissue transglutaminase 2 and bone biological markers osteocalcin, osteopontin and sclerostin expression in human osteoporosis and osteoarthritis," *Amino Acids*, vol. 49, no. 3, pp. 683–693, 2017.
- [31] T. J. C. Komori and T. Research, "Regulation of bone development and extracellular matrix protein genes by RUNX2," *Cell and Tissue Research*, vol. 339, no. 1, pp. 189–195, 2010.

- [32] R. L. Juliano and S. Haskill, "Signal transduction from the extracellular matrix," *The Journal of Cell Biology*, vol. 120, no. 3, pp. 577–585, 1993.
- [33] Z. Hamidouche, O. Fromigue, J. Ringe et al., "Priming integrin alpha5 promotes human mesenchymal stromal cell osteoblast differentiation and osteogenesis," *Proceedings of the National Academy of Sciences of the United States of America*, vol. 106, no. 44, pp. 18587–18591, 2009.
- [34] H. Elkhenany, S. Bourdo, S. Hecht et al., "Graphene nanoparticles as osteoinductive and osteoconductive platform for stem cell and bone regeneration," *Nanomedicine: Nanotechnology, Biology and Medicine*, vol. 13, no. 7, pp. 2117–2126, 2017.
- [35] M. Zayed, S. Newby, N. Misk, R. Donnell, and M. Dhar, "Xenogenic implantation of equine synovial fluid-derived mesenchymal stem cells leads to articular cartilage regeneration," *Stem Cells International*, vol. 2018, Article ID 1073705, 9 pages, 2018.

## Review Article

# Bone Tissue Regeneration in the Oral and Maxillofacial Region: A Review on the Application of Stem Cells and New Strategies to Improve Vascularization

Vivian Wu,<sup>1,2</sup> Marco N. Helder,<sup>2</sup> Nathalie Bravenboer,<sup>3</sup> Christiaan M. ten Bruggenkate,<sup>2</sup> Jianfeng Jin,<sup>1</sup> Jenneke Klein-Nulend <sup>1</sup> and Engelbert A. J. M. Schulten<sup>2</sup>

<sup>1</sup>Department of Oral Cell Biology, Academic Centre for Dentistry Amsterdam (ACTA), University of Amsterdam and Vrije Universiteit Amsterdam, Amsterdam Movement Sciences, Amsterdam, Netherlands

<sup>2</sup>Department of Oral and Maxillofacial Surgery/Oral Pathology, Amsterdam University Medical Centers and Academic Centre for Dentistry Amsterdam (ACTA), Vrije Universiteit Amsterdam, Amsterdam Movement Sciences, Amsterdam, Netherlands

<sup>3</sup>Department of Clinical Chemistry, Amsterdam University Medical Centers, Vrije Universiteit Amsterdam, Amsterdam Movement Sciences, Amsterdam, Netherlands

Correspondence should be addressed to Jenneke Klein-Nulend; [j.kleinnulend@acta.nl](mailto:j.kleinnulend@acta.nl)

Received 15 November 2019; Accepted 13 December 2019; Published 30 December 2019

Guest Editor: Toru Ogasawara

Copyright © 2019 Vivian Wu et al. This is an open access article distributed under the Creative Commons Attribution License, which permits unrestricted use, distribution, and reproduction in any medium, provided the original work is properly cited.

Bone tissue engineering techniques are a promising alternative for the use of autologous bone grafts to reconstruct bone defects in the oral and maxillofacial region. However, for successful bone regeneration, adequate vascularization is a prerequisite. This review presents and discusses the application of stem cells and new strategies to improve vascularization, which may lead to feasible clinical applications. Multiple sources of stem cells have been investigated for bone tissue engineering. The stromal vascular fraction (SVF) of human adipose tissue is considered a promising single source for a heterogeneous population of essential cells with, amongst others, osteogenic and angiogenic potential. Enhanced vascularization of tissue-engineered grafts can be achieved by different mechanisms: vascular ingrowth directed from the surrounding host tissue to the implanted graft, vice versa, or concomitantly. Vascular ingrowth into the implanted graft can be enhanced by (i) optimizing the material properties of scaffolds and (ii) their bioactivation by incorporation of growth factors or cell seeding. Vascular ingrowth directed from the implanted graft towards the host tissue can be achieved by incorporating the graft with either (i) preformed microvascular networks or (ii) microvascular fragments (MF). The latter may have stimulating actions on both vascular ingrowth and outgrowth, since they contain angiogenic stem cells like SVF, as well as vascularized matrix fragments. Both adipose tissue-derived SVF and MF are cell sources with clinical feasibility due to their large quantities that can be harvested and applied in a one-step surgical procedure. During the past years, important advancements of stem cell application and vascularization in bone tissue regeneration have been made. The development of engineered *in vitro* 3D models mimicking the bone defect environment would facilitate new strategies in bone tissue engineering. Successful clinical application requires innovative future investigations enhancing vascularization.

## 1. Introduction

To rehabilitate patients with critical-sized bone defects, surgical reconstructions are required. A critical-sized defect will not heal spontaneously or regenerate more than 10% of the lost bone during patients' lifetime [1]. These bone defects may result from systemic or local causes. Systemic conditions

include congenital abnormalities [2], general diseases [3], and medications [4], while local conditions comprise inflammation [5] or traumatic injuries, such as accidents [6] or dental and surgical treatments. Dental treatments, such as tooth extraction [7], and surgical treatments, such as surgical resection of benign or malignant neoplasms [8], may lead to substantial jaw bone defects.

Bone grafting procedures are carried out to reconstruct a bone defect [9]. In these surgical procedures, autografts are still considered the “gold standard” due to the essential combination of osteogenic, osteoinductive, and osteoconductive properties. However, autografts have some disadvantages, e.g., donor site morbidity and limited amount of graft tissue. In some cases, bone substitutes, such as allografts, xenografts, and alloplasts, are used as alternatives for autologous bone grafts, but these bone substitutes lack osteogenic, osteoinductive, and angiogenic potential [10].

Unfortunately, the ideal bone regeneration technique and material have not yet been developed. However, recent developments in tissue engineering have led to new and better treatment options called “cellular bone tissue engineering.” In this approach, a scaffold with mesenchymal stem cells (MSCs) and/or osteoprogenitor cells of an external source is implanted into the bone defect site. The *ex vivo* seeded cells on the scaffold play a key role and orchestrate the mechanism of bone formation at the target site. Multiple techniques have been investigated, applying a variety of stem cell sources and cell processing protocols [11]. Furthermore, different scaffold types are used for carrying the cells [12].

The rationale behind the application of MSCs and/or osteoprogenitor cells is their key role in bone formation. Natural bone formation in the pre- and postnatal development of the oral and maxillofacial area is performed intramembranously by recruiting mesenchymal bone marrow cells. These cells undergo osteoblastic differentiation and initiate new bone formation in the defect site. In other words, this method is aimed at inducing bone regeneration by mimicking biologic processes that occur during embryogenesis [13, 14].

The mechanism by which MSCs promote bone regeneration can be directed by engraftment of the transplanted cells into the newly regenerated tissue, differentiating into osteoblasts that eventually will secrete osteoid and initiate mineralization [15–17]. In addition, MSCs can enhance bone regeneration indirectly by a paracrine effect, i.e., secretion of cytokines and growth factors such as transforming necrosis factor- $\alpha$  (TNF- $\alpha$ ), platelet-derived growth factor (PDGF), interleukin-1 (IL-1), and IL-6. These secreted factors may recruit resident MSCs to the regenerated site [18, 19].

In cellular bone tissue engineering, MSCs are applied using two different approaches. The first approach is to directly transplant MSCs and/or osteoprogenitor cells combined with a scaffold (external scaffold) into the bone-defected site, which is a kind of an *in situ* tissue engineering [20, 21]. Autogenous particulate cancellous bone and marrow are used as the source of osteoprogenitor cells and MSCs. In this approach, the scaffold functions as a framework [22]. The second approach is to transplant MSCs that are isolated (usually from the patient), expanded *ex vivo*, seeded on adequate three-dimensional (3D) scaffolds (internal scaffolds), and proliferated and/or predifferentiated in controlled culture conditions [23]. Such a scaffold acts as a carrier of the cells and temporary matrix while the cells produce the extracellular matrix (ECM) that is required for bone formation [24].

A major challenge in bone tissue engineering is the vascularization of the implanted graft. Graft survival requires rapid and sufficient vascularization. Since the amount of oxygen is

limited to a diffusion distance of only  $\sim 150$ – $200 \mu\text{m}$  from a supply blood vessel, cells lying beyond this physiological border suffer from hypoxia [25]. Under this condition, MSCs fail to survive, because they are not able to adapt their glucose consumption and do not possess the necessary glycolytic reserves to maintain their metabolism for more than three days [26]. New insights underline the importance of both oxygen and nutrients required for energy-related cellular metabolism and in the end cell survival. Regenerating tissue over  $200 \mu\text{m}$  exceeds the capacity of nutrient supply and waste removal from the tissue and, therefore, requires an intimate supply of vascular networks [25]. Neovascularization along with efficient supply of blood is a prerequisite to this end.

The aim of this review is to present and discuss the advancement of stem cell application, vascularization, and bone regeneration in the oral and maxillofacial region, with emphasis on the human jaw. Moreover, we propose new strategies to improve the current techniques, which may lead to feasible clinical applications.

## 2. Sources of Stem Cells

Somatic stem cells, mainly mesenchymal stem cells (MSCs), that are applied in bone tissue engineering are isolated from various tissues. The clinically applied sources of stem cells in the oral and maxillofacial region originate from bone marrow, adipose tissue [27], and dental tissues [28, 29]. *In vitro* and *in vivo* animal studies reported on the application of embryonic stem cells (ESCs) [30–32] and induced pluripotent stem cells (IPSCs) [33] in bone tissue engineering. However, these ESCs and IPSCs raise several serious ethical and safety concerns, such as teratoma formation, which continue to impede clinical implementation [34]. In Figure 1, the different sources of stem cells and their different stages of application are illustrated: undifferentiated, early differentiated, or differentiated. The different stages of stem cells are categorized as follows:

- (i) Undifferentiated: multipotent adult MSCs, pluripotent ESCs, or IPSCs
- (ii) Early differentiated: MSCs differentiated towards specific lineage, such as osteogenic lineage
- (iii) Differentiated: specialized cell, such as osteoblast

Clinically applicable tissue engineering involving stem cells is focused on the use of patient-derived (adult) stem cells that are undifferentiated, given that terminally differentiated cells are difficult to expand *ex vivo* relative to more highly proliferative stem/progenitor cells. The use of stem cells is also intended to achieve a complete physiological repair process that involves the MSC-mediated activation of not only bone formation but also neovascularization. Nevertheless, it is of pivotal importance to prohibit unwanted side effects such as teratoma formation which may occur by ESCs and IPSCs.

In the following, an overview of the currently *in vivo* applied stem cell sources is given. Besides, Table 1 provides

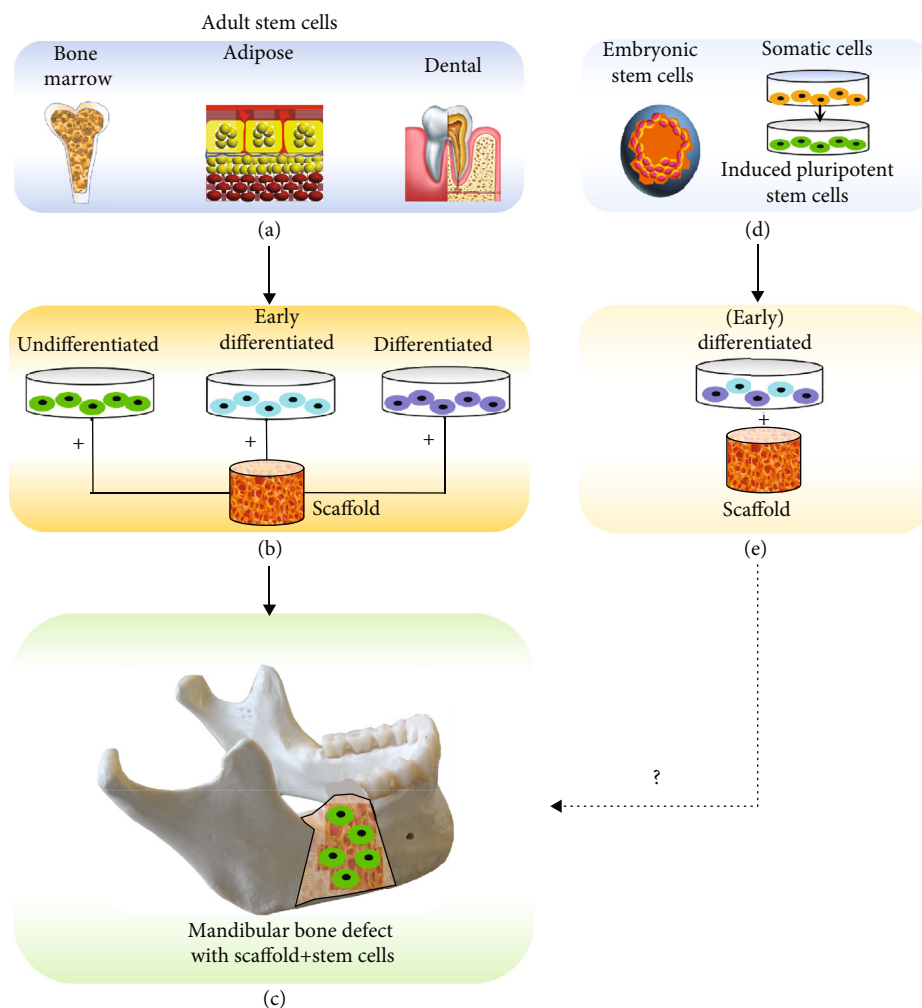


FIGURE 1: Overview of stem cell sources and their stage (undifferentiated, early differentiated, or differentiated) of application. Adult stem cells that are currently applied in clinical studies are retrieved from bone marrow, adipose, or dental tissue (a). These cells are applied in an undifferentiated, early differentiated, or differentiated stage seeded on a scaffold (b). The scaffold with the stem cells is applied in clinical trials to regenerate bone defects, such as mandibular bone defects (c). Embryonic stem cells and somatic stem cells, which are first stimulated into induced pluripotent stem cells (d), are applied in a (early) differentiated stage on a scaffold (e). Their application in clinical trials still needs to be envisioned (c). Note that in the mandibular bone defect shown (c), the stem cells are undifferentiated. However, the stem cells applied in such bone defects could be also early differentiated or differentiated.

an overview of the recent clinical trials, published between January 1, 2015, and November 1, 2019, with successful application of human-derived stem cells. “A successful application” was considered a significant outcome measurement due to the supplementation of MSCs specifically. The majority of these studies investigated bone formation as an outcome measurement based on radiography, (cone beam) computed tomography ((CB)CT), microcomputed tomography (micro-CT), or histomorphometric and/or histologic measurements. As a future direction, it would be interesting to investigate the vascularization in these cases, since enhanced vascularization would be expected in relation to the enhanced osteogenic effects observed due to the supplementation of MSCs. A complete overview of all the clinical studies applying MSCs has been described earlier [35].

Bone marrow was the first source reported to contain MSCs [36]. Until today, adult bone marrow-derived stem

cells (BMSCs) are the most frequently investigated type of MSCs in bone tissue engineering. Several successful applications of BMSCs *in vivo* have been reported in the oral and maxillofacial region (Table 1). There are two different interventions in the application of BMSCs: (1) the use of bone marrow aspirate (concentrated), a whole tissue fraction containing BMSCs, and (2) the use of *in vitro* cultivated BMSCs (expanded with or without differentiation factors) (Table 1). Concentrated bone marrow aspirate compared to nonconcentrated aspirate seems to have a higher osteogenic potential *in vivo* [37]. An overview of the successful clinical trials performed with this cell source is shown in Table 1.

Several studies showed promising results applying BMSCs in surgical procedures in the oral and maxillofacial region. Some maxillary sinus floor elevation studies presented histomorphometrical data that showed increased new bone formation after 3 to 4 months compared to



TABLE 1: Overview of clinical trials applying human-derived stem cells for bone tissue engineering applications/investigations to demonstrate *in vivo* possibilities.

Stem cell source	Intervention	Scaffold material	Clinical procedure	Reference
Bone marrow				
Posterior iliac crest	Aspirate concentrated	FDBA, PRP	Maxillary sinus floor elevation	Bertolai et al. [141]
Posterior iliac crest	Aspirate concentrated	DBBM	Maxillary sinus floor elevation	Pasquali et al. [142]
Posterior iliac crest	<i>In vitro</i> cultivation	$\beta$ -TCP	Maxillary sinus floor elevation	Kaigler et al. [39]
Posterior iliac crest	<i>In vitro</i> cultivation	$\beta$ -TCP	Alveolar cleft reconstruction	Bajestan et al. [43]
Posterior iliac crest	Aspirate concentrated	COL, PRF, nano-HA	Alveolar cleft reconstruction	Al-Ahmady et al. [143]
Posterior iliac crest	<i>In vitro</i> cultivation	HA-SI	Alveolar cleft reconstruction	Khalifa and Gomaa [144]
Posterior iliac crest	Aspirate concentrated	COL, CGF	Jaw defect reconstruction (after enucleation of cyst)	Talaat et al. [145]
Tuberosity	<i>In vitro</i> cultivation	PLA, PRP	Periodontal intrabony defect regeneration	Baba et al. [41]
Adipose tissue				
Abdominal	Aspirate concentrated into SVF	$\beta$ -TCP or BCP	Maxillary sinus floor elevation	Prins et al. [59]
Buccal fat pad	<i>In vitro</i> cultivation	DBBM, AB	Alveolar cleft reconstruction	Khojasteh et al. [60]
Abdominal	<i>In vitro</i> cultivation	—	Mandibular condylar fracture regeneration	Castillo-Cardiel et al. [61]
Dental tissue				
Periosteum	Mechanical disaggregation of sample tissue	PLGA, HA	Maxillary sinus floor elevation	Baena et al. [68]
Pulp	Mechanical disaggregation of sample tissue	COL	Tooth socket preservation	Monti et al. [67]
Periosteum	Mechanical disaggregation of sample tissue	COL	Tooth socket preservation	D' Aquino et al. [66]
Pulp	Mechanical disaggregation of sample tissue	COL	Intrabony periodontal defects	Ferrarotti et al. [69]

PLA: polylactide acid;  $\beta$ -TCP: beta-tricalcium phosphate; FDBA: freeze-dried bone allografts; PRP: platelet-rich plasma; BCP: biphasic calcium phosphate (hydroxyapatite/tricalcium phosphate); DBM: demineralized bone matrix; AB: autologous bone; COL: collagen sponge; CGF: concentrated growth factor; HA: hydroxyapatite; PLGA: poly(lactic-co-glycolic acid); SI: silica.

traditional methods using bone substitutes alone [38, 39]. Kaigler et al. showed accelerated bone regeneration in extraction sockets of teeth when applying BMSCs or gelatin sponge compared to the controls (saline-soaked gelatin sponge) [40]. Baba et al. conducted a phase I/II clinical trial involving ten patients with periodontitis, who required a surgical procedure for intrabony defects, applying bone marrow-derived stem cells with a biodegradable 3D-poly-lactic-acid-based scaffold and platelet-rich plasma. After 12 months, the bone defect showed clinically and radiographically significant improvement compared to conventional periodontal surgical procedures without application of stem cells. These results suggest successful clinical application in regenerating periodontal tissue, including bone tissue [41]. In alveolar cleft surgery, several clinical trials, mainly case reports, suggest promising results with the application of BMSCs, but complete reconstruction (bone fill) of extensive cleft defects has not been demonstrated [42, 43]. In contrast, Hermund

et al. [44] showed no difference in bone density and height between a control group (graft composed of a mixture of bovine bone substitute and autologous bone particles) and a test group (same scaffold, supplemented with BMSCs that were retrieved from the tuberosity and cultivated *in vitro*) after maxillary sinus floor elevation.

Unfortunately, BMSC application comes with limitations: bone marrow aspiration is an invasive and painful procedure for the donor, and cell retrieval is scarce, since the frequency of BMSCs in human bone marrow is rather low (0.001%–0.01%) [45]. Consequently, fresh bone marrow aspirates may result in a too low number and concentration of BMSCs to exert substantial osteogenic effects [37]. Therefore, *in vitro* culture expansion is required to obtain sufficient numbers of cells for clinical application [46]. This cell expansion, however, needs to be done in a laborious, expensive, and time-consuming good manufacturing practice (GMP) laboratory. Other limitations comprise the loss of proliferative

and differentiation capacities during cell expansion [47, 48] and an increased risk for pathogen contamination and genetic transformation [49, 50]. Last but not least, the number, proliferation, and differentiation potential of BMSCs decline with increasing age [51].

Adipose tissue-derived mesenchymal stem cells (ASCs) have opened appealing new possibilities in adult stem cell therapies. ASCs show many similarities with BMSCs with regard to surface marker profiles, multilineage potential, and growth properties [52]. However, in contrast to the other sources (bone marrow, dental, and embryonal), adipose tissue has the following advantages: (a) it has a high stem cell-to-volume ratio [53, 54], (b) the stem cell frequency is far less sensitive to ageing [55], (c) harvesting can easily be upscaled according to the need, and (d) it can be processed within a short time frame to obtain highly enriched ASC preparations (residing in the stromal vascular fraction [SVF]). Furthermore, the multipotent cells within the SVF attach very fast to the scaffold material, proliferate rapidly, and can be differentiated toward amongst others the osteogenic lineage [56, 57].

Helder and colleagues formulated the concept of the one-step surgical procedure (OSP) to apply ASCs in the regeneration of bone tissues [58]. After harvesting the adipose tissue by the surgeon, the SVF-containing ASCs can be seeded onto the scaffold material without culture expansion. Then the ASC scaffold construct can be implanted, all in the same surgical procedure. The obvious advantage of this one-step surgical procedure is not only its patient-friendliness but also its lower costs, since a second surgical intervention and expensive *in vitro* culturing steps can be avoided.

Multiple *in vitro* studies made important advancements in the application of ASCs in bone tissue engineering [32]. Recently, successful results were also obtained in clinical trials (Table 1). The results from a first clinical trial evaluating the application of ASCs showed that it is a feasible, safe, and effective treatment option in jaw bone regeneration [59]. Prins et al. showed in a split-mouth design that patients undergoing maxillary sinus floor elevation for dental implant placement benefitted from the application of ASCs. Bone and osteoid percentages were higher in study biopsies (SVF supplemented to different ceramic bone substitutes) than in control biopsies (ceramic only on contralateral side) (54). The additive effect of SVF supplementation was independent of the bone substitute  $\beta$ -tricalcium phosphate or biphasic calcium phosphate (hydroxyapatite/tricalcium phosphate) [59]. Khojasteh et al. [60] used ASCs derived from the buccal fat pad, *in vitro* cultivated, and seeded on demineralized bovine bone mineral (DBBM) and autologous bone (AB), in alveolar cleft reconstruction. Cone beam-computed tomography 6 months after the treatment showed more bone formation in the test group with supplementation of ASCs. Castillo-Cardiel et al. [61] treated mandibular condylar fractures with abdominal retrieved ASCs that were *in vitro* cultivated and injected at the fracture site. After 12 weeks of the surgical treatment, the test group with the supplemented ASCs had a 37% higher ossification rate compared to the traditional treatment (control group). A disadvantage of SVF harvesting so far is that it is performed

under general anesthesia and requires (short) hospitalization. Also, postoperative care and complaints are to be regarded. However, clinical studies using local anesthesia are currently being undertaken, which may widen the applicability of this intraoperative approach.

Dental tissues provide several populations of stem cells, including the pulp of both exfoliated and adult teeth, periodontal ligament, and dental follicle [62]. Dental tissue-derived stem cells (DSCs) have generic mesenchymal stem cell-like properties such as self-renewal and multilineage differentiation into chondrogenic, osteogenic, and adipogenic cell lineages. In addition, DSCs also show neurogenic and angiogenic potential [62]. It has been demonstrated that DSCs have the ability to generate not only dental tissue such as dentine/pulp-like complexes but also bone tissue [63, 64]. Stem cells from human-exfoliated deciduous teeth exhibit higher proliferation rates and can be easier obtained compared to BMSCs [65].

However, published clinical studies with successful results are scarce (Table 1). D' Aquino et al. [66] used whole tissue fractions from periosteum tissue by mechanically disaggregation, followed by soaking of a collagen sponge in the resulting disaggregated tissue. Calcification was enhanced in tooth socket preservation in the test group with DSCs supplemented to the collagen sponge, compared to the control group with unloaded collagen sponges. Monti et al. [67] used tissue fractions from the dental pulp, followed by soaking of a collagen sponge in a similar clinical model. Sixty days after grafting, the test site (supplemented with DSCs) showed stronger radiopacity when compared with the control site (collagen sponge). Histological analysis showed well-differentiated bone with Haversian system formation in the test site with more bone formation. Baena et al. [68] used whole tissue fractions from periosteum tissue seeded on a poly(lactic-co-glycolic acid) (PLGA) scaffold with hydroxyapatite (HA) in maxillary sinus floor elevation surgery. They showed an increased percentage of vital mineralized tissue in the group treated with both periosteum-derived stem cells and PGLA/HA, with respect to the control group of PGLA/HA or demineralized bovine bone mineral alone, as confirmed by histological analysis and radiographic evaluations at six months after the treatment. Ferrarotti et al. [69] showed clinical success after applying dental pulp stem cells on a collagen sponge in intrabony periodontal regeneration one year after treatment.

The question remains open whether in spite of the low numbers of cells, DSCs might become an attractive source of autologous SCs for bone regeneration. This source is being investigated with at least more than ten new trials underway (<http://www.clinicaltrials.gov>).

### 3. Vascularization in Bone Tissue Regeneration

Successful bone tissue regeneration requires rapid perfusion and integration of the implanted graft with the recipient vasculature. Neovascularization is achieved by both vasculogenesis and angiogenesis. Vasculogenesis is originally described as *de novo* blood vessel formation by differentiation and assembly of angioblastic progenitor cells during

embryogenesis [70]. However, more recently, postnatal vasculogenesis is becoming evident as a major contributor to adult neovascularization. This type of postnatal vasculogenesis is defined as the incorporation of circulating endothelial progenitor cells (EPCs) into the microvascular endothelium of newly developing microvessels [71, 72].

EPCs are mainly located within the stem cell niche in bone marrow, along with some circulating populations in the peripheral blood. When injury or tissue damage occurs, EPCs are thought to mobilize from the bone marrow into the circulation and home to tissue repair sites under the guidance of signals such as hypoxia, growth factors, chemoattractant signals, and chemokines. EPCs then invade and migrate at the same sites and differentiate into mature endothelial cells (ECs) and/or regulate preexisting ECs via paracrine or juxtacrine signals [73].

Angiogenesis is defined as new blood vessel sprouting from preexisting vessels. The first step in this process is the activation of the host microvasculature at the implantation site by angiogenic growth factors, such as vascular endothelial growth factor (VEGF) or basic fibroblast growth factor [74]. These factors may originate from different sources. They may be produced by cells of the host tissue itself due to tissue injury during the implantation procedure or in consequence of an inflammatory response to the implanted graft.

The endothelial cells, which are lining blood vessels, allow the formation of new blood capillaries by the sprouting of an existing small vessel [75, 76]. Upon angiogenic activation, they start to produce matrix metalloproteinases, resulting in the degradation of their basement membrane [77]. This is the prerequisite for their subsequent migration into the surrounding interstitium, which is morphologically reflected by the formation of vascular buds and sprouts. The sprouts progressively grow into the implanted tissue construct and interconnect with each other to develop new blood-perfused microvascular networks [78]. The wall of these networks is finally stabilized by the production of extracellular matrix compounds and the recruitment of smooth muscle cells or pericytes [79].

Accordingly, successful vascularization of an implanted graft via vasculogenesis and angiogenesis is dependent on the coordinated sequence of various humoral and cellular mechanisms and, in particular, the close interaction between the host tissue and the implanted graft. This process allows tissue growth and repair by extending and remodeling the network of blood vessels [73, 80].

#### 4. Vascularization Strategies in Bone Tissue Engineering

Several approaches to improve vascularization, through enhanced vasculogenesis and angiogenesis, of the implanted grafts are currently investigated. The classical vascularization strategies focus on the stimulation of vascular ingrowth into the implanted grafts from the surrounding host tissue by (i) optimizing the material properties of scaffolds and (ii) their bioactivation by incorporation of growth factor delivery systems or by cell seeding. However, endothelial cell migration and physiological growth of new blood vessels has been dem-

onstrated not to be faster than  $\sim 5 \mu\text{m/h}$  [81]. Therefore, these approaches face the problem that sufficient vascularization of the implanted graft requires a prolonged time period which is associated with major tissue loss due to hypoxic conditions.

To overcome this problem, vascular ingrowth directed from the implanted graft towards the host tissue has been proposed to complement vascular ingrowth from the host tissue into the implanted graft. This can be achieved by incorporating the graft with either (i) preformed microvascular networks which can directly be perfused with blood by developing interconnections (inosculation) to the host microvasculature or (ii) microvascular fragments which rapidly develops into microvascular networks after transfer into the host tissue (Figure 2). In the following, an overview of the current possibilities and future perspectives on the above-mentioned strategies to enhance vascularization in bone tissue engineering is provided.

**4.1. Material Properties of Scaffolds.** The characteristics of the scaffold material play an important role in angiogenesis of the graft. Many different scaffold materials for bone tissue engineering have been investigated *in vivo* and *in vitro*, e.g., polymers, bioactive ceramics, and hybrids (composites) [12].

The chemical composition of scaffold materials has been shown to influence the angiogenic process at the implantation site. For instance, poly(lactic-co-glycolic acid) (PLGA), hydroxyapatite (HA), and dentin scaffolds show a slight inflammatory response after implantation, inducing marked angiogenic response and a good vascularization of the grafts after 14 days [78, 82]. In contrast, collagen-chitosan-hydroxyapatite hydrogel scaffolds of identical architecture induce severe inflammation, resulting in apoptotic cell death within the surrounding tissue and a complete lack of ingrowth of newly formed microvessels [78]. Polyurethane scaffolds, which exhibit an excellent *in vivo* biocompatibility, have been shown to be characterized by a poor vascularization [83]. These findings indicate that scaffold materials with slightly proinflammatory properties may stimulate the angiogenic host tissue response to the implanted scaffold material.

Combinations of biomaterials have been investigated to improve the scaffold properties. Composites consist of a combination of two or more materials with different properties, each displaying only some advantages and specific drawbacks. Polymer-ceramic composites have been successful in bone regeneration, exceeding the results obtained when these materials are used separately, showing improved mechanical and biological results [84]. The combination of PLGA (combination of poly lactide and polyglycolide) and HA or  $\beta$ -TCP allows to overcome the problems due to PLGA's acidic degradation products that may induce tissue necrosis and negatively affect neoangiogenesis, since HA and  $\beta$ -TCP neutralize the acidic degradation products of PLGA [85].

Not only the chemical composition but also the architecture of scaffolds is an important determinant for adequate vascularization [86]. It should contain distributed, interconnected pores and display a high porosity in order to ensure cell penetration, vascular ingrowth, nutrient diffusion, and waste product elimination [87]. Another key component to allow proper cell colonization (cells bound to ligands within

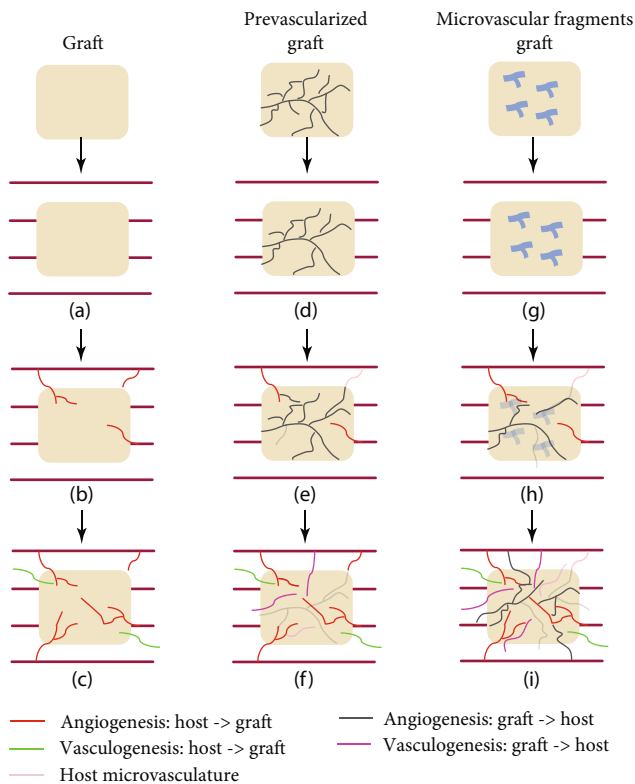


FIGURE 2: Overview of the three different vascularization strategies and their clinical results. First, a graft is implanted (a) which solely depends on the vascularization, angiogenesis, and vasculogenesis, from the host towards the graft (b). This results in insufficient vascularization of the graft (c). Second, a prevascularized graft is implanted in the host tissue (d). A high number of preformed microvessels have a suboptimal lifespan (e), resulting in less microvessels for vascularization from the graft towards the host (f). Third, microvascular fragments in the graft (g) develop rapidly into microvessels when implanted in the host tissue (h). They contribute to vascularization (angiogenesis and vasculogenesis) from the graft towards the host, which results in enhanced vascularization. Vascularization starts from two directions, i.e., from the graft and from the host tissue (i).

the scaffold) is the mean pore size [88]. The minimum recommended pore size for a scaffold is  $100\ \mu\text{m}$  [89] based on the early work of Hulbert et al. [90], but subsequent studies have shown better osteogenesis for implants with pores  $> 300\ \mu\text{m}$  [91, 92]. Relatively larger pores favor direct osteogenesis, since they allow vascularization and high oxygenation, while smaller pores result in endochondral ossification, although the type of bone ingrowth depends on the biomaterial and the geometry of the pores. There is, however, an upper limit in porosity and pore size set by constraints associated with mechanical properties [86, 93].

**4.2. Bioactivation of the Scaffold by Incorporation of Growth Factors or Cell Seeding.** A common strategy to improve scaffold vascularization is the stimulation of the angiogenic host tissue response at the implantation site by incorporation of angiogenic growth factors. For this purpose, VEGF [94, 95], basic fibroblast growth factor [96], platelet-derived

growth factor [97], and angiogenin [98] are the most frequently used factors. However, there are continuing concerns about the cost of multiple cytokines and delivery, potential toxicity, and suboptimal endothelial migration in large tissue grafts.

Another important aspect to consider is that many angiogenic growth factors are known to be released spontaneously by cells under stress-related conditions, including hypoxia. Due to hypoxia, bone-derived osteoblast-like cells as well as bone marrow mesenchymal stem cells (BMSCs) are known to liberate growth factors such as VEGF. Based on this cellular mechanism, an accelerated vascularization of scaffolds is also achieved by seeding the scaffolds with differentiated tissue-specific cells [99, 100] or multipotent stem cells [101, 102]. Although BMSCs are known to have the potential to differentiate into defined vascular cells, it has been shown that the observed acceleration of vascularization at 14 days *in vivo* more strongly depends on the liberation of VEGF by the seeded cells than the differentiation potential of the BMSCs [99]. Even though there is significant acceleration of vascularization after cell seeding, Tavassol et al. [100] showed that the majority of seeded osteoblast-like cells died within the observation period of 14 days after *in vivo* implantation of PGLA scaffolds seeded with osteoblast-like cells. This indicated that this method alone is not sufficient to accelerate the vascularization to ensure the survival of seeded cells. Qu et al. [103] showed that genetically modified cells could have a long-term expression of angiogenic growth factors, independently from their state of hypoxia. They transfected BMSCs with basic fibroblast growth factor seeded on a composite scaffold in a calvarial critical-sized defect model in rats. It accelerated vascularization and bone regeneration at 4 and 8 weeks compared with the controls. However, it was also suggested that overexpression of angiogenic growth factor VEGF may cause a global reduction in bone quantity, consisting of thin trabeculae of immature matrices [104].

**4.3. Preformed Microvascular Networks.** Different approaches to prevascularize the graft *in vitro* by seeding of vessel-forming cells onto scaffolds are being investigated. After seeding onto the scaffold, these cells rapidly assemble into immature microvessels. In contrast to the above-mentioned approaches that focus on the stimulation of vascular ingrowth into the implanted graft, prevascularization is aimed at generating preformed microvascular networks inside the graft prior to their implantation. After implantation, these networks can be rapidly perfused with blood by inosculation with the surrounding host microvasculature [80].

Proangiogenic cells, such as endothelial cells, endothelial progenitor cells, and mural cells (pericytes and smooth muscle cells), are widely used as cell source. Other cell sources including adult stem cells, such as pluripotent mesenchymal stem cells from bone marrow [105, 106] or adipose tissue [106–108], and induced pluripotent stem cells [109] are also suggested as suitable sources for this purpose.

Originally, endothelial and endothelial progenitor cells were used for the formation of blood vessels, but this resulted

in blood vessels with suboptimal lifespan [110]. Due to a limited number of transplanted vascular cells surviving for a prolonged duration, neovasculature fails to recruit the obligatory perivascular cells including mural cells and consequently does not resemble native, multilayered mature microvessels [111]. To overcome this problem, gene transfection to improve the survival and proliferation of the used vascular cells has been suggested [110, 112]. However, this genetic manipulation bears an oncogenic risk [113].

A better alternative being investigated seems to be the cocultivation of endothelial cells with mural cells. These cells are crucial for the stabilization, maturation, and long-term survival of newly formed microvessels. Koike et al. [114] demonstrated stable microvascular networks, which survived for one year *in vivo*, through cocultivation of human umbilical vein endothelial cells (HUVECs) with mural precursor cells. This is in contrast to microvessels engineered with HUVECs alone, which rapidly regressed after 60 days [110]. However, limitations of cell-based prevascularization approaches are that these approaches usually need complex and time-consuming cell isolation and cultivation procedures. Besides, their safety and success are highly sensitive to the quality of the cell isolates, the applied seeding strategy, and the number of cells seeded. Multiple studies reported on a critical optimum ratio between vascular cells and tissue-specific cells within a construct [115, 116]. Therefore, their clinical application is difficult to envision.

**4.4. Microvascular Fragments (MF).** Prevascularization methods by cell seeding using cellular isolates may result in uncertain outcomes. Moreover, the correct ratio of cells to be used is difficult to determine. This led to a novel concept exploiting the use of microvascular fragments (MF) isolated from adipose tissue by short (5–10 min) digestion [117–119]. MF is a mixture of arteriolar, capillary, and venular vessel segments [120]. Several studies successfully isolated MF from mice [117, 118] and human [119] and transplanted adipose tissue-derived MF in animals. These studies further demonstrated that these fragments rapidly develop stable, blood-perfused microvascular networks after implantation into the host tissue. In culture, MF have been shown to release the proangiogenic factors vascular endothelial growth factor (VEGF) and basic fibroblast growth factor (bFGF) [121, 122]. In addition, microvascular fragments contain stem cell antigen (Sca)-1/VEGFR-2-positive endothelial progenitor cells and mesenchymal stem cells expressing common markers, such as CD44, CD73, CD90, and CD117 [123]. It has been speculated that the high vascularization potential of microvascular fragments is (partly) caused by these stem cell populations. Compared to the above described cell seeding strategies to generate *in vitro* preformed microvascular networks, the enzymatic digestion period for the isolation of microvascular fragments is much shorter (5–10 min) than that of single source cells and does not require complex and time-consuming *in vitro* incubation periods. Moreover, MF can also be obtained from patients in a one-step surgical procedure with a liposuction technique under local anesthesia [124].

However, the MF procurement does not avoid the regulatory burden of using stem cell preparations obtained by enzymatic digestion, which are considered “more than minimally manipulated” by the FDA and the European counterpart the EMA. Therefore, recently, much effort was put in the development of mechanical disruption of the tissue creating microfragmented adipose tissue/nanofat (MFAT/N-FAT) (reviewed in Trivisonno et al.’s study [125]).

Strikingly, it was found that the microfragmentation of the adipose tissue, which kept the microarchitecture (extracellular matrix with embedded mesenchymal stem cells and microvascular fragments) of the fat intact but disrupts most mature adipocytes, showed a remarkable enrichment of blood vessel-stabilizing pericytes and release of many more growth factors and cytokines involved in tissue repair and regeneration, noticeably via angiogenesis, compared to enzymatically obtained SVF [126]. Moreover, the microfragmented adipose tissue maintained strong angiogenic and anti-inflammatory properties [127]. Autologous transplantation of such mechanically processed adipose tissue has been used with success in multiple indications, spanning a.o. cosmetics [128, 129], orthopedics [130, 131], and proctology [132].

## 5. Future Directions

Future investigations in cellular bone tissue engineering applications should be focused on enhancing vascularization, since adequate vascularization is a prerequisite for successful clinical bone regeneration. Moreover, due to existing discrepancies in the way human MSC are harvested and whether they are either directly applied without cultivation or isolated and cultured *ex vivo*, in addition to donor-dependent variability regarding the bone forming potency, further investigations are needed to standardize the production and quality of stem cells for therapeutic applications.

A promising future direction for cellular tissue engineering in jaw bone reconstruction with feasible clinical application is the use of the stromal vascular fraction (SVF) of human adipose tissue. SVF is considered a “single source” for cellular tissue engineering due to its heterogeneous population of essential cells, i.e., multipotent stem cells and progenitor cells, including endothelial cells, stroma cells, pericytes, preadipocytes, and hematopoietic cells. SVF also contains macrophages, which secrete a multitude of vascular growth factors and cytokines [133].

The adipose stem cells (ASCs) in SVF have been shown to attach, proliferate, and osteogenically differentiate on calcium phosphate scaffolds [134] and secrete a multitude of growth factors [57]. ASCs not only have been shown to have osteogenic potential *in vivo* [59] but also demonstrated angiogenic potential crucial for bone tissue engineering applications in mice [135]. This is supported by *in vitro* observations that ASCs in SVF secrete a variety of angiogenic and antiapoptotic growth factors [136] and that SVF is highly enriched with CD34+CD45–cells. The CD34+ cells are capable of stimulating angiogenesis and are involved in neovascularization processes that facilitate healing of ischemic tissues in mouse models [137]. Moreover, it has been demonstrated that if cultured within 3D scaffolds, the

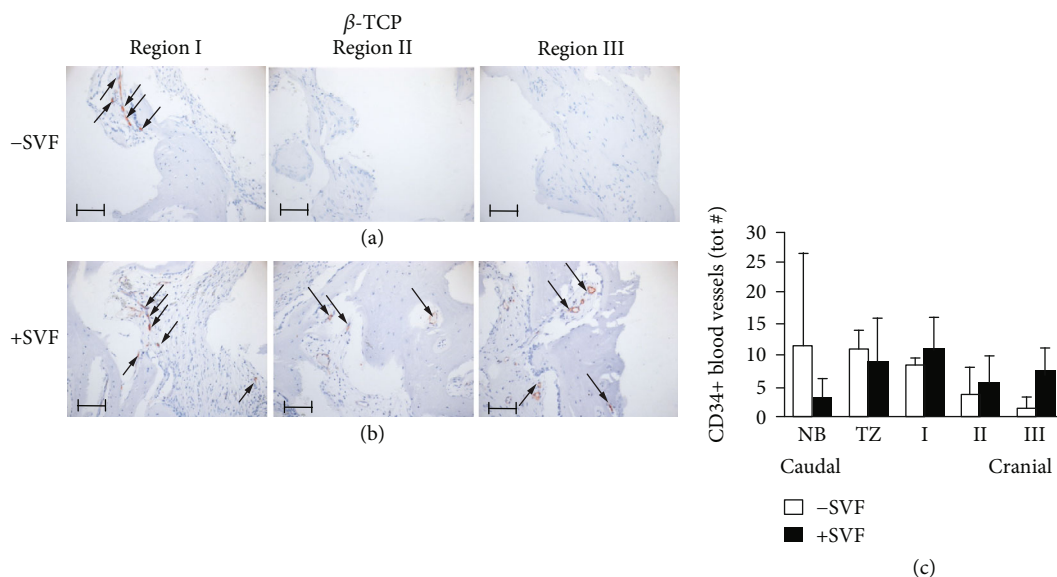


FIGURE 3: Immunohistochemical analysis of CD34, a marker of endothelial cells as well as stem cells such as endothelial progenitor stem cells and hematopoietic stem cells, of a maxillary bone biopsy from a patient treated with  $\beta$ -TCP (a–c). Magnification: 200x. The scale bar represents 100  $\mu$ m. The total number of CD34+ blood vessels of selected bone biopsies taken from control sides without stem cells (white bars;  $n = 3$ ) and study sides with stem cells (black bars;  $n = 4$ ) from patients treated with  $\beta$ -TCP (b).  $\beta$ -TCP:  $\beta$ -tricalcium phosphate; NB: native bone; TZ: transition zone; SVF: stromal vascular fraction; tot #: total number (adapted from Farré-Guasch E, Bravenboer N, Helder MN, Schulten EAJM, Ten Bruggenkate CM, Klein-Nulend J, 2018, Materials, 11, 161).

combination of endothelial cells and stromal cells derived from the SVF assembles into vascular structures, thus actively contributing to the vascularization of tissue-engineered bone grafts and stimulating their engraftment *in vivo* [124].

A first clinical trial confirmed that SVF/ASCs are capable to enhance bone and blood vessel formation [59, 138]. The study group (bone substitute [calcium phosphate] combined with SVF/ASCs) showed a higher bone mass that positively correlated with blood vessel formation versus the control group (only bone substitute) in a maxillary sinus floor elevation model [138]. Immunohistochemical analysis of CD34, a marker of endothelial cells as well as stem cells such as endothelial progenitor stem cells and hematopoietic stem cells, revealed a higher number of CD34+ blood vessels in the SVF-supplemented group (SVF+) than the bone substitute-only group (SVF-) (Figure 3), indicating a proangiogenic effect of the SVF. In addition, the vasculogenic effect of the SVF has been indicated *in vitro* [139].

Further investigations should also address the possibilities to enhance the osteogenic capacity of the ASCs within the treatment time of the “one-step surgery.” *In vitro* results of short (minutes) incubation of ASCs with a low dose of bone morphogenetic protein-2 (BMP-2) before seeding the cells on the scaffold ( $\beta$ -TCP and BCP) showed promising results; i.e., proliferation and osteogenic differentiation were enhanced by BMP-2 pretreatment, with concomitant down-regulation of adipogenic gene expression. Stimulated gene expression of the osteogenic markers core binding factor alpha 1, collagen-1, osteonectin, and osteocalcin in the seeded ASCs was observed [134].

Recently, several studies suggested that adipose tissue-derived microvascular fragments (MF) show higher vascularization potential than SVF [118, 126]. However, further *in vitro* and *in vivo* research needs to confirm these findings. The MF and MFAT/NFAT variants of adipose tissue may spur future developments in particular for homologous applications since the regulatory burden can be avoided and the angiogenic, anti-inflammatory, and regenerative growth factor secretion properties appear at least equal but likely even higher than collagenase-digested SVF [126, 127].

The major clinical benefit of applying adipose tissue-derived SVF, MF, or MFAT/NFAT compared to other single-cell sources is that a native mixture of essential cells can be harvested in large quantities in a one-step surgical procedure. This makes clinical application of adipose tissue-derived SVF or MF feasible, due to its lower morbidity rate and shorter treatment duration compared to the traditional treatment options, such as autologous bone harvesting, bone marrow-derived stem cells, and endothelial cells.

Appropriate *in vitro* 3D models of bone defects to investigate cellular bone tissue engineering techniques, and specifically vascularization, are lacking. Such models would enhance the understanding of the interaction of cells with the host environment for osteogenesis and angiogenesis. Moreover, it would facilitate new possibilities for vascularization strategies. Currently exploited 2D-models and *in vivo* animal models have several limitations, including controllability, reproducibility, and flexibility of design. Recently, novel strategies in 3D-models are investigated to mimic human physiology *in vitro*, including bone niche-on-a-chip and bone bioreactors [140].

## 6. Conclusions

Important advancements have been made regarding the application of stem cells and the development of new strategies to improve vascularization in bone tissue engineering. However, adequate graft vascularization, which is a prerequisite to successful bone regeneration, is still considered a major challenge. The use of SVF of human adipose tissue seems to be a promising source for bone tissue engineering due to its heterogeneous population of essential cells for osteogenesis and angiogenesis. Besides, adipose tissue-derived MF is suggested as a promising cell source, due to its correct native cell ratios, for vascularization strategies. SVF, MF, and MFAT/NFAT are treatment options with clinical feasibility due to their large quantities that can be harvested and applied in a one-step surgical procedure. Appropriate *in vitro* models to study bone tissue engineering are lacking. Engineered *in vitro* 3D models mimicking the bone defect environment are crucial to facilitate new bone regeneration strategies. Successful bone reconstruction in the oral and maxillofacial region, using bone tissue engineering techniques, requires innovative future investigations focusing on the enhancement of vascularization.

## Conflicts of Interest

The authors declare that there is no conflict of interest regarding the publication of this article.

## Authors' Contributions

Jenneke Klein-Nulend and Engelbert A.J.M. Schulten contributed equally as the last authors.

## References

- [1] J. P. Schmitz, "The critical size defect as an experimental model for craniomandibulofacial nonunions," *Clinical Orthopaedics and Related Research*, vol. 205, pp. 299–308, 1986.
- [2] D. J. G. Baxter and M. M. Shroff, "Developmental maxillofacial anomalies," *Seminars in Ultrasound, CT and MRI*, vol. 32, no. 6, pp. 555–568, 2011.
- [3] B. L. Foster, M. S. Ramnitz, R. I. Gafni et al., "Rare bone diseases and their dental, oral, and craniofacial manifestations," *Journal of Dental Research*, vol. 93, pp. 7S–19S, 2014.
- [4] S. Kuroshima, M. Sasaki, and T. Sawase, "Medication-related osteonecrosis of the jaw: a literature review," *Journal of Oral Biosciences*, vol. 61, no. 2, pp. 99–104, 2019.
- [5] A. Terashima and H. Takayanagi, "The role of bone cells in immune regulation during the course of infection," *Seminars in Immunopathology*, vol. 41, no. 5, pp. 619–626, 2019.
- [6] S. Chukwulebe and C. Hogrefe, "The diagnosis and management of facial bone fractures," *Emergency Medicine Clinics of North America*, vol. 37, no. 1, pp. 137–151, 2019.
- [7] M. G. Araújo and J. Lindhe, "Dimensional ridge alterations following tooth extraction. An experimental study in the dog," *Journal of Clinical Periodontology*, vol. 32, no. 2, pp. 212–218, 2005.
- [8] D. Rolski, J. Kostrzewa-Janicka, P. Zawadzki, K. Zycińska, and E. Mierzwińska-Nastalska, "The management of patients after surgical treatment of maxillofacial tumors," *BioMed Research International*, vol. 2016, Article ID 4045329, 7 pages, 2016.
- [9] J. S. Vorrasi and A. Kolokythas, "Controversies in traditional oral and maxillofacial reconstruction," *Oral and Maxillofacial Surgery Clinics of North America*, vol. 29, no. 4, pp. 401–413, 2017.
- [10] G. Fernandez de Grado, L. Keller, Y. Idoux-Gillet et al., "Bone substitutes: a review of their characteristics, clinical use, and perspectives for large bone defects management," *Journal of Tissue Engineering*, vol. 9, 18 pages, 2018.
- [11] H. E. Jazayeri, M. Tahriri, M. Razavi et al., "A current overview of materials and strategies for potential use in maxillofacial tissue regeneration," *Materials Science and Engineering C*, vol. 70, Part 1, pp. 913–929, 2017.
- [12] L. Roseti, V. Parisi, M. Petretta et al., "Scaffolds for bone tissue engineering: state of the art and new perspectives," *Materials Science and Engineering C*, vol. 78, pp. 1246–1262, 2017.
- [13] J. R. Perez, D. Kouroupis, D. J. Li, T. M. Best, L. Kaplan, and D. Correa, "Tissue engineering and cell-based therapies for fractures and bone defects," *Frontiers in Bioengineering and Biotechnology*, vol. 6, pp. 1–23, 2018.
- [14] M. T. Langhans, S. Yu, and R. S. Tuan, "Stem cells in skeletal tissue engineering: technologies and models," *Current Stem Cell Research and Therapy*, vol. 11, no. 6, pp. 453–474, 2015.
- [15] Y. Kinoshita and H. Maeda, "Recent developments of functional scaffolds for craniomaxillofacial bone tissue engineering applications," *The Scientific World Journal*, vol. 2013, Article ID 863157, 21 pages, 2013.
- [16] D. C. Colter, I. Sekiya, and D. J. Prockop, "Identification of a subpopulation of rapidly self-renewing and multipotential adult stem cells in colonies of human marrow stromal cells," *Proceedings of the National Academy of Sciences of the United States of America*, vol. 98, no. 14, pp. 7841–7845, 2001.
- [17] J. A. Andrades, J. A. Santamaria, M. E. Nimni, and J. Becerra, "Selection and amplification of a bone marrow cell population and its induction to the chondro-osteogenic lineage by rhOP-1: an in vitro and in vivo study," *International Journal of Developmental Biology*, vol. 45, no. 4, pp. 689–693, 2001.
- [18] L. C. Gerstenfeld, D. M. Cullinane, G. L. Barnes, D. T. Graves, and T. A. Einhorn, "Fracture healing as a post-natal developmental process: molecular, spatial, and temporal aspects of its regulation," *Journal of Cellular Biochemistry*, vol. 88, no. 5, pp. 873–884, 2003.
- [19] T. Kon, T. Cho, T. Aizawa et al., "Expression of osteoprotegerin, receptor activator of NF- $\kappa$ B ligand (osteoprotegerin ligand) and related proinflammatory cytokines during fracture healing," *Journal of Bone and Mineral Research*, vol. 16, no. 6, pp. 1004–1014, 2001.
- [20] S. M. Meloni, S. A. Jovanovic, I. Urban, L. Canullo, M. Pisano, and M. Tallarico, "Horizontal ridge augmentation using GBR with a native collagen membrane and 1:1 ratio of particulated xenograft and autologous bone: a 1-year prospective clinical study," *Clinical Implant Dentistry and Related Research*, vol. 19, no. 1, pp. 38–45, 2017.
- [21] I. A. Urban, H. Nagursky, J. L. Lozada, and K. Nagy, "Horizontal ridge augmentation with a collagen membrane and a combination of particulated autogenous bone and anorganic bovine bone-derived mineral: a prospective case series in 25

- patients," *The International Journal of Periodontics and Restorative Dentistry*, vol. 33, no. 3, pp. 299–307, 2013.
- [22] K. Yagihara, S. Okabe, J. Ishii et al., "Mandibular reconstruction using a poly(L-lactide) mesh combined with autogenous particulate cancellous bone and marrow: a prospective clinical study," *International Journal of Oral and Maxillofacial Surgery*, vol. 42, no. 8, pp. 962–969, 2013.
- [23] H. Ohgushi, Y. Dohi, T. Yoshikawa et al., "Osteogenic differentiation of cultured marrow stromal stem cells on the surface of bioactive glass ceramics," *Journal of Biomedical Materials Research*, vol. 32, no. 3, pp. 341–348, 1996.
- [24] P. Janicki and G. Schmidmaier, "What should be the characteristics of the ideal bone graft substitute? Combining scaffolds with growth factors and/or stem cells," *Injury*, vol. 42, pp. S77–S81, 2011.
- [25] C. Colton, "Implantable biohybrid artificial organs," *Cell Transplantation*, vol. 4, no. 4, pp. 415–436, 1995.
- [26] A. Moya, J. Paquet, M. Deschepper et al., "Human mesenchymal stem cell failure to adapt to glucose shortage and rapidly use intracellular energy reserves through glycolysis explains poor cell survival after implantation," *Stem Cells*, vol. 36, no. 3, pp. 363–376, 2018.
- [27] A. M. Rodriguez, C. Elabd, E. Z. Amri, G. Ailhaud, and C. Dani, "The human adipose tissue is a source of multipotent stem cells," *Biochimie*, vol. 87, no. 1, pp. 125–128, 2005.
- [28] S. Gronthos, M. Mankani, J. Brahimi, P. G. Robey, and S. Shi, "Postnatal human dental pulp stem cells (DPSCs) in vitro and in vivo," *Proceedings of the National Academy of Sciences of the United States of America*, vol. 97, no. 25, pp. 13625–13630, 2000.
- [29] M. Miura, S. Gronthos, M. Zhao et al., "SHED: stem cells from human exfoliated deciduous teeth," *Proceedings of the National Academy of Sciences of the United States of America*, vol. 100, no. 10, pp. 5807–5812, 2003.
- [30] X. Liu, P. Wang, W. Chen, M. D. Weir, C. Bao, and H. H. K. Xu, "Human embryonic stem cells and macroporous calcium phosphate construct for bone regeneration in cranial defects in rats," *Acta Biomaterialia*, vol. 10, no. 10, pp. 4484–4493, 2014.
- [31] L. D. K. Buttery, S. Bourne, J. D. Xynos et al., "Differentiation of osteoblasts and in Vitro Bone formation from murine embryonic stem cells," *Tissue Engineering*, vol. 7, no. 1, pp. 89–99, 2001.
- [32] K. Rutledge, Q. Cheng, M. Pryzhkova, G. M. Harris, and E. Jabbarzadeh, "Enhanced differentiation of human embryonic stem cells on extracellular matrix-containing osteomimetic scaffolds for bone tissue engineering," *Tissue Engineering - Part C Methods*, vol. 20, no. 11, pp. 865–874, 2014.
- [33] A. Ardeshirylajimi, "Applied induced pluripotent stem cells in combination with biomaterials in bone tissue engineering," *Journal of Cellular Biochemistry*, vol. 118, no. 10, pp. 3034–3042, 2017.
- [34] V. Volarevic, B. S. Markovic, M. Gazdic et al., "Ethical and safety issues of stem cell-based therapy," *International Journal of Medical Sciences*, vol. 15, no. 1, pp. 36–45, 2018.
- [35] S. Shanbhag, S. Suliman, N. Pandis, A. Stavropoulos, M. Sanz, and K. Mustafa, "Cell therapy for orofacial bone regeneration: a systematic review and meta-analysis," *Journal of Clinical Periodontology*, vol. 46, pp. 162–182, 2019.
- [36] A. J. Friedenstein, I. I. Piatetzky-Shapiro, and K. V. Petrakova, "Osteogenesis in transplants of bone marrow cells," *Journal of Embryology and Experimental Morphology*, vol. 16, no. 3, pp. 381–390, 1966.
- [37] P. Hernigou, A. Poignard, F. Beaujean, and H. Rouard, "Percutaneous autologous bone-marrow grafting for nonunions: influence of the number and concentration of progenitor cells," *Journal of Bone and Joint Surgery*, vol. 87, no. 7, pp. 1430–1437, 2005.
- [38] D. Rickert, S. Sauerbier, H. Nagursky, D. Menne, A. Vissink, and G. M. Raghoebar, "Maxillary sinus floor elevation with bovine bone mineral combined with either autogenous bone or autogenous stem cells: a prospective randomized clinical trial," *Clinical Oral Implants Research*, vol. 22, no. 3, pp. 251–258, 2011.
- [39] D. Kaigler, G. Avila-Ortiz, S. Travan et al., "Bone engineering of maxillary sinus bone deficiencies using enriched CD90+ stem cell therapy: a randomized clinical trial," *Journal of Bone and Mineral Research*, vol. 30, no. 7, pp. 1206–1216, 2015.
- [40] D. Kaigler, G. Pagni, C. H. Park et al., "Stem cell therapy for craniofacial bone regeneration: a randomized, controlled feasibility trial," *Cell Transplantation*, vol. 22, no. 5, pp. 767–777, 2013.
- [41] S. Baba, Y. Yamada, A. Komuro et al., "Phase I/II trial of autologous bone marrow stem cell transplantation with a three-dimensional woven-fabric scaffold for periodontitis," *Stem Cells International*, vol. 2016, Article ID 6205910, 7 pages, 2016.
- [42] M. N. Bajestan, A. Rajan, S. P. Edwards et al., "Stem cell therapy for reconstruction of alveolar cleft and trauma defects in adults: a randomized controlled, clinical trial," *Clinical Implant Dentistry and Related Research*, vol. 19, no. 5, pp. 793–801, 2017.
- [43] H. Behnia, A. Khojasteh, M. Soleimani, A. Tehranchi, and A. Atashi, "Repair of alveolar cleft defect with mesenchymal stem cells and platelet derived growth factors: a preliminary report," *Journal of Cranio-Maxillofacial Surgery*, vol. 40, no. 1, pp. 2–7, 2012.
- [44] N. U. Hermund, A. Stavropoulos, O. Donatsky et al., "Reimplantation of cultivated human bone cells from the posterior maxilla for sinus floor augmentation. Histological results from a randomized controlled clinical trial," *Clinical Oral Implants Research*, vol. 23, no. 9, pp. 1031–1037, 2012.
- [45] M. F. Pittenger, A. M. Mackay, S. C. Beck et al., "Multilineage potential of adult human mesenchymal stem cells," *Science*, vol. 284, no. 5411, pp. 143–147, 1999.
- [46] M. E. Bernardo, L. M. Ball, A. M. Cometa et al., "Co-infusion of ex vivo-expanded, parental MSCs prevents life-threatening acute GVHD, but does not reduce the risk of graft failure in pediatric patients undergoing allogeneic umbilical cord blood transplantation," *Bone Marrow Transplantation*, vol. 46, no. 2, pp. 200–207, 2011.
- [47] J. Lienau, H. Schell, D. R. Epari et al., "CYR61 (CCN1) protein expression during fracture healing in an ovine tibial model and its relation to the mechanical fixation stability," *Journal of Orthopaedic Research*, vol. 24, no. 2, pp. 254–262, 2006.
- [48] S. P. Bruder, N. Jaiswal, and S. E. Haynesworth, "Growth kinetics, self-renewal, and the osteogenic potential of purified human mesenchymal stem cells during extensive subcultivation and following cryopreservation," *Journal of Cellular Biochemistry*, vol. 64, no. 2, pp. 278–294, 1997.



- [49] D. Rubio, S. Garcia, M. F. Paz et al., "Molecular characterization of spontaneous mesenchymal stem cell transformation," *PLoS One*, vol. 3, no. 1, p. e1398, 2008.
- [50] R. Izadpanah, D. Kaushal, C. Kriedt et al., "Long-term in vitro expansion alters the biology of adult mesenchymal stem cells," *Cancer Research*, vol. 68, no. 11, pp. 4229–4238, 2008.
- [51] G. F. Muschler, H. Nitto, C. A. Boehm, and K. A. Easley, "Age- and gender-related changes in the cellularity of human bone marrow and the prevalence of osteoblastic progenitors," *Journal of Orthopaedic Research*, vol. 19, no. 1, pp. 117–125, 2001.
- [52] W. J. F. M. Jurgens, M. J. Oedayrajsingh-Varma, M. N. Helder et al., "Effect of tissue-harvesting site on yield of stem cells derived from adipose tissue: implications for cell-based therapies," *Cell and Tissue Research*, vol. 332, no. 3, pp. 415–426, 2008.
- [53] A. J. Katz, A. Tholpady, S. S. Tholpady, H. Shang, and R. C. Ogle, "Cell surface and transcriptional characterization of human adipose-derived adherent stromal (hADAS) cells," *Stem Cells*, vol. 23, no. 3, pp. 412–423, 2005.
- [54] H. Nakagami, R. Morishita, K. Maeda, Y. Kikuchi, T. Ogiwara, and Y. Kaneda, "Adipose tissue-derived stromal cells as a novel option for regenerative cell therapy," *Journal of Atherosclerosis and Thrombosis*, vol. 13, no. 2, pp. 77–81, 2006.
- [55] D. Dufrane, "Impact of age on human adipose stem cells for bone tissue engineering," *Cell Transplantation*, vol. 26, no. 9, pp. 1496–1504, 2017.
- [56] W. J. Jurgens, R. J. Kroeze, R. A. Bank, M. J. P. F. Ritt, and M. N. Helder, "Rapid attachment of adipose stromal cells on resorbable polymeric scaffolds facilitates the one-step surgical procedure for cartilage and bone tissue engineering purposes," *Journal of Orthopaedic Research*, vol. 29, no. 6, pp. 853–860, 2011.
- [57] J. R. Overman, M. N. Helder, C. M. Ten Bruggenkate, E. A. J. M. Schulten, J. Klein-Nulend, and A. D. Bakker, "Growth factor gene expression profiles of bone morphogenetic protein-2-treated human adipose stem cells seeded on calcium phosphate scaffolds *in vitro*," *Biochimie*, vol. 95, no. 12, pp. 2304–2313, 2013.
- [58] M. N. Helder, M. Knippenberg, J. Klein-Nulend, and P. I. J. M. Wuisman, "Stem cells from adipose tissue allow challenging new concepts for regenerative medicine," *Tissue Engineering*, vol. 13, no. 8, pp. 1799–1808, 2007.
- [59] H.-J. Prins, E. A. J. M. Schulten, C. M. ten Bruggenkate, J. Klein-Nulend, and M. N. Helder, "Bone regeneration using the freshly isolated autologous stromal vascular fraction of adipose tissue in combination with calcium phosphate ceramics," *Stem Cells Translational Medicine*, vol. 5, no. 10, pp. 1362–1374, 2016.
- [60] A. Khojasteh, L. Kheiri, H. Behnia et al., "Lateral ramus cortical bone plate in alveolar cleft osteoplasty with concomitant use of buccal fat pad derived cells and autogenous bone: phase I clinical trial," *BioMed Research International*, vol. 2017, Article ID 6560234, 12 pages, 2017.
- [61] G. Castillo-Cardiel, A. C. López-Echaury, J. A. Saucedo-Ortiz et al., "Bone regeneration in mandibular fractures after the application of autologous mesenchymal stem cells, a randomized clinical trial," *Dental Traumatology*, vol. 33, no. 1, pp. 38–44, 2017.
- [62] M. F. H. Yusof, W. Zahari, S. N. M. Hashim et al., "Angiogenic and osteogenic potentials of dental stem cells in bone tissue engineering," *Journal of Oral Biology and Craniofacial Research*, vol. 8, no. 1, pp. 48–53, 2018.
- [63] X. Yang, P. M. Van Der Kraan, Z. Bian, M. Fan, X. F. Walboomers, and J. A. Jansen, "Mineralized tissue formation by BMP2-transfected pulp stem cells," *Journal of Dental Research*, vol. 88, no. 11, pp. 1020–1025, 2009.
- [64] Y. Yamada, M. Ueda, H. Hibi, and S. Baba, "A novel approach to periodontal tissue regeneration with mesenchymal stem cells and platelet-rich plasma using tissue engineering technology: a clinical case report," *The International Journal of Periodontics & Restorative Dentistry*, vol. 26, no. 4, pp. 363–369, 2006.
- [65] S. Nakamura, Y. Yamada, W. Katagiri, T. Sugito, K. Ito, and M. Ueda, "Stem cell proliferation pathways comparison between human exfoliated deciduous teeth and dental pulp stem cells by gene expression profile from promising dental pulp," *Journal of Endodontics*, vol. 35, no. 11, pp. 1536–1542, 2009.
- [66] R. d'Aquino, L. Trovato, A. Graziano et al., "Periosteum-derived micro-grafts for tissue regeneration of human maxillary bone," *Journal of Translational Science*, vol. 2, no. 2, pp. 125–129, 2016.
- [67] M. Monti, A. Graziano, S. Rizzo et al., "In vitro and in vivo differentiation of progenitor stem cells obtained after mechanical digestion of human dental pulp," *Journal of Cellular Physiology*, vol. 232, no. 3, pp. 548–555, 2017.
- [68] R. Rodriguez y Baena, R. D'Aquino, A. Graziano et al., "Autologous periosteum-derived micrografts and PLGA/HA enhance the bone formation in sinus lift augmentation," *Frontiers in Cell and Developmental Biology*, vol. 5, pp. 1–7, 2017.
- [69] F. Ferrarotti, F. Romano, M. N. Gamba et al., "Human intrabony defect regeneration with micrografts containing dental pulp stem cells: a randomized controlled clinical trial," *Journal of Clinical Periodontology*, vol. 45, no. 7, pp. 841–850, 2018.
- [70] W. Risau and I. Flamme, "Vasculogenesis," *Annual Review of Cell and Developmental Biology*, vol. 11, no. 1, pp. 73–91, 1995.
- [71] T. Asahara, H. Masuda, T. Takahashi et al., "Bone marrow origin of endothelial progenitor cells responsible for postnatal vasculogenesis in physiological and pathological neovascularization," *Circulation Research*, vol. 85, no. 3, pp. 221–228, 1999.
- [72] M. Eguchi, H. Masuda, and T. Asahara, "Endothelial progenitor cells for postnatal vasculogenesis," *Clinical and Experimental Nephrology*, vol. 11, no. 1, pp. 18–25, 2007.
- [73] S. Balaji, A. King, T. M. Crombleholme, and S. G. Keswani, "The role of endothelial progenitor cells in postnatal vasculogenesis: implications for therapeutic neovascularization and wound healing," *Advances in Wound Care*, vol. 2, no. 6, pp. 283–295, 2013.
- [74] P. Carmeliet and R. K. Jain, "Molecular mechanisms and clinical applications of angiogenesis," *Nature*, vol. 473, no. 7347, pp. 298–307, 2011.
- [75] E. A. Logsdon, S. D. Finley, A. S. Popel, and F. MacGabhann, "A systems biology view of blood vessel growth and remodeling," *Journal of Cellular and Molecular Medicine*, vol. 18, no. 8, pp. 1491–1508, 2014.
- [76] D. Ribatti and E. Crivellato, "'Sprouting angiogenesis', a reappraisal," *Developmental Biology*, vol. 372, no. 2, pp. 157–165, 2012.

- [77] P. Carmeliet, "Mechanisms of angiogenesis and arteriogenesis," *Nature Medicine*, vol. 6, no. 4, pp. 389–395, 2000.
- [78] M. Rücker, M. W. Laschke, D. Junker et al., "Angiogenic and inflammatory response to biodegradable scaffolds in dorsal skinfold chambers of mice," *Biomaterials*, vol. 27, no. 29, pp. 5027–5038, 2006.
- [79] C. R. Anderson, A. M. Ponce, and R. J. Price, "Immunohistochemical identification of an extracellular matrix scaffold that microguides capillary sprouting in vivo," *Journal of Histochemistry and Cytochemistry*, vol. 52, no. 8, pp. 1063–1072, 2004.
- [80] M. W. Laschke and M. D. Menger, "Vascularization in tissue engineering: angiogenesis versus inosculation," *European Surgical Research*, vol. 48, no. 2, pp. 85–92, 2012.
- [81] H. A. Zarem, "The microcirculatory events within full-thickness skin allografts (homografts) in mice," *Surgery*, vol. 66, no. 2, pp. 392–397, 1969.
- [82] M. Rücker, M. W. Laschke, D. Junker et al., "Vascularization and biocompatibility of scaffolds consisting of different calcium phosphate compounds," *Journal of Biomedical Materials Research - Part A*, vol. 86, no. 4, pp. 1002–1011, 2008.
- [83] M. W. Laschke, A. Strohe, C. Scheuer et al., "In vivo biocompatibility and vascularization of biodegradable porous polyurethane scaffolds for tissue engineering," *Acta Biomaterialia*, vol. 5, no. 6, pp. 1991–2001, 2009.
- [84] S. P. Victor and J. Muthu, "Polymer ceramic composite materials for orthopedic applications—relevance and need for mechanical match and bone regeneration," *Journal of Mechatronics*, vol. 2, no. 1, pp. 1–10, 2014.
- [85] B. Zhang, P. Zhang, Z. Wang, Z. Lyu, and H. Wu, "Tissue-engineered composite scaffold of poly(lactide-co-glycolide) and hydroxyapatite nanoparticles seeded with autologous mesenchymal stem cells for bone regeneration," *Journal of Zhejiang University: Science B*, vol. 18, no. 11, pp. 963–976, 2017.
- [86] V. Karageorgiou and D. Kaplan, "Porosity of 3D biomaterial scaffolds and osteogenesis," *Biomaterials*, vol. 26, no. 27, pp. 5474–5491, 2005.
- [87] Y. Kuboki, H. Takita, D. Kobayashi et al., "BMP-induced osteogenesis on the surface of hydroxyapatite with geometrically feasible and nonfeasible structures: topology of osteogenesis," *Journal of Biomedical Materials Research*, vol. 39, no. 2, pp. 190–199, 1998.
- [88] I. Bruzauskaitė, D. Bironaitė, E. Bagdonas, and E. Bernotienė, "Scaffolds and cells for tissue regeneration: different scaffold pore sizes—different cell effects," *Cytotechnology*, vol. 68, no. 3, pp. 355–369, 2016.
- [89] A. C. Jones, C. H. Arns, A. P. Sheppard, D. W. Huttmacher, B. K. Milthorpe, and M. A. Knackstedt, "Assessment of bone ingrowth into porous biomaterials using MICRO-CT," *Biomaterials*, vol. 28, no. 15, pp. 2491–2504, 2007.
- [90] S. F. Hulbert, F. A. Young, R. S. Mathews, J. J. Klawitter, C. D. Talbert, and F. H. Stelling, "Potential of ceramic materials as permanently implantable skeletal prostheses," *Journal of Biomedical Materials Research*, vol. 4, no. 3, pp. 433–456, 1970.
- [91] Y. Kuboki, Q. Jin, and H. Takita, "Geometry of carriers controlling phenotypic expression in BMP-induced osteogenesis and chondrogenesis," *The Journal of Bone and Joint Surgery-American Volume*, vol. 83, pp. S1–115, 2001.
- [92] E. Tsuruga, H. Takita, H. Itoh, Y. Wakisaka, and Y. Kuboki, "Pore size of porous hydroxyapatite as the cell-substratum controls BMP-induced osteogenesis," *Journal of Biochemistry*, vol. 121, no. 2, pp. 317–324, 1997.
- [93] D. Druecke, S. Langer, E. Lamme et al., "Neovascularization of poly(ether ester) block-copolymer scaffolds in vivo: long-term investigations using intravital fluorescent microscopy," *Journal of Biomedical Materials Research - Part A*, vol. 68, no. 1, pp. 10–18, 2004.
- [94] D. Kaigler, Z. Wang, K. Horger, D. J. Mooney, and P. H. Krebsbach, "VEGF scaffolds enhance angiogenesis and bone regeneration in irradiated osseous defects," *Journal of Bone and Mineral Research*, vol. 21, no. 5, pp. 735–744, 2006.
- [95] L. Chen, Z. He, B. Chen et al., "Loading of VEGF to the heparin cross-linked demineralized bone matrix improves vascularization of the scaffold," *Journal of Materials Science: Materials in Medicine*, vol. 21, no. 1, pp. 309–317, 2010.
- [96] X. Li, B. Guo, Y. Xiao, T. Yuan, Y. Fan, and X. Zhang, "Influences of the steam sterilization on the properties of calcium phosphate porous bioceramics," *Journal of Materials Science*, vol. 27, no. 1, p. 5, 2016.
- [97] B. Li, J. M. Davidson, and S. A. Guelcher, "The effect of the local delivery of platelet-derived growth factor from reactive two-component polyurethane scaffolds on the healing in rat skin excisional wounds," *Biomaterials*, vol. 30, no. 20, pp. 3486–3494, 2009.
- [98] H. Shi, C. Han, Z. Mao, L. Ma, and C. Gao, "Enhanced angiogenesis in porous collagen-chitosan scaffolds loaded with angiogenin," *Tissue Engineering - Part A*, vol. 14, no. 11, pp. 1775–1785, 2008.
- [99] P. Schumann, F. Tavassol, D. Lindhorst et al., "Consequences of seeded cell type on vascularization of tissue engineering constructs in vivo," *Microvascular Research*, vol. 78, no. 2, pp. 180–190, 2009.
- [100] F. Tavassol, P. Schumann, D. Lindhorst et al., "Accelerated angiogenic host tissue response to poly(L-lactide-co-glycolide) scaffolds by vitalization with osteoblast-like cells," *Tissue Engineering - Part A*, vol. 16, no. 7, pp. 2265–2279, 2010.
- [101] E. K. Moiola, P. A. Clark, M. Chen et al., "Synergistic actions of hematopoietic and mesenchymal stem/progenitor cells in vascularizing bioengineered tissues," *PLoS One*, vol. 3, no. 12, article e3992, 2008.
- [102] S. Liu, H. Zhang, X. Zhang et al., "Synergistic angiogenesis promoting effects of extracellular matrix scaffolds and adipose-derived stem cells during wound repair," *Tissue Engineering - Part A*, vol. 17, no. 5–6, pp. 725–739, 2011.
- [103] D. Qu, J. Li, Y. Li et al., "Angiogenesis and osteogenesis enhanced by bFGF ex vivo gene therapy for bone tissue engineering in reconstruction of calvarial defects," *Journal of Biomedical Materials Research - Part A*, vol. 96A, no. 3, pp. 543–551, 2011.
- [104] U. Helmrich, N. di Maggio, S. Güven et al., "Osteogenic graft vascularization and bone resorption by VEGF-expressing human mesenchymal progenitors," *Biomaterials*, vol. 34, no. 21, pp. 5025–5035, 2013.
- [105] J. Liu, C. Liu, B. Sun et al., "Differentiation of rabbit bone mesenchymal stem cells into endothelial cells in vitro and promotion of defective bone regeneration in vivo," *Cell Biochemistry and Biophysics*, vol. 68, no. 3, pp. 479–487, 2014.
- [106] K. Pill, S. Hofmann, H. Redl, and W. Holthöner, "Vascularization mediated by mesenchymal stem cells from bone marrow and adipose tissue: a comparison," *Cell Regeneration*, vol. 4, no. 1, p. 4:8, 2015.

- [107] A. S. Klar, S. Güven, T. Biedermann et al., "Tissue-engineered dermo-epidermal skin grafts prevascularized with adipose-derived cells," *Biomaterials*, vol. 35, no. 19, pp. 5065–5078, 2014.
- [108] A. Miranville, C. Heeschen, C. Sengenès, C. A. Curat, R. Busse, and A. Bouloumié, "Improvement of postnatal neovascularization by human adipose tissue-derived stem cells," *Circulation*, vol. 110, no. 3, pp. 349–355, 2004.
- [109] Z. E. Clayton, S. Sadeghipour, and S. Patel, "Generating induced pluripotent stem cell derived endothelial cells and induced endothelial cells for cardiovascular disease modelling and therapeutic angiogenesis," *International Journal of Cardiology*, vol. 197, pp. 116–122, 2015.
- [110] J. S. Schechner, A. K. Nath, L. Zheng et al., "In vivo formation of complex microvessels lined by human endothelial cells in an immunodeficient mouse," *Proceedings of the National Academy of Sciences of the United States of America*, vol. 97, no. 16, pp. 9191–9196, 2000.
- [111] M. Sweeney and G. Foldes, "It takes two: endothelial-perivascular cell cross-talk in vascular development and disease," *Frontiers in Cardiovascular Medicine*, vol. 5, pp. 1–14, 2018.
- [112] J. Yang, U. Nagavarapu, K. Relloma et al., "Telomerized human microvasculature is functional in vivo," *Nature Biotechnology*, vol. 19, no. 3, pp. 219–224, 2001.
- [113] F. Clément, E. Grockowiak, F. Zylbersztein, G. Fossard, S. Gobert, and V. Maguer-Satta, "Stem cell manipulation, gene therapy and the risk of cancer stem cell emergence," *Stem Cell Investigation*, vol. 4, no. 7, p. 67, 2017.
- [114] N. Koike, D. Fukumura, O. Gralla, P. Au, J. S. Schechner, and R. K. Jain, "Tissue engineering: creation of long-lasting blood vessels," *Nature*, vol. 428, no. 6979, pp. 138–139, 2004.
- [115] K. J. Paik, E. R. Zielins, D. A. Atashroo et al., "Studies in fat grafting: part V. cell-assisted lipotransfer to enhance fat graft retention is dose dependent," *Plastic and Reconstructive Surgery*, vol. 136, no. 1, pp. 67–75, 2015.
- [116] F. Verseijden, S. J. P. V. Sluijs, E. Farrell et al., "Prevascular structures promote vascularization in engineered human adipose tissue constructs upon implantation," *Cell Transplantation*, vol. 19, no. 8, pp. 1007–1020, 2010.
- [117] F. S. Frueh, T. Später, C. Scheuer, M. D. Menger, and M. W. Laschke, "Isolation of murine adipose tissue-derived microvascular fragments as vascularization units for tissue engineering," *Journal of Visualized Experiments*, vol. 122, pp. 1–7, 2017.
- [118] T. Später, F. S. Frueh, R. M. Nickels, M. D. Menger, and M. W. Laschke, "Prevascularization of collagen-glycosaminoglycan scaffolds: stromal vascular fraction versus adipose tissue-derived microvascular fragments," *Journal of Biological Engineering*, vol. 12, no. 1, pp. 1–13, 2018.
- [119] B. R. Shepherd, H. Y. S. Chen, C. M. Smith, G. Gruionu, S. K. Williams, and J. B. Hoying, "Rapid perfusion and network remodeling in a microvascular construct after implantation," *Arteriosclerosis, Thrombosis, and Vascular Biology*, vol. 24, no. 5, pp. 898–904, 2004.
- [120] J. B. Hoying, C. A. Boswell, and S. K. Williams, "Angiogenic potential of microvessel fragments established in three-dimensional collagen gels," *In Vitro Cellular and Developmental Biology - Animal*, vol. 32, no. 7, pp. 409–419, 1996.
- [121] M. W. Laschke, S. Kleer, C. Scheuer et al., "Vascularisation of porous scaffolds is improved by incorporation of adipose tissue-derived microvascular fragments," *European Cells and Materials*, vol. 24, pp. 266–277, 2012.
- [122] M. Pilia, J. S. McDaniel, T. Guda et al., "Transplantation and perfusion of microvascular fragments in a rodent model of volumetric muscle loss injury," *European Cells and Materials*, vol. 28, no. 210, pp. 11–24, 2014.
- [123] J. S. McDaniel, M. Pilia, C. L. Ward, B. E. Pollot, and C. R. Rathbone, "Characterization and multilineage potential of cells derived from isolated microvascular fragments," *Journal of Surgical Research*, vol. 192, no. 1, pp. 214–222, 2014.
- [124] S. V. Koduru, A. N. Leberfinger, D. Pasic et al., "Cellular based strategies for microvascular engineering," *Stem Cell Reviews and Reports*, vol. 15, no. 2, pp. 218–240, 2019.
- [125] A. Trivisonno, R. W. Alexander, S. Baldari et al., "intraoperative strategies for minimal manipulation of autologous adipose tissue for cell- and tissue-based Therapies: Concise Review," *Stem Cells Translational Medicine*, vol. 8, no. 12, pp. 1265–1271, 2019.
- [126] B. Vezzani, I. Shaw, H. Lesme et al., "Higher pericyte content and secretory activity of microfragmented human adipose tissue compared to enzymatically derived stromal vascular fraction," *Stem Cells Translational Medicine*, vol. 7, no. 12, pp. 876–886, 2018.
- [127] V. Ceserani, A. Ferri, A. Berenzi et al., "Angiogenic and anti-inflammatory properties of micro-fragmented fat tissue and its derived mesenchymal stromal cells," *Vascular Cell*, vol. 8, no. 1, pp. 1–12, 2016.
- [128] J. A. van Dongen, H. P. Stevens, M. Parvizi, B. van der Lei, and M. C. Harmsen, "The fractionation of adipose tissue procedure to obtain stromal vascular fractions for regenerative purposes," *Wound Repair and Regeneration*, vol. 24, no. 6, pp. 994–1003, 2016.
- [129] P. Gentile, M. G. Scioli, A. Bielli, A. Orlandi, and V. Cervelli, "Comparing different nanofat procedures on scars: role of the stromal vascular fraction and its clinical implications," *Regenerative Medicine*, vol. 12, no. 8, pp. 939–952, 2017.
- [130] G. Desando, I. Bartolotti, L. Martini et al., "Regenerative features of adipose tissue for osteoarthritis treatment in a rabbit model: enzymatic digestion versus mechanical disruption," *International Journal of Molecular Sciences*, vol. 20, no. 11, article 2636, 2019.
- [131] G. Cattaneo, A. De Caro, F. Napoli, D. Chiapale, P. Trada, and A. Camera, "Micro-fragmented adipose tissue injection associated with arthroscopic procedures in patients with symptomatic knee osteoarthritis," *BMC Musculoskeletal Disorders*, vol. 19, no. 1, pp. 176–177, 2018.
- [132] G. Naldini, A. Sturiale, B. Fabiani, I. Giani, and C. Menconi, "Micro-fragmented adipose tissue injection for the treatment of complex anal fistula: a pilot study accessing safety and feasibility," *Techniques in Coloproctology*, vol. 22, no. 2, pp. 107–113, 2018.
- [133] C.-H. Cho, Y. Jun Koh, J. Han et al., "Angiogenic role of LYVE-1-positive macrophages in adipose tissue," *Circulation Research*, vol. 100, no. 4, pp. e47–e57, 2007.
- [134] J. R. Overman, E. Farré-Guasch, M. N. Helder, C. M. ten Bruggenkate, E. A. J. M. Schulten, and J. Klein-Nulend, "Short (15 minutes) bone morphogenetic protein-2 treatment stimulates osteogenic differentiation of human adipose stem cells seeded on calcium phosphate Scaffolds In vitro," *Tissue Engineering - Part A*, vol. 19, no. 3–4, pp. 571–581, 2012.

- [135] A. Kim, D. H. Kim, H. R. Song et al., "Repair of rabbit ulna segmental bone defect using freshly isolated adipose-derived stromal vascular fraction," *Cytotherapy*, vol. 14, no. 3, pp. 296–305, 2012.
- [136] K. Rubina, N. Kalinina, A. Efimenko et al., "Adipose stromal cells stimulate angiogenesis via promoting progenitor cell differentiation, secretion of angiogenic factors, and enhancing vessel maturation," *Tissue Engineering - Part A*, vol. 15, no. 8, pp. 2039–2050, 2009.
- [137] R. Madonna and R. De Caterina, "In vitro neovasculogenic potential of resident adipose tissue precursors," *American Journal of Physiology-Cell Physiology*, vol. 295, no. 5, pp. C1271–C1280, 2008.
- [138] E. Farré-Guasch, N. Bravenboer, M. Helder, E. Schulten, C. ten Bruggenkate, and J. Klein-Nulend, "Blood vessel formation and bone regeneration potential of the stromal vascular fraction seeded on a calcium phosphate scaffold in the human maxillary sinus floor elevation model," *Materials*, vol. 11, no. 1, p. 161, 2018.
- [139] J. S. Zakhari, J. Zabanick, B. Gettler, and S. K. Williams, "Vasculogenic and angiogenic potential of adipose stromal vascular fraction cell populations in vitro," *In Vitro Cellular and Developmental Biology - Animal*, vol. 54, no. 1, article 213, pp. 32–40, 2018.
- [140] J. Scheinpflug, M. Pfeiffenberger, A. Damerou et al., "Journey into bone models: a review," *Genes*, vol. 9, no. 5, p. 247, 2018.
- [141] R. Bertolai, C. Catelani, A. Aversa, A. Rossi, D. Giannini, and D. Bani, "Bone graft and mesenchymal stem cells: clinical observations and histological analysis," *Clinical Cases in Mineral and Bone Metabolism*, vol. 12, no. 2, pp. 183–187, 2015.
- [142] P. J. Pasquali, M. L. Teixeira, T. A. . Oliveira, L. G. S. de Macedo, A. C. Aloise, and A. A. Pelegrine, "Maxillary sinus augmentation combining bio-oss with the bone marrow aspirate concentrate: a histomorphometric study in humans," *International Journal of Biomaterials*, vol. 2015, Article ID 121286, 7 pages, 2015.
- [143] H. H. al-Ahmady, A. F. Abd Elazeem, N. E. M. Bellah Ahmed et al., "Combining autologous bone marrow mononuclear cells seeded on collagen sponge with nano hydroxyapatite, and platelet-rich fibrin: reporting a novel strategy for alveolar cleft bone regeneration," *Journal of Cranio-Maxillofacial Surgery*, vol. 46, no. 9, pp. 1593–1600, 2018.
- [144] M. E. Khalifa and N. E. Goma, "Dental arch expansion after alveolar cleft repair using autogenous bone marrow derived mesenchymal stem cells versus autogenous chin bone graft," *Journal of Dental Treatment and Oral Care*, vol. 2, no. 1, pp. 1–10, 2017.
- [145] W. M. Talaat, M. M. Ghoneim, O. Salah, and O. A. Adly, "Autologous bone marrow concentrates and concentrated growth factors accelerate bone regeneration after enucleation of mandibular pathologic lesions," *Journal of Craniofacial Surgery*, vol. 29, no. 4, pp. 992–997, 2018.

## Research Article

# Evaluation of Chitosan Hydrogel for Sustained Delivery of VEGF for Odontogenic Differentiation of Dental Pulp Stem Cells

Si Wu <sup>1</sup>, Yachuan Zhou <sup>2</sup>, Yi Yu,<sup>2</sup> Xin Zhou,<sup>1</sup> Wei Du,<sup>2</sup> Mian Wan,<sup>2</sup> Yi Fan,<sup>2</sup> Xuedong Zhou <sup>2</sup>, Xin Xu <sup>2</sup> and Liwei Zheng <sup>1</sup>

<sup>1</sup>State Key Laboratory of Oral Diseases, National Clinical Research Center for Oral Diseases, Department of Pediatric Dentistry, West China Hospital of Stomatology, Sichuan University, Chengdu, Sichuan 610041, China

<sup>2</sup>State Key Laboratory of Oral Diseases, National Clinical Research Center for Oral Diseases, Department of Cariology and Endodontics, West China Hospital of Stomatology, Sichuan University, Chengdu, Sichuan 610041, China

Correspondence should be addressed to Xin Xu; [xin.xu@scu.edu.cn](mailto:xin.xu@scu.edu.cn) and Liwei Zheng; [liweizheng@scu.edu.cn](mailto:liweizheng@scu.edu.cn)

Received 23 September 2019; Revised 14 November 2019; Accepted 25 November 2019; Published 19 December 2019

Guest Editor: Jiashing Yu

Copyright © 2019 Si Wu et al. This is an open access article distributed under the Creative Commons Attribution License, which permits unrestricted use, distribution, and reproduction in any medium, provided the original work is properly cited.

The pulpotomy with pulp capping is aimed at retaining vital pulp with reparative dentin formation. Vascular endothelial growth factor (VEGF) plays a crucial role in dentin regeneration; however, its constant administrations in the human body is still problematic. Chitosan was widely studied as an effective carrier to deliver bioactive molecules in regenerative medicine. In this study, we conducted a chitosan/ $\beta$ -glycerophosphate (CS/ $\beta$ -GP) hydrogel as a VEGF-sustained release system and explored its effects on dental pulp stem cells (DPSCs). CS/ $\beta$ -GP hydrogel was manufactured using a sol-gel method. SEM assay showed the spongy and porous microstructure of the lyophilized hydrogels. DPSCs cultured in the CS/ $\beta$ -GP hydrogel kept adhesion and vitality. CCK-8 assay tested the promoted proliferation activity of DPSCs on the hydrogel. Besides, the added VEGF protein could continually release from VEGF/CS/ $\beta$ -GP hydrogel. The VEGF/CS/ $\beta$ -GP hydrogel could promote the odontogenic differentiation of DPSCs better than VEGF treatment without hydrogel. Our results suggested that CS/ $\beta$ -GP hydrogel could continually release VEGF and contribute to odontogenic differentiation of DPSCs, thus may become a potential carrier of bioactive molecules in pulp capping therapy.

## 1. Introduction

The dental pulpotomy is a kind of dental therapy to retain the vital pulp in accidental pulp exposure caused by trauma or caries removal. The retained radical pulp is valuable for continuous apexogenesis in young permanent teeth with immature root. In pulpotomy, the infected coronal pulp is amputated, and the surface of remaining vital pulp is treated with a sealant, such as calcium hydroxide or mineral trioxide aggregate (MTA) [1]. These sealants, called pulp capping agents, can promote the recruitment, migration, proliferation, and differentiation of human dental pulp stem cells (DPSCs) [2]. Afterwards, a protective mechanism is initiated. The dentin matrix secreted by odontoblast-like cells is laid down on the surface of amputated pulp. As a result, the dentin bridge

or osteodentin is formed to save the vitality of residual pulp [2].

However, as widely used capping agents, the calcium hydroxide has been evaluated with less success in long-term studies, while MTA has drawbacks such as discolor of tooth, high cost, high operational requirements, and longer curing time [3]. Considering the mechanism underlying the reparative dentin formation, bioactive molecules were studied to promote the proliferation and differentiation potential of DPSCs in vital pulp tissue [4–10].

Vascular endothelial growth factor (VEGF) plays a crucial role in dentin formation and regeneration [11]. Studies have evaluated that VEGF can promote the odontogenic differentiation of cultured DPSCs and induce the formation of reparative dentin on the surface of amputated pulp [12–16]. However, the applicable VEGF recombinant

protein has a short half-life in aqueous solutions at 37°C [17]. Most recombinant proteins are susceptible to high temperature or pH levels, and they will be easily degraded by enzymes and lose efficiency. Nowadays, some growth factors have been approved for human therapy as recombinant preparations; however, most of them still carry warnings on clinical application. The use of recombinant proteins without any carriers generally presents side effects to the human body. These proteins are pleiotropic with short half-lives and sometimes functional redundancies and overlapping side effects [18–20]. Many researches and therapies require frequent protein administration and ultimately poor patient compliance [21]. The systemic application of proteins with once large dose or frequent administration may induce a range of flu-like symptoms as well as more severe hematologic, autoimmune, infection, and dermatologic adverse events [18, 22].

In order to effectively extend the residence time and optimize the molecule's concentration, various materials were studied as carriers to deliver bioactive molecules in pulp capping therapy [6, 23, 24]. The carriers have different features like synthetic gel (hydrogel), sponges, scaffolds, and membranes [7, 8, 25–27]. Only the sustained delivery carrier can create a microenvironment to maintain a certain molecule concentration and extend application period. In other words, the carriers could prolong the effective period and minimize the side effects [4, 28].

Chitosan is a kind of polysaccharides derived from chitin which is a natural component of insects' exoskeleton, crustacean shells, and fungi's cell walls. Chitosan has characteristics of bacteriostatic effects, nontoxicity, and biocompatibility [23]. In pharmaceutical industry, chitosan has been widely used as a drug delivery system in different forms, like tablets, microspheres, hydrogels, and nanoparticles [20]. Among these, the chitosan/ $\beta$ -glycerophosphate (CS/ $\beta$ -GP) hydrogel gained attention by its excellent chemical and biological ability to deliver therapeutic agents, molecules, or cells. It has been studied in cartilage repair, bone regeneration, hemostatic agents, and even in endodontic treatment [19, 29–32]. In the study of odontology, chitosan shows good properties as a carrier for some medicaments, such as chlorhexidine, calcium hydroxide, and triple antibiotic paste [33]. The temperature-sensitive CS/ $\beta$ -GP solution can transform into semisolid hydrogel at physiological temperature in human bodies. Besides, the hydrogel protects the agents from physiological degradation and prolongs therapeutic span while minimizing side effects [20].

In this study, we characterized the morphology of CS/ $\beta$ -GP thermosensitive hydrogel and the bioactivity of dental pulp stem cells (DPSCs) on the hydrogel. We also compared the effects of VEGF treatment in CS/ $\beta$ -GP hydrogel and without hydrogel on the behaviors of DPSCs. We hypothesized that the thermosensitive chitosan hydrogel could effectively deliver VEGF protein in a sustained release pattern to stimulate differentiation and mineralization of DPSCs.

## 2. Materials and Methods

**2.1. Isolation and Culture of Dental Pulp Stem Cells.** The procedures were approved by the Ethical Committee of the West

China School of Stomatology, Sichuan University, and performed in accordance with the approved guidelines. Human dental pulp stem cells (DPSCs) were harvested from normal impacted third molars extracted from donors (19–22 years old) in West China Hospital of Stomatology and cultured as previously described [34]. All donors provided informed consent for this study. DPSCs were cultured in Dulbecco's modified Eagle's medium (DMEM) consisting of 10% fetal bovine serum (FBS) and 1% penicillin/streptomycin (PS) at 37°C in moist atmosphere with 5% CO<sub>2</sub> for use. Cells between passages 3 and 4 were used in this study.

To characterize the immunophenotype of DPSCs, flow cytometric analysis was used to measure the expression of mesenchymal and nonmesenchymal stem cell-associated surface markers at passages 3. DPSCs were washed by PBS and liberated by enzymatic digestion for 2 minutes at 37°C. Then, the single cell suspension was washed twice by buffer solution (PBS containing 5% BSA). DPSCs for immunolabeling were resuspended in 0.5 ml blocking buffer and incubated on ice for 30 minutes. Tubes containing  $1 \times 10^6$  of DPSCs were incubated with appropriate antibodies (CD90: 328109, CD29: 303003, CD45: 368507, and CD34: 343603, BioLegend) away from light on ice. The control group was incubated without antibodies in buffer solution. After 30 minutes, cells were washed twice by buffer solution and analyzed on Cytomics™ FC 500 (Beckman Coulter Ltd.).

**2.2. Fabrication of Hydrogel and VEGF Loading.** Chitosan (CS, viscosity: 200–400 mPa·s) was obtained from Aladdin Industrial Corporation (China). Acetic acid and  $\beta$ -glycerophosphate ( $\beta$ -GP) were purchased from Sigma (St. Louis, USA). The 2% (*w/v*) chitosan solution was prepared by stirring chitosan in 0.5% (*v/v*) acetic acid solution at room temperature for at least 3 hours until complete dissolution. Afterwards, the chitosan solution was stored overnight at 4°C to diminish inside bubbles. 56% (*w/v*) beta-sodium glycerophosphate ( $\beta$ -GP) solution was prepared by mixing  $\beta$ -GP with distilled water and then filter sterilized by a 0.22 diameter filter. These two solutions were mixed by adding the  $\beta$ -GP drop by drop into the stirring chitosan solution; the volume ratio of CS:  $\beta$ -GP is 5/1 [31]. After magnetic stirring for 10 minutes under ice bath, the final pH value of the chitosan solution was 7.49. After that, the VEGF/CS/ $\beta$ -GP hydrogel was obtained by adding appropriate amount of recombinant human VEGF protein (PeproTech, China) into CS/ $\beta$ -GP solution under magnetic stirring for 10 minutes; the final concentration of VEGF was 100 ng/ml.

During gelation, these gel solutions were transferred to 37°C baths for 10 minutes. The process of sol-gel transition was observed.

**2.3. Scanning Electron Microscope (SEM) of the Hydrogel and DPSCs.** After gelation in glass containers, hydrogels were lyophilized. The samples were cut into pieces, and the microstructures were observed by SEM (JEOLJEM-1400, Japan) at an acceleration voltage of 20.00 kV. DPSCs were directly seeded and cultured on the surface of CS/ $\beta$ -GP hydrogels. After 24 hours, cell-seeded gels were washed with phosphate buffered saline (PBS) for 3 times and fixed with 2.5%

glutaraldehyde at room temperature for 4 hours. Then, the hydrogels were dehydrated in a graded series of ethanol (30%, 50%, 75%, 85%, 95%, and 100%) for 15 minutes in each concentration and air-dried overnight to be analyzed by SEM (JEOLJEM-1400, Japan).

**2.4. Cell Viability Using AO/EB Staining.** CS/ $\beta$ -GP gel solution was put in the 6-well culture plates for 1 ml/well. After gelation, the culture medium was added into the wells to soak the hydrogels for 10 minutes for 3 times. Then, DPSCs were suspended and cultured on the surface of hydrogels at a density of  $10^6$  cell/well. After 24-hour culture, cells on the surface of hydrogels were stained by 1  $\mu$ l/0.1 ml AO/EB (acridine orange/ethidium bromide) solution (SabbioTech) for 1 minute. The images were captured on a Nikon Eclipse 300 fluorescence microscope (Compix Inc.).

**2.5. Cytotoxicity Using Cell Counting Kit-8 Assay.** The cytotoxicity of CS/ $\beta$ -GP hydrogel was assessed using a Cell Counting Kit-8 (CCK-8, Sigma, St. Louis, MO, USA). DPSCs were cultured in hydrogel leachates or seeded on the surface of hydrogels. The leachates of hydrogels were obtained using an international standard procedure (ISO-10993) [29]. DPSCs were seeded in 96-well culture plates at a density of 2000 cells/well. The medium was replaced by a fresh culture medium or hydrogel leachates every 24 hours. After 1, 3, 5, and 7 days, cells were isolated and incubated with 10  $\mu$ l/0.1 ml CCK-8 solution and then tested using a BioTek ELX800 kit (BioTek, Winooski, VT, USA) in an absorbance of 450 nm.

**2.6. Release Behaviors of VEGF.** The VEGF/CS/ $\beta$ -GP hydrogel leachates were obtained using an international standard procedure (ISO-10993). The leaching solution was collected and immediately frozen at  $-80^\circ\text{C}$ . The same volume of PBS was replenished. The concentrations of VEGF in the leaching solution were measured by using the enzyme-linked immunosorbent assay (ELISA) kit (Dakewe Biotech Company Limited, China). The optical densities were measured at 450 nm using BioTek ELX800. The standard curves were plotted, and the concentrations of VEGF were calculated compared with the standard curves and stated in ng/ml.

**2.7. ALP and Alizarin Red Staining.** DPSCs were cultured in 24-well plates and treated with four different concentrations of VEGF protein (5, 10, 50, and 100 ng/ml) in odontogenic medium (OM, consisting of DMEM, 10% FBS, 1% PS,  $10\text{ mmol l}^{-1}$   $\beta$ -GP, 50  $\mu\text{g/ml}$  ascorbic acid 2-phosphate, and  $10^{-7}$  mol/l dexamethasone). DPSCs in base culture medium (NC, consisting of DMEM, 10% FBS, and 1% PS) were cultured as a negative control group. DPSCs in OM without VEGF were as another control group. Cells were dyed using an alkaline phosphatase (ALP) staining kit (Beyotime, China) after 0, 4, and 7 days, and alizarin red staining (ARS) after 7 and 14 days. For quantitative analysis, 10% ( $w/v$ ) cetylpyridinium chloride resolution was used to elute the alizarin red positive depositions. The absorbance was measured using BioTek ELX800 (BioTek, Winooski, VT, USA) in an optical density of 562 nm.

TABLE 1: Primer names and sequences.

Primer names	Primer sequences
GAPDH	Forward: GGAGCGAGATCCCTCCAAAAT
	Reverse: GGCTGTTGTCATACTTCTCATGG
Runx-2	Forward: CCTTTACTTACACCCCGCCA
	Reverse: GGATCCTGACGAAGTGCCAT
OCN	Forward: ATTGTGGCTCACCTCCATC
	Reverse: CCAGCCTCCAGCACTGTTTA
OSX	Forward: TCTGCGGGACTCAACAACCTC
	Reverse: TAGCATAGCCTGAGGTGGGT
ALP	Forward: CTATCCTGGCTCCGTGCTCC
	Reverse: GTTAACTGATGTTCCAATCCTGCG
DSPP	Forward: ATATTGAGGGCTGGAATGGGGA
	Reverse: TTTGTGGCTCCAGCATTGTCA

The VEGF/CS/ $\beta$ -GP hydrogels were placed on the upper chambers, and DPSCs were cultured on the lower chambers in transwell plates. In the 100 ng/mL VEGF group, DPSCs were cultured in OM containing same amount of VEGF (100 ng/ml) without hydrogels for seven days. DPSCs in NC and OM groups were cultured without hydrogels. DPSCs were dyed using the ALP staining kit after 4 and 7 days, and ARS after 10 and 14 days. Before staining, cells were washed by PBS for 3 times and fixed in 4% paraformaldehyde for 15 minutes in room temperature. The stained cells were observed under light microscopy.

**2.8. RNA Extraction and qRT-PCR.** Total RNAs of DPSCs were extracted using TRIzol reagent according to the manufacturer's protocol. Reverse transcription was performed with a PrimeScript<sup>®</sup> RT reagent kit with gDNA Eraser (TaKaRa). Quantitative real-time PCR (qRT-PCR) was carried out using a standard SYBR Green PCR kit (TaKaRa) on a CFX96 (Bio-Rad). Glyceraldehyde-3-phosphate dehydrogenase (GAPDH) was used to normalize the expression level of each gene. The primer information is shown in Table 1.

**2.9. Western Blot Analyses.** Total proteins of DPSCs were extracted following the kit (KeyGEN, China) protocol. After protein denaturalization, the protein concentrations were measured by bicinchoninic acid (BCA) protein assays (Beyotime, China). Equal amount of each sample was segregated via sodium dodecyl sulfate polyacrylamide gel electrophoresis (SDS-PAGE) gels and then transferred to a nitrocellulose membrane. After blocking, the membranes were incubated with primary antibody: mouse anti- $\beta$ -actin (ab8226, Abcam, 1:1000) and mouse anti-OSX (sc-393325, Santa Cruz Biotechnology, 1:1000). Then, the membranes were incubated with goat anti-mouse IgG-horseradish peroxidase (Santa Cruz Biotechnology) and detected with a chemiluminescent reagent kit (Millipore). The expression level of  $\beta$ -actin was normalized. A GS-700 imaging densitometer (Bio-Rad) was used for image analysis.

**2.10. Statistical Analysis.** The results are revealed as mean  $\pm$  SD from experiments conducted at least 3 times

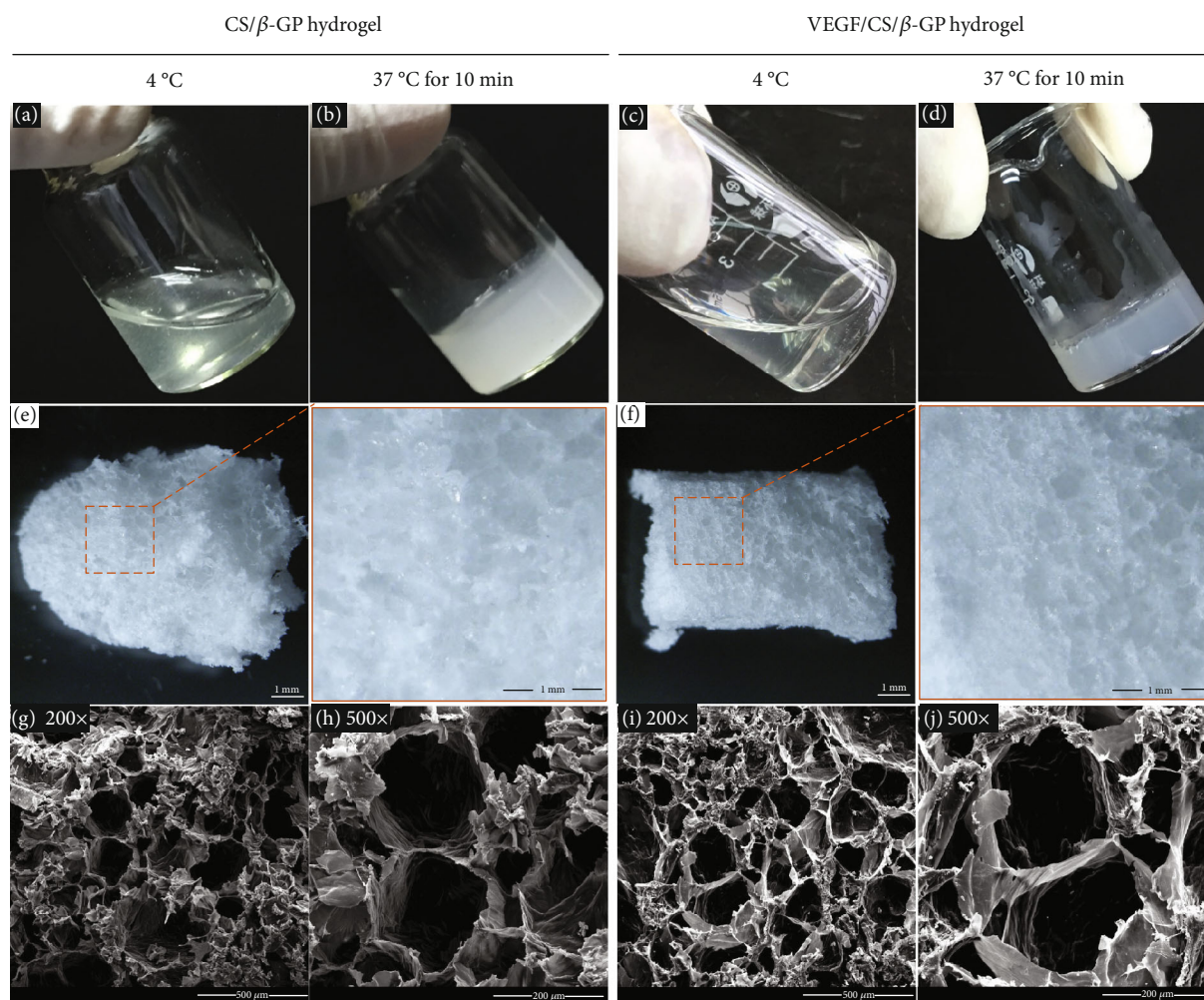


FIGURE 1: The process of gelation and the microstructure of hydrogels. Photographs of CS/ $\beta$ -GP gel before and after gelation (a, b). Photographs of VEGF/CS/ $\beta$ -GP gel before and after gelation (c, d). Photographs of CS/ $\beta$ -GP and VEGF/CS/ $\beta$ -GP hydrogels after lyophilization (e, f). SEM images of CS/ $\beta$ -GP hydrogel in 200x and 500x (g, h). SEM images of VEGF/CS/ $\beta$ -GP hydrogel in 200x and 500x (i, j).

independently and analyzed by two-way ANOVA with SPSS 21.0. When the  $P$  values were  $<0.05$ , data were considered statistically significant. \* $P < 0.05$ , \*\* $P < 0.01$ , and \*\*\* $P < 0.005$ .

### 3. Results

**3.1. Gelation and Microstructure of Hydrogels.** The CS/ $\beta$ -GP gel solution was prepared as procedures described previously [22]. The VEGF/CS/ $\beta$ -GP gel solution was formed by adding VEGF protein into CS/ $\beta$ -GP solutions. The gel solution was transparent liquid at 4°C and transformed into nontransparent semisolid hydrogel after incubation at 37°C for 15 minutes (Figures 1(a)–1(d)). After gelation, the CS/ $\beta$ -GP and VEGF/CS/ $\beta$ -GP hydrogels were lyophilized and observed by SEM (Figures 1(e) and 1(f)). These lyophilized hydrogels showed the spongy and porous microstructure and the average pore diameter range from 100 to

200  $\mu\text{m}$  (Figures 1(g)–1(j)). There was no significantly different appearance of hydrogels with or without VEGF proteins.

**3.2. Adhesion of DPSCs on the Hydrogel.** The flow cytometry detected that the cultured DPSCs were positive for CD29 and CD90, and negative for CD45 and CD34, which are the criteria for mesenchymal stem cell (Figure 2(a)). The DPSCs were planted on the surface of CS/ $\beta$ -GP hydrogel for 24 hours. The microstructure of CS/ $\beta$ -GP hydrogel with DPSCs was analyzed by SEM. DPSCs showed spherical shapes, and the cellular synapses were embedded into the porous hydrogel (Figure 2(b, i and ii)).

**3.3. Cytotoxicity of CS/ $\beta$ -GP Hydrogel to DPSCs.** AO/EB double fluorescence staining was conducted to observe the morphology, distribution, and viability of DPSCs cultured on the surface of CS/ $\beta$ -GP hydrogel after 24 hours (Figure 3(a)). DPSCs cultured without hydrogel were as control groups (Figure 3(b)). Live cells were stained in green



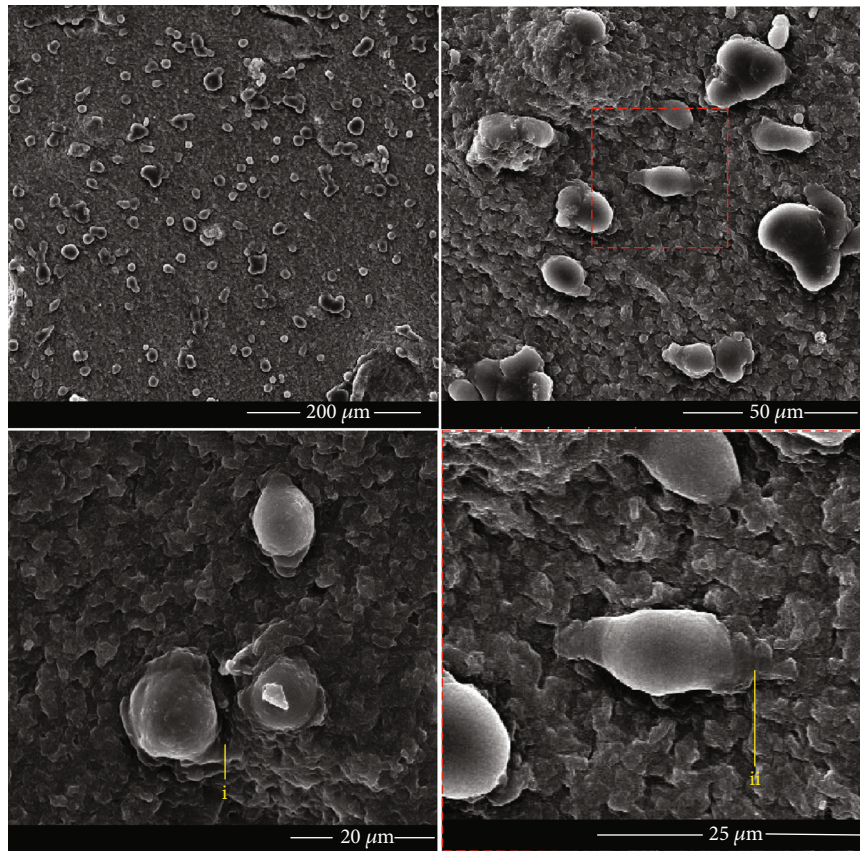
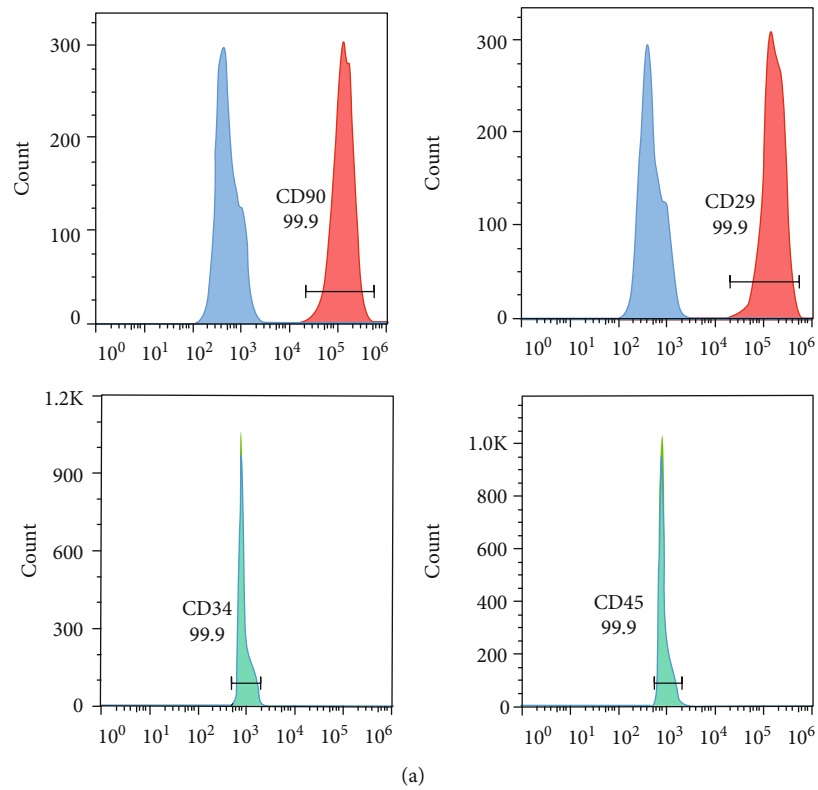


FIGURE 2: Cell surface markers on DPSCs and the morphology of DPSCs cultured on the hydrogel. Flow cytometric analysis was used to test the surface markers of DPSCs. DPSCs were positive for CD29 and CD90, and negative for CD34 and CD45 (a). Morphology of DPSCs cultured on the surface of CS/ $\beta$ -GP hydrogel after 24 h (b). DPSCs embedded their cellular synapses into the pore canal (i, ii).

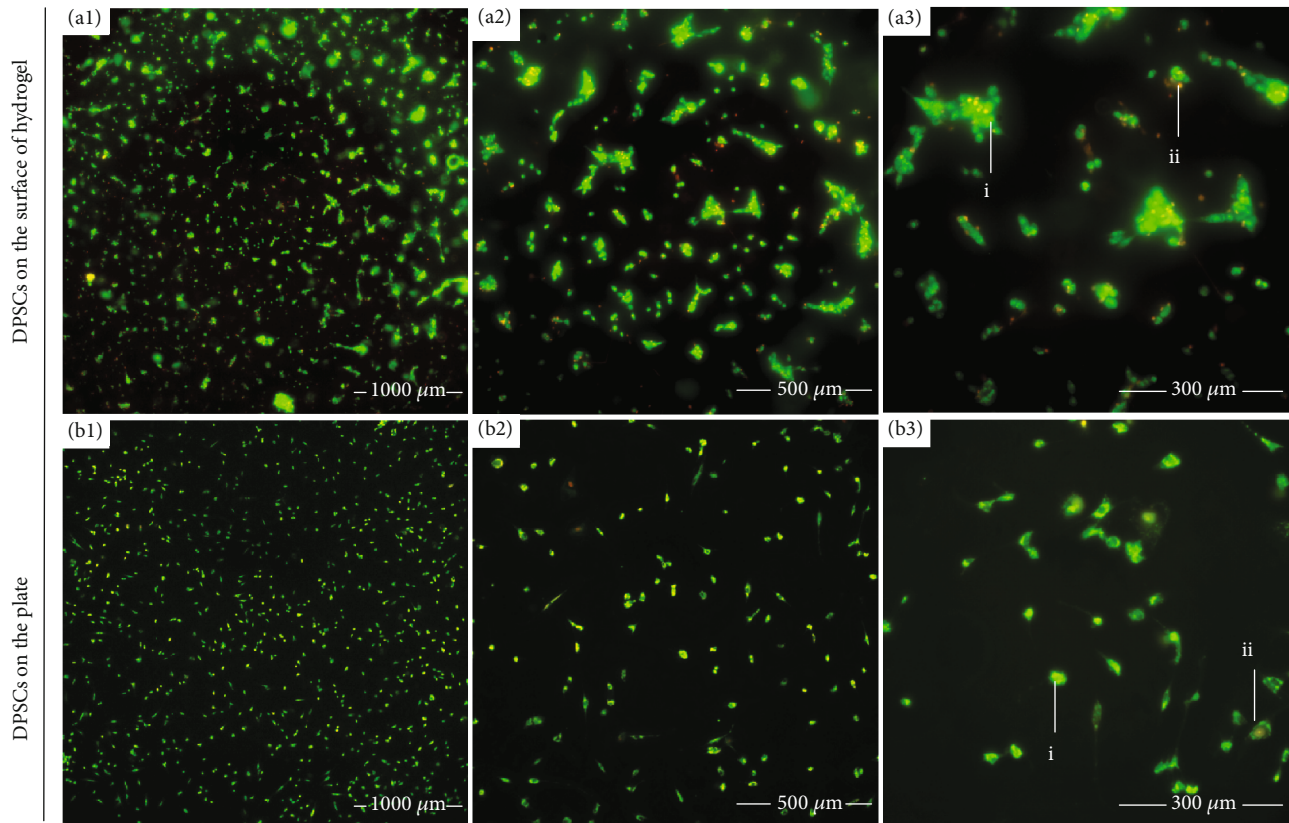


FIGURE 3: The activity of DPSCs cultured on the hydrogel. Distribution and viability of DPSCs cultured on the surface of CS/ $\beta$ -GP hydrogel or on well plates after 24 hours stained by AO/EB. Live cells were shown in green or yellow-green (i), and apoptotic cells were red or orange (ii).

or yellow-green (Figure 3 (i)), and apoptotic cells were red or orange (Figure 3 (ii)). There was no significant difference of cell population in the CS/ $\beta$ -GP hydrogel group compared to cells without hydrogel, and most of DPSCs on the hydrogel kept vitality.

Cell Counting Kit-8 (CCK-8) assay was conducted to test the cytotoxicity of CS/ $\beta$ -GP hydrogel. The proliferation of DPSCs cultured on the surface of hydrogel (Figure 4(a)) and in the hydrogel leachates (Figure 4(b)) was assayed. Cells cultured on the plate were as control groups. The activity of DPSCs showed no difference on the 1<sup>st</sup> and 3<sup>rd</sup> day. Surprisingly, the promoted proliferation of DPSCs was shown in hydrogel and hydrogel leachate groups compared to the control group after 7 days. These results suggested that the CS/ $\beta$ -GP hydrogel was noncytotoxic; furthermore, it has the characteristic to promote the proliferation of DPSCs.

**3.4. VEGF Release from CS/ $\beta$ -GP Hydrogel.** VEGF proteins were added into the CS/ $\beta$ -GP hydrogel to form 100 ng/ml VEGF/CS/ $\beta$ -GP hydrogel, and the release profiles of VEGF were detected using the enzyme-linked immunosorbent assay (ELISA). As a result, a linear increase of VEGF release was observed during the first 5 days. After 8 days, the cumulative release level tended to the peak and levelled out. A total of 12% VEGF proteins were shown to release out of hydrogel after 8 days (Figure 4(c)). The everyday release of VEGF proteins showed a downward trend from the 4th day to reach

a constant concentration (Figure 4(d)). The results suggested that the CS/ $\beta$ -GP hydrogel could be used as a carrier to constantly release VEGF proteins.

**3.5. The Sustained Release of VEGF from Hydrogels Promoted the Odontogenic Differentiation of DPSCs.** VEGF could promote odontogenic differentiation of DPSCs, while the strategy of optimal concentration treatment remains unclear. The effects of VEGF treatment in DPSCs were detected using different concentrations of 5 ng/ml, 10 ng/ml, 50 ng/ml, and 100 ng/ml. The results of ALP staining illustrated induced ALPase activity in DPSCs treated with VEGF compared to cells without VEGF (Figure 5(a)). After 7 days, the VEGF treatment significantly increased the mineralized nodule formation (Figure 5(b)). Cells cultured with 10 ng/ml VEGF exhibited to be higher mineralized than cells with 5 ng/ml VEGF, and cells with 10 ng/ml, 50 ng/ml, and 100 ng/ml did not show an obvious difference in the amounts of mineralized nodules (Figure 5(c)). It suggested that more than 10 ng/ml VEGF may not be needed to induce the odontogenic differentiation of DPSCs, and this result was consistent with previous study [14].

The CS/ $\beta$ -GP hydrogel was evaluated as a valuable sustained delivery system for bioactive molecule release. To further investigate the advantage of hydrogel system compared to the once-add strategy without carriers, we evaluated the cell responses to 100 ng/ml VEGF proteins

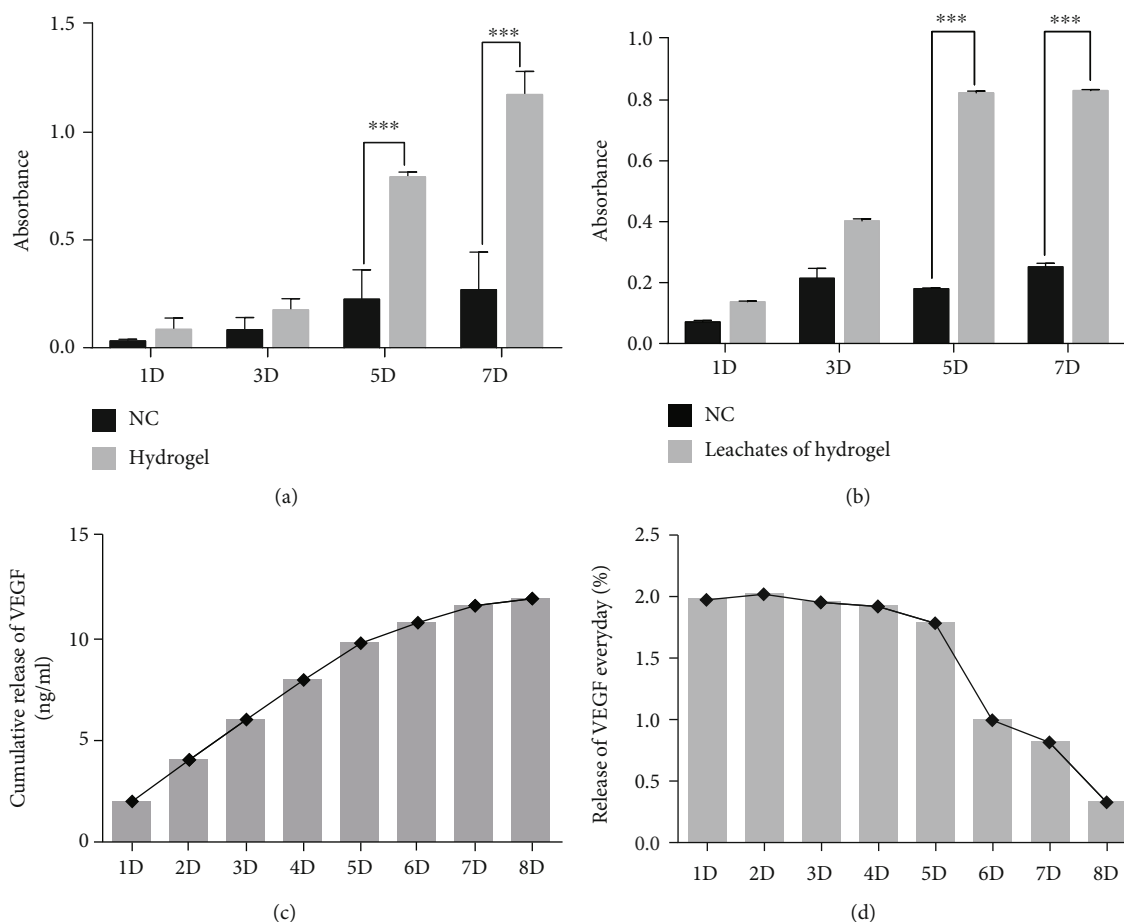


FIGURE 4: The CS/ $\beta$ -GP hydrogel promoted the proliferation of DPSCs and constantly released VEGF. The results of CCK-8 assay showed the promoted proliferation of DPSCs plated on the CS/ $\beta$ -GP hydrogel and in hydrogel leachates (a, b). DPSCs cultured in base culture medium (NC) without hydrogels or hydrogel leachates were as controls. ELISA assay showed the cumulative release profiles of VEGF/CS/ $\beta$ -GP hydrogel (c). ELISA assay showed the release amount of VEGF from hydrogel every day (d).

with or without a CS/ $\beta$ -GP delivery system. Cells without hydrogel cultured in NC and OM were as controls. The results of ALP staining showed that the addition of VEGF protein in the medium and in the hydrogel both increased ALPase activities after 7 days, and no obvious difference was shown between two groups (Figures 6(a1)–6(a4) and 6(b1)–6(b4)).

ARS was further performed to detect the mineralization activity of DPSCs during the late stage of differentiation. After 10 days, the added VEGF proteins increased the formation of mineralized nodules compared to control groups (Figures 6(c1)–6(c4)). Moreover, the sustained VEGF treatment elevated the mineralization activity of DPSCs better than the initial burst release of VEGF without carriers (Figures 6(d3) and 6(d4)). The hydrogel worked as a sustained delivery system and created a steady concentration of VEGF protein, promoting the odontogenic differentiation of DPSCs in the long-term differentiation period.

The expressions of odontogenic markers were further detected using qRT-PCR assay. The alkaline phosphatase (ALP) expression level was higher in the VEGF/CS/ $\beta$ -GP

hydrogel group than other groups, in consistent with the results of ALPase staining (Figure 7(d)). The expression levels of osteocalcin (OCN), osterix (OSX), and dentin sialophosphoprotein (DSPP) were significantly higher in the VEGF/CS/ $\beta$ -GP hydrogel group after 7 days compared to the 100 ng/ml VEGF group (Figures 7(b), 7(c), and 7(e)). The expression of runt-related transcription factor-2 (*RUNX-2*) increased at the 7<sup>th</sup> day while decreased at the 14<sup>th</sup> day in the VEGF/CS/ $\beta$ -GP group (Figure 7(a)). It validated the VEGF/CS/ $\beta$ -GP hydrogel delivery system induced the odontogenic differentiation of DPSCs.

Consistent with the results in gene expression, the protein expressions of osterix (OSX) were also increased in the DPSCs cocultured with VEGF/CS/ $\beta$ -GP hydrogel than cells cultured in 100 ng/ml VEGF (Figures 7(f) and 7(g)).

#### 4. Discussion

The pulpotomy and direct pulp capping in teeth initially establish a nonbacterial environment and maintain the pulpal vitality for further dentin-pulp complex healing [24].

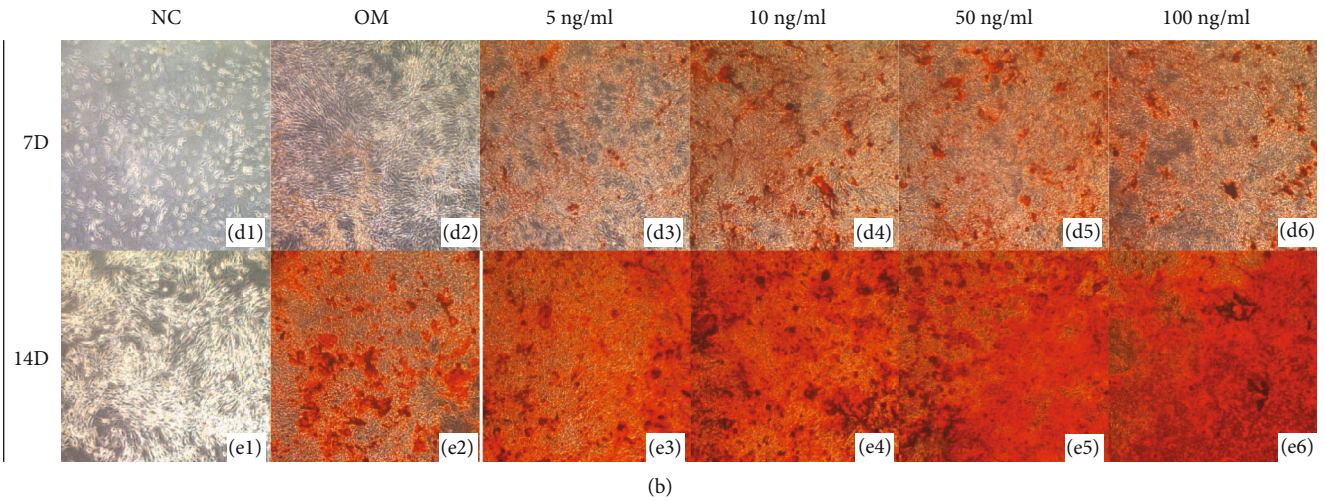
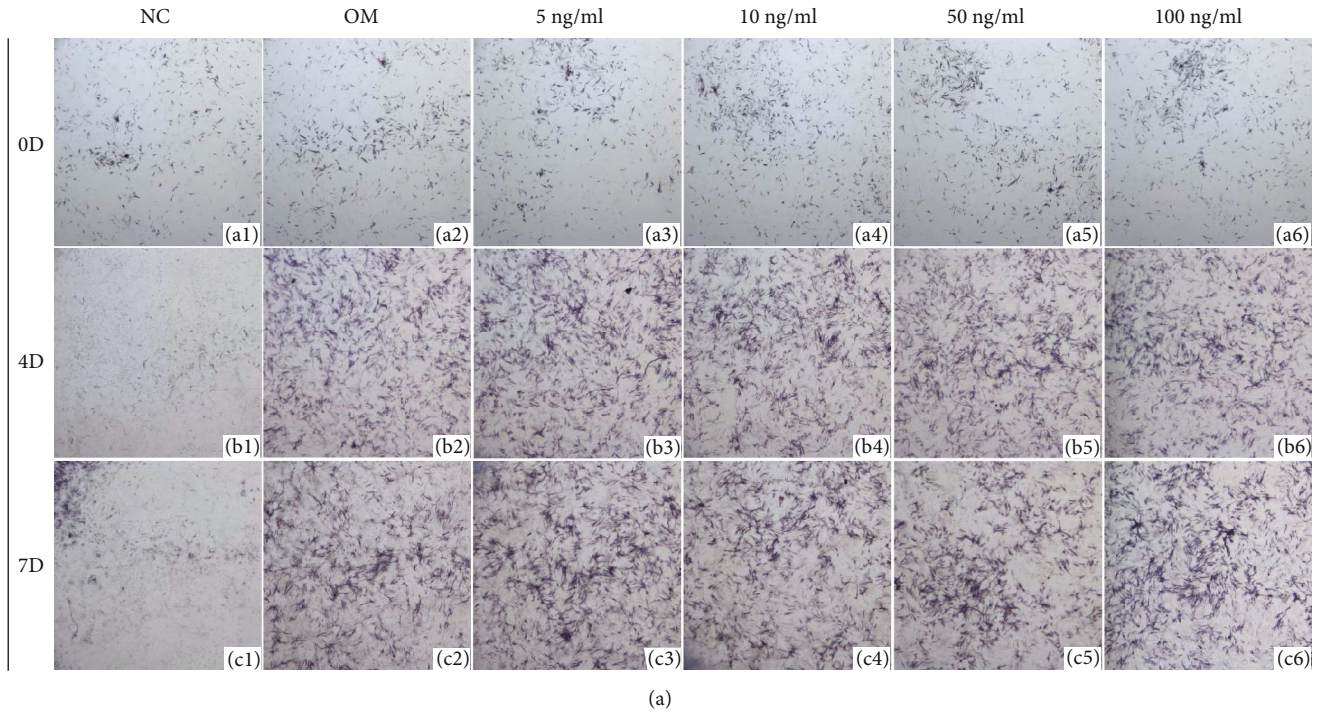


FIGURE 5: Continued.

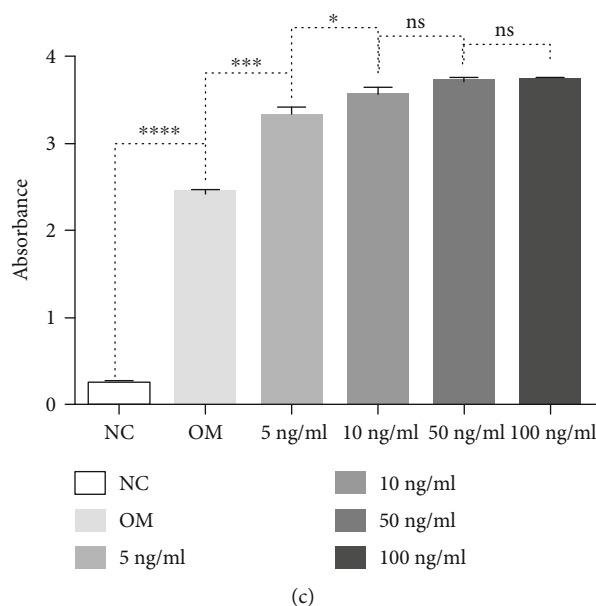


FIGURE 5: VEGF promoted odontogenic differentiation in DPSCs. The induced ALPase activity was tested in DPSCs treated with VEGF compared to cells without VEGF (a). VEGF treatment at 10 ng/ml concentration produced more mineralized nodules than 5 ng/ml VEGF treatment, and cells with 10 ng/ml, 50 ng/ml, and 100 ng/ml did not show an obvious difference in the amount of mineralized nodules (b). The quantitative analysis of ARS was conducted (c). NC: base culture medium; OM: odontogenic culture medium.

Under the condition of dental pulp exposure, stem cells in dental pulp provide the potential of pulp self-healing and tertiary dentin formation. Numerous investigations have concerned that the biological behaviors of DPSCs could be affected and amplified by extracellular environment [35]. Nowadays, an increasing focus on the design of new materials has emerged which are capable of driving DPSC migration and differentiation in dental therapy [36]. Among these, the CS/ $\beta$ -GP hydrogel has been widely used in drug delivery or tissue engineering systems for its biodegradability, biocompatibility, and antibacterial property [37].

The CS/ $\beta$ -GP hydrogel has thermosensitive property. The mixture maintains in the liquid state at room temperature and transforms into gel after 37°C incubation or be injecting into the body [22, 38]. The thermosensitive characteristic has been reported to be helpful in wound healing and bone tissue regeneration [32, 39]. The initial liquid stage can easily flow and fill any target area. Also, the liquid state is useful for encapsulating living cells and therapeutic agents. After the sol-gel transformation in the body, the hydrogel promoted the proliferation of cells. The sol-gel transformation in wound is safe and operable as it does not require externally applied trigger for gelation. Besides, the CS/ $\beta$ -GP hydrogels were elevated to be compatible with DPSCs in this and previous studies [39].

Lyophilization resulted in loss of water in the hydrogel; then, the porous structure of dry hydrogel was observed. The porous and hydrous structure allowed DPSC adhesion with embedded cellular synapses in the hydrogels. Numerous investigations indicated that the extracellular microenvironment can have an impact on cell behaviors. The morphology of cells seeded on different carriers showed in different

shapes. Studies reported that the odontoblastic cell line was spherical on HA sponge, while flattened with stretching processes on collagen sponge [25]. The difference of cell morphology on these carriers may be related to the adhesion receptor. It was previously demonstrated that odontoblastic cell lines KN-3 adhere to HA through surface markers like CD44 and attach to collagen through the integrins and collagen interaction [40, 41]. In the present study, DPSCs on the CS/ $\beta$ -GP hydrogel showed spherical shape. The related adhesion receptors need to be further investigated to identify the adhesion motility of DPSCs on the hydrogel [42, 43].

The AO/EB staining illustrated that the live cells without hydrogel were uniformly distributed on the well, while the live cells grew on the surface of hydrogel showed a status of agminate growth which might be contributed by the advantage of hydrogel for promoting proliferation of DPSCs. The apoptotic cells were stained by EB and less presented on the surface of hydrogels both in the two groups, which was a good proof for the biocompatibility of hydrogel. The well activity of DPSCs was similar with previous studies of human umbilical vein endothelial cells (HUVEC) and mouse embryonic fibroblast cells (NIH 3T3) on other materials composed by chitosan [29, 44]. The results of CCK-8 assay further showed the promoted proliferation of DPSCs with hydrogels. The hydrogel itself is not transparent and may influence the detection of absorbance. DPSCs were cultured in the hydrogel leachates to exclude the hydrogel absorbance in CCK-8 analysis [29]. These evidences were all in agreement with previous studies, suggesting the potential application of CS/ $\beta$ -GP hydrogel with great biocompatibility [45].

The previous studies have suggested that preencapsulating drugs in carriers allow a prolonged release of drugs

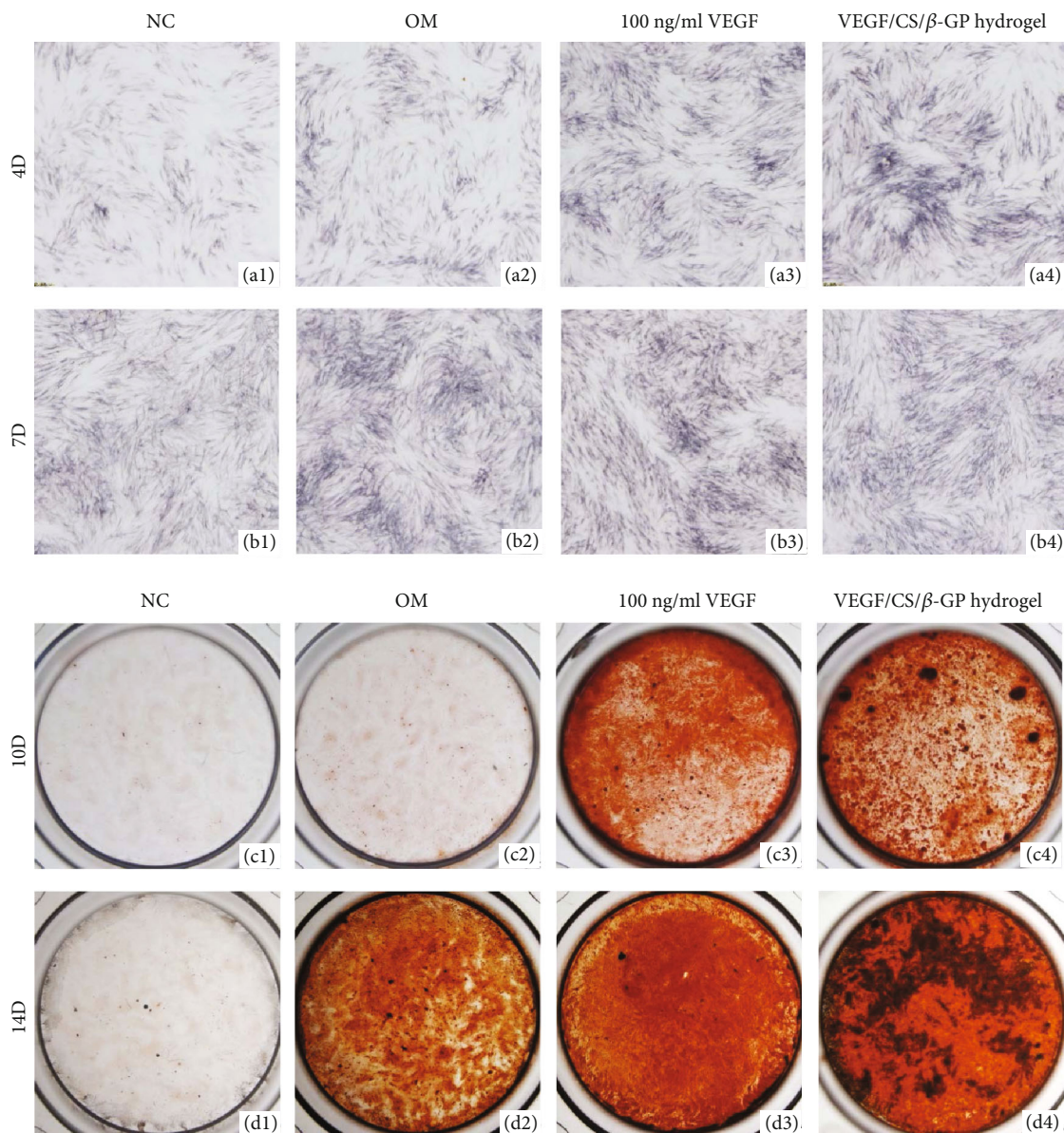


FIGURE 6: The sustained release of VEGF from hydrogels promoted the odontogenic differentiation of DPSCs. The results of ALP staining showed that the addition of VEGF protein in the medium and in the hydrogel both increased ALPase activities of DPSCs after 7 days (a1–a4, b1–b4). The sustained release of VEGF in VEGF/CS/β-GP hydrogels elevated the formation of mineralized nodules better than the initial burst release of VEGF in the medium (c1–c4, d1–d4). NC: base culture medium; OM: odontogenic culture medium.

[46], and the sustained delivery capability of CS/β-GP hydrogel was also evaluated in consistent with previous findings [47, 48]. The results of ELISA showed the incorporation of VEGF into CS/β-GP hydrogel had an initial burst release followed by a sustained release of VEGF over a period of time, and the release cumulation reached a steady level to create a relative steady concentration for cell culture. The similar release status was also observed in CS/β-GP hydrogel with other bioactive molecules [19, 22].

As we found the VEGF/CS/β-GP hydrogel was able to constantly release VEGF, we further compared the effects on the differentiation of DPSCs between VEGF released from hydrogels and once-added 100 ng/ml VEGF treatment.

Generally, agent release from biocompatible materials is related to initial agent loading, agent solubility, carrier material degradation, and so on [49]. In our study, we used the CS/β-GP hydrogel that carried 100 ng/ml of VEGF. Compared to the once-added VEGF treatment, DPSCs with VEGF/CS/β-GP hydrogel showed more mineralized nodule formation in the late differentiation stage. The higher expression levels of osteogenic/odontogenic markers in the VEGF/CS/β-GP hydrogel group were further detected. As a result, we supposed that this delivery system promoted the proliferation and odontogenic differentiation of DPSCs in a period of time, better than 100 ng/ml VEGF treatment without carriers. As described in previous studies [14], VEGF has

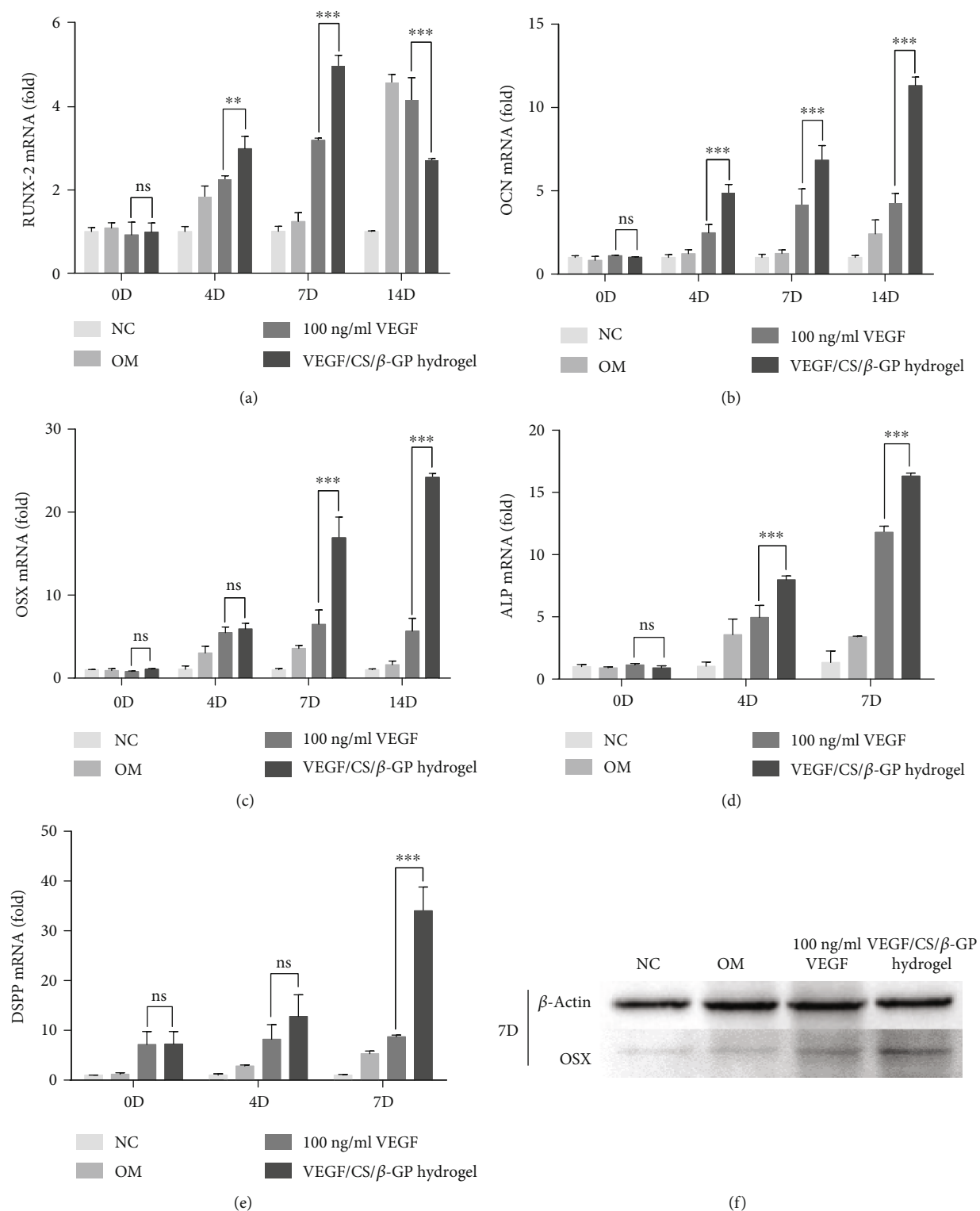


FIGURE 7: Continued.

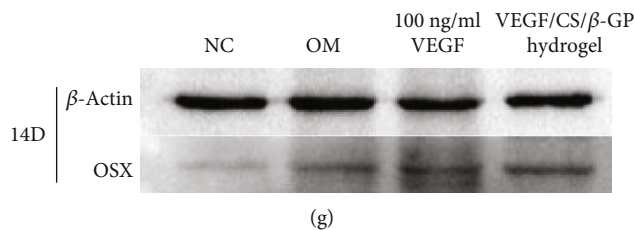


FIGURE 7: The sustained release of VEGF from hydrogels elevated odontogenic marker expressions in DPSCs. The expression levels of RUNX-2, OCN, and OSX during the odontogenic differentiation of DPSCs (a–c). The ALP expression level during the early stage of differentiation in DPSCs (d). The DSPP expression level during the late stage of differentiation in DPSCs (e). Data are presented as mean  $\pm$  SD. ns: no significant, \*\* $P < 0.01$ , \*\*\* $P < 0.005$ . The expression levels of OSX protein in DPSCs after 7 and 14 days (f, g). NC: base culture medium; OM: odontogenic culture medium.

an effect on odontogenic differentiation of DPSCs, while higher concentrations of VEGF may not always show better effects on DPSCs. Our study yielded similar cell responses to VEGF treatment with different concentrations. Based on the VEGF release behavior from hydrogel, it was suspected that the VEGF concentration in the hydrogel group was lower than that of the 100 ng/ml VEGF group. Besides, the  $\beta$ -GP in the CS/ $\beta$ -GP hydrogel not only induced the sol-gel transformation at body temperature but also provided organophosphates, as a result, inducing more calcium deposition [50]. All these data suggested that, even though the hydrogel group creates a lower concentration of VEGF in surroundings, the sustained release and steady concentration of VEGF may better contribute to promote the activity and odontogenic differentiation of DPSCs than the initial burst application of VEGF. These effects were consistent with the BMP-2/CS/ $\beta$ -GP hydrogel delivery system [22]. On the one hand, the CS/ $\beta$ -GP delivery system saves cost and maximizes the effects of VEGF treatment [14, 51, 52]. On the other hand, the delivery system decreased the negative consequence caused by rapid loss of physical stability and bioactivity [22, 32, 44–46]. The transwell technique helps us creating a circumstance to simulate practical application and allowing the VEGF released from hydrogel working on DPSCs.

## 5. Conclusions

In this study, the microstructure and biocompatibility of CS/ $\beta$ -GP hydrogel were identified. As a carrier material, the characteristic of sustained releasing VEGF was profiled and contributed to the proliferation and differentiation of DPSCs. Besides, the angiogenesis is another key step in the dental pulp healing. VEGF has been reported to be a potent factor to promote angiogenesis and might be beneficial to form the pulpodentinal complex. However, the advantages of chitosan carrying VEGF on angiogenesis still need further studies. Also, the pharmaceutical applications of hydrogels need further exploration on animal studies and clinical trials [53].

## Data Availability

The data used to support the findings of the study are available from the corresponding author upon request.

## Conflicts of Interest

The authors declare that there is no conflict of interest regarding the publication of this paper.

## Authors' Contributions

S. W. and Y. Z. designed the study; S. W., Y. Y., and Y. Z. conducted the study; S. W., Y. Z., X. Z., and M. W. collected the data; W. D., Y. F., and M. W. performed data analysis; Y. Z., L. Z., X. X., X. Z., X. Z., and Y. F. participated in data interpretation; S. W. and Y. Z. helped in drafting the manuscript; L. Z., X. X., X. Z., and Y. Z. contributed in revising the manuscript content; L. Z. and Y. Z. approved the final version of the manuscript. L. Z. takes responsibility for the integrity of the data analysis. Si Wu and Yachuan Zhou contributed equally to this work.

## Acknowledgments

This work was supported by the National Natural Science Foundation of China (NSFC) grant 81800927 to Yachuan Zhou, NSFC grant 81771033 to Liwei Zheng, and NSFC grant 81771099 to Xin Xu.

## References

- [1] "Guideline on pulp therapy for primary and immature permanent teeth," *Pediatric Dentistry*, vol. 38, no. 6, pp. 280–288, 2016.
- [2] P. Sangwan, A. Sangwan, J. Duhan, and A. Rohilla, "Tertiary dentinogenesis with calcium hydroxide: a review of proposed mechanisms," *International Endodontic Journal*, vol. 46, no. 1, pp. 3–19, 2013.
- [3] F. G. Aguilar, L. da Fonseca Roberti Garcia, H. L. Rossetto, L. C. Pardini, and F. de Carvalho Panzeri Pires-de-Souza, "Radiopacity evaluation of calcium aluminate cement containing different radiopacifying agents," *Journal of Endodontics*, vol. 37, no. 1, pp. 67–71, 2011.
- [4] M. Goldberg, S. Lacerda-Pinheiro, N. Jegat et al., "The impact of bioactive molecules to stimulate tooth repair and regeneration as part of restorative dentistry," *Dental Clinics of North America*, vol. 50, no. 2, pp. 277–298, 2006.
- [5] M. Nakashima, "Induction of dentin formation on canine amputated pulp by recombinant human bone morphogenetic







- proteins (BMP)-2 and -4,” *Journal of Dental Research*, vol. 73, no. 9, pp. 1515–1522, 1994.
- [6] W. Zhang, X. F. Walboomers, and J. A. Jansen, “The formation of tertiary dentin after pulp capping with a calcium phosphate cement, loaded with PLGA microparticles containing TGF- $\beta$ 1,” *Journal of Biomedical Materials Research Part A*, vol. 85, no. 2, pp. 439–444, 2008.
- [7] F. Li, X. Liu, S. Zhao, H. Wu, and H. H. K. Xu, “Porous chitosan bilayer membrane containing TGF- $\beta$ 1 loaded microspheres for pulp capping and reparative dentin formation in a dog model,” *Dental Materials*, vol. 30, no. 2, pp. 172–181, 2014.
- [8] C. Kitamura, T. Nishihara, M. Terashita, Y. Tabata, and A. Washio, “Local regeneration of dentin-pulp complex using controlled release of fgf-2 and naturally derived sponge-like scaffolds,” *International Journal of Dentistry*, vol. 2012, Article ID 190561, 8 pages, 2012.
- [9] H. Ishimatsu, C. Kitamura, T. Morotomi et al., “Formation of dentinal bridge on surface of regenerated dental pulp in dentin defects by controlled release of fibroblast growth factor-2 from gelatin hydrogels,” *Journal of Endodontia*, vol. 35, no. 6, pp. 858–865, 2009.
- [10] S. Matsumura, A. Quispe-Salcedo, C. M. Schiller et al., “IGF-1 mediates ephrinB1 activation in regulating tertiary dentin formation,” *Journal of Dental Research*, vol. 96, no. 10, pp. 1153–1161, 2017.
- [11] M. Yadlapati, C. Bigueti, F. Cavalla et al., “Characterization of a vascular endothelial growth factor-loaded bioresorbable delivery system for pulp regeneration,” *Journal of Endodontia*, vol. 43, no. 1, pp. 77–83, 2017.
- [12] K. Matsushita, R. Motani, T. Sakutal et al., “The role of vascular endothelial growth factor in human dental pulp cells: induction of chemotaxis, proliferation, and differentiation and activation of the AP-1-dependent signaling pathway,” *Journal of Dental Research*, vol. 79, no. 8, pp. 1596–1603, 2000.
- [13] M. M. L. Deckers, M. Karperien, C. van der Bent, T. Yamashita, S. E. Papapoulos, and C. W. G. M. Löwik, “Expression of vascular endothelial growth factors and their receptors during osteoblast differentiation,” *Endocrinology*, vol. 141, no. 5, pp. 1667–1674, 2000.
- [14] H. Aksel and G. T.-J. Huang, “Combined effects of vascular endothelial growth factor and bone morphogenetic protein 2 on odonto/osteogenic differentiation of human dental pulp stem cells *in vitro*,” *Journal of Endodontia*, vol. 43, no. 6, pp. 930–935, 2017.
- [15] Y. C. Chiang, H. H. Chang, C. C. Wong et al., “Nanocrystalline calcium sulfate/hydroxyapatite biphasic compound as a TGF- $\beta$ 1/VEGF reservoir for vital pulp therapy,” *Dental Materials*, vol. 32, no. 10, pp. 1197–1208, 2016.
- [16] J. Zhang, X. Liu, W. Yu et al., “Effects of human vascular endothelial growth factor on reparative dentin formation,” *Molecular Medicine Reports*, vol. 13, no. 1, pp. 705–712, 2016.
- [17] S. Mathieu, C. Jeanneau, N. Sheibat-Othman, N. Kalaji, H. Fessi, and I. About, “Usefulness of controlled release of growth factors in investigating the early events of dentin-pulp regeneration,” *Journal of Endodontia*, vol. 39, no. 2, pp. 228–235, 2013.
- [18] B. A. Baldo, “Side effects of cytokines approved for therapy,” *Drug Safety*, vol. 37, no. 11, pp. 921–943, 2014.
- [19] L. Mi, H. Liu, Y. Gao, H. Miao, and J. Ruan, “Injectable nanoparticles/hydrogels composite as sustained release system with stromal cell-derived factor-1 $\alpha$  for calvarial bone regeneration,” *International Journal of Biological Macromolecules*, vol. 101, pp. 341–347, 2017.
- [20] R. C. F. Cheung, T. B. Ng, J. H. Wong, and W. Y. Chan, “Chitosan: an update on potential biomedical and pharmaceutical applications,” *Marine Drugs*, vol. 13, no. 8, pp. 5156–5186, 2015.
- [21] D. Gothard, E. L. Smith, J. M. Kanczler et al., “Tissue engineered bone using select growth factors: a comprehensive review of animal studies and clinical translation studies in man,” *European Cells & Materials*, vol. 28, pp. 166–208, 2014.
- [22] S. Kim, H. Tsao, Y. Kang et al., “*In vitro* evaluation of an injectable chitosan gel for sustained local delivery of BMP-2 for osteoblastic differentiation,” *Journal of Biomedical Materials Research Part B: Applied Biomaterials*, vol. 99B, no. 2, pp. 380–390, 2011.
- [23] H. Kaida, T. Hamachi, H. Anan, and K. Maeda, “Wound healing process of injured pulp tissues with emdogain gel,” *Journal of Endodontia*, vol. 34, no. 1, pp. 26–30, 2008.
- [24] D. E. Witherspoon, “Vital pulp therapy with new materials: new directions and treatment perspectives—permanent teeth,” *Pediatric Dentistry*, vol. 30, no. 3, pp. 220–224, 2008.
- [25] Y. Inuyama, C. Kitamura, T. Nishihara et al., “Effects of hyaluronic acid sponge as a scaffold on odontoblastic cell line and amputated dental pulp,” *Journal of Biomedical Materials Research Part B: Applied Biomaterials*, vol. 92B, no. 1, pp. 120–128, 2010.
- [26] X. Niu, Z. Liu, J. Hu, K. J. Rambhia, Y. Fan, and P. X. Ma, “Microspheres assembled from chitosan-graft-poly (lactic acid) micelle-like core-shell nanospheres for distinctly controlled release of hydrophobic and hydrophilic biomolecules,” *Macromolecular Bioscience*, vol. 16, no. 7, pp. 1039–1047, 2016.
- [27] Z. Li and V. Sae-Lim, “Comparison of acidic fibroblast growth factor on collagen carrier with calcium hydroxide as pulp capping agents in monkeys,” *Dental Traumatology*, vol. 23, no. 5, pp. 278–286, 2007.
- [28] W. Luiz de Oliveira da Rosa, T. Machado da Silva, F. Fernando Demarco, E. Piva, and A. Fernandes da Silva, “Could the application of bioactive molecules improve vital pulp therapy success? A systematic review,” *Journal of Biomedical Materials Research Part A*, vol. 105, no. 3, pp. 941–956, 2017.
- [29] A. Deng, X. Kang, J. Zhang, Y. Yang, and S. Yang, “Enhanced gelation of chitosan/ $\beta$ -sodium glycerophosphate thermosensitive hydrogel with sodium bicarbonate and biocompatibility evaluated,” *Materials Science and Engineering: C*, vol. 78, pp. 1147–1154, 2017.
- [30] A. Oryan, S. Alidadi, A. Bigham-Sadegh, A. Moshiri, and A. Kamali, “Effectiveness of tissue engineered chitosan-gelatin composite scaffold loaded with human platelet gel in regeneration of critical sized radial bone defect in rat,” *Journal of Controlled Release*, vol. 254, pp. 65–74, 2017.
- [31] S. Supper, N. Anton, N. Seidel, M. Riemenschnitter, C. Curdy, and T. Vandamme, “Thermosensitive chitosan/glycerophosphate-based hydrogel and its derivatives in pharmaceutical and biomedical applications,” *Expert Opinion on Drug Delivery*, vol. 11, no. 2, pp. 249–267, 2014.
- [32] J. K. Suh and H. W. Matthew, “Application of chitosan-based polysaccharide biomaterials in cartilage tissue engineering: a review,” *Biomaterials*, vol. 21, no. 24, pp. 2589–2598, 2000.

- [33] K. Skoskiewicz-Malinowska, U. Kaczmarek, B. Malicka, K. Walczak, and M. Zietek, "Application of chitosan and propolis in endodontic treatment: a review," *Mini Reviews in Medicinal Chemistry*, vol. 17, no. 5, pp. 410–434, 2017.
- [34] S. Gronthos, M. Mankani, J. Brahim, P. G. Robey, and S. Shi, "Postnatal human dental pulp stem cells (DPSCs) *in vitro* and *in vivo*," *Proceedings of the National Academy of Sciences of the United States of America*, vol. 97, no. 25, pp. 13625–13630, 2000.
- [35] H. Bakhtiar, A. Mazidi S, S. Mohammadi Asl et al., "The role of stem cell therapy in regeneration of dentine-pulp complex: a systematic review," *Progress in Biomaterials*, vol. 7, no. 4, pp. 249–268, 2018.
- [36] T. Giraud, C. Jeanneau, C. Rombouts, H. Bakhtiar, P. Laurent, and I. About, "Pulp capping materials modulate the balance between inflammation and regeneration," *Dental Materials*, vol. 35, no. 1, pp. 24–35, 2019.
- [37] S. Saravanan, S. Vimalraj, P. Thanikaivelan, S. Banudevi, and G. Manivasagam, "A review on injectable chitosan/beta glycerophosphate hydrogels for bone tissue regeneration," *International Journal of Biological Macromolecules*, vol. 121, pp. 38–54, 2018.
- [38] Q. Tang, C. Luo, B. Lu et al., "Thermosensitive chitosan-based hydrogels releasing stromal cell derived factor-1 alpha recruit MSC for corneal epithelium regeneration," *Acta Biomaterialia*, vol. 61, pp. 101–113, 2017.
- [39] Y. Chen, F. Zhang, Q. Fu, Y. Liu, Z. Wang, and N. Qi, "In vitro proliferation and osteogenic differentiation of human dental pulp stem cells in injectable thermo-sensitive chitosan/ $\beta$ -glycerophosphate/hydroxyapatite hydrogel," *Journal of Biomaterials Applications*, vol. 31, no. 3, pp. 317–327, 2016.
- [40] A. Aruffo, I. Stamenkovic, M. Melnick, C. B. Underhill, and B. Seed, "CD44 is the principal cell surface receptor for hyaluronate," *Cell*, vol. 61, no. 7, pp. 1303–1313, 1990.
- [41] C. Hardwick, K. Hoare, R. Owens et al., "Molecular cloning of a novel hyaluronan receptor that mediates tumor cell motility," *The Journal of Cell Biology*, vol. 117, no. 6, pp. 1343–1350, 1992.
- [42] N. Liu, M. Zhou, Q. Zhang et al., "Stiffness regulates the proliferation and osteogenic/odontogenic differentiation of human dental pulp stem cells via the WNT signalling pathway," *Cell Proliferation*, vol. 51, no. 2, article e12435, 2018.
- [43] S. N. Jayash, N. M. Hashim, M. Misran, and N. A. Baharuddin, "Formulation and *in vitro* and *in vivo* evaluation of a new osteoprotegerin-chitosan gel for bone tissue regeneration," *Journal of Biomedical Materials Research Part A*, vol. 105, no. 2, pp. 398–407, 2017.
- [44] K. Liu, P. C. Liu, R. Liu, and X. Wu, "Dual AO/EB staining to detect apoptosis in osteosarcoma cells compared with flow cytometry," *Medical Science Monitor Basic Research*, vol. 21, pp. 15–20, 2015.
- [45] D. D. Li, J. F. Pan, Q. X. Ji et al., "Characterization and cytocompatibility of thermosensitive hydrogel embedded with chitosan nanoparticles for delivery of bone morphogenetic protein-2 plasmid DNA," *Journal of Materials Science: Materials in Medicine*, vol. 27, no. 8, p. 134, 2016.
- [46] E. Ruel-Gariépy, A. Chenite, C. Chaput, S. Guirguis, and J. C. Leroux, "Characterization of thermosensitive chitosan gels for the sustained delivery of drugs," *International Journal of Pharmaceutics*, vol. 203, no. 1-2, pp. 89–98, 2000.
- [47] J. Wu, Z. G. Su, and G. H. Ma, "A thermo- and pH-sensitive hydrogel composed of quaternized chitosan/glycerophosphate," *International Journal of Pharmaceutics*, vol. 315, no. 1-2, pp. 1–11, 2006.
- [48] L. S. Nair, T. Starnes, J.-W. K. Ko, and C. T. Laurencin, "Development of injectable thermogelling chitosan-inorganic phosphate solutions for biomedical applications," *Biomacromolecules*, vol. 8, no. 12, pp. 3779–3785, 2007.
- [49] P. A. Gunatillake and R. Adhikari, "Biodegradable synthetic polymers for tissue engineering," *European Cells & Materials*, vol. 5, pp. 1–16, 2003.
- [50] F. Langenbach and J. Handschel, "Effects of dexamethasone, ascorbic acid and  $\beta$ -glycerophosphate on the osteogenic differentiation of stem cells *in vitro*," *Stem Cell Research & Therapy*, vol. 4, no. 5, p. 117, 2013.
- [51] W. J. Bae, J. K. Yi, J. Park, S. K. Kang, J. H. Jang, and E. C. Kim, "Lysyl oxidase-mediated VEGF-induced differentiation and angiogenesis in human dental pulp cells," *International Endodontic Journal*, vol. 51, no. 3, pp. 335–346, 2018.
- [52] I. D' Alimonte, E. Nargi, F. Mastrangelo et al., "Vascular endothelial growth factor enhances *in vitro* proliferation and osteogenic differentiation of human dental pulp stem cells," *Journal of Biological Regulators and Homeostatic Agents*, vol. 25, no. 1, pp. 57–69, 2011.
- [53] E. Szymanska and K. Winnicka, "Stability of chitosan-a challenge for pharmaceutical and biomedical applications," *Marine Drugs*, vol. 13, no. 4, pp. 1819–1846, 2015.

## Research Article

# Is There a Noninvasive Source of MSCs Isolated with GMP Methods with Better Osteogenic Potential?

Carla C. G. Pinheiro <sup>1</sup>, Alessander Leyendecker Junior <sup>1</sup>, Daniela Y. S. Tanikawa <sup>1</sup>,  
José Ricardo Muniz Ferreira,<sup>2</sup> Reza Jarrahy,<sup>3</sup> and Daniela F. Bueno <sup>1</sup>

<sup>1</sup>Hospital Sírio-Libanês-Instituto de Ensino e Pesquisa, São Paulo, SP 01308-050, Brazil

<sup>2</sup>Instituto Militar de Engenharia (IME), Departamento de Ciências de Materiais, Programa de Pós Graduação em Ciências de Materiais, Rio de Janeiro, RJ 22290-270, Brazil

<sup>3</sup>David Geffen School of Medicine, Division of Plastic and Reconstructive Surgery, University of California Los Angeles (UCLA), Los Angeles, CA, USA

Correspondence should be addressed to Daniela F. Bueno; [dbuenosp@gmail.com](mailto:dbuenosp@gmail.com)

Received 31 May 2019; Revised 11 August 2019; Accepted 11 September 2019; Published 6 November 2019

Guest Editor: Jiashing Yu

Copyright © 2019 Carla C. G. Pinheiro et al. This is an open access article distributed under the Creative Commons Attribution License, which permits unrestricted use, distribution, and reproduction in any medium, provided the original work is properly cited.

**Background.** A new trend in the treatment for alveolar clefts in patients with cleft lip and palate involves the use of bone tissue engineering strategies to reduce or eliminate the morbidity associated with autologous bone grafting. The use of mesenchymal stem cells—autologous cells obtained from tissues such as bone marrow and fat—combined with various biomaterials has been proposed as a viable option for use in cleft patients. However, invasive procedures are necessary to obtain the mesenchymal stem cells from these two sources. To eliminate donor site morbidity, noninvasive stem cell sources such as the umbilical cord, orbicularis oris muscle, and deciduous dental pulp have been studied for use in alveolar cleft bone tissue engineering. In this study, we evaluate the osteogenic potential of these various stem cell types. **Methods.** Ten cellular strains obtained from each different source (umbilical cord, orbicularis oris muscle, or deciduous dental pulp) were induced to osteogenic differentiation *in vitro*, and the bone matrix deposition of each primary culture was quantified. To evaluate whether greater osteogenic potential of the established mesenchymal stem cell strains was associated with an increase in the expression profile of neural crest genes, real-time qPCR was performed on the following genes: SRY-box 9, SRY-box 10, nerve growth factor receptor, transcription factor AP-2 alpha, and paired box 3. **Results.** The mesenchymal stem cells obtained from deciduous dental pulp and orbicularis oris muscle demonstrated increased osteogenic potential with significantly more extracellular bone matrix deposition when compared to primary cultures obtained from the umbilical cord after twenty-one days in culture ( $p = 0.007$  and  $p = 0.005$ , respectively). The paired box 3 gene was more highly expressed in the MSCs obtained from deciduous dental pulp and orbicularis oris muscle than in those obtained from the umbilical cord. **Conclusion.** These results suggest that deciduous dental pulp and orbicularis oris muscle stem cells demonstrate superior osteogenic differentiation potential relative to umbilical cord-derived stem cells and that this increased potential is related to their neural crest origins. Based on these observations, and the distinct translational advantage of incorporating stem cells from noninvasive tissue sources into tissue engineering protocols, greater study of these specific cell lines in the setting of alveolar cleft repair is indicated.

## 1. Background

Tissue bioengineering is characterized by the integration of engineering strategies and biological principles with the aim of restoring, maintaining, or improving the function of tissues affected by various pathologies [1, 2]. The main objective

of tissue bioengineering is to overcome the limitations of conventional treatments that are based on traditional reconstructive surgery or organ transplantation through the combination of cells with great growth potential (e.g., stem cells), biocompatible delivery vehicles, and growth factors. The goal of many tissue engineering protocols is to create

organ and tissue substitutes that exhibit immunologic tolerance and that minimize the disadvantages associated with more traditional techniques [3].

The application of bioengineering principles has rapidly increased in all medical and dental specialties [1, 4]. Congenital malformations associated with cleft and craniofacial syndromes have been extensively studied as part of this expansive research focus. Specifically, tissue engineering approaches to the rehabilitation of the cleft alveolus in patients who are born with complete cleft lip and palate (CLP) have been an area of intense investigation. Currently, the “gold standard” in the treatment of patients with alveolar clefts is the placement of an autologous bone graft. In this surgical procedure, the bone is harvested from the patient—typically from the iliac crest—and used to fill the alveolar cleft [5, 6]. This method, however, has significant drawbacks. For example, the amount of available bone graft donor sites, and the amount of bone that can be procured from these sites, is finite. In cases of large or bilateral clefts, a donor area such as the iliac crest may not provide enough graft material to fill the alveolar cleft. Furthermore, bone resorption in the grafted area may occur, requiring additional procedures. Donor site infection is a reality [7], and, of course, the significant amount of pain that patients experience in the hip region cannot be understated.

Fortunately, with the application of tissue bioengineering principles to this clinical problem, and with our ability to procure autologous stem cells in noninvasive ways, we are now poised to use these cells in innovative ways that might obviate the need for traditional bone grafting and its associated drawbacks. Within this context, mesenchymal stem cells (MSCs) represent a promising biological substrate [1].

MSCs are defined as cells that have the capacity to proliferate and self-renew. They have the ability to respond to external stimuli and give rise to numerous distinct specialized cell lines. MSCs are found in different tissues, are arranged in niches throughout the body, and are responsible for tissue maintenance and repair. MSCs are commonly considered to be of mesodermal origin. Some authors associate various MSC strains with the expression of genes related to embryonic stem cells as well as genes related to the neural crest cell origin [8].

Protocols describing the expansion of MSC populations from umbilical cord isolates, also known as umbilical cord MSCs (UC-MSCs), have been well described. Several authors describe the isolation of UC-MSCs from different components of the umbilical cord, including the cord epithelium and Wharton’s jelly. Different types of enzymatic digestion can be used to isolate UC-MSCs, which are characterized by UC-CD73+, CD90+, and CD105+ expression profiles. Some have described that various UC-MSC strains also express embryonic stem cell markers, such as Podocalyxin (Tra-1-60/Tra-1-81), Stage Specific Embryonic Antigen-1 (SSEA-1), and Stage Specific Embryonic Antigen-4 (SSEA-4) [9–11].

Pluripotency markers, such as octamer-binding transcription factor 4 (Oct-4), SRY-box2 (SOX2), and Nanog markers, are not found in UC-MSCs. UC-MSCs are described as adult MSCs, with intermediate characteristics

between embryonic stem cells and adult multipotent cells and may have better potential than MSCs isolated from bone marrow (BM) or fat for tissue engineering [12].

Due to their origin, MSCs from exfoliated deciduous teeth, or dental pulp stem cells (DPSCs), are noteworthy: they have a faster proliferation rate than the pulp of permanent teeth and they express primitive cell neuronal and glial markers on their surfaces [8, 13]. The expression of neuronal and glial markers in stem cells from human exfoliated deciduous teeth (SHED) is related to their origin, as they originate from the migration of neural crest cells. These cells play a fundamental role in embryonic development, giving rise to all the tissues of the face, except the enamel of the teeth [8, 13, 14].

Orbicularis oris muscle-derived stem cells (OOMDSCs) have been found to represent a noninvasive source of MSCs for CLP patients, with the potential to reconstruct critical size bone defects in animal models [15]. Facial development, including development of the oral cavity and dental structures, is characterized by epithelial-cell interactions between the craniofacial mesoderm and the neural crest-derived mesenchyme. Therefore, all facial tissues, including DPSCs and OOMDSCs, retain some genes that are expressed in neural crest cells in their cellular population [16].

In this study, we compare the osteogenic potential of three different noninvasive sources of MSCs—DPSCs, OOMDSCs, and UC-MSCs—for use in bone tissue engineering. Specifically, we assess their applicability in a bioengineered alternative to traditional alveolar bone graft surgery in CLP patients. We also quantify the expression profile of neural crest genes SRY-box 9 (SOX9), SRY-box 10 (SOX10), nerve growth factor receptor (NGFR), transcription factor AP-2 alpha (TFAP2a), and paired box 3 (PAX3) in DPSCs, OOMDSCs, and UC-MSCs to determine whether the level of expression of these genes in these MSC populations correlates with their osteogenic potential.

## 2. Materials and Methods

*2.1. Obtaining, Isolating, and Characterizing Primary Cultures of MSCs.* Thirty samples of different tissues were obtained from thirty pediatric patients at our affiliate institutions (deciduous dental pulp, 10 samples; orbicularis oris muscle, 10 samples; and umbilical cord, 10 samples). Our research protocol was approved by the Ethics Committee of Hospital Sírio-Libanês, and informed consent was obtained from the legal guardians of all pediatric subjects enrolled in this study. (Of note, these tissues would all be discarded under normal circumstances. The use of these tissues therefore posed no additional burden to the donors.) Cells were isolated according to previously established protocols [15, 17, 18]; however, we added the good manufacturing practice (GMP) grade to the protocols.

For the collection of tissues from a surgical center (muscle fragments and umbilical cords) or dental office (dental pulp), basic care using sterile materials was implemented to avoid contamination. Time from tissue collection to cellular isolation never exceeded 24 hours after collection to avoid cell loss and possible cross-contamination. Our laboratory

has standard biosafety certifications used for the handling and processing of human tissues (e.g., anteroom for paramentation and HEPA air filters). From cell isolation to cryopreservation, reagents that were sterile, apyrogenic, and with batch traceability were used. Aerobic, anaerobic, and fungus contamination tests (BactAlert, bioMérieux) and mycoplasma tests (MycoAlert kit, Lonza) were carried out during cell expansion. Any samples with positive results were discarded.

**2.2. Establishment of Primary Cultures at GMP Laboratory.** Our laboratory facilities are regulated by Brazilian laws and resolutions (National Sanitary Surveillance Agency—ANVISA—RDC No 214, February 8, 2018) that regulate advanced cell therapies. According to the local regulatory committee, our laboratory facilities have regular inspections, conduct staff trainings, perform routine equipment maintenance and risk and adverse event assessments, and use fully traceable reagents and processes [19, 20]. We have recommended infrastructure for clean rooms including airflow and air particulate control (HEPA filter) and antechambers for individual protection paramentation. Only human cells can be processed at our advanced cell therapy laboratory site. Moreover, all reagents from cell isolation to cryopreservation are certified, prion-free, and apyrogenic.

**2.2.1. DPSCs.** The deciduous dental pulp specimens were collected by surgical extraction at a dental office in the Hospital Municipal Infantil Menino Jesus from CLP patients and immediately added to a sterile container with 2 ml of Dulbecco's modified Eagle's medium/Nutrient Mixture F-12 (DMEM-F12; Gibco Invitrogen, Grand Island, NY) solution supplemented with 100 IU/ml penicillin and streptomycin (Penicillin-Streptomycin; Gibco Invitrogen, Grand Island, NY). Afterwards, they were transported to the laboratory of Hospital Sírio-Libanês at 4 to 8°C in a transport box. Deciduous dental pulp was processed on average at 15 hours after initial collection.

In the laboratory, the deciduous dental pulp specimens were washed twice with phosphate-buffered saline (PBS, pH 7.4; Gibco Invitrogen, Grand Island, NY) and digested with a solution containing 1 mg/ml of TrypLE™ Express Enzyme (Gibco Invitrogen, Grand Island, NY) in PBS for 30 minutes at 37°C. After tissue digestion, the samples were centrifuged at  $300 \times g$  for 5 minutes, and then the pulp was cut into two or more  $1 \text{ mm}^3$  fragments. After these procedures, the cells were cultured in a 12-well plate with each fragment in a separate well.

**2.2.2. OOMDSCs.** Fragments of the orbicular oris muscle were collected by surgical extraction at Hospital Municipal Infantil Menino Jesus from CLP patients during cheiloplasty and immediately added to a sterile collector tube with 2 ml of DMEM-F12 solution supplemented with 100 IU/ml penicillin and streptomycin. The orbicular oris muscle fragments were processed on average up to 16 hours after collection.

In the laboratory, fragments of the orbicular oris muscle were washed twice with PBS and digested with a solution containing 1 mg/ml of TrypLE™ Express in PBS for

40 minutes at 37°C. After the enzymatic digestion, the samples were centrifuged at  $300 \times g$  for 10 minutes. The muscle fragments were divided into three parts and cultured in a 12-well plate with each fragment in a separate well. MSCs were expelled from the fragment 10 to 20 days after this procedure.

**2.2.3. UC-MSCs.** The umbilical cord fragments were collected at Maternidade Amparo Maternal, from mothers who previously elected to donate umbilical cord blood to a cord blood bank. After collecting the blood, the umbilical cord was decontaminated with chlorhexidine (0.12%), and the fragment (5 to 8 cm) was immediately added to a sterile collection tube with 2 ml of PBS solution supplemented with 100 IU/ml of penicillin and streptomycin. The fragments were processed on average up to 16 hours after collection.

In the laboratory, the umbilical cord fragments were washed twice with PBS. For better manipulation of the fragments, the tissue was cut into smaller pieces of two to three centimeters, and then the arteries and veins were removed. The stromal tissue was cut into smaller pieces and added to a Falcon-type tube with a 2.0 mg/ml solution of collagenase NB6 (GMP-SERVA Electrophoresis; Nordmark GmbH, Crescent Chemical) diluted in PBS with 2 mM calcium chloride for two hours at 37°C with continuous movement. To remove the digestion solution, the samples were centrifuged at  $300 \times g$  for 10 minutes. The digested tissue was resuspended in 10 ml of a DMEM-F12 culture medium supplemented with 15% Characterized Fetal Bovine Serum (FBS; US Origin HyClone™, GE Healthcare Life Sciences, South Logan, UT), 100 IU/ml of penicillin and streptomycin and nonessential amino acid (MEM Non-Essential Amino Acids Solution; Gibco Invitrogen, Grand Island, NY) and cultured in  $25 \text{ cm}^2$  culture flasks. The successful isolation of MSCs was observed between 15 and 20 days after this process. This culture medium was used for cell expansion in all strains (DPSC, OOMDSCs, and UC-MSC) until the cells reached approximately 80-90% confluence.

**2.3. Cryopreservation.** All 30 strains were cryopreserved before the assays using DMEM-F12 diluted 1:1 with FBS and 10% dimethyl sulfoxide (DMSO; CryoPur™ 100% DMSO; OriGen). The temperature was gradually decreased by 1°C per minute to -80°C, and the cells were stored at -196°C.

**2.4. Characterization by Flow Cytometry.** For all 30 strains between the 4th and the 5th passage, immunophenotyping was performed by flow cytometry in a FACSCalibur flow cytometer (BD, Becton Dickinson Franklin Lakes, NJ) and analyzed in the CellQuest program (BD, Becton Dickinson Franklin Lakes, NJ). Immunophenotyping allows the characterization of cells at different stages of development through the use of fluorescent monoclonal antibodies against surface markers (antigens).

Cells obtained from cell cultures at a concentration of  $1 \times 10^6$  cells/ $100 \mu\text{l}$  were labeled with the following monoclonal antibodies: CD29-PE, CD31-FITC, CD34-FITC, CD45-PE, CD73-FITC, CD90-FITC, CD105-PE, CD166-PE, IgG-FITC, and IgG-PE isotypes (BD Biosciences, Becton

Dickinson, Franklin Lakes, NJ) for 15 minutes at room temperature in the dark. Five hundred microliters of PBS was then added with 3% FBS and incubated for 15 minutes at room temperature in the dark. First, unstained cells were analyzed, and from that analysis, specific isotypes for each antibody were used for staining, with monoclonal antibodies as a negative control for the reaction, and were measured the minimum  $5 \times 10^5$  events.

## 2.5. Characterization by Cell Differentiation Ability

**2.5.1. Osteogenic Differentiation.** The 30 strains between the 4th and the 5th passage were induced for osteogenic differentiation. After the culture in the osteogenic medium for 21 days, we assessed *in vitro* formation of bone matrix by assessing areas of culture that were positive for calcium hydroxyapatite.

In a 12-well plate (Corning® Costar®), the cells obtained from each of the 30 strains were seeded at the same density in triplicate ( $5 \times 10^3$  cells). After 24 hours of culture in DMEM-F12, the culture medium was changed to a specific osteogenic induction medium supplemented with growth factors (StemPro® Osteogenesis Differentiation Kit; Gibco Invitrogen, Grand Island, NY).

After twenty-one days in culture, we stained each culture dish with alizarin red S. The wells were washed twice with PBS and fixed with 70% ethanol (Sigma Aldrich, St. Louis, MO) for 30 minutes. After fixation, the wells were stained with 0.2% alizarin red S solution (pH 4.2; Sigma Aldrich, St. Louis, MO) for 30 minutes. For the final wash, each well was washed with PBS (Gibco Invitrogen, Grand Island, NY) three times. We analyzed the formation of mineralized bone extracellular matrix by microscopy (Olympus CKX31).

**2.5.2. Adipogenic Differentiation.** Primary MSC cultures were cultured in an adipogenic induction medium for eighteen days. After this period, we observed the morphological changes and the formation of intracellular lipid vesicles in the cultured cells.

In a 12-well plate, the cells were seeded at the same density in triplicate ( $5 \times 10^3$  cells). After 24 hours of culture in basal culture medium, the culture medium was changed to the specific adipogenic culture medium supplemented with growth factors (StemPro® Adipogenic Differentiation Kit; Gibco Invitrogen, Grand Island, NY).

For evaluation, the adipogenic induction medium was removed from the cell cultures, and the cells were stained with oil red (Oil Red O, Sigma Aldrich, St. Louis, MO). For the staining, the wells were washed twice with PBS (Gibco Invitrogen, Grand Island, NY) and fixed with 60% isopropanol (Sigma Aldrich, St. Louis, MO) for five minutes at room temperature. After fixation, the cells were stained with oil red (0.5 mg/ml) for 15 minutes under light at room temperature. For the final wash, 60% isopropanol was used once and distilled water twice.

After the staining of the lipid vesicles, the observation of cellular structures was carried out under inverted microscopy (Olympus CKX31).

**2.5.3. Chondrogenic Differentiation.** To perform chondrogenic differentiation, MSCs were induced to differentiate into chondrocytes after twenty-one days of culture in a chondrogenic induction medium supplemented with growth factors.

In a 12-well plate, the cells were seeded at the same concentration in triplicate ( $5 \times 10^4$  cells). After 24 hours of culture in a basal culture medium, the culture medium was changed to the specific chondrogenic differentiation medium supplemented with growth factors (StemPro® Chondrogenic Differentiation Kit; Gibco Invitrogen, Grand Island, NY).

For the evaluation of chondrogenic differentiation, we performed staining with alcian blue after 21 days in differentiation conditions to identify the proteoglycan (extracellular matrix) released by the chondrocytes.

The induction medium was removed from the cell cultures, which were washed twice with PBS (Gibco Invitrogen, Grand Island, NY) and fixed with 4% formaldehyde (Sigma Aldrich, St. Louis, MO) for 20 minutes at room temperature. After fixation, the cells were stained with 1 mg/ml of alcian blue (Sigma Aldrich, St. Louis, MO) for two hours in the dark at room temperature. For the final wash, hydrochloric acid (0.1 M) was used once and with PBS twice.

**2.6. Quantification of Mineralized Bone Matrix.** As one of the objectives of this research was to evaluate the potential for osteogenic differentiation in MSCs from three different sources, 10 primary cultures of DPSCs, 10 primary cultures of OOMDSCs, and 10 primary cultures of UC-MSCs were induced to osteogenic differentiation in a 24-well plate. For this assay,  $2.5 \times 10^3$  cells were seeded in triplicate between the 4th and the 5th passage.

For the initial seeding, the basal culture medium was used after 24 hours when the cells were already adhered to the bottom of the culture plate. The osteogenic induction was initiated by changing the basal culture medium with osteogenic induction medium (StemPro® Osteogenic Differentiation Kit; Gibco Invitrogen, Grand Island, NY). The osteogenic differentiation process was analyzed after 0, 3, 7, 14, and 21 days of culture in osteogenic differentiation medium.

For analysis of bone extracellular matrix formation, the culture medium was removed and 0.5 mg/ml of alizarin red S (pH 4.2; Sigma Aldrich, St. Louis, MO) diluted in PBS (Gibco Invitrogen, Grand Island, NY) was added to each well. Subsequently, the cells were incubated under light for 30 minutes at room temperature.

After 30 minutes, 200  $\mu$ l of 20% methanol solution (Sigma Aldrich, St. Louis, MO) and 10% acetic acid diluted in PBS (Sigma Aldrich, St. Louis, MO) were added to each well and then incubated for 15 minutes in the dark to solubilize the crystal formed by alizarin red S staining. The plate was then agitated for approximately five minutes for complete solubilization. The solution was then transferred to a 96-well plate for the measurement of osteogenic differentiation in a plate reader (Infinite 200 PRO; Tecan, Switzerland). The results were analyzed according to a calibration curve previously performed for each cell type.

**2.7. mRNA Extraction.** RNA extraction was performed when the primary samples presented MSC characteristics such as

being undifferentiated, being in the same stage and passages that were used in the osteogenic differentiation experiments. The MSCs were induced to differentiate into osteoblasts *in vitro* and used in the experiments as described previously.

Total RNA was extracted from cells cultured *in vitro* using the RNeasy Mini Kit (QIAGEN, Hilden, Germany). This kit was developed for the extraction of total RNA from small amounts of starting material. It is a gold standard method that combines the selective binding properties of a silica gel membrane with microcentrifuge velocity.

The protocol used for the extraction technique was provided by the manufacturer.

A Bioanalyzer Kit (Agilent RNA 6000 Nano Kit) was used to evaluate RNA quality. This process allowed us to verify the integrity (RIN) and precise quantification of the samples before any application dependent on the amount of RNA was obtained.

cDNA synthesis was conducted with the SuperScript™ VILO™ cDNA Synthesis Kit (Invitrogen) following the protocol provided by the manufacturer.

**2.8. Quantitative Real-Time PCR Analysis.** By quantitative real-time PCR (qRT-PCR), we evaluated the expression levels of genes related to the expression of neural crest cell markers SOX9, SOX10, NGFR, TFAP2a, and PAX3. The analysis of the gene expression used in our study represents the relative quantification of the genes of interest using an endogenous control (normalizing gene). In this study, the genes SDHA and HPRT1 were used as endogenous controls (supplementary material 1).

For qRT-PCR, we used SYBR Green PCR Master Mix (Applied Biosystems, Warrington, UK) for the amplification and quantification of nucleic acids. Reactions were performed in triplicate with a final volume of 20  $\mu$ l for each reaction. We used 10  $\mu$ l of the real-time SYBR Green PCR Master Mix (2x), 2  $\mu$ l of the cDNA sample at a concentration of 0.2  $\mu$ g/ $\mu$ l, 2  $\mu$ l of a first sense primer, 2  $\mu$ l of a reverse primer, and 4  $\mu$ l of ultrapure water. The quantification was performed by using the Applied Biosystems 7300 Real-Time PCR System, according to the following steps: 95°C for two minutes, 40 cycles at 95°C for 15 seconds and 60°C for 30 seconds, and a subsequent dissociation step.

**2.9. Statistical Analysis.** To analyze the osteogenic differentiation between DPSC, OOMDSCs, and UC-MSC, we used a two-way ANOVA statistic test with repeated measures for a single factor (time). When multiple comparisons of means were necessary, the Bonferroni post hoc test was used. The expression of the genes to be used as normalization factors was determined, that is, genes commonly expressed in MSCs. Expression analysis was calculated from the efficiency of each probe, elevated to the Ct delta of the reference minus the Ct delta of the sample of each gene, as shown in the constitutive ( $\Delta$ Ctref) – ( $\Delta$ Ct sample) formula proposed by Pfaffl in 2001 [21].

To evaluate whether there was a difference between the groups regarding gene expression, the Kruskal-Wallis test was used. When multiple comparisons were required, the Dunn test was used. A type I ( $\alpha$ ) probability of error of 0.05

was considered in all inferential analyses. Descriptive and inferential statistical analyses were performed with SPSS software version 21 (SPSS 21.0 for Windows) with a significance level of  $\alpha = 0.05$ .

### 3. Results

We collected 10 deciduous dental pulp samples, 12 orbicularis oris muscle samples, and 25 umbilical cord samples, with MSC isolation rates of 100%, 83.3%, and 40%, respectively. The failure to achieve a 100% isolation rate was due to microbiological contamination for the orbicularis oris muscle and was due to technical problems in the establishment of the protocols described in the literature for the umbilical cord samples. We used a collagenase developed for use in GMP and we need to increase its concentration over the previously described protocols that used non-GMP collagenase [18, 22–24].

Osteogenic differentiation was performed in each of the 10 different MSC strains, but a cell pool was not performed with respect to the individuality of each MSC strain during the osteogenic differentiation process.

Samples collected from deciduous dental pulp and orbicularis oris muscle underwent enzymatic processing and expelled MSCs 15 days after cell culture (Figure 1). UC-MSCs were obtained after the validation of the MSC isolation protocol and were observed in culture between 20 and 25 days after the enzymatic digestion procedure (Figure 1).

**3.1. Characterization of MSC Strains.** All DPSC, OOMDSC, and UC-MSC primary cultures showed a very similar surface marker expression profile by flow cytometry analysis, as shown in Table 1. The expression of the markers CD29, CD31, CD34, CD45, CD73, CD90, CD105, and CD166 is plotted in the supplementary material.

All primary cultures of DPSCs ( $n = 10$ ), OOMDSCs ( $n = 10$ ), and UC-MSCs ( $n = 10$ ) were able to differentiate into osteoblasts, chondrocytes, and adipocytes (see Figure 2).

**3.2. Quantification of Bone Extracellular Matrix.** We observed osteogenic differentiation after 21 days in all 30 strains obtained; however, we observed a higher deposition of extracellular matrix in OOMDSCs and DPSCs, with a statistically significant difference compared to UC-MSCs (Figure 3). No statistically significant difference was observed when comparing DPSCs to OOMDSCs.

When we observed the initial phase of osteogenic differentiation on days 3 and 7, there was no difference in the production of extracellular matrix between the groups. On day 14, there was deposition of extracellular matrix in the OOMDSC strains compared with the UC-MSC strains that was statistically significant ( $p = 0.023$ ). However, on day 21 of osteogenic differentiation, when all undifferentiated cells were already in the osteoblast stage producing extracellular matrix, higher extracellular matrix deposition was observed in the OOMDSC and DPSC groups than in the UC-MSC group ( $p = 0.005$  and  $p = 0.007$ , respectively) (Figure 3). There was no difference between OOMDSCs and DPSCs in

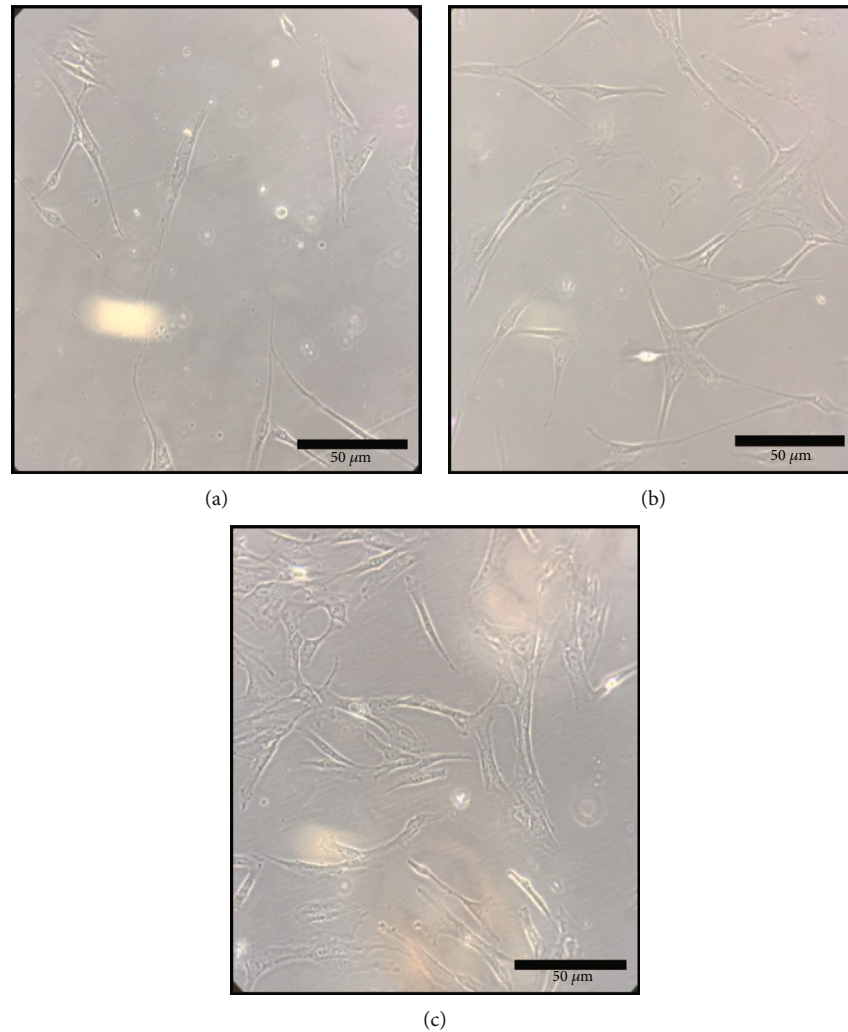


FIGURE 1: Morphology of adherent cells after isolation from corresponding tissue (sources): (a) orbicular oris muscle-derived stem cell (OOMDSC); (b) dental pulp stem cell (DPSC); (c) umbilical cord mesenchymal stem cell (UC-MSC). Similarity in the fibroblastoid morphology among the three different strains is observed.

the formation of extracellular matrix on the 21st day of cell differentiation.

**3.3. Gene Expression Evaluation for Neural Crest Cell Markers.** We observed greater expression of PAX3 in the OOMDSC strains than in the DPSC ( $p = 0.04$ ) and UC-MSC ( $p < 0.001$ ) strains. There was also a trend of increased PAX expression in DPSCs when compared to UC-MSCs ( $p = 0.05$ ) (Figure 4(d)).

The NGFR gene was expressed in all strains obtained from DPSCs, OOMDSCs, and UC-MSCs (Figure 4(e)). Significantly greater expression of this gene was observed in OOMDSCs than in DPSCs ( $p = 0.048$ ) and in UC-MSCs than in DPSCs ( $p = 0.046$ ). No statistically significant difference was observed when comparing the expression profile of the NGFR gene between OOMDSCs and UC-MSCs ( $p > 0.999$ ).

The expression of the TFAP2a, SOX10, and SOX9 genes in all MSC strains was also demonstrated, but there was no significant difference in their expression when the three distinct

strains were compared to one another ( $p = 0.654$ ,  $p = 0.761$ , and  $p = 0.124$ , respectively) (Figures 4(a)–4(c)).

## 4. Discussion

The search for new sources of MSCs as an alternative to the isolation of MSCs from BM has been increasing in the last decade, mainly as a strategy for developing regenerative medicine solutions to clinical problems. Since 2000, studies have described the isolation of stem cells from different sources, such as dental pulp, muscle, fat, and umbilical cord [13, 15, 17, 18, 25–27].

The objective of this study was to determine if there was a correlation between various sources of MSCs and their osteogenic potential. Specifically, we compared the osteogenic potential of cells of neural crest origin to MSCs isolated from the umbilical cord. Our focus on neural crest origin is particularly relevant since the neural crest is responsible for the development of bone and craniofacial connective tissue,



TABLE 1: Characterization of the profile of DPSCs, OOMDSCs, and UC-MSCs.

Cellular type	In vitro analysis		Marker		Immunophenotype	Standard deviation (+/-)
	Multipotency				Positive population (%)	
DPSC	Osteogenic	+	CD29	+	90	4.9
	Chondrogenic	+	CD31	-	0.4	0.2
	Adipogenic	+	CD34	-	0.2	0.1
			CD45	-	0.5	0.2
			CD73	+	90.1	0.9
			CD90	+	97	0.7
			CD105	+	94	2
		CD166	+	91.6	1.3	
OOMDSC	Osteogenic	+	CD29	+	96.3	1.3
	Chondrogenic	+	CD31	-	0.3	0.1
	Adipogenic	+	CD34	-	1.2	0.4
			CD45	-	0.2	0.1
			CD73	+	94	0.6
			CD90	+	97.8	1.3
			CD105	+	92.6	2.1
		CD166	+	90	5	
UC-MSC	Osteogenic	+	CD29	+	90.2	4
	Chondrogenic	+	CD31	-	0.1	0.1
	Adipogenic	+	CD34	-	0.1	0.1
			CD45	-	0.1	0.1
			CD73	+	94.1	4.8
			CD90	+	97.7	2
			CD105	+	90	1.0
		CD166	+	91.6	1.1	

and one of the leading potential clinical applications of this tissue engineering paradigm is in the treatment of patients with CLP-associated bone defects.

Considering the different potential sources of stem cells, umbilical cord and deciduous dental pulp are noteworthy because they are easy to obtain and are considered a noninvasive source. Umbilical cord tissue is discarded at birth, and during early infancy, primary teeth undergo a process of natural exfoliation for the exchange of deciduous for permanent dentition. Both sources of stem cells have great potential for the formation of other tissues, such as bone, muscle, fat, and cartilage [17, 18, 28–35]. Therefore, the cells isolated from these tissues can be cryopreserved in biological storage banks for future use. In the case of patients with CLP, these cells may be thawed for potential use to heal alveolar clefts via a bone tissue engineering approach [36, 37].

For patients with craniofacial malformations, especially CLP patients, another noninvasive source of MSCs is the orbicularis oris muscle. Small fragments of this muscle can be obtained during cheiloplasty surgery and, in fact, are often discarded during the cleft lip repair. MSCs which are capable of osteogenic differentiation can be isolated from these tissues [15].

The results of this study demonstrate that, using good manufacturing practice (GMP) protocols, it is possible to isolate MSCs from deciduous tooth pulp, orbicularis oris mus-

cle, and umbilical cord stroma to be used in clinical interventions, corroborating other studies in the literature. Our results provide further support for the practice of cryopreserving these MSCs for later use in clinical trials and approved cell therapies [38–40]. Our laboratory facilities adhere to all Brazilian laws and regulations governing the use of human tissues in research and advanced cell therapies [19, 20, 37]. Moreover, our group has previously tested genetic stability of the cells used in this study through passage 18; no chromosomal abnormalities at the 1st or at the 18th passage were observed [15, 41]. In obtaining MSCs from deciduous dental pulp, we did not encounter any issues with our GMP laboratory protocols; however, during the establishment of OOMDSC and UC-MSC strains, we had some problems with microbiological contamination and validating the protocols previously described in the literature. To decrease the microbiological contamination in the OOMDSC and UC-MSC strains, antibiotics were added to the culture medium at the time the source tissues were obtained and placed in culture. Additionally, the time between tissue collection and GMP processing to ultimately obtain the MSCs was reduced (from an average of 24 hours to an average of 16 hours). These strategies helped us obtain MSC strains free of contamination with characteristic fibroblastic morphology and adherence to plastic, as recommended by the International Society for Cellular Therapy (ISCT) [42].

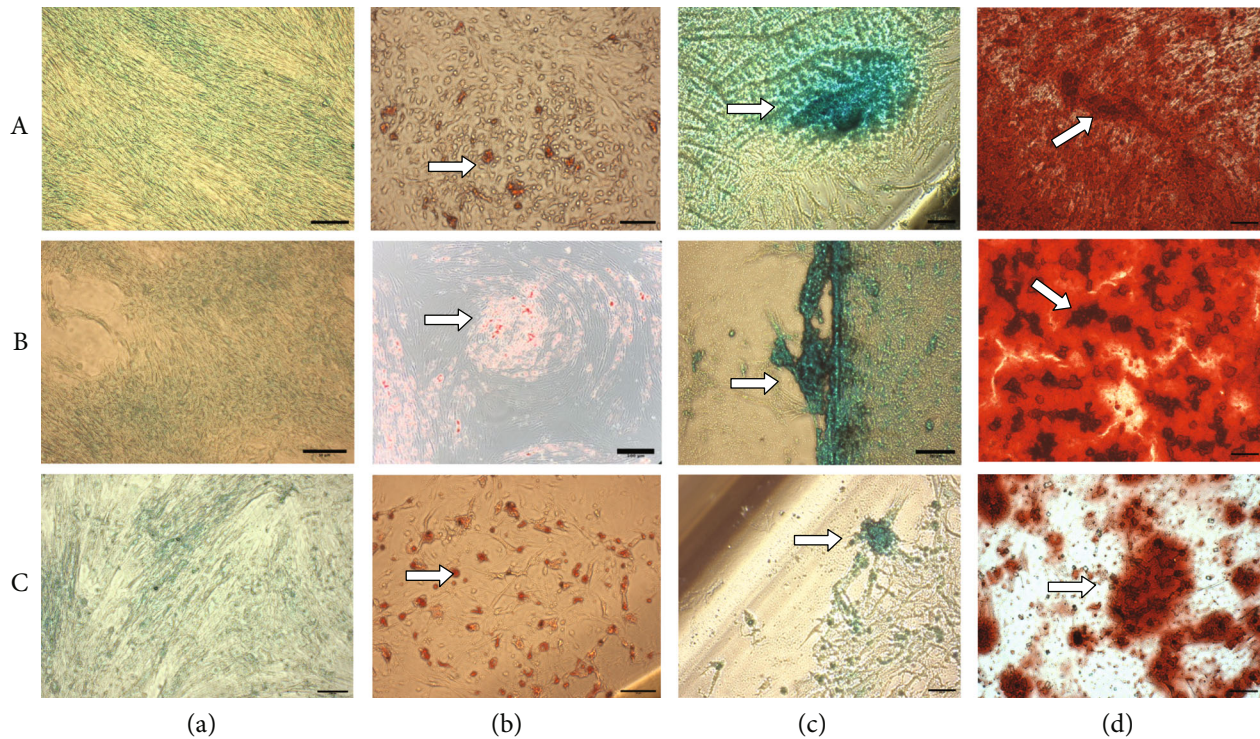


FIGURE 2: Multilineage differentiation in vitro. Row A: OOMDSC; row B: DPSC; and row C: UC-MSC. (a) The control group of undifferentiated strains. (b) Adipogenic differentiation after eighteen days of induction and staining with oil red; white arrows show the fat vesicles. (c) Chondrogenic differentiation after 3 weeks of induction, stained with alcian blue; white arrows show the extracellular matrix formation—mucopolysaccharides. (d) Osteogenic differentiation after 3 weeks of OOMDSC induction, stained with alizarin red S; white arrows show the extracellular matrix deposition.

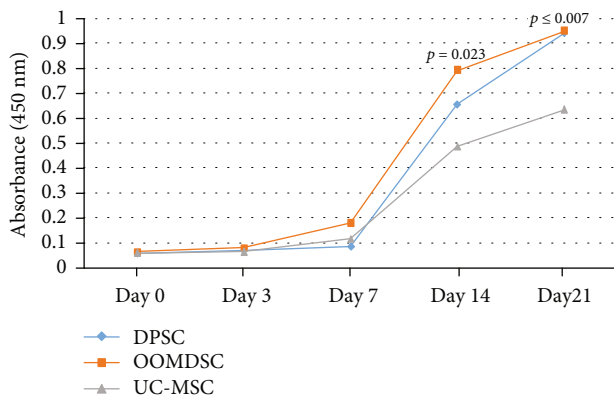


FIGURE 3: Quantitative measurement of the extracellular bone matrix stained with alizarin red S. Graphical representation of the measurement of the extracellular bone matrix deposited during osteogenic differentiation induction at 0, 3, 7, 14, and 21 days, showing the beginning of the deposition of extracellular matrix after 7 days of induction in vitro with increases on days 14 and 21.

In our study, we used bovine serum in cell culture due to our observation of a decrease in cell proliferation when a xeno-free culture medium was used (unpublished data). Alternatives such as platelet lysate or human serum might be more applicable to translational studies. Further investigation of the effects of alternative human-derived culture

products on osteogenic differentiation and gene expression is warranted.

Initially, we had some issues in the isolation of MSCs derived from the umbilical cord stroma since there are several isolation protocols available in the literature [11, 18, 22, 43]. These various protocols call for different methods to dissect and remove the arteries and veins, either by digesting only the Wharton's jelly or by simply explanting a fragment of the cord for processing. The protocol that is implemented can affect the number of cells obtained and their potential for differentiation into bone, cartilage, or fat and may alter their expression of some cell surface markers [11, 44]. Among the compartments of the cord fragment used to isolate UC-MSCs, Wharton's jelly stands out as the best option, and in this present study, Wharton's jelly digested with 2 mg/ml collagenase with 2 mM calcium chloride was used to obtain the UC-MSCs under GMP conditions. We have demonstrated the capacity of UC-MSCs to differentiate in the three mesodermal lines, which is consistent with previous reports [11, 18, 22–24].

The immunophenotypic expression profile of MSCs was determined by the analysis of a set of surface antigen markers in these cells. Research on MSCs derived from dental pulp describes the use of different flow cytometer panels to characterize these cells [45, 46]. Some studies showed the expression of surface antigens for anti-CD117, anti-STRO-1, anti-CD105, anti-CD73, and anti-CD90 antibodies but did not

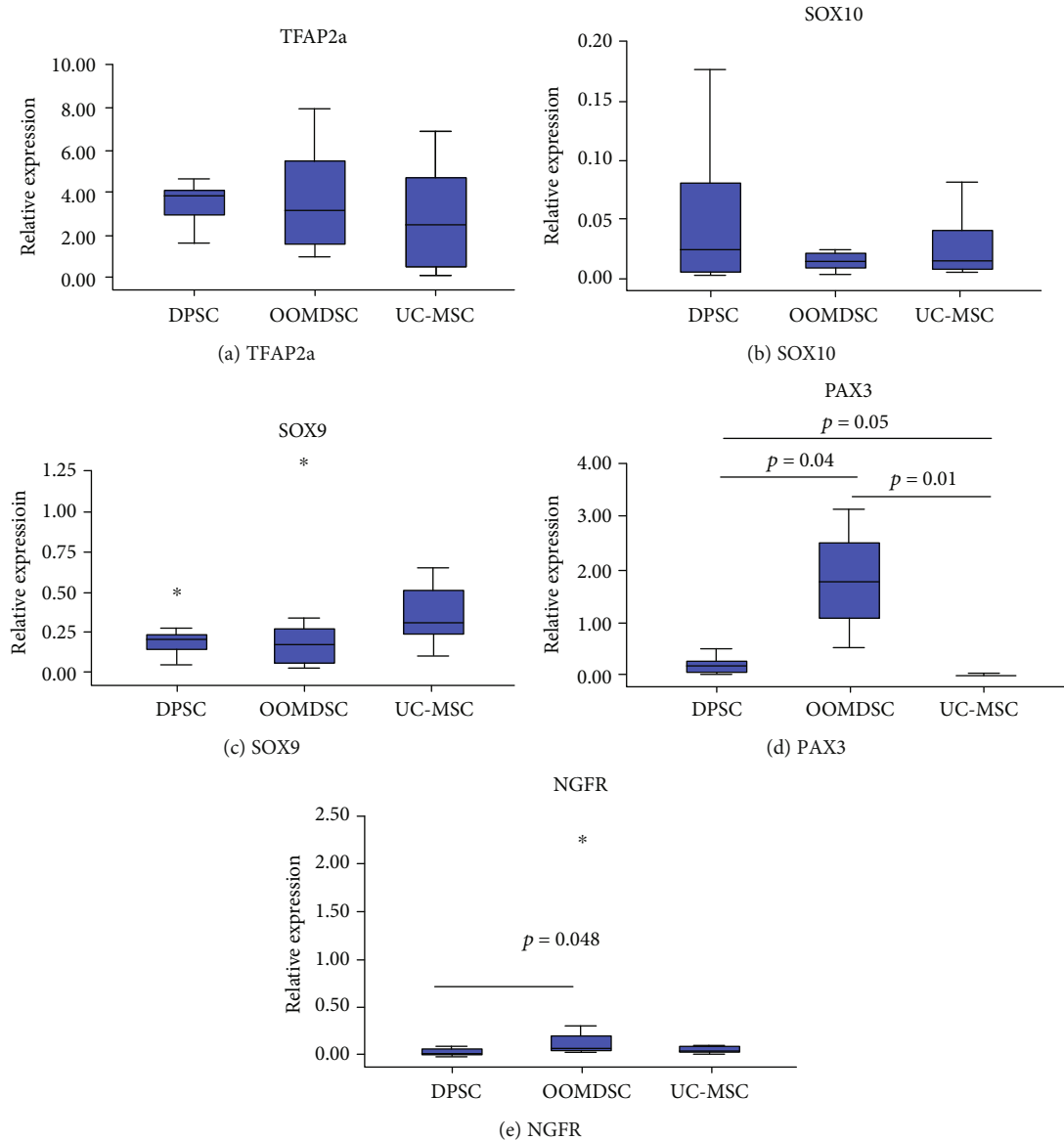


FIGURE 4: Neural crest expression in MSCs: relative expression of 5 neural crest genes in undifferentiated DPSC, OOMDSC, and UC-MSC strains. This experiment was repeated with three replicates for each sample ( $n = 10$ ). The data are presented as the mean  $\pm$  (\* represents the outlier data).

show the expression of the CD45, CD34, and CD14 hematopoietic markers and the CD31 endothelial markers [8, 47]; however, there is no consensus in the literature on which markers should be used [8, 47, 48].

After freezing and thawing, the immunophenotypic characterization of DPSCs, OOMDSCs, and UC-MSCs revealed the presence of cells expressing high levels of MSC markers such as CD105 (endoglin), CD73 (ecto-5'-nucleotidase), CD44 (HCAM), CD90 (Thy-1), CD166 (ALCAM), and CD29 and lacking the expression of CD31 (PECAM-1), CD34, and CD45. The expression of CD117 (c-kit) was low, as has also been reported in other studies with cultures of different MSCs [13, 15]. CD117 is a primitive marker and can be expressed in the first passages of SHED cultures. In this work, we performed cell characterization by flow cytometry analy-

sis at the 4th cell passage, which may be the reason for the low expression of this marker [8, 49].

One of the important biological properties in the characterization of MSCs is their ability to differentiate into at least 3 tissue types of the mesenchymal lineage. Thus, in the present study, primary cultures of all the studied groups demonstrated the capacity for osteogenic, adipogenic, and chondrogenic differentiation when exposed to the appropriate differentiation medium. All experiments used frozen and thawed cells with preserved ability to differentiate into the three different cell lines. This demonstrates that MSCs obtained from different tissues can be cryopreserved after isolation and stored until later use. Our experiments used cells up to 5 passages and stored for up to 2 years in liquid nitrogen at  $-196^{\circ}\text{C}$ . All our DPSC, OOMDSC, and

UC-MSC strains meet the criteria for MSCs according to the requirements of the ISCT [42].

Since the osteogenic potential of MSCs is affected by different factors, such as tissue origin (source) and heterogeneity of the cell population [14], the preselection of subpopulations of cells with greater osteogenic potential is a promising strategy for the complete translation of MSC-based therapies into clinical practice. In this study, we observed the osteogenic potential of DPSCs, OOMDSCs, and UC-MSCs and observed that DPSCs and OOMDSCs had better osteogenic potential than UC-MSCs. Furthermore, we observed that it is possible to isolate these MSCs under GMP conditions and that the cryopreserving and thawing of these cells had no deleterious effect on their osteogenic differentiation.

Fanganiello and colleagues investigated the expression of molecular markers that might be predictive of the osteogenic potential of MSCs, comparing populations of two different sources of MSCs (lipoaspirate and dental pulp). Their results demonstrated that SHED had an intrinsically greater osteogenic potential compared to adipose tissue-derived mesenchymal stem cells (AD-MSCs) when both cell lines were exposed to the same controlled *in vitro* induction system. The transcriptome analysis of these cells during osteogenic differentiation revealed that the upregulated IGF2 gene expression profile may be one of the best predictors of gene expression before and during the onset of osteogenic differentiation in MSCs *in vitro* [50]. In our study, we demonstrated that DPSCs have greater osteogenic potential than UC-MSCs.

Another interesting finding in our study was the similar behavior between strains obtained from DPSCs and OOMDSCs. When these strains were induced to osteogenic differentiation, a significant difference was not observed. One hypothesis for this finding would be that both tissues (sources) have the same origin from neural crest cells [16, 27]. To test this hypothesis, we analyzed the expression of genes directly linked to the neural crest cell population in the three groups of primary cells proposed in this study. TFAP2a, SOX9, and SOX10 genes were expressed by DPSCs, OOMDSCs, and UC-MSCs, but these genes were not differentially expressed between these strains to any significant degree [51–53].

In one published comparison between the osteogenic potential of DPSCs, UC-MSCs, AD-MSCs, MSCs isolated from peripheral blood, and MSCs isolated from the periodontal ligament (PDLSC), DPSCs demonstrated a greater capacity for osteogenic differentiation [54]. Our results also showed a better differentiation capacity in DPSCs than in UC-MSCs. However, in contrast to our findings, in which a significant difference in SOX9 expression was not observed in our tested cell lines, in Trivanović's study, patient DPSCs expressed higher levels of SOX9 than the other MSC lines, even when all of them differentiated into the chondrogenic lineage, where SOX9 staining is presented as a specific marker [54]. However, in cells from the umbilical cord, there was a tendency (without statistical difference) to have greater expression of SOX9, which may be a better alternative when using for chondrogenic differentia-

tion, optimizing protocols for specific use in therapies such as repair of cartilage.

In our results, the expression profile of the PAX3 gene was higher in the primary cultures of DPSCs and OOMDSCs than in the UC-MSCs, corroborating the literature and demonstrating that these lineages maintain a greater expression of PAX3 in their cell population. This observation suggests that these cell lines retain features of neural crest cells that are predisposed to a greater osteogenic differentiation potential [55, 56]. During the development of each line derived from the neural crest, several regulatory genes are involved, including PAX. The genes of the PAX family are essential transcription factors that play important roles during organogenesis and participate in important stages of this process, such as cell migration, cell proliferation, and cell differentiation [57]. PAX3 gene expression is present in immature neural crest cells and in neural cells [56]. In our study, only the PAX3 gene had a different gene expression profile among the cells obtained from the different sources, demonstrating higher expression in OOMDSCs and DPSCs than in UC-MSCs. Since neural crest cells are the origin of all facial tissues except for tooth enamel [55, 58], we suggest that PAX3 is the best marker of neural crest cells for testing samples of MSCs to identify the cell population with a greater predisposition for osteogenic differentiation. In the literature, the PAX3 gene is expressed in myogenic precursor cells at an embryonic stage of development [59]. Because we used orbicularis oris muscle fragments of the lip as a source of MSCs, isolated during cheiloplasty surgery performed in infants approximately 3–6 months of age, there was a greater possibility of finding more premature MSCs with a high expression of PAX3. In the pulp of deciduous teeth, as described in the literature, there is a heterogeneous MSC niche that expresses premature markers [8, 14]. Corroborating this fact, our results demonstrated a high expression of the PAX3 gene in DPSCs.

In the literature, NGFR gene expression in MSCs is unclear but has been shown to be involved in the survival and differentiation of neuronal cells *in vitro* and plays an important role in neuronal development [60]. These genes can be expressed in bone marrow (BM) cells but not in hematopoietic or endothelial cells [61]. The NGFR antigen has also been described on the earlier BM stromal component in the development of the embryo before the onset of BM activity and in 7 to 11% of the cells of the adherent layer of bone marrow mesenchymal stem cell (BM-MSC) cultures in the long term, suggesting that NGFR antibodies may also be present in primitive MSCs. In 2010, Quirici et al. described the presence of this marker in mesenchymal cells derived from adipose tissue, observing that the cell population that retains this marker has greater clonogenic potency and ability to differentiate into bone [62]. Our results demonstrated the expression of this gene in DPSC, OOMDSC, and UC-MSC lines. However, in our results, we observed that the expression of NGFR in OOMDSCs and UC-MSCs was higher than that of DPSCs. In some studies, CD271 (NGFR) has been described as a selective marker for the purification and characterization of MSCs isolated from BM [63, 64]; however, there is no description in the literature of the expression of

this marker in DPSCs. As a consequence, Mikami and colleagues attempted to define the expression of CD271 in DPSCs to elucidate its role in MSCs. They demonstrated that DPSCs have a CD271+/CD90+/CD44+/CD45- expression profile in 2.4% of the cell population. Consistent with our results, this marker was weakly expressed in the DPSC population. The multilineage differentiation potential (osteogenic, adipogenic, chondrogenic, and myogenic) of CD271+/DPSC was compared to that of the CD271-/DPSC population. The results demonstrated the inhibition of the osteogenic capacity of the CD271+/SHED population when compared to the CD271-/DPSC culture, demonstrating lower levels of calcium and alkaline phosphatase. Therefore, DPSCs expressing lower levels of NGFR (CD271-) have superior osteogenic differentiation potential, and over time, the expression of NGFR decreases in CD271+/DPSCs (Mikami et al. [65]). Our findings corroborate the results obtained by Mikami et al. in 2011, suggesting that DPSCs express low levels of the NGFR gene and have a great osteogenic differentiation potential. On the other hand, OOMDSCs were also shown to have a high potential for osteogenic differentiation, and, conversely, it was the cell line that expressed high levels of the NGFR gene [65]. Studies in the literature define the marker CD271 (NGFR) as a potentially specific cell surface marker for a precursor subpopulation of MSCs [63]. However, no study has thus far demonstrated the actual correlation of this marker with proliferative cell potential and *in vitro* and *in vivo* differentiation capabilities. The fact that OOMDSCs exhibit a higher expression profile of the NGFR gene and demonstrate the same osteogenic potential of DPSCs suggests a specific role for this gene in the process of osteogenic differentiation. Furthermore, there are reports in the literature that demonstrate that the greatest potential for osteogenic differentiation of MSCs from different sources is associated with the expression of neural crest genes in the undifferentiated mesenchymal cell populations [51, 65].

According to our findings and relevant published data, we suggest that the NGFR marker may not be a good predictive marker for selecting the best source of MSCs for use in bone tissue engineering. However, we propose that the PAX3 gene may be a potential marker that predicts the osteogenic potential of MSCs obtained from different sources. In our study, higher expression levels of this gene were observed in MSCs that demonstrated greater osteogenic potential. We therefore conclude that DPSCs and OOMDSCs, in part, as indicated by their PAX3 expression, are the best sources of MSCs to be used in bone tissue engineering for CLP patients. These cells can be isolated and cryopreserved under GMP conditions for use in regenerative medicine and therefore represent a very viable substrate for use in translational studies.

## 5. Conclusions

The best sources to obtain MSCs for bone tissue engineering for CLP patients are dental pulp and orbicular oris muscles. MSCs obtained from these tissues have better osteogenic potential than those obtained from umbilical cord. High expression of the PAX3 gene can be a good marker in pre-

dicting which tissues would provide the most ideal MSC strains for use in bone tissue engineering. Our results suggest that the superior osteogenic potential observed in DPSCs and OOMDSCs is due to their neural crest cell origins. Based on these observations, further study of the clinical applicability of MSCs isolated from noninvasive sources, such as DPSCs and OOMDSCs, in innovative translational bone tissue engineering protocols to repair alveolar bone grafts in CLP patients is called for.

## Data Availability

The datasets used during the current study are available from the corresponding author upon reasonable request.

## Ethical Approval

This project was approved by Plataforma Brasil (number: CAAE: 39830214.7.0000.5461) (available in: <http://plataforma.brasil.saude.gov.br/login.jsf>) and by the ethics committee of Hospital Sírio-Libanês/Sociedade Beneficente de Senhoras (number: 5461).

## Consent

Informed consent was obtained from the legal guardians of the donors who donated tissues to the study.

## Conflicts of Interest

The authors declare that they have no competing interests.

## Authors' Contributions

For this research article, the authors contributed as follows: study conceptualization was done by Pinheiro CCG, Jarrahy R, and Bueno DF; methodology by Pinheiro CCG and Bueno DF; formal analysis by Pinheiro CCG; investigation by Pinheiro CCG; resources by Pinheiro CCG, Leyendecker Junior A, and Ferreira JR; collection of samples by Tanikawa DY and Bueno DF; writing and original draft preparation by Pinheiro CCG; writing and review and editing by Bueno DF and Jarrahy R; visualization by Bueno DF; and funding acquisition and supervision by Bueno DF.

## Acknowledgments

This research was supported by the Brazilian Ministry of Health by PROADI-SUS. We thank Hospital Sírio-Libanês for providing physical structure (laboratories) and equipment. We thank Sociedade Beneficente de Senhoras do Hospital Sírio-Libanês and Instituto de Responsabilidade Social Sírio-Libanês through Hospital Municipal Infantil Menino Jesus for providing multidisciplinary cleft lip and palate patient care in São Paulo, Brazil, with endless encouragement for the development of new strategies that could improve patient quality of life and reduce morbidity for their surgeries. We thank the nurses from the Umbilical Cord Blood Bank of the Hospital Sírio-Libanês who helped us in the collection of the cord fragments at Maternidade Amparo

Maternal. We thank all the patients and parents for tissue fragment donation for the establishment of MSC strains and for believing in our research group to advance the development of science.

## Supplementary Materials

Supplementary material 1: all gene sequences used in the neural crest gene profile. Supplementary material 2: the R1, R2, and R3 regions were a population of mesenchymal stem cells: R1: OOMDSC, R2: UC-MSC, and R3: DPSC. The histograms represent the profile markers in the population selected: black line: OOMDSC; green line: UC-MSC; and pink line: DPSC. All strains presented the same profile marker: positive reaction to CD29, CD73, CD90, CD105, and CD166 and negative reaction to CD31, CD34, and CD4. (*Supplementary Materials*)

## References

- [1] M. Gimbel, R. K. Ashley, M. Sisodia et al., "Repair of alveolar cleft defects: reduced morbidity with bone marrow stem cells in a resorbable matrix," *The Journal of Craniofacial Surgery*, vol. 18, no. 4, pp. 895–901, 2007.
- [2] R. Langer and J. Vacanti, "Tissue engineering," *Science*, vol. 260, no. 5110, pp. 920–926, 1993.
- [3] R. M. Shanti, W.-J. Li, L. J. Nesti, X. Wang, and R. S. Tuan, "Adult mesenchymal stem cells: biological properties, characteristics, and applications in maxillofacial surgery," *Journal of Oral and Maxillofacial Surgery*, vol. 65, no. 8, pp. 1640–1647, 2007.
- [4] A.-M. Yousefi, P. F. James, R. Akbarzadeh, A. Subramanian, C. Flavin, and H. Oudadesse, "Prospect of stem cells in bone tissue engineering: a review," *Stem Cells International*, vol. 2016, Article ID 6180487, 13 pages, 2016.
- [5] N. Alonso, D. Y. S. Tanikawa, R. da Silva Freitas, L. Canan, T. O. Ozawa, and D. L. Rocha, "Evaluation of maxillary alveolar reconstruction using a resorbable collagen sponge with recombinant human bone morphogenetic protein-2 in cleft lip and palate patients," *Tissue Engineering Part C: Methods*, vol. 16, no. 5, pp. 1183–1189, 2010.
- [6] L. W. Canan, F. R. da Silva, N. Alonso, D. Y. S. Tanikawa, D. L. Rocha, and J. C. U. Coelho, "Human bone morphogenetic protein-2 use for maxillary reconstruction in cleft lip and palate patients," *Journal of Craniofacial Surgery*, vol. 23, no. 6, pp. 1627–1633, 2012.
- [7] R. Dimitriou, E. Jones, D. McGonagle, and P. V. Giannoudis, "Bone regeneration: current concepts and future directions," *BMC Medicine*, vol. 9, no. 1, article 66, 2011.
- [8] M. Miura, S. Gronthos, M. Zhao et al., "SHED: stem cells from human exfoliated deciduous teeth," *Proceedings of the National Academy of Sciences of the United States of America*, vol. 100, no. 10, pp. 5807–5812, 2003.
- [9] J.-Y. Chen, X.-Z. Mou, X.-C. Du, and C. Xiang, "Comparative analysis of biological characteristics of adult mesenchymal stem cells with different tissue origins," *Asian Pacific Journal of Tropical Medicine*, vol. 8, no. 9, pp. 739–746, 2015.
- [10] H. He, T. Nagamura-Inoue, H. Tsunoda et al., "Stage-specific embryonic antigen 4 in Wharton's jelly-derived mesenchymal stem cells is not a marker for proliferation and multipotency," *Tissue Engineering Part A*, vol. 20, no. 7–8, pp. 1314–1324, 2014.
- [11] A. Subramanian, C.-Y. Fong, A. Biswas, and A. Bongso, "Comparative characterization of cells from the various compartments of the human umbilical cord shows that the Wharton's jelly compartment provides the best source of clinically utilizable mesenchymal stem cells," *PLoS One*, vol. 10, no. 6, article e0127992, 2015.
- [12] R. Carlin, D. Davis, M. Weiss, B. Schultz, and D. Troyer, "Expression of early transcription factors Oct-4, Sox-2 and Nanog by porcine umbilical cord (PUC) matrix cells," *Reproductive Biology and Endocrinology*, vol. 4, no. 1, p. 8, 2006.
- [13] I. Kerkis, A. Kerkis, D. Dozortsev et al., "Isolation and characterization of a population of immature dental pulp stem cells expressing OCT-4 and other embryonic stem cell markers," *Cells, Tissues Organs*, vol. 184, no. 3–4, pp. 105–116, 2006.
- [14] I. Kerkis and A. I. Caplan, "Stem cells in dental pulp of deciduous teeth," *Tissue Engineering Part B: Reviews*, vol. 18, no. 2, pp. 129–138, 2012.
- [15] D. F. Bueno, I. Kerkis, A. M. Costa et al., "New source of muscle-derived stem cells with potential for alveolar bone reconstruction in cleft lip and/or palate patients," *Tissue Engineering Part A*, vol. 15, no. 2, pp. 427–435, 2009.
- [16] D. R. Cordero, S. Brugmann, Y. Chu, R. Bajpai, M. Jame, and J. A. Helms, "Cranial neural crest cells on the move: their roles in craniofacial development," *American Journal of Medical Genetics Part A*, vol. 155, no. 2, pp. 270–279, 2012.
- [17] C. A. de Mendonca, D. F. Bueno, M. T. Martins et al., "Reconstruction of large cranial defects in nonimmunosuppressed experimental design with human dental pulp stem cells," *The Journal of Craniofacial Surgery*, vol. 19, no. 1, pp. 204–210, 2008.
- [18] E. Zucconi, N. M. Vieira, C. R. Bueno Jr. et al., "Preclinical studies with umbilical cord mesenchymal stromal cells in different animal models for muscular dystrophy," *Journal of Biomedicine & Biotechnology*, vol. 2011, Article ID 715251, 9 pages, 2011.
- [19] G. Q. Daley, I. Hyun, J. F. Apperley et al., "Setting global standards for stem cell research and clinical translation: the 2016 ISSCR guidelines," *Stem Cell Reports*, vol. 6, no. 6, pp. 787–797, 2016.
- [20] M. Codinach, M. Blanco, I. Ortega et al., "Design and validation of a consistent and reproducible manufacture process for the production of clinical-grade bone marrow-derived multipotent mesenchymal stromal cells," *Cytotherapy*, vol. 18, no. 9, pp. 1197–1208, 2016.
- [21] M. W. Pfaffl, "A new mathematical model for relative quantification in real-time RT-PCR," *Nucleic Acids Research*, vol. 29, no. 9, article e45, 2001.
- [22] K. Baba, Y. Yamazaki, M. Ishiguro et al., "Osteogenic potential of human umbilical cord-derived mesenchymal stromal cells cultured with umbilical cord blood-derived fibrin: a preliminary study," *Journal of Cranio-Maxillofacial Surgery*, vol. 41, no. 8, pp. 775–782, 2013.
- [23] R. El Omar, J. Beroud, J.-F. Stoltz, P. Menu, E. Velot, and V. Decot, "Umbilical cord mesenchymal stem cells: the new gold standard for mesenchymal stem cell-based therapies?," *Tissue Engineering Part B: Reviews*, vol. 20, no. 5, pp. 523–544, 2014.
- [24] D.-C. Ding, Y.-H. Chang, W.-C. Shyu, and S.-Z. Lin, "Human umbilical cord mesenchymal stem cells: a new era for stem cell

- therapy," *Cell Transplantation*, vol. 24, no. 3, pp. 339–347, 2015.
- [25] P. A. Zuk, M. Zhu, P. Ashjian et al., "Human adipose tissue is a source of multipotent stem cells," *Molecular Biology of the Cell*, vol. 13, no. 12, pp. 4279–4295, 2002.
- [26] M. L. da Silva and P. C. N. N. Chagastelles, "Mesenchymal stem cells reside in virtually all post-natal organs and tissues," *Journal of Cell Science*, vol. 119, no. 11, pp. 2204–2213, 2006.
- [27] J. J. Mao and D. J. Prockop, "Stem cells in the face: tooth regeneration and beyond," *Cell Stem Cell*, vol. 11, no. 3, pp. 291–301, 2012.
- [28] R. Kabir, M. Gupta, A. Aggarwal, D. Sharma, A. Sarin, and M. Z. Kola, "Imperative role of dental pulp stem cells in regenerative therapies: a systematic review," *Nigerian Journal of Surgery*, vol. 20, no. 1, pp. 1–8, 2014.
- [29] T. L. Fernandes, K. Shimomura, A. Asperti et al., "Development of a novel large animal model to evaluate human dental pulp stem cells for articular cartilage treatment," *Stem Cell Reviews*, vol. 14, no. 5, pp. 734–743, 2018.
- [30] A. Leyendecker, C. C. G. Pinheiro, M. T. Amano, and D. F. Bueno, "The use of human mesenchymal stem cells as therapeutic agents for the *in vivo* treatment of immune-related diseases: a systematic review," *Frontiers in Immunology*, vol. 9, article 2056, 2018.
- [31] G. Bonaventura, S. Chamayou, A. Liprino et al., "Different tissue-derived stem cells: a comparison of neural differentiation capability," *PLoS One*, vol. 10, no. 10, article e0140790, 2015.
- [32] J. Hendriks, J. Riesle, and C. A. Blitterswijkvan, "Co-culture in cartilage tissue engineering," *Journal of Tissue Engineering and Regenerative Medicine*, vol. 4, no. 7, pp. 524–531, 2010.
- [33] Y.-B. Park, C.-W. Ha, C.-H. Lee, Y. C. Yoon, and Y.-G. Park, "Cartilage regeneration in osteoarthritic patients by a composite of allogeneic umbilical cord blood-derived mesenchymal stem cells and hyaluronate hydrogel: results from a clinical trial for safety and proof-of-concept with 7 years of extended follow-up," *Stem Cells Translational Medicine*, vol. 6, no. 2, pp. 613–621, 2017.
- [34] E. MacHado, M. H. Fernandes, and P. De Sousa Gomes, "Dental stem cells for craniofacial tissue engineering," *Oral Surgery, Oral Medicine, Oral Pathology and Oral Radiology*, vol. 113, no. 6, pp. 728–733, 2012.
- [35] C. Akyurekli, Y. Le, R. B. Richardson, D. Fergusson, J. Tay, and D. S. Allan, "A systematic review of preclinical studies on the therapeutic potential of mesenchymal stromal cell-derived microvesicles," *Stem Cell Reviews and Reports*, vol. 11, no. 1, pp. 150–160, 2015.
- [36] S.-Y. Lee, P.-C. Chiang, Y.-H. Tsai et al., "Effects of cryopreservation of intact teeth on the isolated dental pulp stem cells," *Journal of Endodontia*, vol. 36, no. 8, pp. 1336–1340, 2010.
- [37] P.-Y. Collart-Dutilleul, F. Chaubron, J. De Vos, and F. J. Cuisinier, "Allogenic banking of dental pulp stem cells for innovative therapeutics," *World Journal of Stem Cells*, vol. 7, no. 7, pp. 1010–1021, 2015.
- [38] M. W. Lee, I. K. Jang, K. H. Yoo, K. W. Sung, and H. H. Koo, "Stem and progenitor cells in human umbilical cord blood," *International Journal of Hematology*, vol. 92, no. 1, pp. 45–51, 2010.
- [39] M. Secco, E. Zucconi, N. M. Vieira et al., "Mesenchymal stem cells from umbilical cord: do not discard the cord!," *Neuromuscular Disorders*, vol. 18, no. 1, pp. 17–18, 2008.
- [40] N. Tsagias, K.-K. Koliakos, T. Spyridopoulos et al., "A simple method for the quantitation of the stem cells derived from human exfoliated deciduous teeth using a luminescent cell viability assay," *Cell and Tissue Banking*, vol. 15, no. 3, pp. 491–499, 2013.
- [41] T. Jazedje, P. M. Perin, C. E. Czeresnia et al., "Human fallopian tube: a new source of multipotent adult mesenchymal stem cells discarded in surgical procedures," *Journal of Translational Medicine*, vol. 7, no. 1, p. 46, 2009.
- [42] M. Dominici, K. Le Blanc, I. Mueller et al., "Minimal criteria for defining multipotent mesenchymal stromal cells. The International Society for Cellular Therapy position statement," *Cytotherapy*, vol. 8, no. 4, pp. 315–317, 2006.
- [43] D.-W. Kim, M. Staples, K. Shinozuka, P. Pantcheva, S.-D. Kang, and C. Borlongan, "Wharton's jelly-derived mesenchymal stem cells: phenotypic characterization and optimizing their therapeutic potential for clinical applications," *International Journal of Molecular Sciences*, vol. 14, no. 6, pp. 11692–11712, 2013.
- [44] A. Can and S. Karahuseyinoglu, "Concise review: human umbilical cord stroma with regard to the source of fetus-derived stem cells," *Stem Cells*, vol. 25, no. 11, pp. 2886–2895, 2007.
- [45] Y. Isobe, N. Koyama, K. Nakao et al., "Comparison of human mesenchymal stem cells derived from bone marrow, synovial fluid, adult dental pulp, and exfoliated deciduous tooth pulp," *International Journal of Oral and Maxillofacial Surgery*, vol. 45, no. 1, pp. 124–131, 2016.
- [46] C. C. G. Pinheiro, M. C. de Pinho, A. C. Aranha, E. Fregnani, and D. F. Bueno, "Low power laser therapy: a strategy to promote the osteogenic differentiation of deciduous dental pulp stem cells from cleft lip and palate patients," *Tissue Engineering Part A*, vol. 24, no. 7–8, pp. 569–575, 2018.
- [47] S. Gronthos, M. Mankani, J. Brahim, P. G. Robey, and S. Shi, "Postnatal human dental pulp stem cells (DPSCs) *in vitro* and *in vivo*," *Proceedings of the National Academy of Sciences of the United States of America*, vol. 97, no. 25, pp. 13625–13630, 2000.
- [48] S.-H. Park, W. Y. Sim, B.-H. Min, S. S. Yang, A. Khademhosseini, and D. L. Kaplan, "Chip-based comparison of the osteogenesis of human bone marrow- and adipose tissue-derived mesenchymal stem cells under mechanical stimulation," *PLoS One*, vol. 7, no. 9, article e46689, 2012.
- [49] S. Nakamura, Y. Yamada, W. Katagiri, T. Sugito, K. Ito, and M. Ueda, "Stem cell proliferation pathways comparison between human exfoliated deciduous teeth and dental pulp stem cells by gene expression profile from promising dental pulp," *Journal of Endodontia*, vol. 35, no. 11, pp. 1536–1542, 2009.
- [50] R. D. Fanganiello, F. A. A. Ishiy, G. S. Kobayashi, L. Alvizi, D. Y. Sunaga, and M. R. Passos-Bueno, "Increased *in vitro* osteopotential in SHED associated with higher *IGF2* expression when compared with hASCs," *Stem Cell Reviews and Reports*, vol. 11, no. 4, pp. 635–644, 2015.
- [51] W.-D. Wang, D. B. Melville, M. Montero-Balaguer, A. K. Hatzopoulos, and E. W. Knapik, "Tfap2a and Foxd3 regulate early steps in the development of the neural crest progenitor population," *Developmental Biology*, vol. 360, no. 1, pp. 173–185, 2011.
- [52] G. Friedl, H. Schmidt, I. Rehak, G. Kostner, K. Schauenstein, and R. Windhager, "Undifferentiated human mesenchymal stem cells (hMSCs) are highly sensitive to mechanical strain: transcriptionally controlled early osteo-chondrogenic

- response *in vitro*,” *Osteoarthritis and Cartilage*, vol. 15, no. 11, pp. 1293–1300, 2007.
- [53] M. Wahlbuhl, S. Reiprich, M. R. Vogl, M. R. Bösl, and M. Wegner, “Transcription factor Sox10 orchestrates activity of a neural crest-specific enhancer in the vicinity of its gene,” *Nucleic Acids Research*, vol. 40, no. 1, pp. 88–101, 2012.
- [54] D. Trivanović, A. Jauković, B. Popović et al., “Mesenchymal stem cells of different origin: comparative evaluation of proliferative capacity, telomere length and pluripotency marker expression,” *Life Sciences*, vol. 141, pp. 61–73, 2015.
- [55] B. Péault, M. Rudnicki, Y. Torrente et al., “Stem and progenitor cells in skeletal muscle development, maintenance, and therapy,” vol. 15, no. 5, pp. 867–877, 2007.
- [56] A. H. Monsoro-Burq, “PAX transcription factors in neural crest development,” *Seminars in Cell & Developmental Biology*, vol. 44, pp. 87–96, 2015.
- [57] J.-L. Plouhinec, D. D. Roche, C. Pegoraro et al., “Pax3 and Zic1 trigger the early neural crest gene regulatory network by the direct activation of multiple key neural crest specifiers,” *Developmental Biology*, vol. 386, no. 2, pp. 461–472, 2014.
- [58] V. Mayo, Y. Sawatari, C. Y. C. Huang, and F. Garcia-Godoy, “Neural crest-derived dental stem cells—where we are and where we are going,” *Journal of Dentistry*, vol. 42, no. 9, pp. 1043–1051, 2014.
- [59] T. Endo, “Molecular mechanisms of skeletal muscle development, regeneration, and osteogenic conversion,” *Bone*, vol. 80, pp. 2–13, 2015.
- [60] T. M. Thomson, W. J. Rettig, P. G. Chesa, S. H. Green, A. C. Mena, and L. J. Old, “Expression of human nerve growth factor receptor on cells derived from all three germ layers,” *Experimental Cell Research*, vol. 174, no. 2, pp. 533–539, 1988.
- [61] N. Quirici, D. Soligo, P. Bossolasco, F. Servida, C. Lumini, and G. L. Delilieri, “Isolation of bone marrow mesenchymal stem cells by anti-nerve growth factor receptor antibodies,” *Experimental Hematology*, vol. 30, no. 7, pp. 783–791, 2002.
- [62] N. Quirici, C. Scavullo, L. de Girolamo et al., “Anti-L-NGFR and -CD34 monoclonal antibodies identify multipotent mesenchymal stem cells in human adipose tissue,” *Stem Cells and Development*, vol. 19, no. 6, pp. 915–925, 2010.
- [63] S. Kuçi, Z. Kuçi, H. Kreyenberg et al., “CD271 antigen defines a subset of multipotent stromal cells with immunosuppressive and lymphohematopoietic engraftment-promoting properties,” *Haematologica*, vol. 95, no. 4, pp. 651–659, 2010.
- [64] A. Attar, A. G. Langeroudi, A. Vassagih, I. Ahrari, M. K. Maharlooei, and A. Monabati, “Role of CD271 enrichment in the isolation of mesenchymal stromal cells from umbilical cord blood,” *Cell Biology International*, vol. 37, no. 9, pp. 1010–1015, 2013.
- [65] Y. Mikami, Y. Ishii, N. Watanabe et al., “CD271/p75<sup>NTR</sup> inhibits the differentiation of mesenchymal stem cells into osteogenic, adipogenic, chondrogenic, and myogenic lineages,” *Stem Cells and Development*, vol. 20, no. 5, pp. 901–913, 2011.



## Review Article

# Dental Follicle Cells: Roles in Development and Beyond

Tao Zhou <sup>1</sup>, Jinhai Pan,<sup>2</sup> Peiyao Wu,<sup>1</sup> Ruijie Huang,<sup>2</sup> Wei Du <sup>3</sup>, Yachuan Zhou <sup>3</sup>,  
Mian Wan,<sup>3</sup> Yi Fan,<sup>3</sup> Xin Xu <sup>3</sup>, Xuedong Zhou <sup>3</sup>, Liwei Zheng <sup>2</sup>, and Xin Zhou <sup>2</sup>

<sup>1</sup>West China School of Stomatology, Sichuan University, Chengdu, Sichuan 610041, China

<sup>2</sup>State Key Laboratory of Oral Diseases, National Clinical Research Center for Oral Diseases, Department of Pediatric Dentistry, West China Hospital of Stomatology, Sichuan University, Chengdu, Sichuan 610041, China

<sup>3</sup>State Key Laboratory of Oral Diseases, National Clinical Research Center for Oral Diseases, Department of Operative Dentistry and Endodontics, West China Hospital of Stomatology, Sichuan University, Chengdu, Sichuan 610041, China

Correspondence should be addressed to Liwei Zheng; [liweizheng@scu.edu.cn](mailto:liweizheng@scu.edu.cn) and Xin Zhou; [xin.zhou@scu.edu.cn](mailto:xin.zhou@scu.edu.cn)

Received 1 June 2019; Accepted 16 August 2019; Published 15 September 2019

Guest Editor: Toru Ogasawara

Copyright © 2019 Tao Zhou et al. This is an open access article distributed under the Creative Commons Attribution License, which permits unrestricted use, distribution, and reproduction in any medium, provided the original work is properly cited.

Dental follicle cells (DFCs) are a group of mesenchymal progenitor cells surrounding the tooth germ, responsible for cementum, periodontal ligament, and alveolar bone formation in tooth development. Cascades of signaling pathways and transcriptional factors in DFCs are involved in directing tooth eruption and tooth root morphogenesis. Substantial researches have been made to decipher multiple aspects of DFCs, including multilineage differentiation, senescence, and immunomodulatory ability. DFCs were proved to be multipotent progenitors with decent amplification, immunosuppressed and acquisition ability. They are able to differentiate into osteoblasts/cementoblasts, adipocytes, neuron-like cells, and so forth. The excellent properties of DFCs facilitated clinical application, as exemplified by bone tissue engineering, tooth root regeneration, and periodontium regeneration. Except for the oral and maxillofacial regeneration, DFCs were also expected to be applied in other tissues such as spinal cord defects (SCD), cardiomyocyte destruction. This article reviewed roles of DFCs in tooth development, their properties, and clinical application potentials, thus providing a novel guidance for tissue engineering.

## 1. Introduction

The dental follicle (DF), a loose ectomesenchymally derived connective tissue surrounding the tooth germ, participates in tooth eruption and contributes extensively to the periodontium by producing osteoblasts, cementoblasts, and periodontal ligament cells (PDLs) in tooth development. In 2002, dental follicle cells (DFCs) were firstly isolated from the molar region of mice and induced to differentiate toward an osteoblast phenotype *in vitro* with exogenous bone morphogenetic protein 2 (BMP2) [1]. Since then, DFCs were successively reported to differentiate into osteoblasts, cementoblasts, adipocytes, chondrocytes, and neuron-like cells with appropriate induction conditions [2, 3]. These researches suggested the existence of heterogeneous cells in DF; some of which possess two main characteristics of stem cells: multipotent

differentiation and self-renewal. Compared with other dental-derived stem cells like dental pulp stem cells (DPSCs), periodontal ligament stem cells (PDLSCs), stem cells from exfoliated deciduous teeth (SHEDs), stem cells from apical papilla (SCAPs), etc., DFCs exhibited robust proliferative capacity, superior pluripotency, and high immunosuppressed effect which favored tissue engineering (see Table 1). Additionally, the ease and high efficiency of isolation and unrelated ethical issues in clinical contributed to a great feasibility for the application of DFC-based therapy. In this article, we reviewed amounts of recent researches about DFCs focusing on their roles in tooth development, characteristics of multipotent differentiation, and immunosuppressed and excellent proliferation properties, as well as the clinical application advances based on these characteristics; therefore, obtaining a comprehensive recognition of DFCs and providing

TABLE 1: Comparison of tooth development-related mesenchymal stem cells/progenitor cells.

Proliferation capacity	Cell surface markers	Negative	Multipotent differentiation in vivo/in vitro	Immunomodulatory properties	Potential clinical application	References
	Cell surface markers Positive					
DFCs	CD9 CD10 CD13 CD29 CD44 CD53 CD56 CD59 CD73 CD90 CD105 CD106 CD146 CD166 CD271 STRO-1 NOTCH-1 HLA-ABC, NANOG SOX2 OCT4, nestin, and beta-III-tubulin	CD31 CD34 CD45 CD133	Alveolar bone, PDL, cementum, adipocyte, osteoblast, cementoblast/chondrocyte, neuron-like cell, cardiomyocyte, and dentin-like tissues	Immunosuppressive properties expressing TLR2, TLR3, and TLR4; increased IL-10, IL-6, TGF- $\beta$ , and IDO-1; decreased IFN- $\gamma$ , IL-4, and IL-8; suppressed proliferation of PBMCs; decreased number of CD4 <sup>+</sup> T cells and increased regulatory T cells	Bone defects, tooth root regeneration, periodontal tissue regeneration, and neural tissue regeneration	[11–16]
DPSCs	CD9 CD10 CD13 CD29 CD44 CD59 CD73 CD90 CD105 CD146 CD106 CD146 CD166 CD271 STRO-1, TRA1-60, and NANOG SOX2 Oct-4 TRA-1-80-1	CD14 CD19 CD24 CD117 CD34 CD45 CD31 CD133	Adipocyte, dentin-pulp, bone muscle/odontoblast, myoblast adipocyte, osteoblast, neuron-like cell, cardiomyocyte, and hepatocyte-like cell	Immunosuppressive properties increased HGF, TGF- $\beta$ , PGE-2, IL-6, IDO, and IL-10; decreased IL-4 and IFN- $\gamma$ ; increased number of regulatory T cells; suppressed proliferation of T cells and PBMCs; inducing activated T cells apoptosis	Bone defects, dentin-pulp repair, and neural tissue regeneration	[11, 15, 17–21]
PDLCs	CD9 CD10 CD13 CD29 CD44 CD59 CD73 CD90 CD105 CD106 CD146 CD166 CD271 STRO-1	CD11b CD14 CD19 CD34 CD45 CD79 $\alpha$ HLA-DR	Cementum, PDL/chondrocyte, osteoblast, cementoblast, and adipocyte neuron-like cell	Immunosuppressive properties expressing TLR2 and TLR4; released IDO, HGF, and TGF- $\beta$ ; suppressed proliferation of PBMCs and reduced induction of Tregs	Tooth root regeneration and periodontal tissue regeneration	[14, 15, 18, 21–24]
ABMSCs	CD13 CD29 CD44 CD71 CD73 CD90 CD105 CD146 CD166 STRO-1, OCT4 NANOG SOX2, and nestin	CD11b CD14 CD19 CD34 CD45 CD31	Bone/osteoblast, chondrocyte, and adipocyte	Expressing TLR2, 4, 5, 7, 1, 10, 8, 3, and 6	Bone defect and periodontal regeneration	[15, 25–29]
SHEDs	CD29 CD73 CD90 CD105 CD146 CD166 STRO-1, NANOG, and nestin	CD14 CD34 CD45	Bone dentin-pulp, microvessels/chondrocyte, myocytes, adipocytes, osteoblasts, and neuron-like cell	Immunosuppressive properties inhibited Th17 cell differentiation; increased number of Tregs; corrected CD4 <sup>+</sup> T cell immune imbalance in allergic diseases; increased IL-10 and decreased IL-4 and IFN- $\gamma$	Craniofacial bone defects, dentin-pulp repair, Neural regeneration, and tooth root regeneration	[11, 30–37]
SCAPs	CD13 CD29 CD49 CD51 CD56 CD61 CD73 CD146 CD90 CD44 CD24 CD106 CD146 CD166 STRO-1, NANOG, and nestin	CD14 CD18 CD34 CD45	Dentin-pulp/osteoblast, adipocyte, odontoblasts, hepatocytes, and neuron-like cell	Low immunogenicity inhibited proliferation of T cells; overexpressed Nfic to suppress LPS-initiated innate immune responses	Bone regeneration, tooth root regeneration, dentin-pulp repair, neural regeneration and	[30, 31, 38–41]

TABLE 1: Continued.

Proliferation capacity	Cell surface markers Positive	Negative	Multipotent differentiation in vivo/in vitro	Immunomodulatory properties	Potential clinical application	References
		CD117 CD150			repair, and periodontal regeneration	
GMSCs	CD29 CD44 CD73 CD90 CD105 CD106 CD166 STRO-1, NANOG, and nestin	CD14 CD117 CD34 CD45	Cartilage, bone, muscle/adipocyte, chondrocyte, osteocyte, and neuron-like cell	Immunosuppressive properties expressing TLR1, 4, 5, 7, and 10; inhibited proliferation of T cells, Th17; increasing CD4 <sup>+</sup> CD25 <sup>+</sup> FoxP3 <sup>+</sup> Tregs; releasing IL-6, IDO, IL-10, COX-2, and iNOS	Calvarial defects, neural regeneration, and periodontal regeneration	[32, 42–45]
TGSCs	Not reported	CD14 CD34 CD45 CD133	Bone/osteoblast, odontoblast, adipocyte, chondrocyte, and endothelial cell	Seldom reported	Bone repair and cartilage regeneration	[30, 46, 47]

DPSCs: dental pulp stem cells; PDLSCs: periodontal ligament stem cells; ABMSCs: alveolar bone-derived mesenchymal stem cells; SHEDs: stem cells from exfoliated deciduous teeth; SCAPs: stem cells from apical papilla; GMSCs: gingiva-derived mesenchymal stem cells; TGSCs: tooth germ stem cells.

theoretical and experimental basis to favor DFCs-based treatment in tissue repairment and regeneration.

## 2. DFCs in Tooth Development

Tooth development initiates from the reciprocal interaction between oral epithelium and neural crest-derived mesenchyme, then develops into integral tooth morphogenesis consisting dental crown and root after bud stage, cap stage, and bell stage. The DF starts from the condensed mesenchyme adjacent to the tip of the bud and harbors mesenchymal progenitor cells for various differentiated lineages to compose the tooth root-bone interface and coordinate tooth eruption [4, 5]. It is known that appropriate stimulation from Hertwig's epithelial root sheath (HERS) is of great necessity for tooth root development via inducing the growth, differentiation, and immigration of DFCs. Lack of stimulation from HERS inhibited the capability of DFCs to form cementum and PDL-like tissues [6], and any disturbance of HERS formation produced malformed cementum, abnormal secretion and distribution of collagen fibers crucial to PDL attachment and orientation [7]. Alternatively, HERS indirectly induced the formation of cementum by regulating dental papilla differentiation toward osteoblasts to secrete dentin matrix exposure to DFCs [8]. In turn, DFCs and cementoblasts collaboratively induced apoptosis of HERS cells in tooth development (*in vitro*) in a Fas-Fas ligand (FasL) pathway, followed with upregulated Fas expression on HERS cells and FasL expression on DFCs, respectively [9]. As the development progressed, HERS cells became fragmented at the apex of the developing root to allow cementoblasts or fibroblasts derived from DF to establish connection with outer surface of the tooth root. The activation of transcriptional growth factor- $\beta$  (TGF- $\beta$ ) signaling induced HERS fragmentation and promoted HERS to form acellular cementum and PDL via epithelial-mesenchymal transition (EMT) [10].

The establishment of tooth root morphogenesis and coordination of tooth eruption associated with DFCs were dependent on an array of growth and transcription factors consisting Gli1, NOTCH, WNT, nuclear factor 1 C-type (Nfic), and TGF- $\beta$  [7, 8], which are critical to form a healthy dentition from primary tooth eruption to permanent dentition establishment [48]. DFCs on the root surface robustly expressed parathyroid hormone-related peptide (PTHrP) during tooth root formation and after tooth eruption, and PTHrP<sup>+</sup> DFCs differentiated into PDLs, alveolar cryptal bone osteoblasts, and cementoblasts in acellular cementum [5, 49]. However, a previous study reported that PTHrP inhibited alveolar bone formation by suppressing WNT/ $\beta$ -catenin signaling in DFCs, exhibiting upregulated RANKL/OPG ratio which was in favor of osteoclastogenesis [50, 51]. PTHrP<sup>+</sup> DFCs subgroups also expressed the PTHrP receptor (PPR) plentifully. PPR-deficient DFCs exhibited obviously truncated roots lacking PDL attachment but enhanced cementoblast differentiation, possibly attributed to the cell fate shift to nonphysiological cementoblast-like cells [5, 49]. Additionally, the cementoblast/osteoblast differentiation of DFCs stimulated by HERS was associated with the

WNT/ $\beta$ -catenin pathway as the WNT3A expressed on HERS increased alkaline phosphatase (ALP) activity [52]. As for tooth eruption, DFCs recruited and activated osteoclasts and DFCs themselves differentiated into osteoblasts to mediate collaboratively bone remodeling and create space for tooth eruption [53]. PTHrP expressed on DFCs inhibited osteogenesis of DFCs but accelerated tooth eruption [51]. Ameloblast-associated protein (OADM) related to mineralization expressed on DFCs in a time-dependent pattern. The gradually increased OADM expression in the early stage of differentiation accelerated osteogenesis to make a normal eruption, and the missing OADM did not influence bone density but resulted in a postponed tooth eruption [54, 55]. Cleidocranial dysplasia (CCD) patients are characterized by delayed tooth eruption due to runt-related transcription factor 2 (*Runx2*) mutation, DFCs-CCD patients displayed significantly lower osteogenic, osteoclast-inductive and matrix-degrading capacities, mechanistically contacted with disturbed RANK/RANKL/OPG signaling and decreased expression of matrix metalloproteinase 9 (MMP9) and MMP2 [56–58].

## 3. DFC Surface Markers

Stem cells retain the ability of self-renewal and multipotent differentiation, and DFCs have been revealed to hold these potentials. Cell surface markers distinctively express among various stem cells and are mainly classified into three types, embryonic stem cell (ESC) markers, mesenchymal stem cell (MSC) markers, and neural stem cell (NSC) markers. Transcriptional factors SOX2, OCT4, and NANOG expressing on hESCs were crucial to maintain undifferentiated pluripotent stem cells. Around 75% DFCs were identified to express OCT4 and SOX2 both in the nucleus and cytoplasm. In the rat model, it displayed that their expression on DFCs were time-independent during development and were upregulated when cocultured with rat dental papilla cells (DPCs) *in vitro* [12, 59]. NANOG was weakly expressed and downregulated gradually in the subsequent passages of DFCs. Alternatively, DFCs expressed a series of MSC surface markers containing NOTCH-1, STRO-1, CD13, CD44, CD73, CD105, CD56, CD271, and HLA-ABC but not hematopoietic stem cell (HSC) markers like CD34, CD45, and CD133 [60, 61]. STRO-1 and CD44 were widely distributed in DFCs, and their expression were downregulated as the passages increased. Therefore, they were the most common surface markers to identify the existence of MSCs in DF [12, 62]. The transmembrane protein NOTCH-1 was important in various cell fate decisions during development and strongly expressed on DFCs. It was reported to promote the capability of self-renewal and proliferation of DFCs by modulating G1/S phase transition and telomerase activity [63]. A recent study also suggested that 90% of cultured DFCs were positive for HLA-ABC which has been reported in PDL and dental pulp [12]. As described previously, DFCs expressed nestin (a neural progenitor cell marker) and beta-III-tubulin (an early neuronal marker), and the presence of neural crest stem cell markers (P75 and HnK1) and glial-like cell markers (GFAP) were also reported in the DF [12, 64, 65].

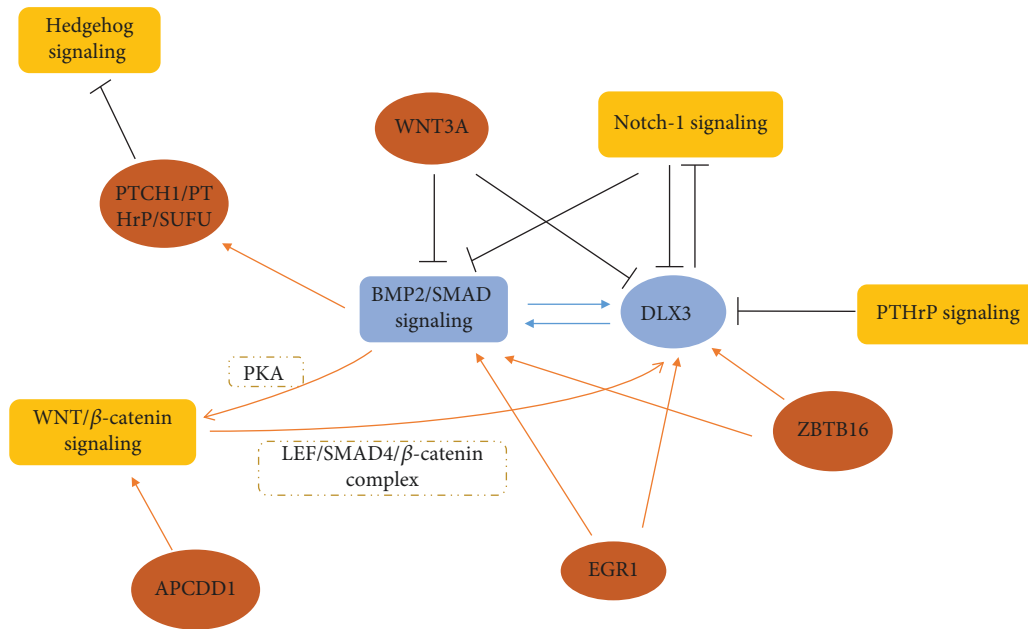


FIGURE 1: BMP2/DLX3 integrated network in DFC osteogenic differentiation.

## 4. Multipotent Differentiation of DFCs

**4.1. Osteogenic Differentiation.** DFCs are responsible to form alveolar bone in tooth development to support and fix the tooth root, which are also capable to differentiate into osteoblasts and form mineralized matrix nodules with appropriate exogenous osteogenic stimulus, such as dexamethasone or BMPs [66, 67]. During the osteogenic differentiation, the proteomic analysis suggested that 115 proteins were differentially regulated, in which 80 proteins like glutamine synthetase and beta-actin were upregulated while 35 proteins like cofilin-1 and pro-alpha1 collagen were downregulated [53]. It is elucidated that the expression of osteogenic-related markers including RUNX2, ALP, bone sialoprotein (BSP), and osteocalcin (OCN) were enhanced in this process [68, 69]. In spite of the complex transcriptomic and proteomic changes during osteogenic differentiation, only a minor number of identified proteins could be assigned to specific pathways currently. These transcriptional factors and signaling pathways collaboratively participating osteogenic differentiation of DFCs are mainly in a BMP2/the distal-less homeobox-3 (DLX3) integrated molecular network. Signaling pathways critical to bone formation such as BMP, NOTCH, Hedgehog, WNT signaling, and transcription factors mainly acted on the BMP2/DLX3 feedback loop to perform a positive or negative regulation for DFC osteogenic differentiation (see Figure 1).

**4.1.1. BMP Signaling.** BMPs are a group of glycoproteins belonging to the TGF- $\beta$  superfamily, and they impact DFC osteogenic differentiation both through the canonical and non-canonical pathways. The signaling transduction of the canonical pathway is initiated when BMPs bind to their receptors BMPRs (BMPRI1A, BMPRI1B, and ActR-1A) to form a heterotetrameric complex composed of two dimers of type I and type II serine/threonine kinase receptors. Subsequently, phosphorylated BMPs activate SMADs, while the noncanonical pathway

is SMAD-independent [70]. More than 20 BMPs are found to modulate osteogenic differentiation directly or act as the intermediate regulator to influence bone formation. BMP2, BMP4, BMP6, BMP7, and BMP9 are five most studied subtypes upon DFC osteogenic differentiation. Though all of them behaved promoted effect on osteogenesis, the mechanisms and effect levels were distinctive. Both BMP2 and BMP7 mediated DFC osteoblast differentiation in a time and dose-dependent manner while others were not [1, 71]. BMP2 and BMP4 were critical to the early stage of osteogenic differentiation while BMP6 functioned both in the early and late stages of this process. Previous evidence supported that high BMP6 expression effectively maintained osteogenic capability of DFCs and exogenous human recombinant (hrBMP6) can partially restore the differentiated capability of DFCs in late passages [72]. Mechanistically, BMP6 enhanced the phosphorylation of SMAD1/5/8 proteins associated with canonical BMP signaling while BMP2 and BMP9 got involved in the MAPK signaling pathway [73, 74]. Secreted BMP6 from other cells in DF also promoted the osteogenesis via a paracrine pathway. Interestingly, BMP6 was also considered as one of the downstream targets of circular RNAs (circRNAs) in DFC differentiation, it was upregulated in circFgfr2-enhanced DFC osteogenesis [75].

In 2012, Viale-Bouroncle et al. firstly put forward the significant status of the BMP2/DLX3 feedback loop in regulating osteogenic differentiation of DFCs. The study displayed that BMP2 induced the expression of DLX, and in turn, DLX3 upregulated BMP2 and activated the BMP/SMAD1 signaling pathway [76]. Furthermore, subsequent evidence supported that BMP/DLX3 acting as the central axis integrated a series of signaling pathways which participated osteogenic differentiation of DFCs. NOTCH-1 expression was regulated as DFCs differentiated and it played a negative role on osteogenic differentiation of DFCs via destroying the expression of DLX3 and activation of SMAD1 [77]. Conversely, DLX3 overexpression enhanced NOTCH signaling in DFCs, displaying a

negative feedback regulation.  $\beta$ -catenin was phosphorylated via intermediate protein kinase A (PKA) induced by BMP2 and DLX3, then formed the lymphoid enhancer factor (LEF)/SMAD4/ $\beta$ -catenin complex to promote DLX3 transcription to facilitate osteogenic differentiation, therefore establishing a cross talk between the WNT/ $\beta$ -catenin and BMP2/SMAD signaling pathways. As the canonical WNT signaling induced by WNT3A negatively adjusted DFCs osteogenic differentiation, the BMP2/DLX3-induced PKA/ $\beta$ -catenin pathway antagonized the inhibitory effect and sustained differentiation capability to some extent [78]. The hedgehog signaling was greatly required in tooth development but slightly inhibited ALP activity and mineralization of differentiated DFCs. With the induction of BMP2 *in vitro*, the hedgehog signaling was repressed during DFC osteogenic differentiation as its inhibitors patched1 (PTCH1), suppressor of fused (SUFU), and PTHrP were upregulated [79]. Except for the suppressor, PTHrP was also the targeted gene of hedgehog signaling, and it was highly concentrated extracellularly and slightly upregulated intracellularly during the osteogenesis in DFCs. PTHrP overexpression inhibited ALP activity and DLX3 transcription but in a hedgehog-independent way [51, 80]. As PKA was regulated downstream in PTHrP signaling and involved the regulation of DLX3 in DFC differentiation, it may be a targeted intermediate in PTHrP-mediated osteogenesis.

**4.1.2. WNT Signaling.** WNT signaling is essential to embryonic development which regulates the proliferation, differentiation, migration of stem cells, and the epithelial-mesenchymal interactions critical to dental tissues. WNTs are secreted glycoproteins acting as the ligands to activate the canonical and noncanonical WNT signaling pathways. The activation of canonical signaling is initiated from the binding of the WNT ligand to Frizzled (Frz) protein and coreceptor, then followed with the phosphorylation of the multiprotein complex and increased cytoplasmic and nuclear  $\beta$ -catenin level, eventually cooperated with T cell factor (TCF)/LEF transcription factors and other coactivators to regulate the target genes [81]. The crucial protein  $\beta$ -catenin expressed in DF and its expression coincided with the period of osteogenesis and cementogenesis. Increased activity of nucleus  $\beta$ -catenin and  $\beta$ -catenin/TCF luciferase induced by lithium chloride (LiCl) led upregulation of OCN, RUNX2, type I collagen (COLI) proteins, and ALP activity, which suggested a positive role of WNT signaling in the DFC osteogenesis [82]. Adenomatous polyposis coli downregulated 1 (APCDD1) was crucial for sustaining the expression of  $\beta$ -catenin and the activity of the TCF/LEF promoter in DFCs. The deletion of APCDD1 reduced the expression of osteogenic markers and matrix mineralization, and it was also regarded to be involved in BMP2/DLX3-directed osteogenic differentiation through  $\beta$ -catenin [83]. The essential ligand WNT3A in WNT signaling impeded mineralized nodule formation and reduced RUNX2, OCN levels, and ALP activity in DFCs, it also suppressed BMP2-induced osteoblast differentiation *in vitro* in a  $\beta$ -catenin/TCF-dependent mechanism [84]. We account that WNT3A may exert a double effect as the DFCs mineralization was enhanced when cocultured

with HERS expressing WNT3A [8]. The available evidence demonstrated that this dual role of WNT3A was mediated through the WNT signaling pathway. However, it is still unclear whether it is led by different cell types or differentiation stages or even the involvement of other signaling pathways. DKK3, an inhibitor of WNT/ $\beta$ -catenin, also negatively regulated osteogenesis of DFCs by influencing formation of calcified nodules [85]. Other proteins also regulated DFCs differentiation indirectly through the WNT/ $\beta$ -catenin pathway. The anterograde intraflagellar transport motor KIF3A in primary cilia activated indirectly the WNT/ $\beta$ -catenin pathway triggered by WNT3A. Deletion of *Kif3a* resulted the attenuation of active  $\beta$ -catenin and LEF1, eventually displayed substantial impairment of mineralization and differentiation-associated marker expression [86]. Naked cuticle homolog 2 (NKD2) has been reported to promote DFCs to differentiate to osteoblasts through WNT/ $\beta$ -catenin as a signal-inducible feedback antagonist [87]. From the perspective of epigenetics, the decrease of maternally expressed 3 (MEG3) or enhancer of zeste homolog 2 (EZH2) activated the WNT/ $\beta$ -catenin signaling pathway via epigenetically regulating the H3K27me3 level on the WNT gene promoters, which offered a new guideline for osteogenesis research in DFCs [88].

The noncanonical WNT signaling is  $\beta$ -catenin independent and is also initiated when WNT ligand binds to Frz and its coreceptor. Then, dishevelled (DSH) is recruited to interact with a series of proteins to activate downstream target molecules like C-Jun N-terminal kinase (JNK). WNT5A mediated the noncanonical WNT signaling pathway and regulated cell proliferation, differentiation, and polarization. WNT5A was expressed in DFCs, especially displayed a robust expression in alveolar bone on postnatal days 1-11. The overexpression of WNT5A in DFCs promoted phosphorylation of JNK1/2, which was similar to that in DPCs and bone marrow stem cells (BMSCs) [89, 90]. Except for acceleration of osteogenesis, WNT5A also took a part in osteoclast lineage by regulating RANKL ligand expression in a positive manner, thus mediating bone resorption and remodeling [91]. Recent evidence demonstrated a complex interaction between canonical and noncanonical WNT signaling in DFC differentiation. Silence of *Wnt5a* in DFCs enhanced WNT3A-mediated increase of ALP expression, while the negative role of WNT5A was not related to nuclear translocation of  $\beta$ -catenin and transcriptional activation of TCF triggered by WNT3A. It was considered to inhibit the downstream part of the  $\beta$ -catenin/TCF pathway [92].

**4.1.3. Transcriptional Factors.** In DFC osteogenesis, around 1/3 regulated genes had promoter binding sites for transcriptional factors TP53 and SP1. TP53 overexpression promoted osteogenic differentiation of DFCs while SP1 showed a more obvious impact on DFC proliferation, whereas the involved mechanism was unclear [93]. Besides, zinc factor and BTB domain containing 16 (ZBTB16) performed multiple and complex functions in DFC osteogenic differentiation. It upregulated late osteogenic marker expression like OCN while ALP and RUNX2 were not affected [68]. And dexamethasone-induced DFC osteogenic differentiation was reported in a

ZBTB16-dependent manner [94, 95]. It was worth mentioning that ZBTB16 also regulated the BMP2/DLX3 feedback loop as it induced the expression of BMP2 and had a binding site on the DLX3 promoter. Another potential mechanism for ZBTB16 in DFC differentiation may associate with the expression of a new target gene stanniocalcin 1 (STC1) which was responsible for mediating osteogenic-related marker OPN and OCN expression [68]. Early growth response protein1 (EGR1) was critical to proliferation, apoptosis, and differentiation. The level of EGR1 was elevated after osteogenic differentiation of DFCs and in turn it regulated the expression of DLX3 and BMP2 to mediate osteogenic differentiation positively [96]. Fractional odontogenic matrix protein such as dentin matrix protein 1 (DMP1) and odontogenic ameloblast-associated protein (ODAM) have been identified to correlate positively with the osteogenic capability of DFCs, which suggested the complex microenvironment in different time and space for DFC differentiation in tooth development [54, 97].

Except for the signaling pathways and biological factors mentioned above, physical factors covering the temperature, stress, and stiffness also influenced DFC osteogenic differentiation. It was reported that soft extracellular matrix, elevated temperature contributed to the proliferation, differentiation, and expression of related markers of DFCs [98, 99]. The role of cell-cell interaction in the complex development microenvironment recently gained increasing attention, except for HERS, *in vitro* studies suggested that the osteogenesis and fibrogenesis abilities of DFCs were inhibited when cocultured with SCAPs [100]. Alternatively, increased angiogenic activity in DFCs and human umbilical vein endothelial cells (HUVECs) cocultures stimulated osteoblast maturation of DFCs [101].

**4.2. Neural Differentiation.** The neural lineage differentiation of DFCs is partially attributable to its origin from neural crest. Early studies reported the neural characteristics of DFCs in specific culture conditions, such as the expression of neural markers and the capability to differentiate to functionally active neurons. When placed DFCs into a neuron induction medium, the differentiated multipolar neuron-like cells expressed late neural markers and exhibited capability to produce a sodium current consistent with functional neuronal cells [2, 102]. The glial cell marker glial fibrillary acidic protein (GFAP) was restrictedly expressed on DFCs, which may suggest a limited differentiation potential of DFCs to glial cells. But the glial cell differentiation can be enhanced remarkably via activating the TGF- $\beta$  signaling pathway through the phosphorylation of SMAD2 in DFCs [103]. Compared with DPSCs and SCAPs, DFCs had a higher proliferation capability and expressed upregulated CNPase (a myelin protein expressed both on oligodendrocytes and Schwann cells) and DCX (a specific protein expressed on neuronal cells) in consistent conditions, which supported that DFCs may act as a better candidate type for neural differentiation [104, 105]. In spite of the neural differentiation potential, superior strategies for DFCs to produce both neural-like and functional neuronal cells are challenges in the complex microenvironment in the body. Previous researches imposed a two-step strategy for neuronal differentiation of DFCs *in vitro* including pre-differentiation and selective induction. DFCs predifferentia-

tion was performed to obtain neurosphere-like cell clusters (NLCCs) in which neural cell markers like beta-III-tubulin, NSE, and nestin were upregulated. Then, these NLCC-derived cells were cultivated in medium whose surface was modified with laminin and poly-L-ornithine, thus exposing neural-like cell morphology with small neurite-like cell extrusions [65]. In view of the two-dimensional culture medium was hard to mimic the highly complex extracellular matrix (ECM) environment of stem cells undergoing neurogenesis *in vivo*. Researchers considered to use decellularized matrix (DECM) extracted from neural stem cells (NSCs) differentiated from hESCs to simulate the natural physiological microenvironment in DFC neurogenesis. The outcome supported that NSC-DSEM was superior in enhancing DFC neural differentiation [106].

**4.3. Periodontium Differentiation.** One of the most important functions of DFCs is to form good root-bone interface, including PDL, cementum, and alveolar bone. Cementum is mineralized tissue covered in the surface of the tooth root and regulates the physical and chemical interaction between PDL and tooth root. In tooth development, cementogenesis initiates at a root-forming stage when epithelial stimulation from HERS induced differentiation of DFCs into cementoblasts/osteoblasts. A combination of DFCs and HERS implanted in immunocompromised mice enhanced the activity of mineralized tissue-forming cementoblasts obviously [107], part of the mechanism resulted from the production of BMP2, BMP4, and BMP7 synthesized by HERS [108]. The structure of the cementum was resembled with the early woven bone; the induction of DFC osteogenic differentiation was usually followed with the formation of a cementoblast phenotype. For example, RUNX2 critical to osteogenesis was present in early proliferative cementoblasts and its overexpression upregulated the expression of cementoblast-related genes of DFCs correspondingly [3]. Specifically, cementoblasts expressed unique markers like cementum-derived attachment proteins (CAP) which promoted the attachment, proliferation, and differentiation of DFCs [109]. DFCs formed cementum-like matrix and expressed osteopontin (OP) and COL1 mRNA when they were transplanted into immunodeficient mice [110, 111]. Odontogenic matrix protein like dentin noncollagenous proteins (dNCPs) and enamel matrix derivatives (EMD) could stimulate DFCs to differentiate cementum-like tissues *in vivo*, and biological activities of EMD were mediated by BMPs [112]. It was also suggested that other factors presented in EMD induced the cementogenesis in a SMAD-independent pathway, such as MAPK signaling [113]. Interestingly, DFCs transplants isolated from human molars at a root-developing stage were able to produce a cementum/PDL-like structure, characterized by a thin layer of cementum-like mineralized tissues and PDL-like collagen fibers connecting with the newly formed cementum [114], which demonstrated a higher activity of DFC differentiation potential in developing stages.

PDL is composed of a fibrous extracellular matrix, including collagens, microfibrils, and proteoglycans to provide resistance against occlusal force and nutrition for the alveolar bone and tooth. DFCs on the surface of hydroxyapatite beads

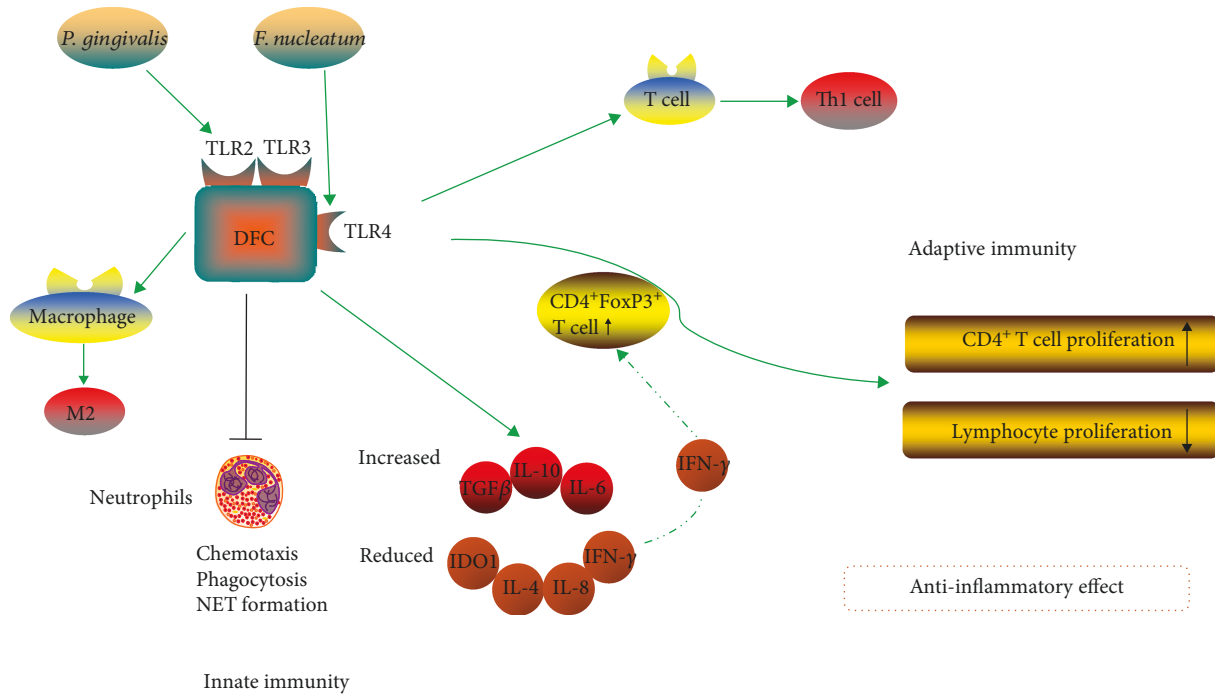


FIGURE 2: The immunosuppression of DFCs linked with innate and adaptive immunity.

formed fibrous tissues when implanted into immunodeficient mice; meanwhile, they expressed mRNA for BSP, OC, OP, and COL1 [111]. Mechanistically, F-spondin expressed on DFCs have been reported to downregulate PDL marker genes through inhibiting TGF- $\beta$  activity, thus suppressing the PDL differentiation of DFCs *in vivo* [115]. In spite of the potential to differentiate PDL-like tissues, it is hard to recover the shape and function of natural PDL utilizing DFCs.

**4.4. Differentiation into Other Lineages.** DFCs were capable of forming adipocytes, and stained adipocytes were observed after placing DFCs in an adipogenic medium for 3 weeks [116]. The transient receptor potential melastatin 4 (TRPM4), an ion channel that controls Ca<sup>2+</sup> signal was necessary for DFCs adipogenesis while it acted as an inhibitory regulator in osteogenic differentiation [117]. The relatively lower chondrocyte differentiation of DFCs than adipocyte differentiation was also reported in previous studies. Interestingly, with the induction of treated dentin matrix (TDM), DFCs differentiated to odontoblasts to form dentin-like tissues via expressing a higher level of odontogenic markers such DMP-1 and DSP than DPCs [118, 119]. Additionally, a recent study also reported that DFCs differentiated into cardiomyocytes with suberoylanilide hydroxamic acid (SAHA) *in vitro*, which extended the recognition of DFCs [120]. In conclusion, DFCs possessed superior multilineage differentiation capabilities, which provided a significant prerequisite and research foundation for DFC treatment in repairment and regeneration of tissue defects.

## 5. Immunomodulatory Properties of DFCs

In spite of the multidifferentiation of DFCs expected to be used in tissue repairment, damaged or exposed tissue wounds

are often accompanied by inflammatory infections which suppressed the differentiation of stem cells. In patients with periodontitis, the complex oral microenvironment accumulating amounts of anaerobic periodontal pathogens and bacterial toxins is the main issue leading to the failure of multiple treatment. Besides, we have to pay attention to the immune responses caused by the proliferation and differentiation of allogeneic cells in cell-based therapy.

DFCs surface expressed Toll-like receptors (TLR) like TLR2, TLR3, and TLR4. They are a kind of pattern recognition receptors which are broadly distributed on immune system cells to connect innate and adaptive immune responses (see Figure 2). TLR4 can be activated by the lipopolysaccharide (LPS) of gram-negative species such as *F. nucleatum*, while *P. gingivalis* LPS conveyed signals via TLR2 [121, 122]. LPS-pretreated DFCs suppressed peripheral blood mononuclear cell (PBMC) proliferation at the cell ratios, which may be a consequence of significantly downregulated TLR4 in DFCs [121]. In the existence of pathogenic bacterium, DFCs released amounts of cytokines to perform immunomodulation through the innate immune system. When cocultured with lymphocytes from healthy peripheral venous blood, DFCs exhibited decreased IL-4 and IFN- $\gamma$  levels and increased anti-inflammatory cytokine IL-10 [11]. In a cocultured inflammatory environment combining *P. gingivalis* and *F. nucleatum* with DFCs, DFCs behaved higher secretion of IL-10 than proinflammatory cytokine IL-8 at all measured time points and obviously lowered bacterial adherence and internalization capacity [123]. Additionally, after the pretreatment with LPS, it was followed by a higher production of TGF- $\beta$ , anti-inflammatory cytokine IL-6, and reduced indoleamine 2,3-dioxygenase 1 (IDO-1) expression [13]. In comparative studies, LPS from different kinds of pathogenic



bacterium behaved distinguished impact on dental stem cells. LPS especially *P. gingivalis* LPS induced the expression of pro-inflammatory cytokines therefore inhibiting the differentiation of DPSCs [124]. Conversely, the proinflammatory cytokine induction was absent after the administration of *P. gingivalis* LPS in DFCs while *Escherichia coli* LPS induced the expression of IL-6, IL-8, and IL-1 $\beta$  in DFCs, thus inhibiting DFC osteoblast differentiation and mineralization [125]. And the inhibition of DFC osteogenic differentiation in an inflammatory microenvironment was related to the increase in TGF- $\beta$ 2 levels [126]. This specific reaction may provide a target choice of appropriate cell types for repairment after bacterial culture experiment. Furthermore, DFCs with infection of periodontopathogens behaved a direct impact on chemotactic attraction, phagocytic activity, and NET formation of neutrophils (PMN), reducing PMN-induced tissue and bone degradation via suppression of PMN activity [127]. DFCs also reprogrammed macrophages into the anti-inflammatory M2 phenotype by secreting paracrine factors TGF- $\beta$ 3 and TSP-1, which ameliorated LPS-induced inflammation [128].

In addition, DFCs were capable to regulate the adaptive immunity. Cytokines secreted by DFCs exhibited suppressive effect on lymphocyte proliferation and T lymphocyte apoptosis, and the presence of IFN- $\gamma$  strengthened the suppression of DFCs on these cells. Mechanistically, the immunosuppressive effects on lymphocyte proliferation are related to an upregulated frequency FoxP3 which expressed on CD4<sup>+</sup>CD25<sup>+</sup> regulatory T cells [11, 129]. Asthma is an allergic disease in which inflammatory responses involve the polarization of CD4<sup>+</sup> T cells to Th2 cells. The study showed that DFCs exhibited an antiproliferative response to CD4<sup>+</sup> T lymphocytes by increasing the levels of CD4<sup>+</sup>CD25<sup>+</sup>FoxP3<sup>+</sup> T regulatory cell frequency and the IDO and TGF- $\beta$  pathways were involved in the induction of T regulatory cells. Besides, DFCs suppressed allergen-induced Th2 cell polarization while supported the differentiation of T lymphocytes toward Th1 cells. In conclusion, the downregulated effect of DFCs on allergen-induced effector, effector memory, and central memory T cell subsets in asthma patients behaved a protective mechanism on naïve T lymphocyte population [130]. Apart from allergic diseases, DFCs were effective to treat autoimmune diseases like MuSK-related myasthenia gravis (MG) through reducing proliferation of lymph node cells and producing IL-6 and IL-12 [131].

## 6. Senescence and Apoptosis Characteristics of DFCs

DF tissue is a potential stem cell bank which can be harvested abundantly from extracted teeth, especially in the case of impacted wisdom teeth extraction. After appropriate isolation procedure and expansion *in vitro*, a sufficient number of DFCs are expected to obtain [132–134]. Unfortunately, even under standard cell culture conditions, DFCs face the challenge of limited cell divisions and enter cellular senescence after a prolonged cell culture [135]. Senescent cells usually behave shortened telomere, changes in morphology and expression of  $\beta$ -galactosidase, and the loss of cell prolifera-

tion potency [136]. A previous study suggested that DFCs exhibited features of cellular senescence after being expanded after more than 14 cell passages, displaying decreased cell proliferation, enlarged cell size, and upregulated expression of  $\beta$ -galactosidase [137]. Short telomeres and increased DNA damage with genomic instability were correlated with the accelerated induction of cellular senescence [138]. Moreover, the osteogenic differentiation of DFCs was inhibited due to cellular senescence, followed with a lower extent to differentiate into biomineralizing cells [137]. During the process of cellular senescence, expression of cyclin-dependent kinase 2 (CDK2) and CDK4 were modulated, and the cell cycle regulatory protein P21, P27, and P18 were all downregulated while P16 was upregulated. The cell cycle protein P16-dependent pathway was considered to drive the induction of cellular senescence of DFCs as the number of senescent cells reduced when P16 gene was silenced [139]. NOTCH signaling was essential to control the proliferation and apoptosis of DFCs. NOTCH-1 signaling regulated the proliferation and self-renewal capacity of DFCs through modulation of the G1/S phase transition and telomerase activity, active NOTCH-1 promoted G1/S transition via decreasing the number of the G1 phase cells and accelerating the S phase transition in DFCs [63, 140]. In addition, NOTCH signaling was elucidated to exhibit a suppressive effect on DFC apoptosis through reducing cytoplasmic apoptotic effects in the classical mitochondrial pathway and the noncanonical NOTCH-1-AKT module, together with repression of *p53* transcription in nuclei [141]. It is worth noting that some biomaterials or chemical substances accelerated the senescence of DFCs. The  $\beta$ -tricalcium phosphate (TCP) induced programmed cell death while enhanced bone differentiation, and the survived DFCs exhibited a highly upregulated expression of antiapoptotic genes [142]. Hydroxyurea induced premature via influencing genes associated with DNA damage and repair, mitochondrial dysfunction, and it also increased reactive oxygen species levels. The age was another crucial factor as DFCs from young donors were more resistant to apoptosis and behaved increased nonhomologous end joining activity compared to old donors [143].

## 7. Clinical Application Potential of DFCs

From what were mentioned above, DFCs had multilineage differentiation potential, excellent anti-inflammatory capability, and accessibility to obtain and expand *in vitro*, which lay the foundation for DFC clinical application. To date, the key steps in tissue engineering contain methods of cell isolation, expansion, transplantation, and specific lineage differentiation. The use of bioactive matrix materials such as tissue scaffolds, addition of various hormones, and growth factors or other chemical compounds optimized the strategies in tissue repairment and regeneration. Previous studies have reported the formation of bone-like, PDL-like tissues successfully both *in vitro* and *in vivo* utilizing DFCs combined with various approaches.

**7.1. Bone Tissue Engineering.** Osteogenic differentiation potential makes DFCs an attractive type of stem cells for

repairing bone defects or loss caused by periodontal diseases, trauma, or degenerative diseases. Honda et al. initially obtained new bone formation after DFCs transplantation in surgically created calvarial defects in immunosuppressed mice [53]. However, it was difficult to obtain effective tissue repairment relying on cell differentiation singly. Recent views supported a combination of dental stem cells with bioactive materials, an alternative to autologous bone transplants without impairing the proliferation and differentiation of dental stem cells [144]. Early studies considered hydroxylapatite (HAP) and  $\beta$ -tricalcium phosphates (TCP) as scaffolds for DFC osteogenic differentiation. TCP was an excellent scaffold for DFC osteogenesis while HAP contributed to a modest differentiation [145]. However, TCP-induced apoptosis of DFCs is unbeneficial for cell-based therapy. A better bone regeneration for healing calvarial critical-size defects was achieved through transplanting DFCs loaded into polycaprolactone (PCL) scaffold that was covered with hyaluronic acid and  $\beta$ -TCP. This method promoted cell proliferation, migration, and even dispersion [146]. A novel scaffold composed of biodegradable coralline hydroxyapatite (CHA) seeded with BMP9-transfected rat DFCs (rDFCs) induced new alveolar bone formation. It achieved optimal effects in repairing the alveolar bone defects for forming more new bone and blood vessels, and the osteogenesis was associated with the activation of SMAD1/5/8 signaling induced by BMP9 [147]. Recently, alloplastic materials like titanium and ceramics gained increasingly focus in recovering bone defects. Even without exogenous osteogenic factors like BMP2, titanium with different bioactive coatings was capable of sustaining osteogenic differentiation of DFCs and titanium implants with hydroxyapatite (TiHA) seemed more favorable [148]. To imitate the complex microenvironment *in vivo*, DFCs were precultured from the 5th to 8th passages in a three-dimensional (3D) culture using gelatin sponges and then were transplanted to immunodeficient rats. After 28 days, numerous woven osteoids, enlarged capillary vessels, and spindle-shaped cells were observed and osteoblasts were accumulated around osteoids. Micro-CT as the gold standard for assessing bone morphology and microarchitecture demonstrated a higher quality than the control group [149]. With the advancement of materials science, nanocomposite was applied into tissue engineering, a trilayered nanocomposite hydrogel scaffold implanted into rabbit maxillary periodontal defects with growth factors supported new formation of the alveolar bone [150]. It is also highlighted that nanosilicates with fluoride additive (NS+F) aid evidently enhanced the osteogenic differentiation capabilities of DFCs. Therefore, nanobiomaterials are expected to be a type of a good carrier used for periodontal bone tissue regeneration [151].

**7.2. Tooth Root Regeneration.** Tooth is another type of mineralized tissue in the human body. As DFCs are responsible for forming a tooth root and its supporting tissues in odontogenesis, DFCs were mainly studied to apply in tooth root regeneration. Previous studies isolated DFCs from developing root and loaded them on an absorptive root-shaped scaffold in regular sequence. By this way, they mimicked a biophysiological root *in vivo* and regenerated a functional

root/periodontal tissue complex able to support a porcelain crown [114]. The strategy was optimized by combining DFCs seeding cells, TDM scaffolds, and an inductive alveolar fossa microenvironment, successfully forming root-like tissues with a pulp-dentin complex, and a PDL connecting a cementum-like layer with the host alveolar bone [152]. This bioroot complex performed the masticatory function and kept a stable structure for around three months after crown restoration [153]. Alternatively, eight weeks after *in situ* implantation of DFCs/TDM, it displayed a soft tissue clearance between the TDM and jaw bone similar to the native tooth root, consisting of dense and well-aligned collagen fibers, fibroblasts, and blood vessels beneficial for PDL formation [33]. Considering the scant sources of allogeneic TDM (aTDM), xenogeneic TDM (xTDM) was a possible substitute for aTDM but it caused osteolysis and resorption lacunae and led to regenerated root failure. The *tert*-butylhydroquinone (*t*BHQ), an antioxidant, can reduce osteolysis and osteoclastic resorption when added in xTDM/aDFCs scaffolds [154].

**7.3. Periodontium Regeneration.** Periodontal tissue destruction caused by periodontal diseases has become the main cause of tooth loss and a huge challenge in oral treatment. The connection between the tooth root and alveolar bone decreases obviously due to the damage of collagen fiber of PDL. In the current treatment for periodontal diseases, the application of alloplastic materials and autografts are dependent on autologous tissue grafts or artificial implants, which are limited as a result of insufficient biocompatibility, the risks of reinfection, and bone resorption [116]. As a consequence, cell-based techniques have been a new trend for periodontal regeneration [155]. As the vital precursor cells to form periodontal tissues in tooth development, DFCs are excellent potential resources for periodontium regeneration. Oshima et al. developed a novel fibrous-connected tooth implant using a HA-coated dental implant and DFCs, which successfully restored physiological functions of the tooth, including the ability to respond to mechanical stress and noxious stimulation, bone remodeling in severe bone defects [156]. Later, a multilayer construct emerged to induce simultaneous regeneration of PDL, cementum, and alveolar bone in periodontium repairment. A bilayered construct with DFCs consisting of a polycaprolactone (PCL) multiscale electrospun membrane and a chitosan/2 wt% CaSO<sub>4</sub> scaffold regenerated PDL and alveolar bone separately, and it showed better protein adsorption beneficial for cell attachment and proliferation [157]. Trilayered nanocomposite hydrogel scaffolding, composed of chitin poly(lactic-co-glycolic) acid (PLGA)/nanobioactive glass ceramic (nBGC)/cementum protein 1 (CEMP1), chitin-PLGA/fibroblast growth factor 2 (FGF2), and chitin-PLGA/nBGC/platelet-rich plasma- (PRP-) derived growth factors acting as the cementum layer, PDL layer, and alveolar bone layer, respectively, achieved a complete healing with the formation of new cementum, fibrous PDL, and alveolar bone with well-defined trabeculae, which served as a good alternative regenerative approach for periodontal diseases [150].

**7.4. Other Tissue Regeneration.** DFCs are also an alternative source for the regeneration of other tissues in addition to the

tooth and bone. Due to neural differentiation capability of DFCs, an approach utilized human DFCs (hDFCs) and aligned electrospun PCL/PLGA material (AEM) to reconstruct SCD, the developed oriented fibers *in vitro* and trend to differentiate an oligodendrogenic lineage in the SCD microenvironment may contribute to remyelination [158]. Alternatively, DFCs behaved a cardiomyogenic differentiation potential with the influence of SAHA *in vitro* and a small number of induced cardiomyocytes (iCMs) homed to the heart muscle without leading inflammatory or immune responses via systemic administration. However, the low homing ratio was unfavorable factors for standardized treatment [120].

DFCs, which possess multipotent differentiation ability and excellent immunosuppression capacities, are regarded as an alternative resource for repairing both hard tissue and soft tissue defects. However, the restoration of both morphology and function of damaged and infected tissues bring about enormous challenges. Quantities of researches were carried out to optimize the regenerative strategies depending on the rapid development of other subjects. In spite of a great prospect for DFCs in clinical application, the following points have been taken into account. Firstly, the requirement of donors including the age and health condition of periodontium should be emphasised since they impacted the regenerative properties of stem cells. Then, optimizing the strategy of DFC isolation and expansion *in vitro* beforehand is necessary. Proper heat stress conditions were beneficial to obtain the DFCs population containing more stem cells. Some isolation strategies such as the enzymatic digestion (EZ) and the outgrowth (OG) method did not affect DFCs-derived cell growth and isolated DFCs were capable of forming cementum-like matrix *in vitro* and acellular cementum structures *in vivo* [132, 159]. Besides, age-related cellular changes of DFCs regarding the loss of stemness and differentiation capability are expected to be improved [160]. More importantly, preclinical evaluations of dental stem cells especially on large animal models followed by randomized clinical trials are required [161]. Also, clinical trials evaluating DFC application in bone or tooth tissue engineering should be carried out to identify the actual feasibility of clinical application. Therefore, we are faced with the coexistence of opportunities and challenges and there is a long way to go.

## 8. Conclusion

In this article, we reviewed roles of DFCs in tooth development, the characteristics of DFCs including their multilineage differentiation, immunosuppressed capability, and excellent amplification ability and their tissue engineering potentials. Meanwhile, experimental or clinical application progresses on tissue regeneration such as the bone regeneration, dental root establishment, and periodontium recovery. Therefore, DFCs can act as a group of excellent cells for future cell-based treatment for tissue repairment and regeneration.

## Conflicts of Interest

The authors declare that there is no conflict of interests regarding the publication of this paper.

## Acknowledgments

This work was supported by the China Postdoctoral Science Foundation 2018M643508 to Xin Zhou, SCU Postdoctoral Science Foundation 2018SCU12022 to Xin Zhou, Young Scientist Foundation of West China Hospital of Stomatology WCHS-201709 to Xin Zhou, and National Natural Science Foundation of China (NSFC) Grant 81771033 to Liwei Zheng.

## References

- [1] M. Zhao, G. Xiao, J. E. Berry, R. T. Franceschi, A. Reddi, and M. J. Somerman, "Bone morphogenetic protein 2 induces dental follicle cells to differentiate toward a cementoblast/osteoblast phenotype," *Journal of Bone and Mineral Research*, vol. 17, no. 8, pp. 1441–1451, 2002.
- [2] S. Yao, F. Pan, V. Prpic, and G. E. Wise, "Differentiation of stem cells in the dental follicle," *Journal of Dental Research*, vol. 87, no. 8, pp. 767–771, 2008.
- [3] K. Pan, Q. Sun, J. Zhang et al., "Multilineage differentiation of dental follicle cells and the roles of Runx2 over-expression in enhancing osteoblast/cementoblast-related gene expression in dental follicle cells," *Cell Proliferation*, vol. 43, no. 3, pp. 219–228, 2010.
- [4] D. K. Yoshikawa and E. J. Kollar, "Recombination experiments on the odontogenic roles of mouse dental papilla and dental sac tissues in ocular grafts," *Archives of Oral Biology*, vol. 26, no. 4, pp. 303–307, 1981.
- [5] A. Takahashi, M. Nagata, A. Gupta et al., "Autocrine regulation of mesenchymal progenitor cell fates orchestrates tooth eruption," *Proceedings of the National Academy of Sciences of the United States of America*, vol. 116, no. 2, pp. 575–580, 2019.
- [6] Y. Guo, W. Guo, J. Chen, G. Chen, W. Tian, and D. Bai, "Are Hertwig's epithelial root sheath cells necessary for periodontal formation by dental follicle cells?," *Archives of Oral Biology*, vol. 94, pp. 1–9, 2018.
- [7] J. Li, C. Parada, and Y. Chai, "Cellular and molecular mechanisms of tooth root development," *Development*, vol. 144, no. 3, pp. 374–384, 2017.
- [8] Y. Yang, Y. Ge, G. Chen et al., "Hertwig's epithelial root sheath cells regulate osteogenic differentiation of dental follicle cells through the Wnt pathway," *Bone*, vol. 63, pp. 158–165, 2014.
- [9] J. H. Lee, D. S. Lee, H. Nam et al., "Dental follicle cells and cementoblasts induce apoptosis of ameloblast-lineage and Hertwig's epithelial root sheath/epithelial rests of Malassez cells through the Fas-Fas ligand pathway," *European Journal of Oral Sciences*, vol. 120, no. 1, pp. 29–37, 2012.
- [10] S. Itaya, K. Oka, K. Ogata et al., "Hertwig's epithelial root sheath cells contribute to formation of periodontal ligament through epithelial-mesenchymal transition by TGF- $\beta$ ," *Bio-medical Research*, vol. 38, no. 1, pp. 61–69, 2017.
- [11] S. Yildirim, N. Zibandeh, D. Genc, E. M. Ozcan, K. Goker, and T. Akkoc, "The comparison of the immunologic properties of stem cells isolated from human exfoliated deciduous teeth, dental pulp, and dental follicles," *Stem Cells International*, vol. 2016, Article ID 4682875, 15 pages, 2016.

- [12] R. L. Lima, R. C. Holanda-Afonso, V. Moura-Neto, A. M. Bolognese, M. F. DosSantos, and M. M. Souza, "Human dental follicle cells express embryonic, mesenchymal and neural stem cells markers," *Archives of Oral Biology*, vol. 73, pp. 121–128, 2017.
- [13] S. Tomic, J. Djokic, S. Vasilijic et al., "Immunomodulatory properties of mesenchymal stem cells derived from dental pulp and dental follicle are susceptible to activation by toll-like receptor agonists," *Stem Cells and Development*, vol. 20, no. 4, pp. 695–708, 2011.
- [14] Y. Tian, D. Bai, W. Guo et al., "Comparison of human dental follicle cells and human periodontal ligament cells for dentin tissue regeneration," *Regenerative Medicine*, vol. 10, no. 4, pp. 461–479, 2015.
- [15] J. Liu, F. Yu, Y. Sun et al., "Concise reviews: characteristics and potential applications of human dental tissue-derived mesenchymal stem cells," *Stem Cells*, vol. 33, no. 3, pp. 627–638, 2015.
- [16] T. Fu, P. Liang, J. Song et al., "Matrigel scaffolding enhances BMP9-induced bone formation in dental follicle stem/precursor cells," *International Journal of Medical Sciences*, vol. 16, no. 4, pp. 567–575, 2019.
- [17] F. Ferro, R. Spelat, and C. S. Baheney, "Dental pulp stem cell (DPSC) isolation, characterization, and differentiation," *Methods in Molecular Biology*, vol. 1210, pp. 91–115, 2014.
- [18] M. Lei, K. Li, B. Li, L. N. Gao, F. M. Chen, and Y. Jin, "Mesenchymal stem cell characteristics of dental pulp and periodontal ligament stem cells after in vivo transplantation," *Biomaterials*, vol. 35, no. 24, pp. 6332–6343, 2014.
- [19] J. M. Campos, A. C. Sousa, A. R. Caseiro et al., "Dental pulp stem cells and Bonelike® for bone regeneration in ovine model," *Regenerative Biomaterials*, vol. 6, no. 1, pp. 49–59, 2019.
- [20] A. T. Özdemir, R. B. Özgül Özdemir, C. Kırmaz et al., "The paracrine immunomodulatory interactions between the human dental pulp derived mesenchymal stem cells and CD4 T cell subsets," *Cellular Immunology*, vol. 310, pp. 108–115, 2016.
- [21] N. Wada, D. Menicanin, S. Shi, P. M. Bartold, and S. Gronthos, "Immunomodulatory properties of human periodontal ligament stem cells," *Journal of Cellular Physiology*, vol. 219, no. 3, pp. 667–676, 2009.
- [22] J. Xiong, D. Menicanin, P. S. Zilm, V. Marino, P. M. Bartold, and S. Gronthos, "Investigation of the cell surface proteome of human periodontal ligament stem cells," *Stem Cells International*, vol. 2016, Article ID 1947157, 13 pages, 2016.
- [23] A. Tomokiyo, N. Wada, and H. Maeda, "Periodontal ligament stem cells: regenerative potency in periodontium," *Stem Cells and Development*, vol. 28, no. 15, pp. 974–985, 2019.
- [24] A. Tomokiyo, S. Yoshida, S. Hamano, D. Hasegawa, H. Sugii, and H. Maeda, "Detection, characterization, and clinical application of mesenchymal stem cells in periodontal ligament tissue," *Stem Cells International*, vol. 2018, Article ID 5450768, 9 pages, 2018.
- [25] S. Onizuka and T. Iwata, "Application of periodontal ligament-derived multipotent mesenchymal stromal cell sheets for periodontal regeneration," *International Journal of Molecular Sciences*, vol. 20, no. 11, p. 2796, 2019.
- [26] K. T. Lim, J. Kim, H. Seonwoo et al., "Enhanced osteogenesis of human alveolar bone-derived mesenchymal stem cells for tooth tissue engineering using fluid shear stress in a rocking culture method," *Tissue Engineering. Part C, Methods*, vol. 19, no. 2, pp. 128–145, 2013.
- [27] X. Wang, H. Xing, G. Zhang et al., "Restoration of a critical mandibular bone defect using human alveolar bone-derived stem cells and porous nano-HA/collagen/PLA scaffold," *Stem Cells International*, vol. 2016, Article ID 8741641, 13 pages, 2016.
- [28] S. Mason, S. A. Tarle, W. Osibin, Y. Kinfu, and D. Kaigler, "Standardization and safety of alveolar bone-derived stem cell isolation," *Journal of Dental Research*, vol. 93, no. 1, pp. 55–61, 2014.
- [29] K. Pekovits, J. M. Kröpfl, I. Stelzer, M. Payer, H. Hutter, and G. Dohr, "Human mesenchymal progenitor cells derived from alveolar bone and human bone marrow stromal cells: a comparative study," *Histochemistry and Cell Biology*, vol. 140, no. 6, pp. 611–621, 2013.
- [30] S. Aydin and F. Sahin, "Stem cells derived from dental tissues," *Advances in Experimental Medicine and Biology*, vol. 1144, pp. 123–132, 2019.
- [31] D. Whiting, W. O. Chung, J. D. Johnson, and A. Paranjpe, "Characterization of the cellular responses of dental mesenchymal stem cells to the immune system," *Journal of Endodontics*, vol. 44, no. 7, pp. 1126–1131, 2018.
- [32] J. Li, S. Q. Xu, Y. M. Zhao, S. Yu, L. H. Ge, and B. H. Xu, "Comparison of the biological characteristics of human mesenchymal stem cells derived from exfoliated deciduous teeth, bone marrow, gingival tissue, and umbilical cord," *Molecular Medicine Reports*, vol. 18, no. 6, pp. 4969–4977, 2018.
- [33] X. Yang, Y. Ma, W. Guo, B. Yang, and W. Tian, "Stem cells from human exfoliated deciduous teeth as an alternative cell source in bio-root regeneration," *Theranostics*, vol. 9, no. 9, pp. 2694–2711, 2019.
- [34] T. Yamaza, A. Kentaro, C. Chen et al., "Immunomodulatory properties of stem cells from human exfoliated deciduous teeth," *Stem Cell Research & Therapy*, vol. 1, no. 1, p. 5, 2010.
- [35] Y. Y. Dai, S. Y. Ni, K. Ma, Y. S. Ma, Z. S. Wang, and X. L. Zhao, "Stem cells from human exfoliated deciduous teeth correct the immune imbalance of allergic rhinitis via Treg cells in vivo and in vitro," *Stem Cell Research & Therapy*, vol. 10, no. 1, p. 39, 2019.
- [36] B. M. Seo, W. Sonoyama, T. Yamaza et al., "SHED repair critical-size calvarial defects in mice," *Oral Diseases*, vol. 14, no. 5, pp. 428–434, 2008.
- [37] F. P. dos Santos, T. Peruch, S. J. V. Katami et al., "Poly (lactide-co-glycolide) (PLGA) scaffold induces short-term nerve regeneration and functional recovery following sciatic nerve transection in rats," *Neuroscience*, vol. 396, pp. 94–107, 2019.
- [38] J. Kang, W. Fan, Q. Deng, H. He, and F. Huang, "Stem cells from the apical papilla: a promising source for stem cell-based therapy," *BioMed Research International*, vol. 2019, Article ID 6104738, 8 pages, 2019.
- [39] B. C. Kim, S. M. Jun, S. Y. Kim et al., "Engineering three dimensional micro nerve tissue using postnatal stem cells from human dental apical papilla," *Biotechnology and Bioengineering*, vol. 114, no. 4, pp. 903–914, 2017.
- [40] G. Ding, Y. Liu, Y. An et al., "Suppression of T cell proliferation by root apical papilla stem cells in vitro," *Cells, Tissues, Organs*, vol. 191, no. 5, pp. 357–364, 2010.
- [41] J. Zhang, Y. Zhang, H. Lv et al., "Human stem cells from the apical papilla response to bacterial lipopolysaccharide

- exposure and anti-inflammatory effects of nuclear factor I C,” *Journal of Endodontics*, vol. 39, no. 11, pp. 1416–1422, 2013.
- [42] S. Ansari, I. M. Diniz, C. Chen et al., “Human periodontal ligament- and gingiva-derived mesenchymal stem cells promote nerve regeneration when encapsulated in alginate/hyaluronic acid 3D scaffold,” *Advanced Healthcare Materials*, vol. 6, no. 24, 2017.
- [43] W. Sun, Z. Wang, Q. Xu et al., “The treatment of systematically transplanted gingival mesenchymal stem cells in periodontitis in mice,” *Experimental and Therapeutic Medicine*, vol. 17, no. 3, pp. 2199–2205, 2019.
- [44] Q. Zhang, S. Shi, Y. Liu et al., “Mesenchymal stem cells derived from human gingiva are capable of immunomodulatory functions and ameliorate inflammation-related tissue destruction in experimental colitis,” *Journal of Immunology*, vol. 183, no. 12, pp. 7787–7798, 2009.
- [45] M. Chen, W. Su, X. Lin et al., “Adoptive transfer of human gingiva-derived mesenchymal stem cells ameliorates collagen-induced arthritis via suppression of Th1 and Th17 cells and enhancement of regulatory T cell differentiation,” *Arthritis and Rheumatism*, vol. 65, no. 5, pp. 1181–1193, 2013.
- [46] A. C. Calikoglu Koyuncu, G. Gurel Pekozer, M. Ramazanoglu, G. Torun Kose, and V. Hasirci, “Cartilage tissue engineering on macroporous scaffolds using human tooth germ stem cells,” *Journal of Tissue Engineering and Regenerative Medicine*, vol. 11, no. 3, pp. 765–777, 2017.
- [47] D. Guzmán-Urbe, K. N. A. Estrada, A. d. J. P. Guillén, S. M. Pérez, and R. R. Ibáñez, “Development of a three-dimensional tissue construct from dental human ectomesenchymal stem cells: in vitro and in vivo study,” *The Open Dentistry Journal*, vol. 6, no. 1, pp. 226–234, 2012.
- [48] J. Zou, M. Meng, C. S. Law, Y. Rao, and X. Zhou, “Common dental diseases in children and malocclusion,” *International Journal of Oral Science*, vol. 10, no. 1, 2018.
- [49] W. Ono, N. Sakagami, S. Nishimori, N. Ono, and H. M. Kronenberg, “Parathyroid hormone receptor signalling in osterix-expressing mesenchymal progenitors is essential for tooth root formation,” *Nature Communications*, vol. 7, no. 1, article 11277, 2016.
- [50] H. Sun, Q. Li, Y. Zhang et al., “Regulation of OPG and RANKL expressed by human dental follicle cells in osteoclastogenesis,” *Cell and Tissue Research*, vol. 362, no. 2, pp. 399–405, 2015.
- [51] J. Zhang, L. Liao, Y. Li et al., “Parathyroid hormone-related peptide (1-34) promotes tooth eruption and inhibits osteogenesis of dental follicle cells during tooth development,” *Journal of Cellular Physiology*, vol. 234, no. 7, pp. 11900–11911, 2019.
- [52] E. Nemoto, Y. Sakisaka, M. Tsuchiya et al., “Wnt3a signaling induces murine dental follicle cells to differentiate into cementoblastic/osteoblastic cells via an osterix-dependent pathway,” *Journal of Periodontal Research*, vol. 51, no. 2, pp. 164–174, 2016.
- [53] M. J. Honda, M. Imaizumi, S. Tsuchiya, and C. Morsczeck, “Dental follicle stem cells and tissue engineering,” *Journal of Oral Science*, vol. 52, no. 4, pp. 541–552, 2010.
- [54] S. Yao, C. Li, M. Beckley, and D. Liu, “Expression of odontogenic ameloblast-associated protein in the dental follicle and its role in osteogenic differentiation of dental follicle stem cells,” *Archives of Oral Biology*, vol. 78, pp. 6–12, 2017.
- [55] R. M. Wazen, P. Moffatt, K. J. Ponce, S. Kuroda, C. Nishio, and A. Nanci, “Inactivation of the odontogenic ameloblast-associated gene affects the integrity of the junctional epithelium and gingival healing,” *European Cells & Materials*, vol. 30, pp. 187–199, 2015.
- [56] J. Ge, S. Guo, Y. Fu et al., “Dental follicle cells participate in tooth eruption via the RUNX2-MiR-31-SATB2 loop,” *Journal of Dental Research*, vol. 94, no. 7, pp. 936–944, 2015.
- [57] Y. Liu, X. Zhang, X. Sun, X. Wang, C. Zhang, and S. Zheng, “Abnormal bone remodelling activity of dental follicle cells from a cleidocranial dysplasia patient,” *Oral Diseases*, vol. 24, no. 7, pp. 1270–1281, 2018.
- [58] Y. Liu, X. Sun, X. Zhang, X. Wang, C. Zhang, and S. Zheng, “RUNX2 mutation impairs osteogenic differentiation of dental follicle cells,” *Archives of Oral Biology*, vol. 97, pp. 156–164, 2019.
- [59] Z. Peng, L. Liu, X. Wei, and J. Ling, “Expression of Oct-4, SOX-2, and MYC in dental papilla cells and dental follicle cells during in-vivo tooth development and in-vitro co-culture,” *European Journal of Oral Sciences*, vol. 122, no. 4, pp. 251–258, 2014.
- [60] F. Angiero, C. Rossi, A. Ferri et al., “Stromal phenotype of dental follicle stem cells,” *Frontiers in Bioscience*, vol. E4, no. 3, pp. 1009–1014, 2012.
- [61] G. T. Huang, S. Gronthos, and S. Shi, “Mesenchymal stem cells derived from dental tissues vs. those from other sources: their biology and role in regenerative medicine,” *Journal of Dental Research*, vol. 88, no. 9, pp. 792–806, 2009.
- [62] S. Guo, W. Guo, Y. Ding et al., “Comparative study of human dental follicle cell sheets and periodontal ligament cell sheets for periodontal tissue regeneration,” *Cell Transplantation*, vol. 22, no. 6, pp. 1061–1073, 2013.
- [63] X. Chen, T. Zhang, J. Shi et al., “Notch1 signaling regulates the proliferation and self-renewal of human dental follicle cells by modulating the G1/S phase transition and telomerase activity,” *PLoS One*, vol. 8, no. 7, article e69967, 2013.
- [64] C. Morsczeck, W. Götz, J. Schierholz et al., “Isolation of precursor cells (PCs) from human dental follicle of wisdom teeth,” *Matrix Biology*, vol. 24, no. 2, pp. 155–165, 2005.
- [65] F. Vollner, W. Ernst, O. Driemel, and C. Morsczeck, “A two-step strategy for neuronal differentiation in vitro of human dental follicle cells,” *Differentiation*, vol. 77, no. 5, pp. 433–441, 2009.
- [66] G. Mori, A. Ballini, C. Carbone et al., “Osteogenic differentiation of dental follicle stem cells,” *International Journal of Medical Sciences*, vol. 9, no. 6, pp. 480–487, 2012.
- [67] C. Morsczeck, “Gene expression of runx2, Osterix, c-fos, DLX-3, DLX-5, and MSX-2 in dental follicle cells during osteogenic differentiation in vitro,” *Calcified Tissue International*, vol. 78, no. 2, pp. 98–102, 2006.
- [68] O. Felthaus, M. Gosau, and C. Morsczeck, “ZBTB16 induces osteogenic differentiation marker genes in dental follicle cells independent from RUNX2,” *Journal of Periodontology*, vol. 85, no. 5, pp. e144–e151, 2014.
- [69] Y. Tamaki, T. Nakahara, H. Ishikawa, and S. Sato, “In vitro analysis of mesenchymal stem cells derived from human teeth and bone marrow,” *Odontology*, vol. 101, no. 2, pp. 121–132, 2013.
- [70] A. Kaneda, T. Fujita, M. Anai et al., “Activation of Bmp2-Smad1 signal and its regulation by coordinated alteration of

- H3K27 trimethylation in Ras-induced senescence,” *PLoS Genetics*, vol. 7, no. 11, article e1002359, 2011.
- [71] Y. Açı, F. Yang, A. Gulsels, M. Ayna, J. Wiltfang, and M. Gierloff, “Isolation, characterization and investigation of differentiation potential of human periodontal ligament cells and dental follicle progenitor cells and their response to BMP-7 in vitro,” *Odontology*, vol. 104, no. 2, pp. 123–135, 2016.
- [72] S. Yao, H. He, D. L. Gutierrez et al., “Expression of bone morphogenetic protein-6 in dental follicle stem cells and its effect on osteogenic differentiation,” *Cells, Tissues, Organs*, vol. 198, no. 6, pp. 438–447, 2014.
- [73] C. Li, X. Yang, Y. He et al., “Bone morphogenetic protein-9 induces osteogenic differentiation of rat dental follicle stem cells in P38 and ERK1/2 MAPK dependent manner,” *International Journal of Medical Sciences*, vol. 9, no. 10, pp. 862–871, 2012.
- [74] K. Takahashi, N. Ogura, H. Aonuma et al., “Bone morphogenetic protein 6 stimulates mineralization in human dental follicle cells without dexamethasone,” *Archives of Oral Biology*, vol. 58, no. 6, pp. 690–698, 2013.
- [75] Y. Du, J. Li, Y. Hou, C. Chen, W. Long, and H. Jiang, “Alteration of circular RNA expression in rat dental follicle cells during osteogenic differentiation,” *Journal of Cellular Biochemistry*, vol. 120, no. 8, pp. 13289–13301, 2019.
- [76] S. Viale-Bouroncle, O. Felthaus, G. Schmalz, G. Brockhoff, T. E. Reichert, and C. Morsczeck, “The transcription factor DLX3 regulates the osteogenic differentiation of human dental follicle precursor cells,” *Stem Cells and Development*, vol. 21, no. 11, pp. 1936–1947, 2012.
- [77] S. Viale-Bouroncle, M. Gosau, and C. Morsczeck, “NOTCH1 signaling regulates the BMP2/DLX-3 directed osteogenic differentiation of dental follicle cells,” *Biochemical and Biophysical Research Communications*, vol. 443, no. 2, pp. 500–504, 2014.
- [78] S. Viale-Bouroncle, C. Klingelhofer, T. Ettl, T. E. Reichert, and C. Morsczeck, “A protein kinase A (PKA)/ $\beta$ -catenin pathway sustains the BMP2/DLX3-induced osteogenic differentiation in dental follicle cells (DFCs),” *Cellular Signalling*, vol. 27, no. 3, pp. 598–605, 2015.
- [79] C. Morsczeck, A. Reck, and H. C. Beck, “The hedgehog-signaling pathway is repressed during the osteogenic differentiation of dental follicle cells,” *Molecular and Cellular Biochemistry*, vol. 428, no. 1-2, pp. 79–86, 2017.
- [80] C. Klingelhofer, A. Reck, T. Ettl, and C. Morsczeck, “The parathyroid hormone-related protein is secreted during the osteogenic differentiation of human dental follicle cells and inhibits the alkaline phosphatase activity and the expression of DLX3,” *Tissue & Cell*, vol. 48, no. 4, pp. 334–339, 2016.
- [81] C. Y. Logan and R. Nusse, “The Wnt signaling pathway in development and disease,” *Annual Review of Cell and Developmental Biology*, vol. 20, no. 1, pp. 781–810, 2004.
- [82] Y. du, J. Ling, X. Wei et al., “Wnt/ $\beta$ -catenin signaling participates in cementoblast/osteoblast differentiation of dental follicle cells,” *Connective Tissue Research*, vol. 53, no. 5, pp. 390–397, 2012.
- [83] S. Viale-Bouroncle, C. Klingelhofer, T. Ettl, and C. Morsczeck, “The WNT inhibitor APCDD1 sustains the expression of  $\beta$ -catenin during the osteogenic differentiation of human dental follicle cells,” *Biochemical and Biophysical Research Communications*, vol. 457, no. 3, pp. 314–317, 2015.
- [84] K. G. Silvério, K. C. Davidson, R. G. James et al., “Wnt/ $\beta$ -catenin pathway regulates bone morphogenetic protein (BMP2)-mediated differentiation of dental follicle cells,” *Journal of Periodontal Research*, vol. 47, no. 3, pp. 309–319, 2012.
- [85] X. Zhang, Y. du, J. Ling, W. Li, Y. Liao, and X. Wei, “Dickkopf-related protein 3 negatively regulates the osteogenic differentiation of rat dental follicle cells,” *Molecular Medicine Reports*, vol. 15, no. 4, pp. 1673–1681, 2017.
- [86] S. Jiang, G. Chen, L. Feng et al., “Disruption of kif3a results in defective osteoblastic differentiation in dental mesenchymal stem/precursor cells via the Wnt signaling pathway,” *Molecular Medicine Reports*, vol. 14, no. 3, pp. 1891–1900, 2016.
- [87] C. Chen, J. Zhan, J. Ling, Y. du, and Y. Hou, “Nkd2 promotes the differentiation of dental follicle stem/progenitor cells into osteoblasts,” *International Journal of Molecular Medicine*, vol. 42, no. 5, pp. 2403–2414, 2018.
- [88] L. Deng, H. Hong, X. Zhang et al., “Down-regulated lncRNA MEG3 promotes osteogenic differentiation of human dental follicle stem cells by epigenetically regulating Wnt pathway,” *Biochemical and Biophysical Research Communications*, vol. 503, no. 3, pp. 2061–2067, 2018.
- [89] C. Wang, Y. Zhao, Y. Su et al., “C-Jun N-terminal kinase (JNK) mediates Wnt5a-induced cell motility dependent or independent of RhoA pathway in human dental papilla cells,” *PLoS One*, vol. 8, no. 7, article e69440, 2013.
- [90] L. Fu, T. Tang, Y. Miao, S. Zhang, Z. Qu, and K. Dai, “Stimulation of osteogenic differentiation and inhibition of adipogenic differentiation in bone marrow stromal cells by alendronate via ERK and JNK activation,” *Bone*, vol. 43, no. 1, pp. 40–47, 2008.
- [91] L. Xiang, M. Chen, L. He et al., “Wnt5a regulates dental follicle stem/progenitor cells of the periodontium,” *Stem Cell Research & Therapy*, vol. 5, no. 6, p. 135, 2014.
- [92] Y. Sakisaka, M. Tsuchiya, T. Nakamura, M. Tamura, H. Shimauchi, and E. Nemoto, “Wnt5a attenuates Wnt3a-induced alkaline phosphatase expression in dental follicle cells,” *Experimental Cell Research*, vol. 336, no. 1, pp. 85–93, 2015.
- [93] O. Felthaus, S. Viale-Bouroncle, O. Driemel, T. E. Reichert, G. Schmalz, and C. Morsczeck, “Transcription factors TP53 and SP1 and the osteogenic differentiation of dental stem cells,” *Differentiation*, vol. 83, no. 1, pp. 10–16, 2012.
- [94] O. Felthaus, M. Gosau, S. Klein et al., “Dexamethasone-related osteogenic differentiation of dental follicle cells depends on ZBTB16 but not Runx2,” *Cell and Tissue Research*, vol. 357, no. 3, pp. 695–705, 2014.
- [95] C. Morsczeck and T. E. Reichert, “The dexamethasone induced osteogenic differentiation of dental follicle cells,” *Histology and Histopathology*, vol. 32, no. 12, pp. 1223–1229, 2017.
- [96] T. Press, S. Viale-Bouroncle, O. Felthaus, M. Gosau, and C. Morsczeck, “EGR1 supports the osteogenic differentiation of dental stem cells,” *International Endodontic Journal*, vol. 48, no. 2, pp. 185–192, 2015.
- [97] M. Rezaei Rad, D. Liu, H. He et al., “The role of dentin matrix protein 1 (DMP1) in regulation of osteogenic differentiation of rat dental follicle stem cells (DFSCs),” *Archives of Oral Biology*, vol. 60, no. 4, pp. 546–556, 2015.
- [98] S. Viale-Bouroncle, F. Völlner, C. Möhl et al., “Soft matrix supports osteogenic differentiation of human dental follicle cells,” *Biochemical and Biophysical Research Communications*, vol. 410, no. 3, pp. 587–592, 2011.
- [99] M. Rezaei Rad, G. E. Wise, H. Brooks, M. B. Flanagan, and S. Yao, “Activation of proliferation and differentiation of

- dental follicle stem cells (DFSCs) by heat stress," *Cell Proliferation*, vol. 46, no. 1, pp. 58–66, 2013.
- [100] X. Wu, L. Hu, Y. Li et al., "SCAPs regulate differentiation of DFSCs during tooth root development in swine," *International Journal of Medical Sciences*, vol. 15, no. 4, pp. 291–299, 2018.
- [101] J. S. Bok, S. H. Byun, B. W. Park et al., "The role of human umbilical vein endothelial cells in osteogenic differentiation of dental follicle-derived stem cells in in vitro co-cultures," *International Journal of Medical Sciences*, vol. 15, no. 11, pp. 1160–1170, 2018.
- [102] W. Ernst, M. Saugspier, O. Felthaus, O. Driemel, and C. Morsczeck, "Comparison of murine dental follicle precursor and retinal progenitor cells after neural differentiation in vitro," *Cell Biology International*, vol. 33, no. 7, pp. 758–764, 2009.
- [103] O. Felthaus, W. Ernst, O. Driemel, T. E. Reichert, G. Schmalz, and C. Morsczeck, "TGF-beta stimulates glial-like differentiation in murine dental follicle precursor cells (mDFPCs)," *Neuroscience Letters*, vol. 471, no. 3, pp. 179–184, 2010.
- [104] N. Daviaud, E. Garbayo, P. C. Schiller, M. Perez-Pinzon, and C. N. Montero-Menei, "Organotypic cultures as tools for optimizing central nervous system cell therapies," *Experimental Neurology*, vol. 248, pp. 429–440, 2013.
- [105] C. Yang, L. Sun, X. Li et al., "The potential of dental stem cells differentiating into neurogenic cell lineage after cultivation in different modes in vitro," *Cellular Reprogramming*, vol. 16, no. 5, pp. 379–391, 2014.
- [106] B. C. Heng, T. Gong, S. Wang, L. W. Lim, W. Wu, and C. Zhang, "Decellularized matrix derived from neural differentiation of embryonic stem cells enhances the neurogenic potential of dental follicle stem cells," *Journal of Endodontics*, vol. 43, no. 3, pp. 409–416, 2017.
- [107] H. S. Jung, D. S. Lee, J. H. Lee et al., "Directing the differentiation of human dental follicle cells into cementoblasts and/or osteoblasts by a combination of HERS and pulp cells," *Journal of Molecular Histology*, vol. 42, no. 3, pp. 227–235, 2011.
- [108] H. Yamamoto, S. W. Cho, E. J. Kim, J. Y. Kim, N. Fujiwara, and H. S. Jung, "Developmental properties of the Hertwig's epithelial root sheath in mice," *Journal of Dental Research*, vol. 83, no. 9, pp. 688–692, 2004.
- [109] M. Saito, M. Iwase, S. Maslan et al., "Expression of cementum-derived attachment protein in bovine tooth germ during cementogenesis," *Bone*, vol. 29, no. 3, pp. 242–248, 2001.
- [110] K. Handa, M. Saito, A. Tsunoda et al., "Progenitor cells from dental follicle are able to form cementum matrix in vivo," *Connective Tissue Research*, vol. 43, no. 2-3, pp. 406–408, 2002.
- [111] K. Handa, M. Saito, M. Yamauchi et al., "Cementum matrix formation in vivo by cultured dental follicle cells," *Bone*, vol. 31, no. 5, pp. 606–611, 2002.
- [112] J. Wu, F. Jin, L. Tang et al., "Dentin non-collagenous proteins (dNCPs) can stimulate dental follicle cells to differentiate into cementoblast lineages," *Biology of the Cell*, vol. 100, no. 5, pp. 291–302, 2008.
- [113] P. Kémoun, S. Laurencin-Dalicieux, J. Rue et al., "Human dental follicle cells acquire cementoblast features under stimulation by BMP-2/-7 and enamel matrix derivatives (EMD) in vitro," *Cell and Tissue Research*, vol. 329, no. 2, pp. 283–294, 2007.
- [114] C. Han, Z. Yang, W. Zhou et al., "Periapical follicle stem cell: a promising candidate for cementum/periodontal ligament regeneration and bio-root engineering," *Stem Cells and Development*, vol. 19, no. 9, pp. 1405–1415, 2010.
- [115] A. Orimoto, M. Kurokawa, K. Handa et al., "F-spondin negatively regulates dental follicle differentiation through the inhibition of TGF- $\beta$  activity," *Archives of Oral Biology*, vol. 79, pp. 7–13, 2017.
- [116] Y. Y. Jo, H. J. Lee, S. Y. Kook et al., "Isolation and characterization of postnatal stem cells from human dental tissues," *Tissue Engineering*, vol. 13, no. 4, pp. 767–773, 2007.
- [117] P. Nelson, T. D. Ngoc Tran, H. Zhang et al., "Transient receptor potential melastatin 4 channel controls calcium signals and dental follicle stem cell differentiation," *Stem Cells*, vol. 31, no. 1, pp. 167–177, 2013.
- [118] L. Guo, J. Li, X. Qiao et al., "Comparison of odontogenic differentiation of human dental follicle cells and human dental papilla cells," *PLoS One*, vol. 8, no. 4, article e62332, 2013.
- [119] G. Chen, Q. Sun, L. Xie et al., "Comparison of the odontogenic differentiation potential of dental follicle, dental papilla, and cranial neural crest cells," *Journal of Endodontics*, vol. 41, no. 7, pp. 1091–1099, 2015.
- [120] I. Y. Sung, H. N. Son, I. Ullah et al., "Cardiomyogenic differentiation of human dental follicle-derived stem cells by suberoylanilide hydroxamic acid and their in vivo homing property," *International Journal of Medical Sciences*, vol. 13, no. 11, pp. 841–852, 2016.
- [121] K. Chatzivasilieou, C. A. Lux, G. Steinhoff, and H. Lang, "Dental follicle progenitor cells responses to Porphyromonas gingivalis LPS," *Journal of Cellular and Molecular Medicine*, vol. 17, no. 6, pp. 766–773, 2013.
- [122] P. G. Stathopoulou, M. R. Benakanakere, J. C. Galicia, and D. F. Kinane, "Epithelial cell pro-inflammatory cytokine response differs across dental plaque bacterial species," *Journal of Clinical Periodontology*, vol. 37, no. 1, pp. 24–29, 2010.
- [123] A. Biedermann, K. Kriebel, B. Kreikemeyer, and H. Lang, "Interactions of anaerobic bacteria with dental stem cells: an in vitro study," *PLoS One*, vol. 9, no. 11, article e110616, 2014.
- [124] K. Nomiya, C. Kitamura, T. Tsujisawa et al., "Effects of lipopolysaccharide on newly established rat dental pulp-derived cell line with odontoblastic properties," *Journal of Endodontics*, vol. 33, no. 10, pp. 1187–1191, 2007.
- [125] C. O. Morsczeck, J. Dress, and M. Gosau, "Lipopolysaccharide from Escherichia coli but not from Porphyromonas gingivalis induce pro-inflammatory cytokines and alkaline phosphatase in dental follicle cells," *Archives of Oral Biology*, vol. 57, no. 12, pp. 1595–1601, 2012.
- [126] S. Um, J. H. Lee, and B. M. Seo, "TGF- $\beta$ 2 downregulates osteogenesis under inflammatory conditions in dental follicle stem cells," *International Journal of Oral Science*, vol. 10, no. 3, p. 29, 2018.
- [127] C. Hieke, K. Kriebel, R. Engelmann, B. Müller-Hilke, H. Lang, and B. Kreikemeyer, "Human dental stem cells suppress PMN activity after infection with the periodontopathogens Prevotella intermedia and Tannerella forsythia," *Scientific Reports*, vol. 6, no. 1, article 39096, 2016.
- [128] X. Chen, B. Yang, J. Tian et al., "Dental follicle stem cells ameliorate lipopolysaccharide-induced inflammation by secreting TGF- $\beta$ 3 and TSP-1 to elicit macrophage M2 polarization," *Cellular Physiology and Biochemistry*, vol. 51, no. 5, pp. 2290–2308, 2018.
- [129] D. Genç, N. Zibandeh, E. Nain et al., "IFN- $\gamma$  stimulation of dental follicle mesenchymal stem cells modulates immune

- response of CD4<sup>+</sup> T lymphocytes in Der p1<sup>+</sup> asthmatic patients in vitro," *Allergologia et Immunopathologia*, vol. 47, no. 5, pp. 467–476, 2019.
- [130] D. Genç, N. Zibandeh, E. Nain et al., "Dental follicle mesenchymal stem cells down-regulate Th2-mediated immune response in asthmatic patients mononuclear cells," *Clinical and Experimental Allergy*, vol. 48, no. 6, pp. 663–678, 2018.
- [131] C. Ulusoy, N. Zibandeh, S. Yıldırım et al., "Dental follicle mesenchymal stem cell administration ameliorates muscle weakness in MuSK-immunized mice," *Journal of Neuroinflammation*, vol. 12, no. 1, p. 231, 2015.
- [132] R. Shinagawa-Ohama, M. Mochizuki, Y. Tamaki, N. Suda, and T. Nakahara, "Heterogeneous human periodontal ligament-committed progenitor and stem cell populations exhibit a unique cementogenic property under in vitro and in vivo conditions," *Stem Cells and Development*, vol. 26, no. 9, pp. 632–645, 2017.
- [133] H. Yang, J. Li, J. Sun et al., "Cells isolated from cryopreserved dental follicle display similar characteristics to cryopreserved dental follicle cells," *Cryobiology*, vol. 78, pp. 47–55, 2017.
- [134] B. W. Park, S. J. Jang, J. H. Byun et al., "Cryopreservation of human dental follicle tissue for use as a resource of autologous mesenchymal stem cells," *Journal of Tissue Engineering and Regenerative Medicine*, vol. 11, no. 2, pp. 489–500, 2017.
- [135] J. C. Estrada, Y. Torres, A. Benguría et al., "Human mesenchymal stem cell-replicative senescence and oxidative stress are closely linked to aneuploidy," *Cell Death & Disease*, vol. 4, no. 6, article e691, 2013.
- [136] R. A. J. Signer and S. J. Morrison, "Mechanisms that regulate stem cell aging and life span," *Cell Stem Cell*, vol. 12, no. 2, pp. 152–165, 2013.
- [137] C. Morsczeck, J. Gresser, and T. Ettl, "The induction of cellular senescence in dental follicle cells inhibits the osteogenic differentiation," *Molecular and Cellular Biochemistry*, vol. 417, no. 1–2, pp. 1–6, 2016.
- [138] C. Morsczeck, A. Reck, and T. E. Reichert, "Short telomeres correlate with a strong induction of cellular senescence in human dental follicle cells," *BMC Molecular and Cell Biology*, vol. 20, no. 1, p. 5, 2019.
- [139] C. Morsczeck, M. Hullmann, A. Reck, and T. E. Reichert, "The cell cycle regulator protein P16 and the cellular senescence of dental follicle cells," *Molecular and Cellular Biochemistry*, vol. 439, no. 1–2, pp. 45–52, 2018.
- [140] L. Borghese, D. Dolezalova, T. Opitz et al., "Inhibition of notch signaling in human embryonic stem cell-derived neural stem cells delays G1/S phase transition and accelerates neuronal differentiation in vitro and in vivo," *Stem Cells*, vol. 28, no. 5, pp. 955–964, 2010.
- [141] X. Chen, S. Li, Z. Zeng et al., "Notch1 signalling inhibits apoptosis of human dental follicle stem cells via both the cytoplasmic mitochondrial pathway and nuclear transcription regulation," *The International Journal of Biochemistry & Cell Biology*, vol. 82, pp. 18–27, 2017.
- [142] S. Viale-Bouroncle, R. Buegers, C. Morsczeck, and M. Gosau, "β-tricalcium phosphate induces apoptosis on dental follicle cells," *Calcified Tissue International*, vol. 92, no. 5, pp. 412–417, 2013.
- [143] Y. Zhai, R. Wei, J. Liu et al., "Drug-induced premature senescence model in human dental follicle stem cells," *Oncotarget*, vol. 8, no. 5, pp. 7276–7293, 2017.
- [144] M. Gosau, S. Viale-Bouroncle, H. Eickhoff et al., "Evaluation of implant-materials as cell carriers for dental stem cells under in vitro conditions," *International Journal of Implant Dentistry*, vol. 1, no. 1, p. 2, 2015.
- [145] S. Viale-Bouroncle, B. Bey, T. E. Reichert, G. Schmalz, and C. Morsczeck, "β-tricalcium-phosphate stimulates the differentiation of dental follicle cells," *Journal of Materials Science: Materials in Medicine*, vol. 22, no. 7, pp. 1719–1724, 2011.
- [146] M. Rezai-Rad, J. F. Bova, M. Orooji et al., "Evaluation of bone regeneration potential of dental follicle stem cells for treatment of craniofacial defects," *Cytotherapy*, vol. 17, no. 11, pp. 1572–1581, 2015.
- [147] L. Nie, X. Yang, L. Duan et al., "The healing of alveolar bone defects with novel bio-implants composed of Ad-BMP9-transfected rDFCs and CHA scaffolds," *Scientific Reports*, vol. 7, no. 1, article 6373, 2017.
- [148] O. Lucaci, O. Sorițău, D. Gheban et al., "Dental follicle stem cells in bone regeneration on titanium implants," *BMC Biotechnology*, vol. 15, no. 1, p. 114, 2015.
- [149] K. Takahashi, N. Ogura, R. Tomoki et al., "Applicability of human dental follicle cells to bone regeneration without dexamethasone: an in vivo pilot study," *International Journal of Oral and Maxillofacial Surgery*, vol. 44, no. 5, pp. 664–669, 2015.
- [150] S. Sowmya, U. Mony, P. Jayachandran et al., "Tri-layered nanocomposite hydrogel scaffold for the concurrent regeneration of cementum, periodontal ligament, and alveolar bone," *Advanced Healthcare Materials*, vol. 6, no. 7, 2017.
- [151] I. Veernala, J. Giri, A. Pradhan, P. Polley, R. Singh, and S. K. Yadava, "Effect of fluoride doping in laponite nanoplatelets on osteogenic differentiation of human dental follicle stem cells (hDFSCs)," *Scientific Reports*, vol. 9, no. 1, p. 915, 2019.
- [152] W. Guo, K. Gong, H. Shi et al., "Dental follicle cells and treated dentin matrix scaffold for tissue engineering the tooth root," *Biomaterials*, vol. 33, no. 5, pp. 1291–1302, 2012.
- [153] X. Luo, B. Yang, L. Sheng et al., "CAD based design sensitivity analysis and shape optimization of scaffolds for bio-root regeneration in swine," *Biomaterials*, vol. 57, pp. 59–72, 2015.
- [154] J. Sun, J. Li, H. Li et al., "tBHQ suppresses osteoclastic resorption in xenogeneic-treated dentin matrix-based scaffolds," *Advanced Healthcare Materials*, vol. 6, no. 18, 2017.
- [155] K. Hynes, D. Menicanin, S. Gronthos, and P. M. Bartold, "Clinical utility of stem cells for periodontal regeneration," *Periodontology 2000*, vol. 59, no. 1, pp. 203–227, 2012.
- [156] M. Oshima, K. Inoue, K. Nakajima et al., "Functional tooth restoration by next-generation bio-hybrid implant as a bio-hybrid artificial organ replacement therapy," *Scientific Reports*, vol. 4, no. 1, article 6044, 2015.
- [157] M. Nivedhitha Sundaram, S. Sowmya, S. Deepthi, J. D. Bumgardener, and R. Jayakumar, "Bilayered construct for simultaneous regeneration of alveolar bone and periodontal ligament," *Journal of Biomedical Materials Research: Part B, Applied Biomaterials*, vol. 104, no. 4, pp. 761–770, 2016.
- [158] X. Li, C. Yang, L. Li et al., "A therapeutic strategy for spinal cord defect: human dental follicle cells combined with aligned PCL/PLGA electrospun material," *BioMed Research International*, vol. 2015, Article ID 197183, 12 pages, 2015.
- [159] S. Yao, D. L. Gutierrez, H. He, Y. Dai, D. Liu, and G. E. Wise, "Proliferation of dental follicle-derived cell populations in heat-stress conditions," *Cell Proliferation*, vol. 44, no. 5, pp. 486–493, 2011.



- [160] B. C. Kim, H. Bae, I. K. Kwon et al., "Osteoblastic/cementoblastic and neural differentiation of dental stem cells and their applications to tissue engineering and regenerative medicine," *Tissue Engineering Part B: Reviews*, vol. 18, no. 3, pp. 235–244, 2012.
- [161] P. Ercal, G. G. Pekozer, and G. T. Kose, "Dental stem cells in bone tissue engineering: current overview and challenges," *Advances in Experimental Medicine and Biology*, vol. 1107, pp. 113–127, 2018.

## Research Article

# Local Application of Semaphorin 3A Combined with Adipose-Derived Stem Cell Sheet and Anorganic Bovine Bone Granules Enhances Bone Regeneration in Type 2 Diabetes Mellitus Rats

Xiaoru Xu , Kaixiu Fang, Lifeng Wang, Xiangwei Liu, Yuchao Zhou, and Yingliang Song 

State Key Laboratory of Military Stomatology & National Clinical Research Center for Oral Diseases & Shaanxi Engineering Research Center for Dental Materials and Advanced Manufacture, Department of Implantology, School of Stomatology, The Fourth Military Medical University, Xi'an, 710032 Shaanxi, China

Correspondence should be addressed to Yingliang Song; [songyingliang@163.com](mailto:songyingliang@163.com)

Received 4 April 2019; Accepted 8 July 2019; Published 31 July 2019

Guest Editor: Toru Ogasawara

Copyright © 2019 Xiaoru Xu et al. This is an open access article distributed under the Creative Commons Attribution License, which permits unrestricted use, distribution, and reproduction in any medium, provided the original work is properly cited.

Bone tissue regeneration is considered to be the optimal solution for bone loss. However, diabetic patients have a greater risk of poor bone healing or bone grafting failure than nondiabetics. The purpose of this study was to investigate the influence of the complexes of an adipose-derived stem cell sheet (ASC sheet) and Bio-Oss® bone granules on bone healing in type 2 diabetes mellitus (T2DM) rats with the addition of semaphorin 3A (Sema3A). The rat ASC sheets showed stronger osteogenic ability than ASCs *in vitro*, as indicated by the extracellular matrix mineralization and the expression of osteogenesis-related genes at mRNA level. An ASC sheet combined with Bio-Oss® bone granules promoted bone formation in T2DM rats as indicated by microcomputed tomography (micro-CT) and histological analysis. In addition, Sema3A promoted the osteogenic differentiation of ASC sheets *in vitro* and local injection of Sema3A promoted T2DM rats' calvarial bone regeneration based on ASC sheet and Bio-Oss® bone granule complex treatment. In conclusion, the local injection of Sema3A and the complexes of ASC sheet and Bio-Oss® bone granules could promote osseous healing and are potentially useful to improve bone healing for T2DM patients.

## 1. Background/Introduction

Bone regeneration of bone defects is a challenge in patients with type 2 diabetes mellitus (T2DM). Diabetic patients have a greater risk of poor bone healing or bone grafting failure than nondiabetics [1–3]. Hundreds of millions of people suffer from diabetes, and China has the largest amount of diabetic patients in the world [4]; therefore, there is a high demand for improving the healing of alveolar bone defects in T2DM patients. In addition to traditional tissue transplants like autografts, allografts, and xenografts, stem cell-based tissue engineering of bone has become a brand-new and prospective remedy for bone healing. Many kinds of MSCs, such as bone marrow mesenchymal stem cells (BMSCs) [5], adipose-derived stem cells (ASCs) [6], human umbilical cord mesenchymal stromal cells [7], and human periodontal ligament stem cells (PDLSCs) [8] have been used to improve the bone healing in diabetics. ASCs have a good

capacity for self-renewal, have a multipotential ability, are abundantly available, and are less likely to cause donor-associated morbidity [9–11]; thus, they provide promising seed cells for bone tissue engineering. Studies have proved that the local application of ASCs could enhance bone regeneration in the T2DM model [12, 13]. However, T2DM can affect biological characteristics and osteoblastic differentiation of MSCs through many factors [14, 15]. Measures should be taken to improve the osteogenic ability of ASCs in T2DM. Cell sheet engineering is one of the most promising approaches of tissue engineering in recent years. It can perfectly preserve cultured cells, extracellular matrix (ECM), and cell-cell and cell-ECM connections, avoiding the use of enzymes [16]. Semaphorin 3A (Sema3A) is a member of the semaphorin family. Researches show that Sema3A can promote osteogenic differentiation and inhibit osteoclast differentiation, in addition to the important role on neurological development and healing [17, 18]. Our previous study

showed that overexpression of Sema3A in ASCs significantly enhanced the osteogenic ability of ASCs [19]. Bio-Oss® bone granules are anorganic bovine bone substitutes that are widely used in clinics due to their osteoconductivity and good biological compatibility [20, 21]. To compensate for their poor osteoinductivity, Bio-Oss® bone granules can be used as a scaffold in combination with MSCs. The present study assessed the osteogenic capacity of adipose-derived stem cell sheets (ASC sheets) *in vitro*. ASC sheets and Bio-Oss® bone granules were used to make tissue-engineered bone and were applied to T2DM rats. We found that ASC sheets with strong osteogenic capacity could promote bone healing in the T2DM model. Besides, the local injection of Sema3A could further improve bone regeneration in the T2DM model. Our study has revealed that tissue engineering of bone which was established using an ASC sheet, Bio-Oss® bone granules, as well as Sema3A holds a promising approach for bone regeneration in the future.

## 2. Materials and Methods

**2.1. Animals.** All animal experimental procedures were conducted in accordance with the committee guidelines of the Laboratory Animal Care & Welfare Committee, School of Stomatology, Fourth Military Medical University, China. Four-week-old Sprague-Dawley rats were used for the isolation of ASCs. Eight-week-old male SD rats were purchased to induce T2DM models and then used in animal experiments. Animals were maintained in specific pathogen-free conditions under a 12h light/dark cycle with access to a high-fat diet, at 26°C and a humidity of 30-70% throughout the study.

**2.2. Isolation and Characterization of Adipose-Derived Stem Cells (ASCs).** After being executed by cervical dissection, the rats were submerged in 70% ethanol for 5 min. The inguinal fat pads were obtained under sterile conditions. After being washed with phosphate-buffered saline (PBS) (Gibco, USA), the fresh adipose tissue was minced into paste, digested in an equal volume of 0.1% collagenase type I (Sigma-Aldrich, USA) at 37°C for 40 min, and filtered with a sterile stainless steel sieve (75  $\mu$ m mesh). The filtrate was centrifuged at 1,200 rpm for 5 min, resuspended in 10 mL PBS, and centrifuged again. The cells were cultured in a complete medium consisting of  $\alpha$ -minimum essential media ( $\alpha$ -MEM) (Gibco, USA), 10% fetal bovine serum (Sijiqing, China), and 1% penicillin/streptomycin (HyClone, USA) and incubated at 37°C in a humidified atmosphere of 5% CO<sub>2</sub> and 95% air. Cells of passage 3 were used for the follow-up experiments.

To determine the multilineage differentiation capacity of the ASCs, the cells were plated in six-well culture plates and the culture medium was changed to osteogenic or adipogenic medium when the cells reached 80% confluence. The osteoinductive medium was prepared using  $\alpha$ -MEM (Gibco, USA) supplemented with 10% FBS (Sijiqing, China), 0.1 mM dexamethasone (Sigma-Aldrich, USA), 5 mM  $\beta$ -glycerophosphate (Sigma-Aldrich, USA), 50  $\mu$ g/mL L-ascorbic acid (Sigma-Aldrich, USA), and 1% penicillin/streptomycin (HyClone, USA). The adipogenic medium was composed of

$\alpha$ -MEM (Gibco, USA) containing 10% FBS (Sijiqing, China), 1% penicillin/streptomycin (HyClone, USA), 0.5 mM 3-isobutyl-1-methylxanthine (IBMX, France), 1  $\mu$ M dexamethasone (Sigma-Aldrich, USA), 0.1 mM indomethacin (Sigma-Aldrich, USA), and 10  $\mu$ g/mL insulin (Sigma-Aldrich, USA). The osteogenic or adipogenic induction medium was changed every 3 days. The calcium deposits yielded by the ASCs were visualized by Alizarin Red staining (Sigma-Aldrich, USA) after osteogenic induction for 28 days, while lipid droplets were revealed by Oil Red O staining (Sigma-Aldrich, USA) after adipogenic induction for 14 days.

**2.3. Immunophenotype of ASCs.** Some  $1 \times 10^6$  third-passage ASCs were fixed with 4% paraformaldehyde for 15 min and then incubated with phycoerythrin- (PE-) or fluorescein isothiocyanate- (FITC-) conjugated monoclonal antibodies for rat CD34 (R&D Systems, USA), CD44 (Santa Cruz Biotechnology, USA), CD45 (eBioscience, USA), and CD90 (eBioscience, USA) at room temperature for 1 h and then at 4°C in the dark. The labeled ASCs were assessed using a flow cytometer (Beckman Coulter, USA). The monoclonal antibodies CD44-PE and CD90-FITC were used to identify the mesenchymal phenotype, and CD34-PE and CD45-PE were applied to exclude the hematopoietic and angiogenic lineages.

**2.4. Fabricating ASC Sheets.** The third-generation ASCs were seeded at  $1 \times 10^6$  cells/well in 6-well plates. After reaching about 90% confluence, the basal medium was changed to a cell sheet induction medium, which was composed of  $\alpha$ -MEM (Gibco, USA), 10% bovine fetal serum (Sijiqing, China), 1% penicillin/streptomycin (HyClone, USA), and 50 mg/mL vitamin C (Kehao, China). ASCs were cultured for 7 to 10 days, and the nutrient solution was replaced every 2 to 3 days. When the curly edge appeared at the plate rim, the whole cell sheets were peeled off with a scraper or tweezers. The ASC sheets were always kept moist during the peeling process.

**2.5. Osteogenesis Capability of ASCs and ASC Sheets.** For *in vitro* osteogenic differentiation analysis, both the ASC group and the ASC sheet group were started with a  $1 \times 10^6$  cells/well seeding in 6-well plates. The ASC group was osteoinduced once the cell confluence reached 90%, while the ASC sheet group was osteoinduced only after a 7-day cell sheet induction. The osteoinductive medium was prepared using  $\alpha$ -MEM (Gibco, USA) supplemented with 10% FBS (Sijiqing, China), 0.1 mM dexamethasone (Sigma-Aldrich, USA), 5 mM  $\beta$ -glycerophosphate (Sigma-Aldrich, USA), 50  $\mu$ g/mL L-ascorbic acid (Sigma-Aldrich, USA), and 1% penicillin/streptomycin (HyClone, USA).

**2.5.1. Osteogenesis Staining.** Both groups were subjected to ALP staining (Leagene, China) at the 7th day of osteogenic induction and to Alizarin Red staining (Sigma-Aldrich, USA) at the 28th day. The results were observed and recorded by digital camera (Nikon, Japan).

**2.5.2. Real-Time RT-qPCR.** At the 7th day of osteogenic differentiation, the relative mRNA expressions of alkaline phosphatase (ALP), bone morphogenetic protein 2 (BMP2),

TABLE 1: Primers used for real-time quantitative polymerase chain reaction.

Gene	Forward primer sequence (5'-3')	Reverse primer sequence (5'-3')
GAPDH	CAAGTTCAACGGCACAGTCA	CCATTTGATGTTAGCGGGAT
ALP	ATGGCTCACCTGCTTCACG	TCAGAACAGGGTGCCTAGG
BMP2	GAGGAGAAGCCAGGTGTCT	GTCCACATACAAAGGGTGC
OCN	CCACCCGGGAGCAGTGT	GAGCTGCTGTGACATCCATACTTG
OPG	ACAATGAACAAGTGGCTGTGCTG	CGGTTTCTGGGTCATAATGCAAG
RUNX-2	GCACCCAGCCCATAATAGA	TTGGAGCAAGGAGAACCC

osteocalcin (OCN), and runt-related transcription factor 2 (Runx-2) in the ASC group and in the ASC sheet group were determined. The total RNA of ASCs and ASC sheets was extracted using the TRIzol Reagent (Invitrogen, USA) according to the manufacturer's protocol. After quantification by optical density measurement, 1  $\mu$ g total RNA was converted to cDNA using the PrimeScript™ RT Reagent Kit (Takara, Japan). RT-PCR was performed using the SYBR Premix Ex Taq™ II Kit (Takara, Japan) in a quantitative PCR system (Bio-Rad, USA) under the following conditions: 3 min of denaturation at 95°C, 40 rounds of 10 s of annealing at 95°C, and 30 s of extension at 60°C. The primers used in the present study are listed in Table 1; GAPDH was monitored as a housekeeping gene. The results were evaluated by the CFX96™ RT-PCR System (Bio-Rad, USA).

**2.6. In Vitro Osteogenesis of ASC Sheets with Sema3A.** The procedures for ASC isolation and ASC sheet fabrication were the same as mentioned above. After a 7-day cell sheet induction, ASC sheets were treated with osteoinductive medium as mentioned above with or without 1  $\mu$ g/mL Sema3A (PeproTech, USA). The treatment groups were then named the control group and the Sema3A group. ALP staining and Alizarin Red staining, as well as osteogenesis-related gene expression were tested as mentioned above.

**2.7. Induction of T2DM Rat Model.** A high-fat diet with 69.5% basal feed, 10.0% sucrose, 10.0% egg yolk granules, 0.5% cholesterol, and 10.0% lard (Experimental Animal Center of the Fourth Military Medical University) for four weeks and a single low dose (30 mg/kg) of streptozotocin (STZ) via intraperitoneal injection were administered to rats to induce type 2 DM models as previously described [22]. After 7 days of STZ injection, blood was collected by tail cutting to test the random plasma glucose levels (PGLs) using a glucometer. Rats with PGL above 16.7 mmol/L were considered as diabetics, but PGL below this value were excluded from the experiment.

## 2.8. Characteristics and Preparation of Implants

**2.8.1. ASC+Bone Granule Complex.** Biomembranes (Heal-All, China) were cut into 7 mm  $\times$  7 mm squares. Bio-Oss® bone granules (0.02 g) (Geistlich, Switzerland) were loaded on the biomembrane.  $3 \times 10^6$  ASCs were dropped on bone granules and cocultured for 4 hours (Figures 1(a)–1(c)).

**2.8.2. ASC Sheet+Bone Granule Complex.**  $3 \times 10^6$  ASCs were seeded into 60 mm petri dishes and induced to the ASC sheet as mentioned earlier for 7 days. Then, 0.02 g bone granules (Geistlich, Switzerland) were mixed evenly with each ASC sheet in a 1.5 mL EP tube (Figures 1(d)–1(f)).

**2.8.3. Scanning Electron Microscopy (SEM) Observation of the Two Complexes.** The surface morphologies of the two kinds of complexes were observed by JEOL JSM-6700F Field Emission SEM (JEOL Ltd., Japan).

**2.9. Implantation of Two Complexes in T2DM Rats.** A total of 20 rats with T2DM were randomly divided into two groups ( $n = 10$ ): the ASC+bone granule group and the ASC sheet +bone granule group. Animals were anesthetized by an intraperitoneal injection of 2% pentobarbital sodium solution (Sigma-Aldrich, USA) (0.25 mL/100 g body weight). Following shaving and sterilization, a 5 mm critical-sized calvarial defect (CSD) was drilled carefully penetrating through the calvarial bone without damage to the dura mater. CSDs were randomly filled with the different complexes in the two groups. The complexes were placed over the dura mater and covered with the 7 mm  $\times$  7 mm biomembrane (Heal-All, China). The periosteum and skin were sutured separately with 4-0 silk sutures. Antibiotics based on body weight were administered for 3 consecutive days post surgery. The healing process was 4 or 8 weeks, then the rats were euthanized with an overdose of anesthetic. Calvarial specimens were harvested, fixed in 4% paraformaldehyde for 2 days, and analyzed by microcomputed tomography (micro-CT) and histomorphology.

**2.10. Micro-CT Scanning.** A micro-CT scanner (Inveon CT, Siemens, Germany) was used to scan the samples at a scanning resolution of 56  $\mu$ m to evaluate bone formation in the CSDs of the T2DM rats. Three-dimensional models were reconstructed from the micro-CT scanning datasets for the quantitative analysis of bone formation within the CSDs (Figures 2(a) and 2(d)). The region of interest (ROI) was defined as a cylinder with a radius of 5 mm and a height of 1 mm (about the full thickness of the calvarial bone) from the surgery area. The Inveon Research Workplace software package, version 2.2.0 (Siemens Healthcare GmbH, Erlangen, Germany) was used for 3D reconstruction of the image and data analysis. Tissue with a CT value between 700 and 2000 Hounsfield units (Hu) is defined as new bone (Figure 2(b)). Tissue with a CT value above 2000 Hu is defined as

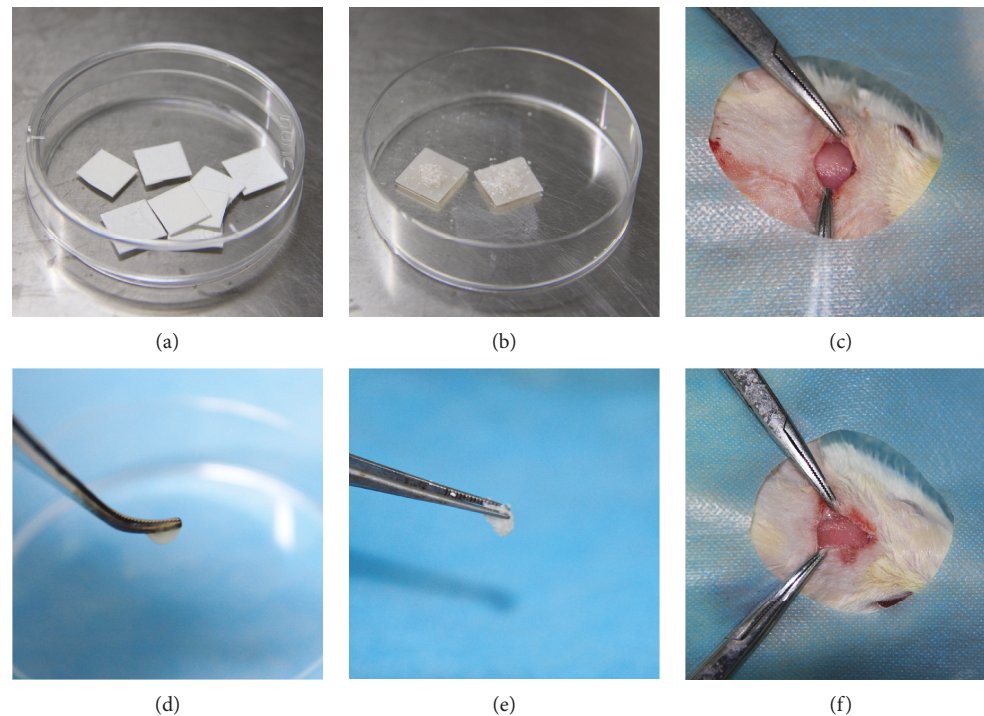


FIGURE 1: Preparation and transplantation of different implants. (a–c) ASC+bone granule complex: (a) 7 mm × 7 mm biomembranes, (b)  $3 \times 10^6$  ASCs were seeded on 0.02 g bone granules above the biomembrane, and (c) the ASC+bone granule complex together with the biomembrane were transplanted in the CSD of T2DM rat. (d–f) ASC sheet+bone granule complex: (d) ASC sheet pellet which started from  $3 \times 10^6$  ASCs in 60 mm petri dishes and cultured in cell sheet induction medium for 7 days, (e) the complex of the ASC sheet and 0.02 g bone granules, and (f) the ASC sheet+bone granule complex was transplanted in CSD of the T2DM rat and covered by the 7 mm × 7 mm biomembrane.

Bio-Oss® bone granules (Figure 2(c)). The bone volume/total volume (BV/TV), trabecular thickness (Tb.Th), trabecular number (Tb.N), and trabecular spacing (Tb.Sp) were calculated.

**2.11. Histomorphologic Analyses.** The calvarial specimens were decalcified in 17% EDTA in a 37°C incubator for 20–30 days until the bone tissue became soft and could be easily penetrated by needles. The EDTA was changed twice weekly. After embedding in paraffin, representative coronal sections were taken and hematoxylin and eosin (HE) staining was performed. The sections were observed using a stereo microscope (Olympus Corporation, Tokyo, Japan).

**2.11.1. Vascular Counting.** Three HE-stained sections were selected from each sample. Three fields were randomly selected for each section and the number of blood vessels was counted at 40 times magnification. An average value was calculated.

**2.12. Bone Healing in T2DM Rats with Sema3A.** A total of 20 rats with T2DM were randomly divided into two groups ( $n = 10$ ): the control group and the Sema3A group. CSDs were drilled penetrating through the calvarial bone and filled with the ASC sheet+bone granule complex as mentioned above in all the rats. Rats received a local injection of Sema3A (100 µg/mL in sterile saline, 20 µg/kg) into the surgery site in the Sema3A group or vehicle (sterile saline) in the control

group on the 1st, 4th, and 7th day after operation. All animals were euthanized 4 or 8 weeks later with an overdose of anesthetic. Samples were harvested and examined by micro-CT and histomorphology. The procedure was the same as mentioned above.

**2.13. Statistical Analysis.** All experiments were repeated at least three times and the results were displayed as mean ± standard deviation. Comparisons were performed by Student's *t*-test or one-way ANOVA followed by LSD-*t*-test or Games-Howell test using SPSS 19.0 (SPSS Inc., USA). Significance was considered as *P* value < 0.05.

### 3. Results

**3.1. Characterization of ASCs.** Primary culture of ASCs emerged as colonies with spindle-shaped morphology (Figure 3(a)). Cell population appeared to be more homogeneous by the third passage (P3, Figure 3(b)). In osteogenic culture, calcium nodules were stained with Alizarin Red S (Figure 3(c)). In adipogenic culture, intercellular lipid vacuoles were stained with Oil Red O (Figure 3(d)). ASCs were positive for the MSC markers CD44 ( $99.8\% \pm 0.1\%$ ) and CD90 ( $99.9\% \pm 0.1\%$ ) but negative for the hematopoietic and angiogenic markers CD34 ( $0.4\% \pm 0.2\%$ ) and CD45 ( $0.5\% \pm 0.2\%$ ) (Figure 3(e)).

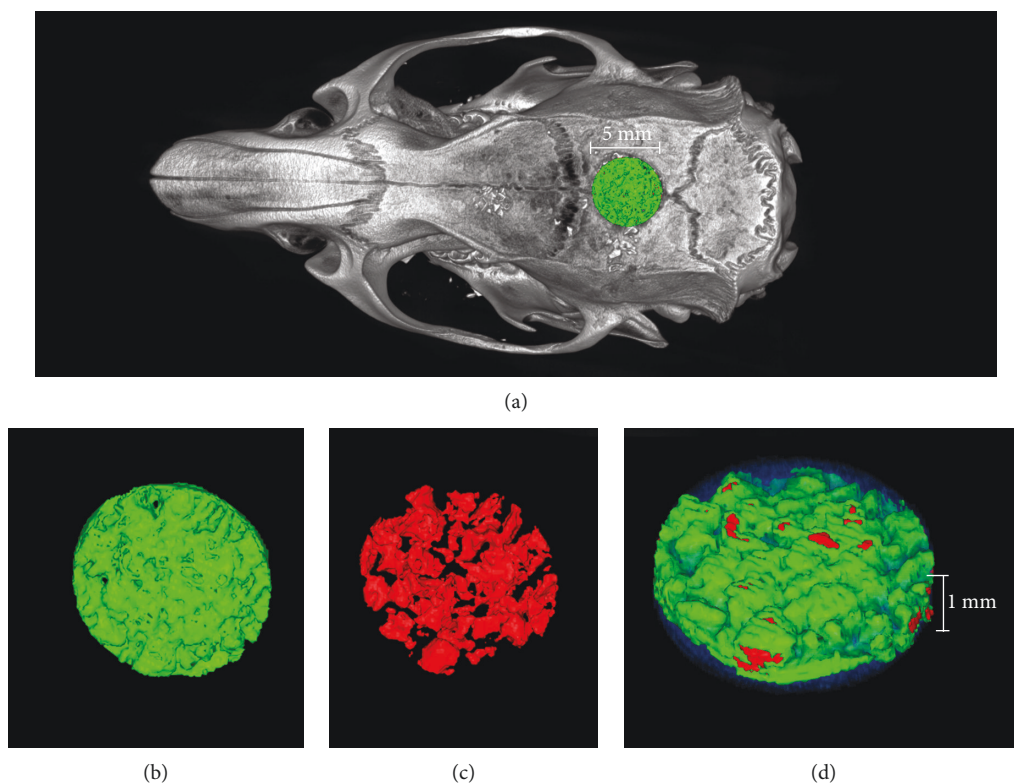


FIGURE 2: Definition of the region of interest (ROI). (a) The ROI was defined as a cylinder with a radius of 5 mm and a height of 1 mm from the surgery area. (b) Tissue with a CT value between 700 and 2000 Hu was defined as new bone; green=new bone. (c) Tissue with a CT value above 2000 Hu was defined as Bio-Oss® bone granules; red=bone granules. (d) Three-dimensional reconstruction of the ROI, translucent blue=CT value below 700 Hu.

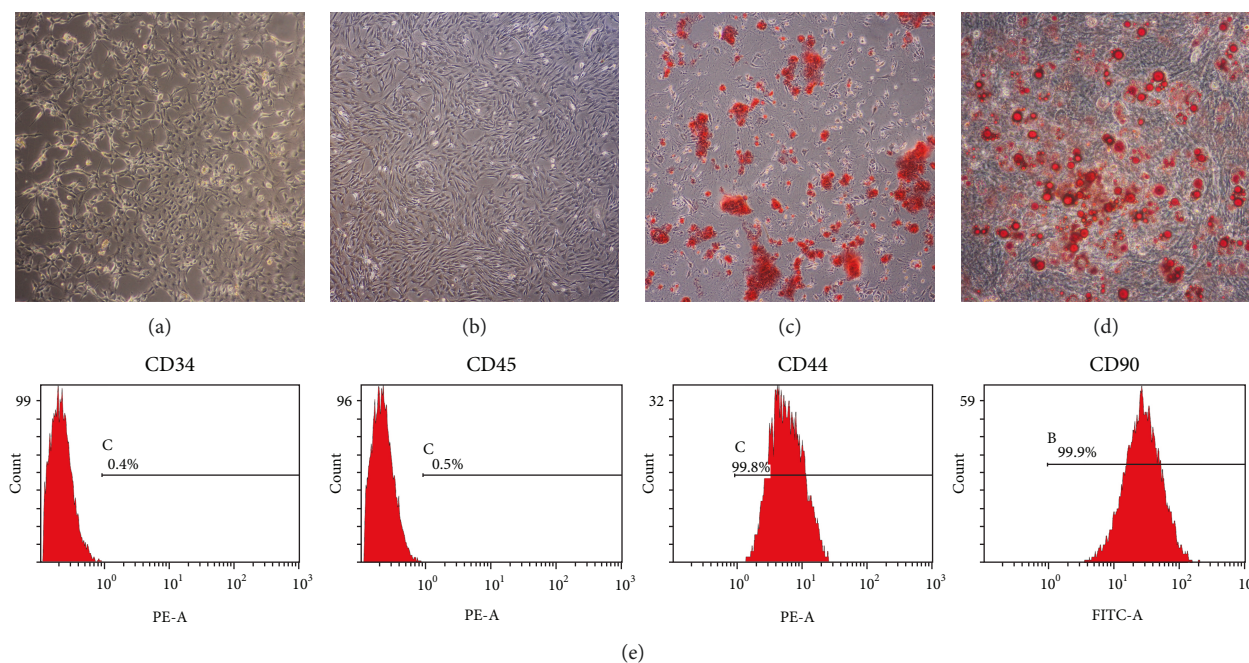


FIGURE 3: Characterization of ASCs. (a) Primary culture of ASCs (original magnification  $\times 100$ ). (b) Subculture of ASCs (P3, original magnification  $\times 100$ ). (c) Mineral node stained with Alizarin Red S (original magnification  $\times 40$ ). (d) Fat droplets stained with Oil Red O (original magnification  $\times 200$ ). (e) Flow cytometry analysis of ASC surface markers.

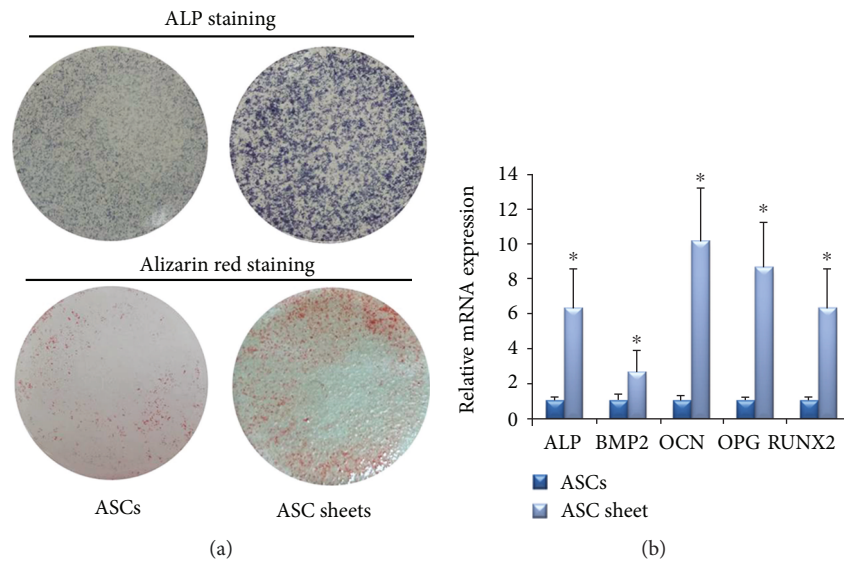


FIGURE 4: Osteogenic differentiation of the ASCs and ASC sheets. (a) ALP staining after osteogenic induction for 7 days and Alizarin Red staining after osteogenic induction for 28 days. (b) Osteogenesis-related gene expression quantified by RT-PCR after osteogenic induction for 7 days. Mean  $\pm$  SD,  $n = 3$ , and  $*P < 0.05$ .

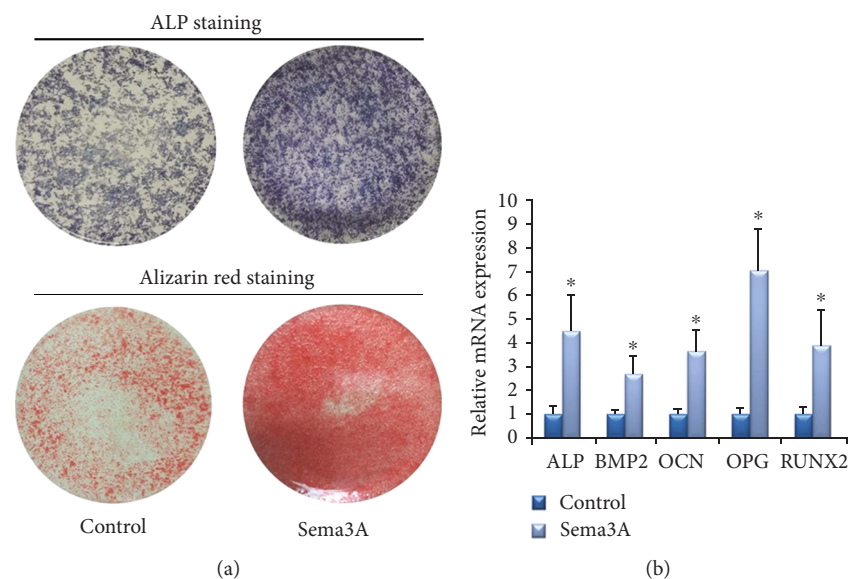


FIGURE 5: The effect of Sema3A on osteogenic differentiation of ASC sheets. (a) ALP staining after osteogenic induction for 7 days and Alizarin Red staining after osteogenic induction for 28 days. (b) Osteogenesis-related gene expression quantified by RT-PCR after osteogenic induction for 7 days. Mean  $\pm$  SD,  $n = 3$ , and  $*P < 0.05$ .

**3.2. Osteogenic Differentiation of the ASCs and ASC Sheets.** The results of ALP staining showed that ASC sheets after osteogenic induction for 7 days were deeper colored than ASCs (Figure 4(a)). The areas of mineralization nodules in the ECM of ASC sheets after osteogenic induction for 28 days were significantly larger and denser than ASCs (Figure 4(a)).

At the 7th day of osteogenic differentiation, the relative mRNA expressions of ALP, BMP2, OCN, OPG, and Runx2 in ASC sheets were higher than those in the ASC group

(Figure 4(b)). The data of the two groups were statistically significant ( $P < 0.05$ ).

**3.3. In Vitro Osteogenesis of ASC Sheets with Sema3A.** To evaluate the effect of Sema3A on osteogenic differentiation, ASC sheets were treated with osteoinductive medium with Sema3A. Both ALP activity and deposition of calcified extracellular matrix were increased, as detected by ALP staining and Alizarin Red staining results (Figure 5(a)). In addition, the mRNA levels of osteogenic markers, including ALP,

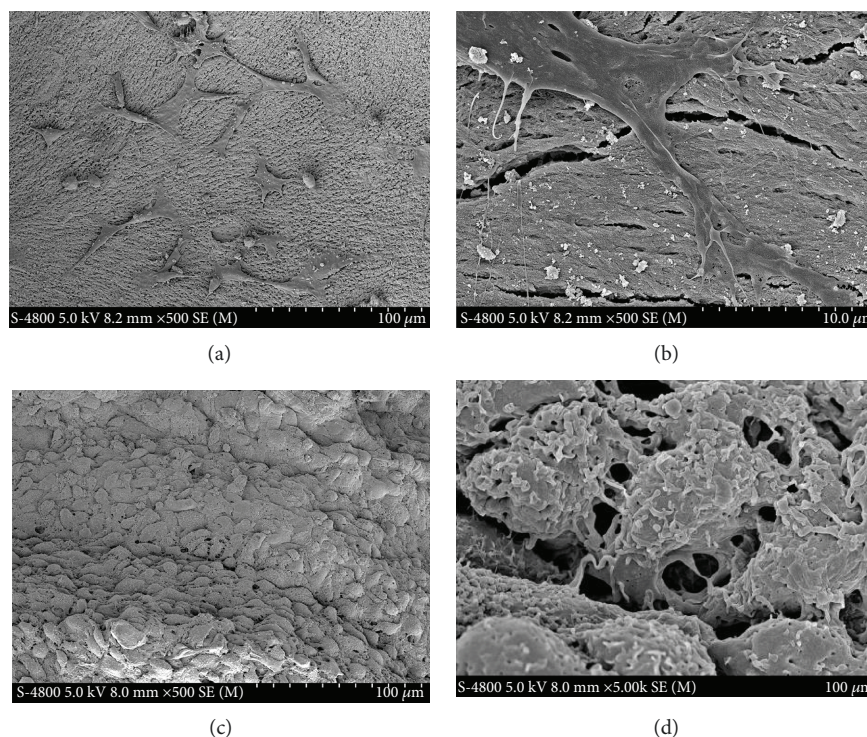


FIGURE 6: Surface morphologies of two kinds of complexes by SEM. (a, b) ASC+bone granule coculture complex. (c, d) ASC sheet+bone granule complex. Scale bar of (a) and (c), 100  $\mu\text{m}$ ; scale bar of (b) and (d), 10.0  $\mu\text{m}$ .

BMP2, OCN, OPG, and Runx2 were significantly higher in the Sema3A group after 7-day osteogenic inductions (Figure 5(b)). All these results verified that Sema3A significantly increased the osteogenic capacity of ASC sheets *in vitro*.

**3.4. SEM Observation of Two Kinds of Complexes.** In the ASC+bone granule complex, ASCs adhered tightly to the Bio-Oss® bone granules by protruding their projections on the surface of the bone granules (Figures 6(a) and 6(b)). In the ASC sheet+bone granule complex, numerous ASCs were densely populated in the ASC sheet and abundant cellular junctions were observed between the cells (Figures 6(c) and 6(d)). Under the same magnification, the ASC sheet+bone granule complex contained more cells.

### 3.5. Osseointegration of Different Types of Tissue Engineering Bone in T2DM Rats

#### 3.5.1. The ASC Sheet+Bone Granule Group and the ASC+Bone Granule Group

**(1) Rat Physical Health.** All the rats were successfully modeled. The average blood glucose of T2DM rats was  $24.9 \pm 2.8$  mmol/L, and the average body weight was  $375 \pm 26.5$  g before surgery. Blood glucose was stable throughout the experiment. All animals survived, and none showed signs of infection during the experiment.

**(2) Micro-CT Analysis.** Three-dimensional images on micro-CT showed massive newly formed bone in both two groups (Figure 7(a)). More new bone was observed in the ASC sheet+bone granule group than in the ASC+bone granule

group. All the BV/TV, Tb.Sp, Tb.N, and Tb.Th were statistically different ( $P < 0.05$ ) between the two groups except BV/TV at 8 weeks and Tb.Th at 4 weeks (Figure 7(b)). The results showed that new bone formation was significantly improved in the ASC sheet+bone granule group.

**(3) Histologic Analysis of New Bone within the CSDs.** To further investigate the newly formed bone within the CSDs, histologic analysis was performed using HE staining under light microscopy (Figure 8(a)). A large number of active osteoblasts and woven bone were observed around bone granules in both groups. New bone was observed only around the margin of CSDs in the ASC+bone granule group, while new bone started to grow into the central area in the ASC sheet+bone granule group at 4 weeks. At 8 weeks, the difference was more obvious with bone remodeling. In the ASC sheet+bone granule group, more mature new bone was creeping from the periphery to the center of the CSDs, and osseous islands and bridges were observed in the center of the CSDs. In addition, more blood vessels were observed in the ASC sheet+bone granule group than in the ASC+bone granule group (Figure 8(b)).

#### 3.5.2. The Sema3A Group and the Control Group

**(1) Rat Physical Health.** All the rats were successfully modeled. The average blood glucose of T2DM rats was  $25.7 \pm 3.4$  mmol/L, and the average body weight was  $383 \pm 28.7$  g before surgery. Blood glucose was stable throughout the experiment. All animals survived, and none showed signs of infection during the experiment.



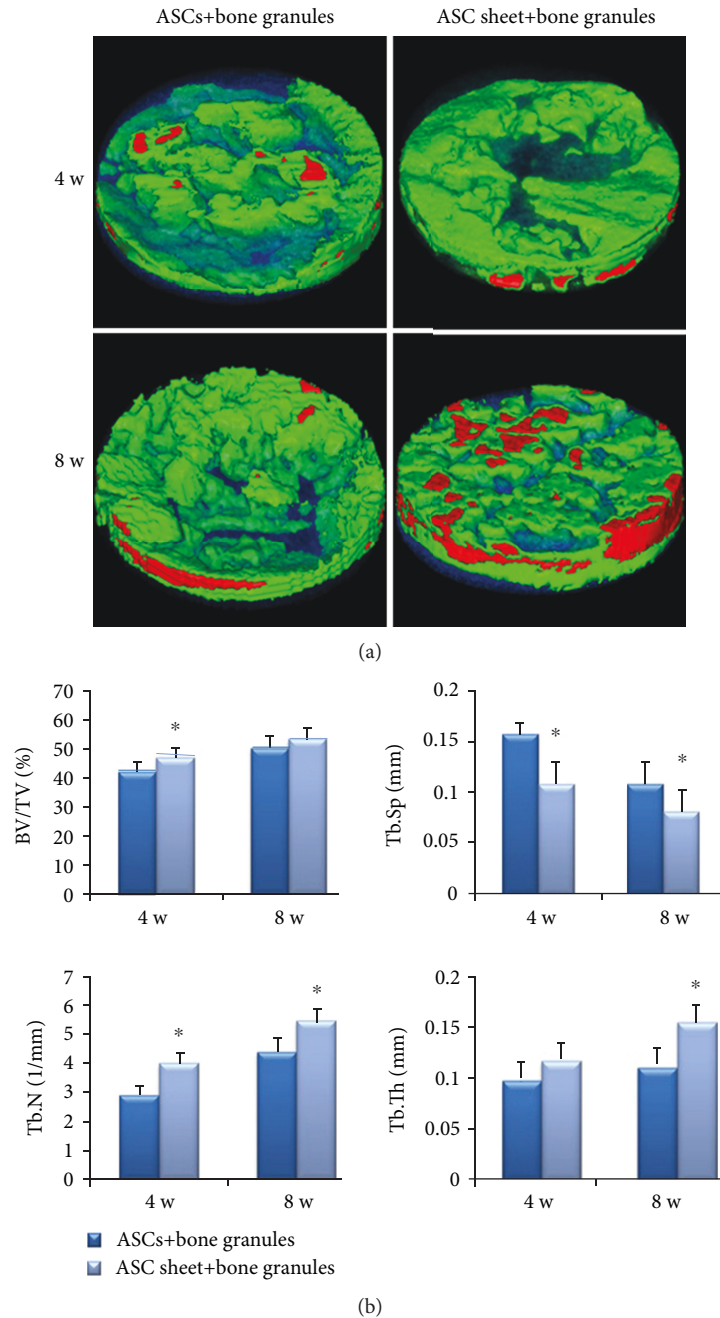


FIGURE 7: Micro-CT evaluation of the ASC+bone granule group and the ASC sheet+bone granule group. (a) Three-dimensional images of micro-CT reconstruction of ROI (a cylinder with a radius of 5 mm and a height of 1 mm). Green=new bone (CT value between 700 and 2000 Hu), red=bone granules (CT value above 2000 Hu), and translucent blue=trabecular spacing (CT value below 700 Hu). (b) BV/TV, Tb.Sp, Tb.N, and Tb.Th evaluation of ROI. One-way ANOVA, followed by LSD-*t*-test or the Games-Howell test; \* $P < 0.05$ . BV/TV, bone volume/total volume; Tb.Th, trabecular thickness; Tb.N, trabecular number; Tb.Sp, trabecular spacing; ROI, region of interest.

(2) *Micro-CT Analysis*. Three-dimensional images on micro-CT showed massive newly formed bone in both two groups (Figure 9(a)). More new bone was observed in the Sema3A group than in the control group. At 8 weeks, the morphology of the bone granules was blurred and the new bone almost completely filled the bone defect area in the Sema3A group. Besides, more red area in the Sema3A group suggested that the degree of new bone mineralization was higher as well. The BV/TV, Tb.N, and Tb.Th were higher and Tb.Sp was less

in the Sema3A group (Figure 9(b)). The results showed that Sema3A significantly improved new bone formation in the T2DM model.

(3) *Histologic Analysis of New Bone within the CSDs*. At 4 weeks, osseous islands were observed in the center of the CSDs in the Sema3A group, while new bone was observed only around the margin of CSDs in the control group. At 8 weeks, new bone in the Sema3A group was thicker and fused

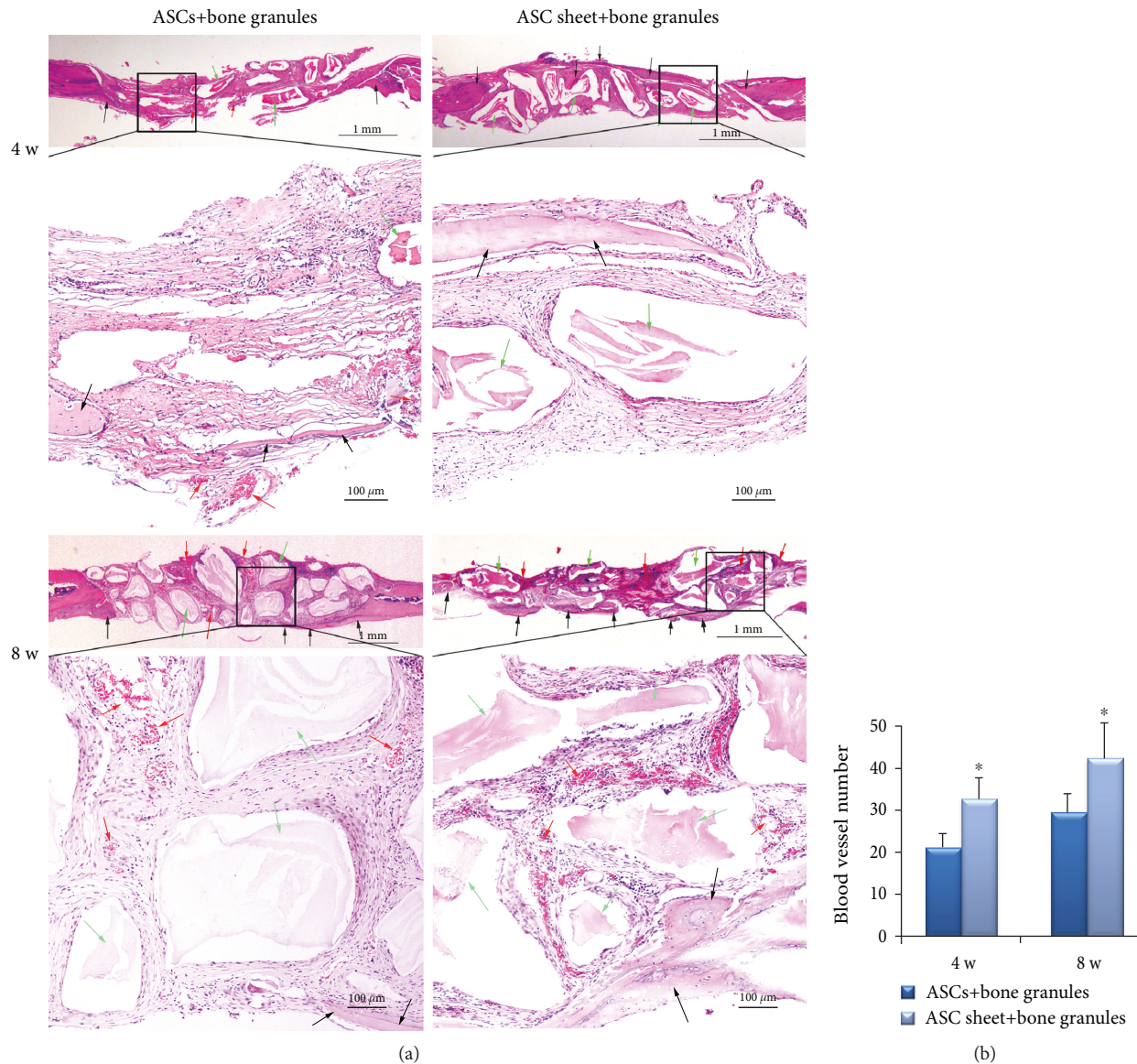


FIGURE 8: Histomorphologic analyses of the ASC+bone granule group and the ASC sheet+bone granule group. (a) New bone formation of the calvarial defect sections of the two groups was detected by H&E staining. Scale bar of upper images, 1 mm; scale bar of lower images, 0.5 mm. (b) Blood vessel number of the calvarial defect sections of the two groups. Black arrows indicate new bone, red arrows indicate blood vessels, and green arrows indicate bone granules; the lower panels are the magnifications of the insets in each group. Mean  $\pm$  SD,  $n = 3$ , and  $*P < 0.05$ .

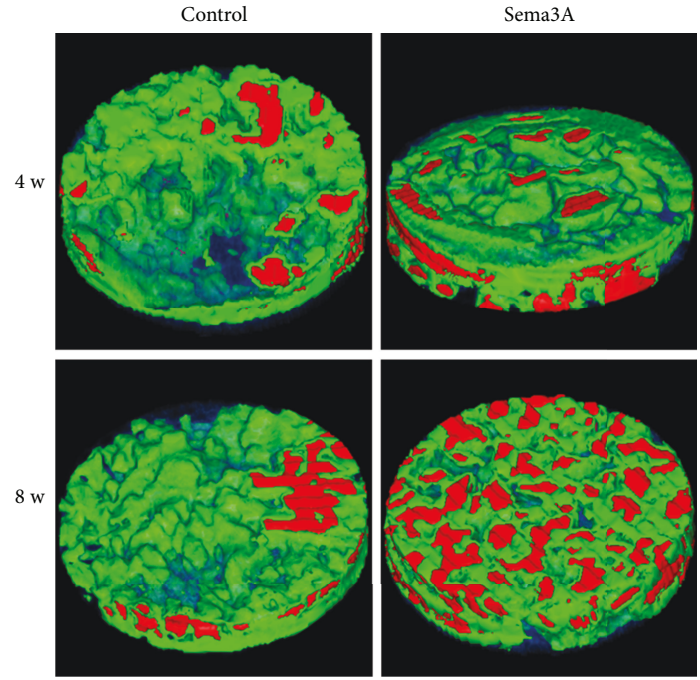
continuously, almost completely covering the bone defect area (Figure 10(a)). Less blood vessels were observed in the Sema3A group at 4 weeks while the difference was not significant at 8 weeks (Figure 10(b)).

#### 4. Discussion

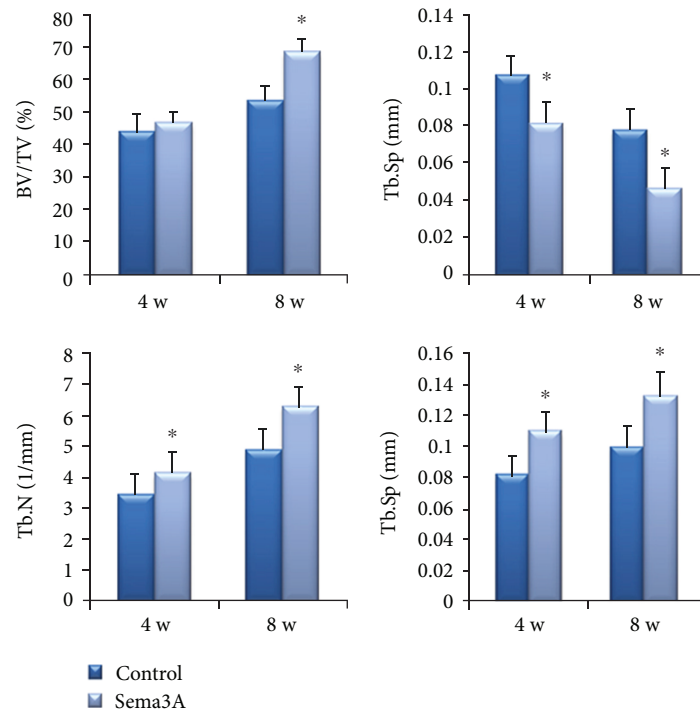
Quite a few T2DM patients suffer from impaired bone healing [1] and bone grafting failure [2], which is often associated with the suppression of osteogenic differentiation of MSCs [14] and thus become a crucial issue hindering clinical application of MSCs in patients with T2DM. In this study, we found that ASC sheets preserved more cells and had better osteogenic ability than ASCs *in vitro*. Importantly, based on critical calvarial defect repair in the T2DM model, we

certified that ASC sheets improved bone regeneration *in vivo*. We further confirmed that Sema3A significantly increased the osteogenic capacity of the ASC sheets *in vitro* and *in vivo*. Taken together, our study highlights the promising effect of bone tissue engineering based on ASC sheets, Bio-Oss® bone granules, and Sema3A on bone healing in the T2DM model.

In bone tissue engineering, the traditional method of seeding MSCs onto scaffolds often results in a great loss of cells. In order to solve the problem, we loaded scaffolds on a biomembrane when seeding stem cells in a previous study [13], where cells that failed to attach to scaffolds could adhere to the biomembrane below, maximizing the utilization of stem cells *in vivo*. However, the effect is still limited and the prepared complexes with the specific biomembrane can



(a)



(b)

FIGURE 9: Micro-CT evaluation of the control group and the Sema3A group. (a) Three-dimensional images of micro-CT reconstruction of ROI (a cylinder with a radius of 5 mm and a height of 1 mm). Green=new bone (CT value between 700 and 2000 Hu), red=bone granules (CT value above 2000 Hu), and translucent blue=trabecular spacing (CT value below 700 Hu). (b) BV/TV, Tb.Sp, Tb.N, and Tb.Th evaluation of ROI. One-way ANOVA, followed by LSD-*t*-test or the Games-Howell test; \**P* < 0.05. BV/TV, bone volume/total volume; Tb.Th, trabecular thickness; Tb.N, trabecular number; Tb.Sp, trabecular spacing; ROI, region of interest.

hardly be adjusted to the irregular shape of bone defects in clinics. Cell sheet technology is an alternative approach of tissue engineering that binds cells tightly in a sheet form

via temperature-responsive culture [23], electron beam irradiation [24], mechanical methods [25], or vitamin C [26] application, to prevent cell loss, provide an ideal

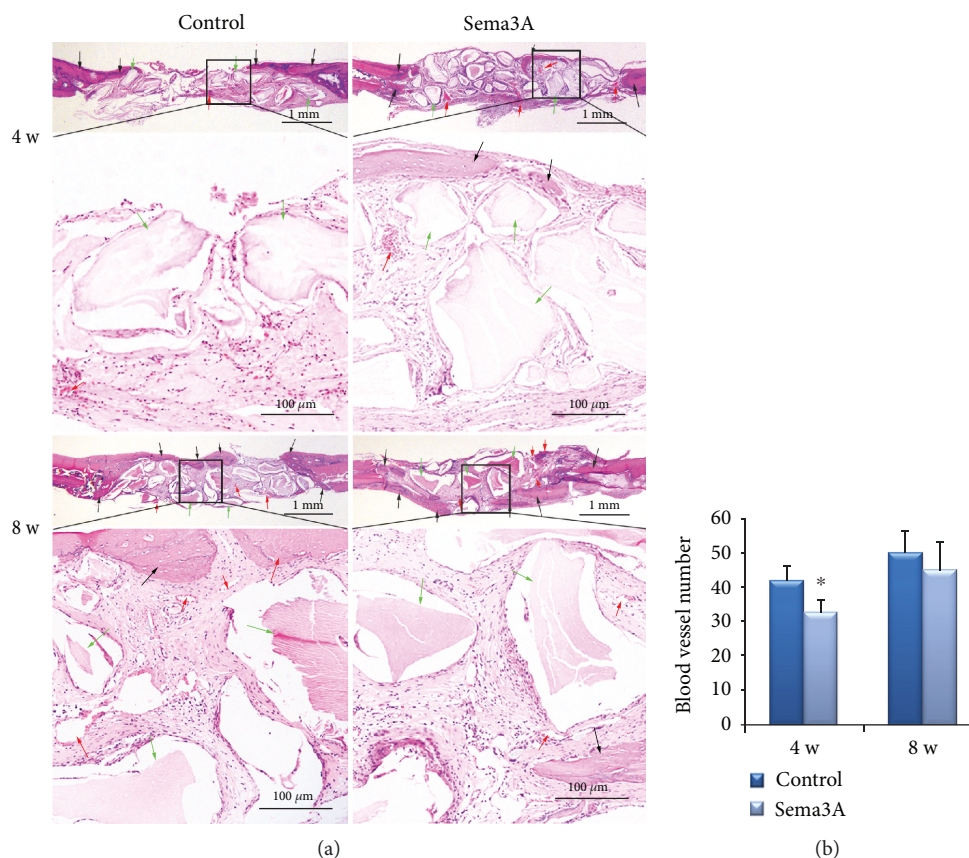


FIGURE 10: Histomorphologic analyses of the control group and the Sema3A group. (a) New bone formation of the calvarial defect sections of the two groups was detected by H&E staining. Scale bar of upper images, 1 mm; scale bar of lower images, 0.5 mm. (b) Blood vessel number of the calvarial defect sections of the two groups. Black arrows indicate new bone, red arrows indicate blood vessels, and green arrows indicate bone granules; the lower panels are the magnifications of the insets in each group. Mean  $\pm$  SD,  $n = 3$ , and  $*P < 0.05$ .

microenvironment, and obtain a certain degree of mechanical strength for the seed cells by preserving both cell surface proteins and ECM to the utmost [27]. Therefore, we used cell sheet technology in this study.

Considering the low price, convenient operation, and satisfactory film-inductive effect, we constructed ASC sheets with vitamin C in this study. In the osteogenic experiments, ASC sheets showed better osteogenic ability with enhanced ALP activity, more calcium deposition, and the elevated expression level of osteogenesis-related genes. These results claimed a positive effect of cell sheets on the osteogenesis of ASCs, just as what has been proven with many other MSCs including BMSCs and PDLSCs [16, 28].

Stem cell sheets are now generally used as a periosteum, wrapping scaffolds to repair bone defects [29–34]. However, cells cannot be evenly distributed on the scaffolds in this way, and this method has limits on osteoinductivity. In this study, we thoroughly mixed ASC sheets and Bio-Oss® bone granules in an EP tube to make sure that ASCs exist in the center of the defect and intact ASC sheets act as a whole to contact the bone tissue of the host. The results of SEM showed that the ASC sheet+bone granule complex perfectly guaranteed the number of ASCs, intercellular connection, and cell-ECM connection. This may facilitate cell signaling, thereby promoting cell differentiation and new bone

formation. Besides, the complexes can fit bone defects of different sizes and shapes in clinics only by adjusting the amount of the bone granules and cell sheets during the operation. Our study provided a novel strategy with high efficiency and convenience to perform bone tissue engineering only by mixing cell sheets and scaffold granules during surgery, which is very practical when applied in clinics.

Many *in vitro* and *in vivo* studies have shown that Sema3A can promote osteogenic differentiation and new bone formation [35–38]. Sema3A has a good curative effect on the osteoporosis model, the cortical bone defect model [17], and the rat osteoporotic fracture model [39], which can promote bone regeneration, increase bone mass, and reduce bone loss in injured parts. The mechanism may be that Sema3A binds to the neuropilin-1 (Nrp1) receptor and activates  $\beta$ -catenin, which promotes osteogenesis through the Wnt/ $\beta$ -catenin signaling pathway [17]. In addition, Hayashi et al. confirmed that Sema3A, like OPG, also has an inhibitory effect on osteoclast formation with OPG-deficient mice; this may be due to the fact that the binding of Sema3A to Nrp1 inhibited osteoclast differentiation by intervening in the ITAM and RhoA pathway [17]. Consistent with a previous study, our group showed that the stimuli of Sema3A can promote the osteogenic ability of the ASC sheets of 7-day induction as revealed by improved ECM

mineralization and a higher expression of osteogenesis-related genes. Moreover, *in vitro* studies further confirmed the osteogenic role of Sema3A in the T2DM model. It is notable that the Sema3A group had relatively few new blood vessels at 4 weeks after surgery compared with the control group. This may be related to the fact that the receptor NRP-1 is shared by Sema3A and vascular endothelial growth factor (VEGF). Many studies on tumors have shown that Sema3A competes with VEGF for the receptor NRP-1, which inhibits VEGF-mediated angiogenesis, thereby further inhibiting the growth, invasion, and metastasis of tumor [40]. However, 8 weeks after surgery, the difference in the number of blood vessels between the two groups was not obvious. The possible mechanism may be that Sema3A injected locally on days 1, 4, and 7 may decrease as time flows and the autocrine or paracrine VEGF of ASCs may increase at the later stage.

The present study demonstrated that ASC sheets and the Bio-Oss® bone granule complex combined with a local injection of Sema3A can greatly promote bone healing under T2DM conditions.

## 5. Conclusion

Our study has identified that rat ASC sheets have stronger osteogenic ability than ASCs *in vitro*. ASC sheets combined with Bio-Oss® bone granules promoted bone formation in T2DM rats. In addition, Sema3A promoted the osteogenic differentiation of ASC sheets *in vitro* and local injection of Sema3A promoted T2DM rats' calvarial bone regeneration based on ASC sheets and Bio-Oss® bone granule complex treatment. Our study provided a novel strategy with high efficiency and convenience to perform bone tissue engineering only by mixing cell sheets with scaffold granules. Moreover, bone tissue engineering based on ASC sheets combined with a local injection of Sema3A provides a promising strategy to repair bone defects in T2DM patients.

## Abbreviations

ASCs:	Adipose-derived stem cells
ASC sheets:	Adipose-derived stem cell sheets
T2DM:	Type 2 diabetes mellitus
BMSCs:	Bone marrow mesenchymal stem cells
PDLSCs:	Periodontal ligament stem cells
PBS:	Phosphate-buffered saline
$\alpha$ -MEM:	$\alpha$ -Minimum essential media
ALP:	Alkaline phosphatase
PE:	Phycocerythrin
FITC:	Fluorescein isothiocyanate
OPG:	Osteoprotegerin
BMP2:	Bone morphogenetic protein 2
OCN:	Osteocalcin
RUNX-2:	Runt-related transcription factor 2
STZ:	Streptozotocin
CSD:	Critical-sized calvarial defect
ECM:	Extracellular matrix
HA:	Hydroxyapatite
Micro-CT:	Microcomputed tomography
ROI:	Region of interest

Hu:	Hounsfield units
BV:	Bone volume
TV:	Total volume
Tb.Th:	Trabecular thickness
Tb.N:	Trabecular number
Tb.Sp:	Trabecular spacing
Sema3A:	Semaphorin 3A
VEGF:	Vascular endothelial growth factor.

## Data Availability

The data used to support the findings of this study are available from the corresponding author upon request.

## Conflicts of Interest

The authors declare that they have no conflicts of interest.

## Acknowledgments

We thank the Research and Development Center for Tissue Engineering, Fourth Military Medical University (Xi'an, China) for the technical assistance. We express our thanks to Dr. Wen Song in the Department of Prosthodontics, School of Stomatology, Fourth Military Medical University for the critical reading of this manuscript. This study was supported by the National Nature Science Foundation of China (NSFC) (grant numbers 81771107, 81470775, 81170984, 81271579, and 81300918). The authors acknowledge colleagues from the Research and Development Center for Tissue Engineering, Fourth Military Medical University for the help and support rendered.

## References

- [1] C. Marin, F. P. Luyten, B. Van der Schueren, G. Kerckhofs, and K. Vandamme, "The impact of type 2 diabetes on bone fracture healing," *Frontiers in Endocrinology*, vol. 9, p. 6, 2018.
- [2] W. A. Camargo, R. de Vries, J. van Luijk et al., "Diabetes mellitus and bone regeneration: a systematic review and meta-analysis of animal studies," *Tissue Engineering Part B: Reviews*, vol. 23, no. 5, pp. 471–479, 2017.
- [3] D. Schwartz-Arad, L. Levin, and L. Sigal, "Surgical success of intraoral autogenous block onlay bone grafting for alveolar ridge augmentation," *Implant Dentistry*, vol. 14, no. 2, pp. 131–138, 2005.
- [4] D. R. Whiting, L. Guariguata, C. Weil, and J. Shaw, "IDF diabetes atlas: global estimates of the prevalence of diabetes for 2011 and 2030," *Diabetes Research and Clinical Practice*, vol. 94, no. 3, pp. 311–321, 2011.
- [5] Q. Qiao, X. Xu, Y. Song, S. Song, W. Zhu, and F. Li, "Semaphorin 3A promotes osteogenic differentiation of BMSC from type 2 diabetes mellitus rats," *Journal of Molecular Histology*, vol. 49, no. 4, pp. 369–376, 2018.
- [6] K. Fang, W. Song, L. Wang et al., "Semaphorin 3A-modified adipose-derived stem cell sheet may improve osseointegration in a type 2 diabetes mellitus rat model," *Molecular Medicine Reports*, vol. 14, no. 3, pp. 2449–2456, 2016.
- [7] F. E. Al Jofi, T. Ma, D. Guo et al., "Functional organic cation transporters mediate osteogenic response to metformin in

- human umbilical cord mesenchymal stromal cells,” *Cytherapy*, vol. 20, no. 5, pp. 650–659, 2018.
- [8] Z. Liu, T. Chen, W. Sun et al., “DNA demethylation rescues the impaired osteogenic differentiation ability of human periodontal ligament stem cells in high glucose,” *Scientific Reports*, vol. 6, no. 1, article 27447, 2016.
- [9] J. A. Semon, C. Maness, X. Zhang et al., “Comparison of human adult stem cells from adipose tissue and bone marrow in the treatment of experimental autoimmune encephalomyelitis,” *Stem Cell Research & Therapy*, vol. 5, no. 1, p. 2, 2014.
- [10] C. Romagnoli and M. L. Brandi, “Adipose mesenchymal stem cells in the field of bone tissue engineering,” *World Journal of Stem Cells*, vol. 6, no. 2, pp. 144–152, 2014.
- [11] N. Hiwatashi, S. Hirano, M. Mizuta et al., “Adipose-derived stem cells versus bone marrow-derived stem cells for vocal fold regeneration,” *Laryngoscope*, vol. 124, no. 12, pp. E461–E469, 2014.
- [12] C. Wallner, S. Abraham, J. M. Wagner et al., “Local application of isogenic adipose-derived stem cells restores bone healing capacity in a type 2 diabetes model,” *Stem Cells Translational Medicine*, vol. 5, no. 6, pp. 836–844, 2016.
- [13] L. Liang, Y. Song, L. Li et al., “Adipose-derived stem cells combined with inorganic bovine bone in calvarial bone healing in rats with type 2 diabetes,” *Journal of Periodontology*, vol. 85, no. 4, pp. 601–609, 2014.
- [14] J. Tan, L. Zhou, Y. Zhou et al., “The influence of diabetes mellitus on proliferation and osteoblastic differentiation of MSCs,” *Current Stem Cell Research & Therapy*, vol. 12, no. 5, pp. 388–400, 2017.
- [15] B. Zhang, N. Liu, H. Shi et al., “High glucose microenvironments inhibit the proliferation and migration of bone mesenchymal stem cells by activating GSK3 $\beta$ ,” *Journal of Bone and Mineral Metabolism*, vol. 34, no. 2, pp. 140–150, 2016.
- [16] F. Wei, C. Qu, T. Song et al., “Vitamin C treatment promotes mesenchymal stem cell sheet formation and tissue regeneration by elevating telomerase activity,” *Journal of Cellular Physiology*, vol. 227, no. 9, pp. 3216–3224, 2012.
- [17] M. Hayashi, T. Nakashima, M. Taniguchi, T. Kodama, A. Kumanogoh, and H. Takayanagi, “Osteoprotection by semaphorin 3A,” *Nature*, vol. 485, no. 7396, pp. 69–74, 2012.
- [18] R. Xu, “Semaphorin 3A: a new player in bone remodeling,” *Cell Adhesion & Migration*, vol. 8, no. 1, pp. 5–10, 2014.
- [19] X. Liu, N. Tan, Y. Zhou et al., “Semaphorin 3A shifts adipose mesenchymal stem cells towards osteogenic phenotype and promotes bone regeneration in vivo,” *Stem Cells International*, vol. 2016, Article ID 2545214, 13 pages, 2016.
- [20] B. Wessing, S. Lettner, and W. Zechner, “Guided bone regeneration with collagen membranes and particulate graft materials: a systematic review and meta-analysis,” *The International Journal of Oral & Maxillofacial Implants*, vol. 33, no. 1, pp. 87–100, 2018.
- [21] M. Sanz and F. Vignoletti, “Key aspects on the use of bone substitutes for bone regeneration of edentulous ridges,” *Dental Materials*, vol. 31, no. 6, pp. 640–647, 2015.
- [22] M. Yu, W. Zhou, Y. Song et al., “Development of mesenchymal stem cell-implant complexes by cultured cells sheet enhances osseointegration in type 2 diabetic rat model,” *Bone*, vol. 49, no. 3, pp. 387–394, 2011.
- [23] T. Okano, N. Yamada, H. Sakai, and Y. Sakurai, “A novel recovery system for cultured cells using plasma-treated polystyrene dishes grafted with poly(N-isopropylacrylamide),” *Journal of Biomedical Materials Research*, vol. 27, no. 10, pp. 1243–1251, 1993.
- [24] O. H. Kwon, A. Kikuchi, M. Yamato, Y. Sakurai, and T. Okano, “Rapid cell sheet detachment from poly(N-isopropylacrylamide)-grafted porous cell culture membranes,” *Journal of Biomedical Materials Research*, vol. 50, no. 1, pp. 82–89, 2000.
- [25] D. Ma, C. Zhong, H. Yao et al., “Engineering injectable bone using bone marrow stromal cell aggregates,” *Stem Cells and Development*, vol. 20, no. 6, pp. 989–999, 2011.
- [26] A. Nakamura, M. Akahane, H. Shigematsu et al., “Cell sheet transplantation of cultured mesenchymal stem cells enhances bone formation in a rat nonunion model,” *Bone*, vol. 46, no. 2, pp. 418–424, 2010.
- [27] I. Elloumi-Hannachi, M. Yamato, and T. Okano, “Cell sheet engineering: a unique nanotechnology for scaffold-free tissue reconstruction with clinical applications in regenerative medicine,” *Journal of Internal Medicine*, vol. 267, no. 1, pp. 54–70, 2010.
- [28] E. Y.-S. See, S. L. Toh, and J. C. H. Goh, “Multilineage potential of bone-marrow-derived mesenchymal stem cell sheets: implications for tissue engineering,” *Tissue Engineering Part A*, vol. 16, no. 4, pp. 1421–1431, 2010.
- [29] Q. Xing, Z. Qian, B. Kannan, M. Tahtinen, and F. Zhao, “Osteogenic differentiation evaluation of an engineered extracellular matrix based tissue sheet for potential periosteum replacement,” *ACS Applied Materials & Interfaces*, vol. 7, no. 41, pp. 23239–23247, 2015.
- [30] F. N. Syed-Picard, G. A. Shah, B. J. Costello, and C. Sfeir, “Regeneration of periosteum by human bone marrow stromal cell sheets,” *Journal of Oral and Maxillofacial Surgery*, vol. 72, no. 6, pp. 1078–1083, 2014.
- [31] Y. Kang, L. Ren, and Y. Yang, “Engineering vascularized bone grafts by integrating a biomimetic periosteum and  $\beta$ -TCP scaffold,” *ACS Applied Materials & Interfaces*, vol. 6, no. 12, pp. 9622–9633, 2014.
- [32] W. Geng, D. Ma, X. Yan et al., “Engineering tubular bone using mesenchymal stem cell sheets and coral particles,” *Biochemical and Biophysical Research Communications*, vol. 433, no. 4, pp. 595–601, 2013.
- [33] K. Uematsu, M. Nagata, T. Kawase, K. Suzuki, and R. Takagi, “Application of stem-cell media to explant culture of human periosteum: an optimal approach for preparing osteogenic cell material,” *Journal of Tissue Engineering*, vol. 4, Article ID 204173141350964, 2013.
- [34] D. Ma, H. Yao, W. Tian et al., “Enhancing bone formation by transplantation of a scaffold-free tissue-engineered periosteum in a rabbit model,” *Clinical Oral Implants Research*, vol. 22, no. 10, pp. 1193–1199, 2011.
- [35] Y. Li, L. Yang, S. He, and J. Hu, “The effect of semaphorin 3A on fracture healing in osteoporotic rats,” *Journal of Orthopaedic Science*, vol. 20, no. 6, pp. 1114–1121, 2015.
- [36] T. Fukuda, S. Takeda, R. Xu et al., “Sema3A regulates bone-mass accrual through sensory innervations,” *Nature*, vol. 497, no. 7450, pp. 490–493, 2013.
- [37] T. Negishi-Koga and H. Takayanagi, “Bone cell communication factors and semaphorins,” *BoneKey Reports*, vol. 1, p. 183, 2012.
- [38] C. Gomez, B. Burt-Pichat, F. Mallein-Gerin et al., “Expression of Semaphorin-3A and its receptors in endochondral ossification: potential role in skeletal development and innervation,” *Developmental Dynamics*, vol. 234, no. 2, pp. 393–403, 2005.

- [39] D. M. Liu, N. Lu, L. Zhao et al., "Serum Sema3A is in a weak positive association with bone formation marker osteocalcin but not related to bone mineral densities in postmenopausal women," *The Journal of Clinical Endocrinology and Metabolism*, vol. 99, no. 12, pp. E2504–E2509, 2014.
- [40] D. E. Hansel, R. E. Wilentz, C. J. Yeo, R. D. Schulick, E. Montgomery, and A. Maitra, "Expression of neuropilin-1 in high-grade dysplasia, invasive cancer, and metastases of the human gastrointestinal tract," *The American Journal of Surgical Pathology*, vol. 28, no. 3, pp. 347–356, 2004.

## Review Article

# New Insights on Properties and Spatial Distributions of Skeletal Stem Cells

Jun-qi Liu,<sup>1</sup> Qi-wen Li ,<sup>1</sup> and Zhen Tan <sup>2</sup>

<sup>1</sup>State Key Laboratory of Oral Diseases, National Clinical Research Centre for Oral Diseases, West China Hospital of Stomatology, Sichuan University, Chengdu 610041, China

<sup>2</sup>Department of Oral Implantology, West China Hospital of Stomatology, Sichuan University, Chengdu 610041, China

Correspondence should be addressed to Zhen Tan; tzdentist@163.com

Received 10 April 2019; Accepted 13 May 2019; Published 3 June 2019

Guest Editor: Toru Ogasawara

Copyright © 2019 Jun-qi Liu et al. This is an open access article distributed under the Creative Commons Attribution License, which permits unrestricted use, distribution, and reproduction in any medium, provided the original work is properly cited.

Skeletal stem cells (SSCs) are postnatal self-renewing, multipotent, and skeletal lineage-committed progenitors that are capable of giving rise to cartilage, bone, and bone marrow stroma including marrow adipocytes and stromal cells in vitro and in an exogenous environment after transplantation in vivo. Identifying and isolating defined SSCs as well as illuminating their spatiotemporal properties contribute to our understating of skeletal biology and pathology. In this review, we revisit skeletal stem cells identified most recently and systematically discuss their origin and distributions.

## 1. Introduction

Skeletal system, comprised of over 200 individual bones, is essential for general health. Robust skeleton facilitates movement and offers protection for inner organs. Furthermore, mounting evidence showed that the skeleton system is inextricably related with energy metabolism, vascular homeostasis, and immune homeostasis [1–3].

Skeletal homeostasis largely relies on the equilibrium between bone formation mediated by osteoblasts and bone resorption induced by osteoclasts. Perturbation of either of the two processes will cause skeletal disorders. For example, increased bone formation or lack of bone resorption could lead to high bone mass phenotype and reciprocally, excessive osteoclastogenesis or defective osteoblastogenesis can result in diseases like osteopenia, osteoporosis, rheumatoid arthritis, and increased risk of bone fracture [4–7].

Mesenchymal stromal/stem cells (MSCs), main source of osteoblasts, hold great promise for treating skeletal anomalies [8]. Recently, a lot of advancements have made to clarify the mechanism of osteogenic and chondrogenic differentiation of MSCs [9–13]. Over the past few years, many scholars including the concept inventor have been insisting that the term “MSC” should be abandoned or revised due to hetero-

geneity and overestimated stemness. Under such circumstances, the concept “skeletal stem cells” emerged [14–19].

Mesenchymal stromal/stem cells and skeletal stem cells are two confounding terms for most researchers. Mesenchymal stem cells are referred in most cases and according to the International Society for Cellular Therapy, MSCs should at least meet three minimal criteria: Firstly, they can adhere on plastic when cultured in standard conditions. Secondly, several surface molecules (CD73, CD90, and CD105) should be expressed by MSCs while some other markers should be excluded (CD34, CD45, CD14 or CD11b, CD79a or CD19, and HLA-DR). Thirdly, MSCs must possess trilineage differentiation capacity to osteoblasts, adipocytes, and chondroblasts in vitro [20]. These criteria help researchers identify and isolate stem cells easily. Nevertheless, such definitions are based on in vitro properties and can lead to misjudgment sometimes as in vitro experiments cannot represent in vivo characteristics. For instance, myxovirus resistance-1- (Mx1-) positive population of bone marrow mesenchymal stem cells are tripotent ex vivo (osteoblasts, adipocytes, and chondrocytes) but are defective in chondrogenic and adipocytic lineage differentiation in vivo [21]. By contrast, the definition of skeletal stem cells is more stringent. They are defined as a group of self-renewable cells that are restricted within the



skeleton and multipotent to give rise to skeleton-related progenies including osteoblasts, chondrocytes, and adipocytes both in vitro and in an exogenous environment after transplantation in vivo.

Here, a detailed comparison of MSCs and SSCs is provided (Table 1). Firstly, MSCs consist of stem cells of both skeletal lineages and nonskeletal lineages, which means MSCs are distributed ubiquitously [22], while SSCs are inherently restricted to and contribute to skeletal-related tissue including bone, cartilage, bone marrow stroma, and adipose tissue [15, 17]. Secondly, the minimal criteria defining MSCs inevitably lead to cell heterogeneity and variability. Their biological behavior such as colony-forming unit and multipotent differentiation ability varies with donors [23]. In comparison, SSCs are more defined and expected to exhibit more stable properties, largely owing to the discovery of exact cell surface markers as well as a comprehensive in vivo lineage tracing study. Further, SSCs possess multilineage differentiation (osteoblasts, chondrocytes, and adipocytes) capacity both in vitro and in an exogenous environment after transplantation in vivo. Transplantation of SSCs into nonskeletal tissue (e.g., kidney capsule) leads to ectopic bone organoid formation, including bone marrow. Furthermore, serial transplantation of isolated SSCs from the primary donor results in de novo formation of heterotopic ossicles. In comparison, MSCs barely exhibit aforementioned potential [17, 18, 24–26].

In the last decade, the isolation of MSCs was based on their plastic-adherent ability and expression of limited surface markers [20, 27, 28]. Emergence and advancement of research protocols, for instance, combined with the use of fluorescent reporter mouse, lineage tracing, and fluorescence-activated cell sorting (FACS), makes isolation and functional assessment of a precise SSC accessible [29]. Recently, a cohort of candidate markers were identified to label different SSC populations. Most of these populations are self-renewable, clonogenic, and multipotent. In addition, these cells are instrumental in bone injury healing, which is in accordance with the description that a true SSC is capable of responding to injury [30]. At the same time, SSCs in different developmental stages and locations often exhibit distinctive properties. For example, most perivascular SSCs play a role in maintaining hematopoiesis and cranial suture SSCs contribute exclusively to intramembranous ossification. Properties of SSCs change with age too. Together, in this review, we systematically discuss about the recent discovery of SSCs, with specific focus on their origin, stemness, and spatial-temporal variation. Moreover, similarities and differences among these cells are also indicated.

## 2. Growth Plate

The growth plate (or epiphyseal plate) is a type of hyaline cartilage that exists between the epiphysis and metaphysis of a long bone. The growth plate plays a critical role in bone elongation through endochondral ossification [31]. Several growth factors including Indian hedgehog (Ihh), parathyroid hormone-related protein (PTHrP), fibroblast growth factors (FGF), bone morphogenetic proteins (BMP), and vascular

TABLE 1: Comparison of MSCs and SSCs.

	MSCs	SSCs
Location	Ubiquitously	Skeleton
Skeletal lineage restricted	No	Yes
Homogeneity	Low	High
Stability	Low	High
Multilineage differentiation in vivo	Unpredictable	Yes
Ectopic bone formation	Unpredictable	Yes

endothelial growth factor (VEGF) regulate this endochondral bone formation process [31–35]. Depending on different stages of chondrocytes, the growth plate is divided into a resting zone, a proliferation zone, a prehypertrophic zone, and a hypertrophic zone [32]. A resting zone is considered as an enrichment area of stem-like cells especially chondroprogenitors and sustains the development of the other zones and longitudinal bone growth [36]. A very recent research revealed that a stem cell niche exists in the growth plate of mice, providing new insights into treating children growth disorders [37]. These features make the growth plate an ideal place to find skeletal stem cells.

*2.1. CD45<sup>-</sup>Ter-119<sup>-</sup>Tie2<sup>-</sup>AlphaV<sup>+</sup>Thy<sup>+</sup>6C3<sup>-</sup>CD105<sup>-</sup>CD200<sup>+</sup> Cells.* Chan et al. isolated cells from femoral growth plates of mice through enzymatic and mechanical dissociation. FACS showed that a large group of cells were CD45<sup>-</sup>Ter-119<sup>-</sup>Tie2<sup>-</sup>AlphaV<sup>+</sup> (hereafter termed as [AlphaV<sup>+</sup>]). Subsequent microarray analysis of [AlphaV<sup>+</sup>] further divided this population into eight subpopulations, based on different expressions of CD105, Thy, 6C3, and CD200.

CD45 and Ter-119 are universally expressed in hematopoietic cells. Tie2 is an angiopoietin receptor mostly expressed by endothelial cells and hematopoietic cells. Therefore, CD45, Ter-119, and Tie2 are markers to exclude hematopoietic lineages from bone marrow. AlphaV, as a member of the integrin family, is recently identified as a receptor for irisin, a kind of myokines that promote bone remodeling [38–40]. Thy is a heavily N-glycosylated glycoposphatidylinositol which is expressed on MSCs, fibroblasts, microvascular endothelial cells, neurons, hematopoietic stem cells (HSCs), and mouse T cells [41–43]. CD105 (also known as endoglin) is a type I membrane glycoprotein and a part of the TGF- $\beta$  receptor complex. CD105 can act as a marker of bone marrow colony-forming unit-fibroblasts (CFU-Fs) [21]. The type I membrane glycoprotein CD200 is predominantly expressed on some thymocytes, lymphocytes, neurons, and endothelial and follicular dendritic cells.

Experiment showed that both the [CD45<sup>-</sup>Ter-119<sup>-</sup>Tie2<sup>-</sup>AlphaV<sup>+</sup>Thy<sup>+</sup>6C3<sup>-</sup>CD105<sup>-</sup>CD200<sup>+</sup>] (hereafter short termed as [AlphaV<sup>+</sup>Thy<sup>+</sup>6C3<sup>-</sup>CD105<sup>-</sup>CD200<sup>+</sup>]) subpopulation and single cell sorted from it could generate the other seven subpopulations in a linear fashion both in vitro and in an exogenous environment after transplantation in vivo, indicating that [AlphaV<sup>+</sup>Thy<sup>+</sup>6C3<sup>-</sup>CD105<sup>-</sup>CD200<sup>+</sup>] cells lie at the apex of the skeletogenic differentiation hierarchy [25]. In addition, the [AlphaV<sup>+</sup>Thy<sup>+</sup>6C3<sup>-</sup>CD105<sup>-</sup>CD200<sup>+</sup>]

population possesses the ability of self-renewal and multipotency (bone, cartilage, and stroma). Please note that single cell sorted from the [AlphaV<sup>+</sup>Thy<sup>+</sup>6C3<sup>-</sup>CD105<sup>-</sup>CD200<sup>+</sup>] subgroup requires the help of a “supportive niche” to give rise to chondrocytes and osteocytes upon kidney capsule transplantation. In this experiment, 5000 unsorted cells from the long bones were used to provide the “supportive niche.” Without them, the individual [AlphaV<sup>+</sup>Thy<sup>+</sup>6C3<sup>-</sup>CD105<sup>-</sup>CD200<sup>+</sup>] cell cannot survive beneath the renal capsule. Compared with uninjured sites, callus of an injured site had more SSCs and these cells were more osteogenic, revealing a pivotal role of mSSCs in fracture healing. Taken together, researchers conclude that the [AlphaV<sup>+</sup>Thy<sup>+</sup>6C3<sup>-</sup>CD105<sup>-</sup>CD200<sup>+</sup>] cell represents a kind of mouse skeletal stem cell (mSSC) population and that the seven other subpopulations of [AlphaV<sup>+</sup>] are descendants of mSSC [44].

Some factors were identified that could influence the activity and differentiation of the [AlphaV<sup>+</sup>Thy<sup>+</sup>6C3<sup>-</sup>CD105<sup>-</sup>CD200<sup>+</sup>] mSSCs and their progenies. Firstly, Gene Expression Commons analysis of microarray data and single-cell RNA sequencing both indicated that autocrine signaling and/or paracrine signaling are present in this mSSCs and descendants. Secondly, the proliferation of the [AlphaV<sup>+</sup>Thy<sup>+</sup>6C3<sup>-</sup>CD105<sup>-</sup>CD200<sup>+</sup>] mSSCs could be induced by recombinant BMP and inhibited by the BMP2 antagonist in culture. Interestingly, some progenies of the mSSCs expressed antagonists of the BMP2 signaling pathway, such as Gremlin-2 and Noggin, suggesting that downstream skeletal progenitors can regulate mSSC activity.

Fate commitment of these skeletal stem/progenitor cells can be shifted between the bone and cartilage. On the one hand, prochondrogenic progenitors (PCPs or [CD45<sup>-</sup>Ter-119<sup>-</sup>Tie2<sup>-</sup>AlphaV<sup>+</sup>Thy<sup>+</sup>6C3<sup>-</sup>CD105<sup>-</sup>CD200<sup>+</sup>] cells), the skeletal progenitors that are directed primarily toward cartilage formation, can differentiate into a bone when cotransplanted with the bone, cartilage, and stromal progenitors (BCSPs), a progeny of the [AlphaV<sup>+</sup>Thy<sup>+</sup>6C3<sup>-</sup>CD105<sup>-</sup>CD200<sup>+</sup>] mSSCs. On the other hand, VEGF blockade can promote chondrogenesis of SSCs, probably at the expense of osteogenesis. BMP2 can induce de novo formation of [AlphaV<sup>+</sup>Thy<sup>+</sup>6C3<sup>-</sup>CD105<sup>-</sup>CD200<sup>+</sup>] cells in some extraskelatal locations. Considering the aforementioned results, it is understandable that code-livery of the BMP2 and VEGF inhibitor can induce de novo formation of cartilage in adipose tissue.

**2.2. PDPN<sup>+</sup>CD146<sup>+</sup>CD73<sup>+</sup>CD164<sup>+</sup> Cells.** After identifying a kind of SSCs in the mouse (CD45<sup>-</sup>Ter-119<sup>-</sup>Tie2<sup>-</sup>AlphaV<sup>+</sup>Thy<sup>+</sup>6C3<sup>-</sup>CD105<sup>-</sup>CD200<sup>+</sup> cells), Chan et al. found that PDPN<sup>+</sup>CD146<sup>+</sup>CD73<sup>+</sup>CD164<sup>+</sup> cells represent a type of human skeletal stem cell, which can be obtained from fetal and adult bones, BMP2-treated human adipose stroma, and iPSCs [24].

Podoplanin (PDPN) is a conserved mucin-type protein found among species. PDPN can act as a diagnostic marker in certain types of cancer [45]. CD146 (also known as MCAM) is a cell adhesion molecule that closely related with melanoma. A previous study revealed that CD146 can mark a type of self-renewing osteoprogenitors in human bone marrow and the CD146<sup>+</sup> osteoprogenitors

can establish a hematopoietic microenvironment [46]. CD73 is a glycosylphosphatidylinositol-linked cell surface protein and is considered as a potential target of several cancers [47]. CD164 is a mucin-like receptor mainly expressed by CD34<sup>+</sup> hematopoietic progenitor cells and can suppress hematopoietic cell proliferation [48].

In this experiment, seven distinct cell populations were isolated in the human fetal growth plate based on their different surface expressions of PDPN, CD146, CD73, CD164, and THY1 by FACS. These cells were neither endothelial nor hematopoietic. Among them, PDPN<sup>+</sup>CD146<sup>+</sup>CD73<sup>+</sup>CD164<sup>+</sup> cells are at the apex of the skeletal lineage hierarchy, with the ability of self-renewal and multipotency (cartilage, bone, and stroma but not fat) in vitro and in vivo. It is noteworthy that PDPN<sup>+</sup>CD146<sup>+</sup>CD73<sup>+</sup>CD164<sup>+</sup> cells managed to form ectopic ossicles with marrow cavity after serial renal capsule transplantation. Additionally, PDPN<sup>+</sup>CD146<sup>+</sup>CD73<sup>+</sup>CD164<sup>+</sup> cells can respond to skeletal injury through expansion of cell numbers and cell size. Based on the results mentioned above, PDPN<sup>+</sup>CD146<sup>+</sup>CD73<sup>+</sup>CD164<sup>+</sup> cells meet the rigorous standards of SSCs [44].

Similar with the mSSCs identified previously, BMP2 can cause de novo bone formation in human adipose stroma (HAS) and the newly formed ossicles housed PDPN<sup>+</sup>CD146<sup>+</sup>CD73<sup>+</sup>CD164<sup>+</sup> hSSCs and downstream PDPN<sup>+</sup>CD146<sup>+</sup> human osteoprogenitors (hOPs). Codelivery of the VEGF inhibitor and BMP2 can promote chondrogenesis at the expense of bone formation. Despite similarities mentioned above, differences of the gene expression profile during bone development including WNT, BMP, hedgehog, FGF, and Notch signaling pathways were identified between mSSCs and hSSCs. Some of these genes were exclusively expressed by hSSCs or mSSCs, for example, *SOST*, *CXXC4*, and *DNAJB6* were absent in mSSCs. At the same time, genes like *RUNX2* and *SOX9* were both expressed by mSSCs and hSSCs but showed different activity. The analysis about gene expression partially explains the divergencies on the formation of the ectopic bone and CFUs.

It is noteworthy that there exists a crosstalk between hSSCs and human hematopoietic stem cells (hHSCs). The two groups of cells support each other mainly through cytokines. On the one hand, hSSCs and its subpopulations expressed varieties of hematopoiesis-supportive cytokines such as ANGPT1, CSF1, SDF, IL27, IL7, and SCF, whose matching cognate receptors are expressed on hHSCs and progenies. On the other hand, hHSCs secrete a variety of factors to support the hSSC lineage, such as BMP2, BMP8A, DHH, FGF3, WNT1, and WNT8.

**2.3. PTHrP-Positive Resting Chondrocytes.** As it is widely accepted that stem cells are quiescent before they are needed and the resting zone of the growth plate is abundant in stem cell-like cells especially chondroprogenitors, it seems reasonable to find skeletal stem cells in the resting zone of the growth plate, where PTHrP plays a critical role in delaying hypertrophy of chondrocytes through interactions with Ihh [34, 49]. Based on this assumption, PTHrP<sup>+</sup> chondrocytes from the resting zone of the postnatal growth plate were identified as skeletal stem cells [50].

PTHrP<sup>+</sup> cells were distributed in the perichondrial region during a fetal stage. At postnatal day (P) 3, PTHrP<sup>+</sup> cells appeared at the resting zone. During P6 to P9, they proliferated markedly. The number of PTHrP<sup>+</sup> chondrocytes peaked at P15 and formed columnar chondrocytes longitudinally that were not restricted in the resting zone. They could gradually extend to primary spongiosa and bone marrow. Lineage tracing showed that besides giving rise to hypertrophic chondrocytes, a fraction of the PTHrP<sup>+</sup> resting chondrocytes can differentiate into *coll1a1* (2.3 kb)-GFP<sup>+</sup> osteoblasts and *Cxcl12*-GFP<sup>+</sup> stromal cells in vivo. In contrast, PTHrP<sup>+</sup> chondrocytes ineffectively give rise to adipocytes either in lineage tracing or subcutaneous transplantation but can be induced to adipocytes under adipogenic differentiation conditions in vitro. Under pathological conditions such as growth plate injury, PTHrP<sup>+</sup> resting chondrocytes lose their physiological fate and directly differentiate into osteoblasts instead.

In addition to multipotency, PTHrP<sup>+</sup> resting chondrocytes are self-renewing and clonogenic. Interestingly, PTHrP<sup>+</sup> resting chondrocytes developing before (P9) or after (P12) secondary ossification center formation possess distinct self-renewability. P9 PTHrP<sup>+</sup> cells failed to survive the third passage while a fraction of P12 PTHrP<sup>+</sup> cells can survive even after nine passages. Taken together, PTHrP<sup>+</sup> cells are heterogeneous populations consist of transient, short-term, and long-term skeletal stem cells.

Of note, flow cytometry analysis of PTHrP<sup>+</sup> resting chondrocytes demonstrates a portion of overlap with the mouse skeletal stem and progenitor cells identified previously by Chan and colleagues but not *Gremlin1*<sup>+</sup> cells [25], further proving that PTHrP<sup>+</sup> resting chondrocytes represent a type of skeletal stem cells from immunophenotypical perspective. Collectively, these observations suggest that PTHrP<sup>+</sup> resting chondrocytes are a unique type of SSCs.

Probably due to the function of PTHrP and hedgehog (Hh) signaling on delaying hypertrophy of chondrocytes, PTHrP<sup>+</sup> resting chondrocytes are critical in maintaining the integrity of the growth plate. Partial loss of PTHrP<sup>+</sup> resting cells is enough to induce premature hypertrophic differentiation of chondrocytes in the proliferating zone. Differentiation of PTHrP<sup>+</sup> resting cells toward columnar chondrocytes can be repressed regardless of using an agonist or an antagonist of Hh signaling.

**2.4. *Gli1*-Expressing Cells.** Glioma-associated oncogene 1 (*Gli1*) is a transcription factor and an effector of the Hh pathways. *Gli1* is closely related to osteoblast differentiation and marks MSCs in several organs of adult mice, like craniofacial bones and incisors [51–53]. For instance, a very recent experiment revealed that *Gli1* play a key part in mediating *Numb*-deficient osteoblasts and bone resorption through Hh pathways [54].

Shi et al. discovered that a group of *Gli1*<sup>+</sup> cells termed “metaphyseal mesenchymal progenitors” (MMPs) was pivotal for cancellous bone formation. MMPs are located in chondroosseous junction immediately under the growth plate in young postnatal mice. Subsequent genetic lineage tracing experiments unveiled several unique features of MMPs [55].

Firstly, a large number of MMPs were enriched in mRNA associated with some MSC markers, including *CD146/Mcam*, *CD44*, *CD106/Vcam1*, *Pdgfra*, *Pdgfrb*, *αSma*, and *Lepr*. Secondly, MMPs were at least tripotent to generate osteoblasts, bone marrow stromal cells (BMSCs), and bone marrow adipocytes in vivo. Of note, the experiment data showed that 20% and <10% of *Gli1*<sup>+</sup> cells were positive for *Osx* and *Col1*, respectively, at 1 month of age and after one-month chasing, the proportion increased to 50% and 80%. Ablation of MMPs reduced the bone mass because of defective bone formation rather than bone resorption, which is evidenced by decreased serum propeptide of type I procollagen (P1NP) and a normal level of C-telopeptide (CTX-I) in *Gli1-CreER<sup>T2</sup>;Ai9;Rosa-DTA* mice.

It is noteworthy that MMP-derived osteoblasts supported cancellous bone formation mainly at a very young age (juvenile mice, till 4 months of age), while the MMP-derived BMSCs about half of which expressed *Lepr* (49.1 ± 9.5%, 6 months of age) may took the responsibility for long-term skeletogenesis in adult mice by generating osteoblasts, adipocytes, and bone marrow stroma. As for fracture healing, MMPs can contribute to bone regeneration by promoting bone (~50% osteocalcin<sup>+</sup> cells) and cartilage (~63% aggrecan<sup>+</sup> cells) formation. Overall, MMPs can be regarded as a type of SSCs or at least a source of SSCs if not.

Previous studies have revealed the role of *Ihh* signaling on osteoblast differentiation, and *Gli1* is an important transcription factor of *Ihh*-*Smo* signaling pathways [51]. Expectedly, blockade of Hh signaling in MMPs caused reduced bone mass and trabecular bone number in juvenile mice without affecting bone resorption. *Smo* deletion decreased the proliferation of MMPs and impaired their osteogenic differentiation. In addition, conditional knockout of *β*-catenin in MMPs leads to decreased cancellous bone mass and increased marrow adiposity, corresponding with the previous observations on *Osx-Cre;β-catenin<sup>fl/fl</sup>* mice [56]. This result indicates the determinant role of *β*-catenin in the fate commitment of MMPs.

**2.5. *Gremlin 1*-Expressing Cells.** *Gremlin1* (*Grem1*), as a BMP antagonist and a VEGFR2 agonist, has been recognized that it functions in embryonic and postnatal skeletogenesis [57–59]. Worthley et al. demonstrated that *Grem1* may mark a small group of “skeletal stem cells” immediately adjacent to the growth plate. The number of *Grem1*<sup>+</sup> cells was rare, only comprised 0.0025% of the live, mononucleated bone marrow cells after collagenase digestion [60]. Distinct from perivascular MSCs like *Nestin*<sup>+</sup> cells and *LepR*<sup>+</sup> cells which contribute to skeletogenesis mainly in later adulthood, *Grem1*<sup>+</sup> cells can function in both development and adult stage, especially in early life [61, 62].

*Grem1*<sup>+</sup> cells are clonogenic in vitro and in vivo, and this ability is stronger than *Nestin*<sup>+</sup> MSCs. *Grem1*<sup>+</sup> cells were tripotent to produce bone, cartilage, and reticular marrow stromal cells, but not fat, in development and adulthood of mice (~64% of the bone and 50% of the chondrocytes of the metaphyseal and epiphyseal bone, at the age of 4 weeks). Thus, the *Grem1*<sup>+</sup> cells are termed as osteochondroreticular (OCR) stem cells. Gene expression profile showed that several pathways relating to osteochondral differentiation rather than

adipocytic differentiation were elevated in the Grem1<sup>+</sup> cells. Grem1<sup>+</sup> cells are highly active in BMP signaling, ECM-receptor interaction, PI3K-AKT signaling, and focal adhesion pathways, which correlates with osteochondral differentiation potential of Grem1<sup>+</sup> cells. Moreover, Grem1<sup>+</sup> cells and descendants highly expressed adipogenesis inhibitors. Grem1<sup>+</sup> cells were critical for bone formation. *Grem1* null mice were osteopenic [58], and an incomplete ablation of Grem1<sup>+</sup> cells using Grem1-creER<sup>T</sup>;R26-LSL-DTA leads to less total bone volume and trabecular bone fraction of mice. Moreover, Grem1<sup>+</sup> cells could function in fracture repair by generating osteoblasts and chondrocytes in vivo.

### 3. Perivascular

Mesenchymal cells in hematopoietic niche often provide regulatory cues for HSC development and homeostasis. At the same time, many important discoveries of SSCs are based on vasculature, indicating a function of the vascular microenvironment for SSCs [26, 63–65]. The association between MSCs/SSCs and hematopoiesis is the focus of the study [66]. A crowd of perivascular MSC/SSC markers have been identified, such as Nestin, LepR, Prx1, Mx1, PDGFR, CD51, and CD146 [21, 46, 61, 62, 67, 68]. Nestin-GFP cells, for example, found perivascular in the bone marrow, were capable of trilineage differentiation (osteoblasts, chondrocytes, and adipocytes) and possess SSC-related activities. In addition, Nestin-GFP cells expressed high levels of HSC maintenance genes like *Cxcl12*, *angiopoietin-1* (*Angpt1*), and *interleukin-7*<sup>61</sup>. In this chapter, we will describe three groups of perivascular SSCs in detail. Among them, LepR<sup>+</sup> cells and CD45<sup>-</sup>CD31<sup>-</sup>Sca1<sup>+</sup>CD24<sup>+</sup> cells play a regulatory role in hematopoiesis, while the association between Hox<sup>+</sup> cells and hematopoiesis remains unclear.

**3.1. CD45<sup>-</sup>CD31<sup>-</sup>Sca1<sup>+</sup>CD24<sup>+</sup> Cells.** Flow cytometric sorting of CD45 and CD31 excludes the hematopoietic and endothelial lineages in bone marrow [69]. Sca1 (stem cell antigen-1), as a mouse glycosyl phosphatidylinositol-anchored cell surface protein, has been commonly used as a marker for HSCs. More importantly, Sca1 is also used in isolating stem/progenitor cells from the skeletal system [70]. CD24 is a mucin-type sialoglycoprotein that is expressed mainly by immature hematopoietic cells [71].

CD45<sup>-</sup>CD31<sup>-</sup>Sca1<sup>+</sup>CD24<sup>+</sup> cells are mostly located in the perivascular niche and more abundant in the metaphyseal area than diaphyseal area [72]. CD45<sup>-</sup>CD31<sup>-</sup>Sca1<sup>+</sup>CD24<sup>+</sup> cells possess the following skeletal stem cell-like characteristics. Firstly, it has marked colony-forming unit ability. Secondly, CD45<sup>-</sup>CD31<sup>-</sup>Sca1<sup>+</sup>CD24<sup>+</sup> cell population had an excellent multipotent capacity to give rise to osteochondrogenic progenitor cells (OPCs: CD45<sup>-</sup>CD31<sup>-</sup>Sca1<sup>+</sup>PDGFα<sup>+</sup>) and two subsets of adipogenic populations: fate-committed adipogenic progenitor cells (APCs: CD45<sup>-</sup>CD31<sup>-</sup>Sca1<sup>+</sup>CD24<sup>-</sup>) and a more mature preadipocyte (preAd: CD45<sup>-</sup>CD31<sup>-</sup>Sca1<sup>+</sup>Zfp423<sup>+</sup>). Thirdly, CD45<sup>-</sup>CD31<sup>-</sup>Sca1<sup>+</sup>CD24<sup>+</sup> cells were able to contribute to bone healing when these cells were transplanted into the defect through generating some osteogenic and chondrogenic structures as with OPCs. The

two aforementioned adipocytic populations can delay the healing process, which is at least partially attributed to DPP4 (dipeptidyl peptidase-4), a protease acts commonly as a target of treating diabetes clinically and can be released by CD45<sup>-</sup>CD31<sup>-</sup>Sca1<sup>+</sup>CD24<sup>+</sup> cells and APCs after adipogenic differentiation. DPP4 inhibitors can promote osteogenic differentiation of CD45<sup>-</sup>CD31<sup>-</sup>Sca1<sup>+</sup>CD24<sup>+</sup> cells and OPCs, reversing the inhibitory effect of the APCs and preAd on bone healing. Moreover, the adipocytic lineage of CD45<sup>-</sup>CD31<sup>-</sup>Sca1<sup>+</sup>CD24<sup>+</sup> cells can be influenced by age and diet, with increased accumulation of APCs instead of OPCs

CD45<sup>-</sup>CD31<sup>-</sup>Sca1<sup>+</sup>CD24<sup>+</sup> cells and adipogenic progenies have distinct effect on hematopoiesis. On the one hand, CD45<sup>-</sup>CD31<sup>-</sup>Sca1<sup>+</sup>CD24<sup>+</sup> population itself can promote the hematopoietic regeneration in irradiated mice with increased hematopoietic progenitor cells. On the other hand, the transplantation of APCs or preAds could impair hematopoietic reconstitution, which was consistent with the previous view that bone marrow adipocytes act negatively on hematopoietic homeostasis [73].

**3.2. Leptin Receptor-Expressing Cells.** Leptin is a fat-derived hormone that plays a crucial part in regulating appetite and energy expenditure [74]. Moreover, leptin is involved in osteogenesis via central and peripheral pathways [75, 76]. The leptin receptor is a class I cytokine receptor that gradually appears postnatally, and deficiency of it can lead to obesity [77].

Nowadays, leptin receptor (LepR) is widely used to mark SSCs of adult mice as leptin receptor-expressing (LepR<sup>+</sup>) cells occur almost specifically in adult mice [62]. LepR<sup>+</sup> cells reside around sinusoids and arterioles and significantly overlap with other MSC markers including PDGFα, CD51, PDGFβ, CD105, *Prx1*, and Nestin-GFP<sup>low</sup> but rarely express Nestin-GFP<sup>high</sup>. LepR<sup>+</sup> cells only comprise 0.3% of bone marrow cells but are highly clonogenic, consisting of most bone marrow CFU-Fs (94% ± 4%). LepR<sup>+</sup> cells are tripotent to give rise to the bone, cartilage, and fat in vitro and upon subcutaneous injection and are a major source of the bone and adipocytes from 2 months of age. The capacity of LepR<sup>+</sup> cells to generate bone and adipocytes increases with age.

LepR<sup>+</sup> cells are quiescent physiologically but can be activated upon irradiation or bone fracture. Irradiation activates LepR<sup>+</sup> cells to give rise to osteoblasts and adipocytes, and LepR<sup>+</sup> cells are considered as the main source of bone marrow adipocytes of adult mice [62]. LepR<sup>+</sup> cells can contribute to bone and cartilage healing while chondrogenesis is hardly seen under physiological conditions in vivo.

It should be noted that there is a close correlation between LepR<sup>+</sup> cells and hematopoiesis. LepR<sup>+</sup> cells express HSC niche factors like stem cell factor (SCF) and CXCL12 in a high level, and the ablation of LepR<sup>+</sup> cells impairs hematopoiesis. Further research unveiled that LepR<sup>+</sup> cells contribute to hematopoietic regeneration through adipogenic differentiation. The bone marrow adipocytes can synthesize SCF and adiponectin to support hematopoietic stem cell proliferation [78, 79], which is contradictory with the previous view that bone marrow adipocytes act negatively on hematopoiesis [73, 80].

Further experiment revealed that LepR also plays a critical role in regulating the differentiation of SSCs through the Jak2/Stat3 signaling pathway. A high-fat diet or adiposity can activate Lep/LepR signaling, which promotes adipogenesis at the expense of osteogenesis and acts as a negative factor in bone fracture regeneration [81].

**3.3. *Hox11*-Expressing Cells.** *Hox* genes are comprised of 13 sets of transcription factors that play a critical part in regulating the formation and regeneration of vertebral and limb skeleton and, additionally, differentiation of stem cells [82–84]. *Hox* genes are expressed in a spatiotemporal sequence, which means *Hox1* and *Hox2* appear early and anteriorly while *Hox13* is expressed late and posteriorly. Among them, *Hox11* expressed in zeugopod (tibia/fibula and radius/ulna) [85, 86].

*Hox11*<sup>+</sup> cells in adult mice are nonendothelial, nonhematopoietic, and undifferentiated cells [86]. They are restricted within zeugopod, specifically speaking, in the periosteal and perivascular areas throughout the adulthood [87]. Most adult *Hox11*<sup>+</sup> cells were found to express other classic SSC markers including PDGFR $\alpha$ , CD51, and LepR. In addition, perivascular *Hox11*<sup>+</sup> cells in adult mice were supposed to represent a group of SSCs due to the following reasons. Firstly, they were clonogenic in vitro and cells positive for *Hox11*, PDGFR $\alpha$ , and CD51 exhibit almost three times greater self-renewal ability than cells only positive for PDGFR $\alpha$  and CD51. Secondly, perivascular *Hox11*<sup>+</sup> cells were tripotent to give rise to osteoblasts, chondrocytes, and adipocytes in vitro and vivo. Thirdly, *Hox11*<sup>+</sup> cells were crucial for fracture repair of zeugopod [88]. They can respond to injury through self-expansion, and they could differentiate into osteoblasts and chondrocytes upon transplantation into fracture callus. Dysfunction of *Hox11* would cause defective fracture repairment, which was reflected in reduced cartilage formation, delayed ossification, and increased adipogenic differentiation of *Hox11*<sup>+</sup> cells. Of note, these effects were zeugopod-specific. In other words, fracture healing of other regions was not influenced by function loss of *Hox11*. Collectively, it is believed that *Hox11* can be regarded as a marker of SSCs.

#### 4. Periosteum

Periosteum is the membrane that lines the outer surface of bones. It can be divided into two layers, and the inner layer is known as a reservoir of osteogenic progenitors, which play an important part in bone formation and bone generation [89]. Considering its easy access and minimal invasiveness, periosteum is supposed to be a good place to find SSCs for clinical treatment [90].

Over the past few years, several markers have been reported for potential identification of SSCs in the periosteum, but due to a low purity and stemness, these markers cannot be used alone [90, 91]. A recent study demonstrated that there exists a pool of SSCs within the periosteum. These cells can give rise to osteocytes, adipocytes, and chondrocytes in vitro. Compared with bone marrow SSCs, the SSCs in the periosteum were more clonogenic and possessed greater ability of cell growth and bone regeneration. More importantly,

this pool of SSCs can survive after periosteum grafting. Periostin, a secreted extracellular matrix protein, was believed to be essential for maintaining the pool of periosteal skeletal stem cells [92]. However, a long-standing question impeding translational research is a lack of specific markers for this pool. Until recently, cathepsin K was identified.

Cathepsin K (CTSK) is a lysosomal cysteine protease that mainly secreted by activated osteoclasts [93]. Cathepsin K can play a major part in bone remodeling and resorption by degrading collagen and matrix proteins. Bone resorption can be reversed by inactivation or deletion of *Ctsk*. Thus, *Ctsk* is a recognized marker for marrow mature osteoclasts both in vivo and in vitro [93–95]. In 2013, Yang et al. accidentally identified a pool of *Ctsk*<sup>+</sup> cells within Ranvier's groove. Conditional knockout of tyrosine phosphatase SHP2 in *Ctsk*<sup>+</sup> cells leads to metachondromatosis, a disease characterized by the presence of multiple enchondromas and osteochondromas, indicating that *Ctsk*<sup>+</sup> cells in Ranvier's groove exhibit functional properties consistent with mesenchymal progenitors. They termed these cells as *Ctsk*<sup>+</sup> chondroid progenitors (CCPs) [96].

Recently, Debnath et al. discovered that *Ctsk* could label a type of skeletal stem cells that exist in the periosteal mesenchyme of the long bones or calvarium, termed as periosteal stem cells (PSCs) [97]. Three groups of nonhematopoietic CTSK-mGFP mesenchymal cells were identified: PSCs and periosteal progenitors 1 and 2 (PP1 and PP2), among which only PSCs were constantly positive for CD200 [98]. PSCs can give rise to all the CTSK-mGFP cells, but other cells cannot, namely, PSCs lie at the top of the CTSK-mGFP differentiation hierarchy. Transcriptional analysis and single-cell RNA sequencing showed that PSCs express MSC-related gene. Besides, PSCs possess the ability of self-renewal and multipotency to differentiate into osteoblasts, adipocytes, and chondrocytes. Critically, PSCs can retain these abilities even after serial transplantation into the mammary fat pad and kidney capsule.

PSC-derived osteoblasts were so crucial that lack of it can cause reduced periosteal bone formation and abnormal cortical structure. PSCs can contribute to fracture healing via self-expansion and increased osteogenic and chondrogenic differentiation, which is intriguing as the periosteum is involved in intramembranous instead of endochondral bone formation. Moreover, PSCs isolated from the fracture callus promoted endochondral ossification after ectopic transplantation into the kidney capsule. The plasticity of PSCs partially explains the contradiction.

It is noteworthy that researchers managed to isolate human periosteal stem cells (h-PSCs) in human periosteal tissue of the femur. The h-PSCs were analogous to m-PSCs in immunophenotype and are multipotent both in vivo and in vitro, which provides a feasible way for treating human skeletal disorders.

#### 5. Cranial Suture

Different from long bones, craniofacial bones are developed via intramembranous bone formation without intermediate cartilage, indicating that SSCs residing here prefer bone

formation to chondrogenesis [99, 100]. Besides, there is little bone marrow space inside of the craniofacial bones compared with the long bones [101]. The gap between craniofacial bones is known as a suture. Premature closure of the suture characterizes craniosynostosis, a developmental craniofacial deformity accompanying with a series of severe consequences including increased intracranial pressure and craniofacial dysmorphism [102]. A cranial suture acts as the growth site for osteogenesis of craniofacial bones, and therefore, suture mesenchyme is postulated as a main source of craniofacial SSCs. The two SSCs we described in the following passage both reside within suture mesenchyme [103].

**5.1. *Gli1*-Expressing Cells.** Besides as a marker of MMPs (previously described in this review), *Gli1* was initially regarded as a marker of MSCs in the cranial suture of adult mice [52]. Cranial *Gli1*<sup>+</sup> cells share a lot of characteristics with MMPs. Cranial *Gli1*<sup>+</sup> cells are capable of trilineage differentiation (osteogenic, chondrogenic, and adipogenic), but adipogenic differentiation ability of them was not comparable to that of the MMPs. *Gli1*<sup>+</sup> cells can contribute to bone injury healing. Besides, they are regulated by *Ihh* signaling pathways, blockade of which could cause reduced bone volume.

However, compared with MMPs, *Gli1*<sup>+</sup> cells in cranial sutures can generate periosteum and dura but contribute little to bone marrow and vasculature. More importantly, *Gli1*<sup>+</sup> cells in the suture mesenchyme are crucial for local homeostasis, and ablation of them using diphtheria toxin (DTA) resulted in a typical symptom of craniosynostosis, growth arrest, osteoporosis, and compromised injury repair.

**5.2. *Axin2*-Expressing Cells.** *Axin2*, also known as conductin or Axil, is a negative regulator of *Wnt*/ $\beta$ -catenin pathways and thus plays a critical role in skeletogenesis. *Axin2* can inhibit intramembranous bone formation, and the inactivation of *Axin2* leads to craniosynostosis because of excessive intramembranous ossification [104, 105]. Of note, fate commitment of *Axin2* stem cells is tightly regulated by interaction of several signaling pathways including FGF, BMP, and *Wnt* [106, 107].

Maruyama et al. identified that *Axin2* can mark a group of SSCs or specifically termed as suture stem cells (SuSCs) [108]. *Axin2*<sup>+</sup> SuSCs and their descendants were restricted within calvarial sutures and nearly absent in long bones, indicating that *Axin2*<sup>+</sup> cells represent a totally distinct group of SSCs from those populations in the long bones. *Axin2*<sup>+</sup> cells possess the capacity of self-renewal and colony forming and were able to give rise to osteogenic lineages during the developmental period and adulthood of mice. *Axin2*<sup>+</sup> cells could strongly respond to bone injury through self-expansion and producing skeletogenic cell types including osteoprogenitors and osteocytes in vivo. Although *Axin2*<sup>+</sup> cells did not differentiate into chondrogenic cells under normal conditions, they are committed to cartilage formation with BMP2 induction. Importantly, *Axin2*<sup>+</sup> cells showed a great ability of bone regeneration upon implantation into the kidney capsule and they could contribute to the formation of the ectopic bone that appears to share morphological features with calvarial skeletons, which had little marrow structure. Further experi-

ment indicated that the *Axin2*<sup>+</sup> cells applied into the injury site can directly engraft into the regenerated bone and promoted osteogenesis.

*Axin2*<sup>+</sup> cells in the suture mesenchyme express little markers of MSCs except *LepR* but overlap a lot with *Gli1*<sup>+</sup> cell population. Distinct from *Gli1*<sup>+</sup> cells which appear to be located within the whole suture and contribute to calvarial maintenance of the vicinity of central bone plates, *Axin2*<sup>+</sup> SuSCs were mainly located in the midline of the suture mesenchyme. The aforementioned differences indicate that the two groups of stem cells contribute to different parts of calvarium.

## 6. Conclusion

In this review, we emphasize four places of bones (growth plate, perivascular areas, periosteum, and cranial suture) as a possible source of SSCs and evaluate these cells from a SSC perspective. Compared with traditional mesenchymal stem cells, these identified “skeletal stem cells” are more defined and therefore more efficient in clinical utility. However, not all of them can differentiate into osteoblasts, chondrocytes, and adipocytes both in vitro and in vivo. More importantly, some markers are not precise enough to represent a pure group of SSCs, resulting from a contamination by their descendants or other cells. Hopefully, this flaw would be alleviated when used in combination with other markers. Looking back on these cells, we notice that different SSCs may share the same markers in space and time. Meanwhile, SSCs exhibit site-specific characteristics, indicating that distinct but somewhat overlapped pools of SSCs contribute to skeletogenesis altogether. In conclusion, to make the best use of SSCs, the mechanism of their fate commitment requires further research.

## Abbreviations

SSCs:	Skeletal stem cells
MSCs:	Mesenchymal stromal/stem cells
Mx1:	Myxovirus resistance-1
FACS:	Fluorescence-activated cell sorting
<i>Ihh</i> :	Indian hedgehog
PTHrP:	Parathyroid hormone-related protein
FGF:	Fibroblast growth factors
BMP:	Bone morphogenetic proteins
VEGF:	Vascular endothelial growth factor
HSCs:	Hematopoietic stem cells
CFU-Fs:	Colony-forming unit-fibroblasts
mSSC:	Mouse skeletal stem cell
PCPs:	Prochondrogenic progenitors
BCSPs:	Bone, cartilage, and stromal progenitors
PDPN:	Podoplanin
HAS:	Human adipose stroma
hOPs:	Human osteoprogenitors
hHSCs:	Human hematopoietic stem cells
Hh:	Hedgehog
<i>Gli1</i> :	Glioma-associated oncogene 1
MMPs:	Metaphyseal mesenchymal progenitors
BMSCs:	Bone marrow stromal cells

PINP: Propeptide of type I procollagen  
 CTX-I: C-telopeptide  
 Grem1: Gremlin1  
 OCR: Osteochondroreticular  
 Angpt1: Angiopoietin-1  
 Sca1: Stem cell antigen-1  
 OPCs: Osteochondrogenic progenitor cells  
 APCs: Adipogenic progenitor cells  
 preAd: Preadipocyte  
 DPP4: Dipeptidyl peptidase-4  
 LepR: Leptin receptor  
 LepR+: Leptin receptor-expressing  
 SCF: Stem cell factor  
 CTSK: Cathepsin K  
 CCPs: Ctsk<sup>+</sup> chondroid progenitors  
 PSCs: Periosteal stem cells  
 PP1: Periosteal progenitor 1  
 PP2: Periosteal progenitor 2  
 h-PSCs: Human periosteal stem cells  
 DTA: Diphtheria toxin  
 SuSCs: Suture stem cells.

## Conflicts of Interest

The authors declare no conflicts of interest.

## References

- [1] J. O. Manilay and M. Zouali, "Tight relationships between B lymphocytes and the skeletal system," *Trends in Molecular Medicine*, vol. 20, no. 7, pp. 405–412, 2014.
- [2] R. C. Riddle and T. L. Clemens, "Bone cell bioenergetics and skeletal energy homeostasis," *Physiological Reviews*, vol. 97, no. 2, pp. 667–698, 2017.
- [3] E. C. Watson and R. H. Adams, "Biology of bone: the vasculature of the skeletal system," *Cold Spring Harbor Perspectives in Medicine*, vol. 8, no. 7, 2018.
- [4] J. R. Edwards and G. R. Mundy, "Advances in osteoclast biology: old findings and new insights from mouse models," *Nature Reviews Rheumatology*, vol. 7, no. 4, pp. 235–243, 2011.
- [5] S. Harada and G. A. Rodan, "Control of osteoblast function and regulation of bone mass," *Nature*, vol. 423, no. 6937, pp. 349–355, 2003.
- [6] S. R. Cummings and L. J. Melton, "Epidemiology and outcomes of osteoporotic fractures," *Lancet*, vol. 359, no. 9319, pp. 1761–1767, 2002.
- [7] D. M. Lee and M. E. Weinblatt, "Rheumatoid arthritis," *Lancet*, vol. 358, no. 9285, pp. 903–911, 2001.
- [8] L. Aghebati-Maleki, S. Dolati, R. Zandi et al., "Prospect of mesenchymal stem cells in therapy of osteoporosis: a review," *Journal of Cellular Physiology*, vol. 234, no. 6, pp. 8570–8578, 2018.
- [9] W. Liu, L. Zhou, C. Zhou et al., "GDF11 decreases bone mass by stimulating osteoclastogenesis and inhibiting osteoblast differentiation," *Nature Communications*, vol. 7, no. 1, article 12794, 2016.
- [10] Y. C. Guo, M. Y. Wang, S. W. Zhang et al., "Ubiquitin-specific protease USP34 controls osteogenic differentiation and bone formation by regulating BMP2 signaling," *The EMBO Journal*, vol. 37, no. 20, p. e99398, 2018.
- [11] Y. Fan, J. I. Hanai, P. T. Le et al., "Parathyroid hormone directs bone marrow mesenchymal cell fate," *Cell Metabolism*, vol. 25, no. 3, pp. 661–672, 2017.
- [12] Y. Wu, L. Xie, M. Wang et al., "Mettl3-mediated m<sup>6</sup>A RNA methylation regulates the fate of bone marrow mesenchymal stem cells and osteoporosis," *Nature Communications*, vol. 9, no. 1, article 4772, 2018.
- [13] C. C. Zhou, Q. C. Xiong, X. X. Zhu et al., "AFF1 and AFF4 differentially regulate the osteogenic differentiation of human MSCs," *Bone Research*, vol. 5, no. 1, article 17044, 2017.
- [14] D. Sipp, P. G. Robey, and L. Turner, "Clear up this stem-cell mess," *Nature*, vol. 561, no. 7724, pp. 455–457, 2018.
- [15] P. Bianco, P. G. Robey, and P. J. Simmons, "Mesenchymal stem cells: revisiting history, concepts, and assays," *Cell Stem Cell*, vol. 2, no. 4, pp. 313–319, 2008.
- [16] J. Galipeau, D. J. Weiss, and M. Dominici, "Response to *Nature* commentary "Clear up this stem-cell mess"," *Cytotherapy*, vol. 21, no. 1, pp. 1–2, 2019.
- [17] P. Bianco and P. G. Robey, "Skeletal stem cells," *Development*, vol. 142, no. 6, pp. 1023–1027, 2015.
- [18] P. Bianco, X. Cao, P. S. Frenette et al., "The meaning, the sense and the significance: translating the science of mesenchymal stem cells into medicine," *Nature Medicine*, vol. 19, no. 1, pp. 35–42, 2013.
- [19] G. Nusspaumer, S. Jaiswal, A. Barbero et al., "Ontogenic identification and analysis of mesenchymal stromal cell populations during mouse limb and long bone development," *Stem Cell Reports*, vol. 9, no. 4, pp. 1124–1138, 2017.
- [20] M. Dominici, K. le Blanc, I. Mueller et al., "Minimal criteria for defining multipotent mesenchymal stromal cells. The International Society for Cellular Therapy position statement," *Cytotherapy*, vol. 8, no. 4, pp. 315–317, 2006.
- [21] D. Park, J. A. Spencer, B. I. Koh et al., "Endogenous bone marrow MSCs are dynamic, fate-restricted participants in bone maintenance and regeneration," *Cell Stem Cell*, vol. 10, no. 3, pp. 259–272, 2012.
- [22] A. I. Caplan, "Review: mesenchymal stem cells: cell-based reconstructive therapy in orthopedics," *Tissue Engineering*, vol. 11, no. 7–8, pp. 1198–1211, 2005.
- [23] C. M. McLeod and R. L. Mauck, "On the origin and impact of mesenchymal stem cell heterogeneity: new insights and emerging tools for single cell analysis," *European Cells & Materials*, vol. 34, pp. 217–231, 2017.
- [24] C. K. F. Chan, G. S. Gulati, R. Sinha et al., "Identification of the human skeletal stem cell," *Cell*, vol. 175, no. 1, pp. 43–56.e21, 2018.
- [25] C. K. F. Chan, E. Y. Seo, J. Y. Chen et al., "Identification and specification of the mouse skeletal stem cell," *Cell*, vol. 160, no. 1–2, pp. 285–298, 2015.
- [26] F. F. Mohamed and R. T. Franceschi, "Skeletal stem cells: origins, functions and uncertainties," *Current Molecular Biology Reports*, vol. 3, no. 4, pp. 236–246, 2017.
- [27] H. Zhu, Z. K. Guo, X. X. Jiang et al., "A protocol for isolation and culture of mesenchymal stem cells from mouse compact bone," *Nature Protocols*, vol. 5, no. 3, pp. 550–560, 2010.
- [28] P. Bianco, "Mesenchymal" stem cells," *Annual Review of Cell and Developmental Biology*, vol. 30, no. 1, pp. 677–704, 2014.

- [29] G. S. Gulati, M. P. Murphy, O. Marecic et al., "Isolation and functional assessment of mouse skeletal stem cell lineage," *Nature Protocols*, vol. 13, no. 6, pp. 1294–1309, 2018.
- [30] E. D. Tichy and F. Mourkioti, "Human skeletal stem cells: the markers provide some clues in the hunt for hidden treasure," *Cell Stem Cell*, vol. 23, no. 4, pp. 462–463, 2018.
- [31] H. M. Kronenberg, "Developmental regulation of the growth plate," *Nature*, vol. 423, no. 6937, pp. 332–336, 2003.
- [32] B. C. J. van der Eerden, M. Karperien, and J. M. Wit, "Systemic and local regulation of the growth plate," *Endocrine Reviews*, vol. 24, no. 6, pp. 782–801, 2003.
- [33] F. Long and D. M. Ornitz, "Development of the endochondral skeleton," *Cold Spring Harbor Perspectives in Biology*, vol. 5, no. 1, p. a008334, 2013.
- [34] U. I. Chung, E. Schipani, A. P. McMahon, and H. M. Kronenberg, "Indian hedgehog couples chondrogenesis to osteogenesis in endochondral bone development," *The Journal of Clinical Investigation*, vol. 107, no. 3, pp. 295–304, 2001.
- [35] W. A. Horton and C. R. Degnin, "FGFs in endochondral skeletal development," *Trends in Endocrinology and Metabolism: TEM*, vol. 20, no. 7, pp. 341–348, 2009.
- [36] V. Abad, J. L. Meyers, M. Weise et al., "The role of the resting zone in growth plate chondrogenesis," *Endocrinology*, vol. 143, no. 5, pp. 1851–1857, 2002.
- [37] P. T. Newton, L. Li, B. Zhou et al., "A radical switch in clonality reveals a stem cell niche in the epiphyseal growth plate," *Nature*, vol. 567, no. 7747, pp. 234–238, 2019.
- [38] H. Kim, C. D. Wrann, M. Jedrychowski et al., "Irisin mediates effects on bone and fat via  $\alpha V$  integrin receptors," *Cell*, vol. 175, no. 7, pp. 1756–1768.e17, 2018.
- [39] C. F. Lai and S. L. Cheng, " $\alpha v \beta$  integrins play an essential role in BMP-2 induction of osteoblast differentiation," *Journal of Bone and Mineral Research*, vol. 20, no. 2, pp. 330–340, 2005.
- [40] M. M. Thi, S. O. Suadicani, M. B. Schaffler, S. Weinbaum, and D. C. Spray, "Mechanosensory responses of osteocytes to physiological forces occur along processes and not cell body and require  $\alpha V \beta 3$  integrin," *Proceedings of the National Academy of Sciences of the United States of America*, vol. 110, no. 52, pp. 21012–21017, 2013.
- [41] W. Craig, R. Kay, R. L. Cutler, and P. M. Lansdorp, "Expression of Thy-1 on human hematopoietic progenitor cells," *The Journal of Experimental Medicine*, vol. 177, no. 5, pp. 1331–1342, 1993.
- [42] A. K. Picke, G. M. Campbell, F. N. Schmidt et al., "Thy-1 deficiency augments bone loss in obesity by affecting bone formation and resorption," *Frontiers in Cell and Developmental Biology*, vol. 6, p. 127, 2018.
- [43] A. F. Williams and A. N. Barclay, "The immunoglobulin superfamily—domains for cell surface recognition," *Annual Review of Immunology*, vol. 6, no. 1, pp. 381–405, 1988.
- [44] M. Kassem and P. Bianco, "Skeletal stem cells in space and time," *Cell*, vol. 160, no. 1–2, pp. 17–19, 2015.
- [45] J. L. Astarita, S. E. Acton, and S. J. Turley, "Podoplanin: emerging functions in development, the immune system, and cancer," *Frontiers in Immunology*, vol. 3, p. 283, 2012.
- [46] B. Sacchetti, A. Funari, S. Michienzi et al., "Self-renewing osteoprogenitors in bone marrow sinusoids can organize a hematopoietic microenvironment," *Cell*, vol. 131, no. 2, pp. 324–336, 2007.
- [47] B. Zhang, "CD73: a novel target for cancer immunotherapy," *Cancer Research*, vol. 70, no. 16, pp. 6407–6411, 2010.
- [48] A. C. Zannettino, H. J. Bühring, S. Niutta, S. M. Watt, M. A. Benton, and P. J. Simmons, "The sialomucin CD164 (MGC-24v) is an adhesive glycoprotein expressed by human hematopoietic progenitors and bone marrow stromal cells that serves as a potent negative regulator of hematopoiesis," *Blood*, vol. 92, no. 8, pp. 2613–2628, 1998.
- [49] B. Lanske, A. C. Karaplis, K. Lee et al., "PTH/PTHrP receptor in early development and Indian hedgehog-regulated bone growth," *Science*, vol. 273, no. 5275, pp. 663–666, 1996.
- [50] K. Mizuhashi, W. Ono, Y. Matsushita et al., "Resting zone of the growth plate houses a unique class of skeletal stem cells," *Nature*, vol. 563, no. 7730, pp. 254–258, 2018.
- [51] H. Hojo, S. Ohba, F. Yano et al., "Gli1 protein participates in Hedgehog-mediated specification of osteoblast lineage during endochondral ossification," *The Journal of Biological Chemistry*, vol. 287, no. 21, pp. 17860–17869, 2012.
- [52] H. Zhao, J. Feng, T. V. Ho, W. Grimes, M. Urata, and Y. Chai, "The suture provides a niche for mesenchymal stem cells of craniofacial bones," *Nature Cell Biology*, vol. 17, no. 4, pp. 386–396, 2015.
- [53] H. Zhao, J. Feng, K. Seidel et al., "Secretion of shh by a neurovascular bundle niche supports mesenchymal stem cell homeostasis in the adult mouse incisor," *Cell Stem Cell*, vol. 14, no. 2, pp. 160–173, 2014.
- [54] L. Ye, F. Lou, F. Yu et al., "NUMB maintains bone mass by promoting degradation of PTEN and GLI1 via ubiquitination in osteoblasts," *Bone Research*, vol. 6, no. 1, p. 32, 2018.
- [55] Y. Shi, G. He, W. C. Lee, J. A. McKenzie, M. J. Silva, and F. Long, "Gli1 identifies osteogenic progenitors for bone formation and fracture repair," *Nature Communications*, vol. 8, no. 1, p. 2043, 2017.
- [56] L. Song, M. Liu, N. Ono, F. R. Bringhurst, H. M. Kronenberg, and J. Guo, "Loss of wnt/ $\beta$ -catenin signaling causes cell fate shift of preosteoblasts from osteoblasts to adipocytes," *Journal of Bone and Mineral Research*, vol. 27, no. 11, pp. 2344–2358, 2012.
- [57] M. K. Khokha, D. Hsu, L. J. Brunet, M. S. Dionne, and R. M. Harland, "Gremlin is the BMP antagonist required for maintenance of Shh and Fgf signals during limb patterning," *Nature Genetics*, vol. 34, no. 3, pp. 303–307, 2003.
- [58] E. Canalis, K. Parker, and S. Zanotti, "Gremlin1 is required for skeletal development and postnatal skeletal homeostasis," *Journal of Cellular Physiology*, vol. 227, no. 1, pp. 269–277, 2012.
- [59] R. Merino, J. Rodriguez-Leon, D. Macias, Y. Gañan, A. N. Economides, and J. M. Hurler, "The BMP antagonist Gremlin regulates outgrowth, chondrogenesis and programmed cell death in the developing limb," *Development*, vol. 126, no. 23, pp. 5515–5522, 1999.
- [60] D. L. Worthley, M. Churchill, J. T. Compton et al., "Gremlin 1 identifies a skeletal stem cell with bone, cartilage, and reticular stromal potential," *Cell*, vol. 160, no. 1–2, pp. 269–284, 2015.
- [61] S. Méndez-Ferrer, T. V. Michurina, F. Ferraro et al., "Mesenchymal and haematopoietic stem cells form a unique bone marrow niche," *Nature*, vol. 466, no. 7308, pp. 829–834, 2010.
- [62] B. O. Zhou, R. Yue, M. M. Murphy, J. G. Peyer, and S. J. Morrison, "Leptin-receptor-expressing mesenchymal stromal cells represent the main source of bone formed by adult



- bone marrow," *Cell Stem Cell*, vol. 15, no. 2, pp. 154–168, 2014.
- [63] M. Zhao, F. Tao, A. Venkatraman et al., "N-cadherin-expressing bone and marrow stromal progenitor cells maintain reserve hematopoietic stem cells," *Cell Reports*, vol. 26, no. 3, pp. 652–669.e6, 2019.
- [64] M. Crisan, S. Yap, L. Casteilla et al., "A perivascular origin for mesenchymal stem cells in multiple human organs," *Cell Stem Cell*, vol. 3, no. 3, pp. 301–313, 2008.
- [65] S. Shi and S. Gronthos, "Perivascular niche of postnatal mesenchymal stem cells in human bone marrow and dental pulp," *Journal of Bone and Mineral Research*, vol. 18, no. 4, pp. 696–704, 2003.
- [66] C. K. F. Chan, C.-C. Chen, C. A. Luppen et al., "Endochondral ossification is required for haematopoietic stem-cell niche formation," *Nature*, vol. 457, no. 7228, pp. 490–494, 2009.
- [67] A. Greenbaum, Y. M. S. Hsu, R. B. Day et al., "CXCL12 in early mesenchymal progenitors is required for haematopoietic stem-cell maintenance," *Nature*, vol. 495, no. 7440, pp. 227–230, 2013.
- [68] S. Pinho, J. Lacombe, M. Hanoun et al., "PDGFR $\alpha$  and CD51 mark human nestin+sphere-forming mesenchymal stem cells capable of hematopoietic progenitor cell expansion," *The Journal of Experimental Medicine*, vol. 210, no. 7, pp. 1351–1367, 2013.
- [69] S. A. Boxall and E. Jones, "Markers for characterization of bone marrow multipotential stromal cells," *Stem Cells International*, vol. 2012, Article ID 975871, 12 pages, 2012.
- [70] C. Holmes and W. L. Stanford, "Concise review: stem cell antigen-1: expression, function, and enigma," *Stem Cells*, vol. 25, no. 6, pp. 1339–1347, 2007.
- [71] Y. Tan, M. Zhao, B. Xiang, C. Chang, and Q. Lu, "CD24: from a hematopoietic differentiation antigen to a genetic risk factor for multiple autoimmune diseases," *Clinical Reviews in Allergy and Immunology*, vol. 50, no. 1, pp. 70–83, 2016.
- [72] T. H. Ambrosi, A. Scialdone, A. Graja et al., "Adipocyte accumulation in the bone marrow during obesity and aging impairs stem cell-based hematopoietic and bone regeneration," *Cell Stem Cell*, vol. 20, no. 6, pp. 771–784.e6, 2017.
- [73] O. Naveiras, V. Nardi, P. L. Wenzel, P. V. Hauschka, F. Fahey, and G. Q. Daley, "Bone-marrow adipocytes as negative regulators of the haematopoietic microenvironment," *Nature*, vol. 460, no. 7252, pp. 259–263, 2009.
- [74] J. S. Flier and E. Maratos-Flier, "Leptin's physiologic role: does the emperor of energy balance have no clothes?," *Cell Metabolism*, vol. 26, no. 1, pp. 24–26, 2017.
- [75] R. T. Turner, S. P. Kalra, C. P. Wong et al., "Peripheral leptin regulates bone formation," *Journal of Bone and Mineral Research*, vol. 28, no. 1, pp. 22–34, 2013.
- [76] S. Takeda, F. Eleftheriou, R. Levasseur et al., "Leptin regulates bone formation via the sympathetic nervous system," *Cell*, vol. 111, no. 3, pp. 305–317, 2002.
- [77] K. Clément, C. Vaisse, N. Lahlou et al., "A mutation in the human leptin receptor gene causes obesity and pituitary dysfunction," *Nature*, vol. 392, no. 6674, pp. 398–401, 1998.
- [78] L. DiMascio, C. Voermans, M. Uqoezwa et al., "Identification of adiponectin as a novel hemopoietic stem cell growth factor," *Journal of Immunology*, vol. 178, no. 6, pp. 3511–3520, 2007.
- [79] B. O. Zhou, H. Yu, R. Yue et al., "Bone marrow adipocytes promote the regeneration of stem cells and haematopoiesis by secreting SCF," *Nature Cell Biology*, vol. 19, no. 8, pp. 891–903, 2017.
- [80] Q. Li, Y. Wu, and N. Kang, "Marrow adipose tissue: its origin, function, and regulation in bone remodeling and regeneration," *Stem Cells International*, vol. 2018, Article ID 7098456, 11 pages, 2018.
- [81] R. Yue, B. O. Zhou, I. S. Shimada, Z. Zhao, and S. J. Morrison, "Leptin receptor promotes adipogenesis and reduces osteogenesis by regulating mesenchymal stromal cells in adult bone marrow," *Cell Stem Cell*, vol. 18, no. 6, pp. 782–796, 2016.
- [82] M. C. Gonzalez-Martin, M. Mallo, and M. A. Ros, "Long bone development requires a threshold of Hox function," *Developmental Biology*, vol. 392, no. 2, pp. 454–465, 2014.
- [83] A. Seifert, D. F. Werheid, S. M. Knapp, and E. Tobiasch, "Role of Hox genes in stem cell differentiation," *World Journal of Stem Cells*, vol. 7, no. 3, pp. 583–595, 2015.
- [84] P. Leucht, J. B. Kim, R. Amasha, A. W. James, S. Girod, and J. A. Helms, "Embryonic origin and Hox status determine progenitor cell fate during adult bone regeneration," *Development*, vol. 135, no. 17, pp. 2845–2854, 2008.
- [85] D. M. Wellik and M. R. Capecchi, "Hox10 and Hox11 genes are required to globally pattern the mammalian skeleton," *Science*, vol. 301, no. 5631, pp. 363–367, 2003.
- [86] I. T. Swinehart, A. J. Schlientz, C. A. Quintanilla, D. P. Mortlock, and D. M. Wellik, "Hox11 genes are required for regional patterning and integration of muscle tendon and bone," *Development*, vol. 140, no. 22, pp. 4574–4582, 2013.
- [87] D. R. Rux, J. Y. Song, I. T. Swinehart et al., "Regionally restricted Hox function in adult bone marrow multipotent mesenchymal stem/stromal cells," *Developmental Cell*, vol. 39, no. 6, pp. 653–666, 2016.
- [88] D. R. Rux, J. Y. Song, K. M. Pineault et al., "Hox11 function is required for region-specific fracture repair," *Journal of Bone and Mineral Research*, vol. 32, no. 8, pp. 1750–1760, 2017.
- [89] M. R. Allen, J. M. Hock, and D. B. Burr, "Periosteum: biology, regulation, and response to osteoporosis therapies," *Bone*, vol. 35, no. 5, pp. 1003–1012, 2004.
- [90] Y. K. Kim, H. Nakata, M. Yamamoto, M. Miyasaka, S. Kasugai, and S. Kuroda, "Osteogenic potential of mouse periosteum-derived cells sorted for CD90 in vitro and in vivo," *Stem Cells Translational Medicine*, vol. 5, no. 2, pp. 227–234, 2016.
- [91] B. G. Matthews, D. Grcevic, L. Wang et al., "Analysis of  $\alpha$ SMA-labeled progenitor cell commitment identifies notch signaling as an important pathway in fracture healing," *Journal of Bone and Mineral Research*, vol. 29, no. 5, pp. 1283–1294, 2014.
- [92] O. Duchamp de Lageneste, A. Julien, R. Abou-Khalil et al., "Periosteum contains skeletal stem cells with high bone regenerative potential controlled by Periostin," *Nature Communications*, vol. 9, no. 1, p. 773, 2018.
- [93] S. Lotinun, R. Kiviranta, T. Matsubara et al., "Osteoclast-specific cathepsin K deletion stimulates SIP-dependent bone formation," *The Journal of Clinical Investigation*, vol. 123, no. 2, pp. 666–681, 2013.
- [94] P. Panwar, L. Xue, K. Sjøe et al., "An ectosteric inhibitor of cathepsin K inhibits bone resorption in ovariectomized mice," *Journal of Bone and Mineral Research*, vol. 32, no. 12, pp. 2415–2430, 2017.

- [95] N. Bonnet, J. Brun, J. C. Rousseau, L. T. Duong, and S. L. Ferrari, "Cathepsin K controls cortical bone formation by degrading periostin," *Journal of Bone and Mineral Research*, vol. 32, no. 7, pp. 1432–1441, 2017.
- [96] W. Yang, J. Wang, D. C. Moore et al., "Ptpn11 deletion in a novel progenitor causes metachondromatosis by inducing hedgehog signalling," *Nature*, vol. 499, no. 7459, pp. 491–495, 2013.
- [97] S. Debnath, A. R. Yallowitz, J. McCormick et al., "Discovery of a periosteal stem cell mediating intramembranous bone formation," *Nature*, vol. 562, no. 7725, pp. 133–139, 2018.
- [98] C. K. F. Chan, P. Lindau, W. Jiang et al., "Clonal precursor of bone, cartilage, and hematopoietic niche stromal cells," *Proceedings of the National Academy of Sciences of the United States of America*, vol. 110, no. 31, pp. 12643–12648, 2013.
- [99] J. J. Mao and D. J. Prockop, "Stem cells in the face: tooth regeneration and beyond," *Cell Stem Cell*, vol. 11, no. 3, pp. 291–301, 2012.
- [100] Y. Chai and R. E. Maxson, "Recent advances in craniofacial morphogenesis," *Developmental Dynamics*, vol. 235, no. 9, pp. 2353–2375, 2006.
- [101] M. Yang, H. Zhang, and R. Gangolli, "Advances of mesenchymal stem cells derived from bone marrow and dental tissue in craniofacial tissue engineering," *Current Stem Cell Research & Therapy*, vol. 9, no. 3, pp. 150–161, 2014.
- [102] G. M. Morriss-Kay and A. O. M. Wilkie, "Growth of the normal skull vault and its alteration in craniosynostosis: insights from human genetics and experimental studies," *Journal of Anatomy*, vol. 207, no. 5, pp. 637–653, 2005.
- [103] L. A. Opperman, "Cranial sutures as intramembranous bone growth sites," *Developmental Dynamics*, vol. 219, no. 4, pp. 472–485, 2000.
- [104] H. M. Yu, B. Jerchow, T. J. Sheu et al., "The role of Axin2 in calvarial morphogenesis and craniosynostosis," *Development*, vol. 132, no. 8, pp. 1995–2005, 2005.
- [105] B. Liu, H. M. I. Yu, and W. Hsu, "Craniosynostosis caused by Axin2 deficiency is mediated through distinct functions of  $\beta$ -catenin in proliferation and differentiation," *Developmental Biology*, vol. 301, no. 1, pp. 298–308, 2007.
- [106] T. Maruyama, A. J. Mirando, C. X. Deng, and W. Hsu, "The balance of WNT and FGF signaling influences mesenchymal stem cell fate during skeletal development," *Science Signaling*, vol. 3, no. 123, p. ra40, 2010.
- [107] T. Maruyama, M. Jiang, A. Abbott et al., "Rap1b is an effector of Axin2 regulating crosstalk of signaling pathways during skeletal development," *Journal of Bone and Mineral Research*, vol. 32, no. 9, pp. 1816–1828, 2017.
- [108] T. Maruyama, J. Jeong, T. J. Sheu, and W. Hsu, "Stem cells of the suture mesenchyme in craniofacial bone development, repair and regeneration," *Nature Communications*, vol. 7, no. 1, article 10526, 2016.